ANALYSES OF GAS-LIQUID AND GAS-LIQUID-SOLID FOAM-BED REACTORS

By

ISHA ARYA

(2008RCH101)

Department of Chemical Engineering

Submitted as a partial fulfillment of the requirements for the degree of

DOCTOR OF PHYLOSOPHY

IN

CHEMICAL ENGINEERING

Malaviya National Institute of Technology, Jaipur

JULY 2014

Certificate

This is to certify that the thesis entiled, **ANALYSES OF GAS-LIQUID AND GAS-LIQUID-SOLID FOAM-BED REACTORS**, being submitted by **Mrs. Isha Arya** to the Malaviya National Institute of technology, Jaipur for the award of the degree of **DOCTOR OF PHILOSOPHY** is a record of the bonafide research work carried out by her. She worked under my guidance for the submission of this thesis which to my knowledge has reached the requisite standard.

The thesis or any part of it has not been submitted to any university or institute for the award of any degree or diploma.

Date:

Dr. S.K. Jana
Associate Professor
Department of Chemical Engineering
Malaviya National Institute of
Technology, Jaipur, Rajasthan, 302017

Declaration

This is to certify that the data presented in the current Ph.D. thesis entitled *"ANALYSES OF GAS-LIQUID AND GAS-LIQUID-SOLID FOAM-BED REACTORS"* is the outcome of the study conducted by me for the present work. These data have not been published anywhere else to the best of my knowledge. The data referred/taken from other papers/reports have been duly acknowledged by citing references at appropriate places. I have checked plagiarism through software *"turnitin"*. The report showed 86% original and 14% plagiarism in the whole thesis.

Isha Arya

(2008RCH101)

Acknowledgement

I am grateful to the almighty, the most benevolent and merciful, for giving me the strength and zeal to complete this endeavor. Tremendous praise for God, who is forever a torch of guidance for knowledge seekers and whole humanity.

*Foremost, I would like to express my sincere gratitude to my advisor **Dr. S. K. Jana** Dept. of Chemical Engineering, Malaviya National Institute of Technology, Jaipur for the continuous support of my Ph.D. study and research, for his patience, motivation, enthusiasm, and immense knowledge. His nonpareil guidance helped me in all the time of research and writing of this thesis. I could not have imagined having a better advisor and mentor for my Ph.D. study.*

*I am highly thankful to **Dr. Suja George** Head, Department of Chemical Engineering for providing infra-structure support and facilities. All DREC members specially Prof. Dilip Sharma, Dr. P. Pandit and Dr. Virendra Saharan for their continuous evaluation and suggestions throughout my Ph.D. studies.*

*I am indebted to **Dr. Ashok Bhaskarwar**, Head, Department of Chemical Engineering, Indian Institute of Technology, New Delhi for his support and giving all help which was needed from time to time in the course of present investigation.*

*A non-payable debt to my loving father **Mr. Mohan Lal Arya** and mother **Mrs. Usha Arya** for their unflagging love, blessings and moral support throughout my research work. They prayed for me, shared the burdens and made sure that I sailed through smoothly. Their boundless affection has been my great strength during the moment of stress. I thank them for being my strength always.*

*It is impossible to express my sincere and heartfelt thanks to my adorable sister and brothers **Miss Khushaboo Arya, Mr. Nitesh Arya** and*

Mr. Sandeep Tamoli for their persistent co-operation, patience, moral support and endurance.

The constant co-operation, inspiration and moral support accorded by my soul mate **Dr. Yogesh Kumar** is beyond any acknowledgement. His patient and love enable me to complete this work. My deepest gratitude goes for standing by me like a rock during critical periods and helping me a great deal to fulfill my scientific pursuits and preparation of this manuscript. I have no doubt in my mind that without his invaluable guidance and help, this stupendous work would not have been completed. I shall remain indebted to my adorable daughter **Miss Manasvini** because her childhood was affected because of my full occupation with my own research work.

I would like to express my gratitude and indebtedness to my grandfather **Mr. Jaswant Singh Tamoli,** grandmother **Mrs. Shiv Kumari**, Father-in-law Late Pitram Chandelia Mother-in law Mrs. Santara Devi for their strong inspiration, encouragement, blessings and wishes. They offered me their silent contribution and moral support when it was most needed.

I feel extremely thankful to all the non-teaching staff of the Department namely **Mr. Ramesh Sharma** and **Rajiv Goswami** also deserves mention for helping me with the experimental set-up and acquisitions of reagents and other requirements.

I wish to thank my collesgues **Mr. Avnish,** Mr. Vivek, Mr Praveen, Mrs. Parul Bhatt and Ms Neha Sharma for their assistance in preparation of the manuscript of this thesis.

I sincerely thank all those people whose names I have not mentioned here, but directly or indirectly have contributed in making this thesis a success.

July 2014

Isha Arya

ABSTRACT

The present investigation concerns itself with the re-analyses of mathematical models reported in the literature for mass-transfer accompanied by chemical reaction in gas liquid and gas-liquid-solid *foam-bed reactors* for typically two different reaction systems, development of new models and their experimental verification. The systems chosen for studies are, absorption of CO_2 in NaOH solution under conditions of pseudo-first order reaction and the other, for a gas-liquid-solid system: carbonation of hydrated lime slurry using lean CO_2 gas. The former system corresponds to a fast chemical reaction and it occurs in a zone within the liquid film close to the gas-liquid interface. The latter reaction is moderately fast and occurs in the bulk of the liquid. Carbonation of hydrated lime in slurry using carbon-dioxide gas is an industrially important process for the manufacture of precipitated calcium carbonate (PCC). The performance of a short slurry bubble-column reactor has been compared with that of the slurry-foam reactor using experimental data collected for the above-mentioned reaction.

Mathematical models for these two systems have been reported in the literature for carrying out the reactions in a foam-bed reactor. This reactor comprises of two sections, (i) the lower section, called the storage, is a shallow pool of liquid containing a surfactant through which gas bubbles rise and (ii) the upper section is a tall column of foam, called the foam section. The total amount of liquid contained in the foam, for the typical foam heights reported in the literature, is normally less than 15 percent of the total liquid fed to the reactor. In spite of this fact, models reported in the literature for the two systems assume extent of gas absorption and reaction in the storage section to be negligible. The above mentioned work was therefore undertaken in the present work.

Models have been developed for absorption of lean carbon dioxide gas, 0.22% to 0.49%, from its mixture with air in sodium hydroxide solution, 0.23 to 0.87 (N) in semi-batch bubble column- and foam-bed reactors. Experimental studies with this low concentration of CO_2 and relatively high concentration of NaOH were performed with the objective of verifying the contribution of the storage section of a foam bed reactor towards conversion of reactants which was considered negligible in the previous studies, developing a new model, verifying its validity with the data generated and at the same time comparing the

present model with that already reported in the literature in which about the same concentrations of CO_2 and NaOH were used in the gas and liquid phase respectively. Mass transfer with chemical reaction is treated using the principle of absorption into agitated liquids for the development of models for the bubble column. Model for the storage section of a foam-bed reactor is developed following a similar concept to that of the bubble column. In the foam section, on the other hand, mass transfer occurs into the foam films primarily by molecular diffusion and the model is developed using the theories of absorption into quiescent liquids. Concentration of reactant B (i.e., NaOH) in the bulk of the liquid is maintained substantially high compared to a low concentration of dissolved CO_2. Reactant B diffuses from the bulk of liquid to the reaction zone located close to the gas-liquid interface to nullify its depletion by reaction and maintain the same concentration of B upto the reaction zone as that existed in the bulk liquid. Rate of consumption of B is obtained by using the reaction stoichiometry and the average flux equation for CO_2 (component A). Calculations for concentration of component B in the storage section of a foam-bed reactor proceed by repeating the process over a small time step. For the development of model for the foam section, it is assumed that all the A absorbed in the storage section get reacted there itself and none of it goes to the foam section and *vis-à-vis*. Predictions for the extent of reaction over a small time interval in storage and foam sections are made using separate modules. The resulting concentration of component B in the storage section is estimated and the calculations are repeated over small time interval till the desired time of reactor operation.

For validation of the models developed, experiments in the bubble column reactor were performed on absorption of CO_2 in NaOH solution without any surfactant added to the reaction mixture. Similar experiments were conducted under otherwise identical operating conditions in a foam reactor with the addition of cetyl trimethyl ammonium bromide (CTAB), a cationic surfactant (0.054% w/w) as the foaming agent. The variables and parameters studied include, effects of initial concentration of NaOH, superficial velocity of gas, volume of solution charged into the reactor and concentration of CO_2 gas on conversion of NaOH. After 2 minutes of reactor operation, a conversion 6 to20 percent higher than that obtained in a bubble column reactor, was obtained in the foam reactor. ***Conversion of sodium hydroxide reduces with an increase in the concentration***

of NaOH in the feed solution when other variables are kept unchanged. This is attributed to the reduced solubility of CO_2 with an increase in the concentration of NaOH in the solution and that the fraction of the total initial mass of NaOH reacted during the same time interval reduced with each successive increment in concentration and caused a reduction in conversion. Conversions of sodium hydroxide after a definite time of reactor operation and under otherwise similar experimental conditions are found to be substantially higher in a foam-bed reactor than that in the bubble column reactor. Large increase in the interfacial area is considered to be the primary reason for this increase in conversion of NaOH. With an increase in the *superficial velocity of gas,* conversion of NaOH is found to increase. Larger size of bubbles and higher bubble-rise velocity at higher superficial velocity of gas reduce the specific interfacial area and gas-liquid contact time in the bubble column or in the storage section of the foam reactor. These lead to a reduction in the level of conversion. On the contrary, turbulence in the bubble column increases with an increase in the superficial velocity of gas and leads to higher values of gas-liquid mass transfer coefficient in the column. These result in higher rates of gas absorption, reaction and conversion. Percent conversion of NaOH reduces as *volume of solution fed to the reactor is increased*, concentration and all the other variables being kept unchanged. Total amount of NaOH is larger in the larger volume of solution fed to the reactor and conversion is found to reduce mainly because of the higher total initial mass appearing in the denominator in the definition used for conversion calculation. Conversion of NaOH increases with an increase in the concentration of CO_2 gas. Interfacial concentration of CO_2 in the liquid phase increases and the increased driving force for mass transfer causes an increase in the rates of gas absorption, reaction and therefore the conversion.

Model for the *bubble column slurry reactor* has been developed for simultaneous dissolution of sparingly soluble hydrated lime particles and reaction with the dissolved gaseous species in the liquid phase. The slurry in the reactor is assumed to be well mixed by the rising gas bubbles. The reaction between hydroxide ions in solution and dissolved carbon-dioxide occurs in accordance with a second-order kinetics (Danckwerts and Sharma, 1966). Particle-size distribution has been incorporated in the model for evaluation of the reactor performance as lime samples having different initial particle-size

distributions have been used in the experiments and the rate of dissolution of particles in liquid depends on its surface area.

In the development of the **slurry-foam reactor** model, combined contributions of both the storage and foam sections towards gas absorption and reaction have been taken into account. That the storage section contributes significantly have been verified through experiments. The entire foam section is assumed to be equivalent to a single stage with an average liquid hold-up (Bhaskarwar and Kumar, 1984). In the course of reaction, as the dissolved species *B* gets consumed by reaction with component *A* absorbed in the liquid phase, concentration of *B* tends to reduce and more solid (*B*) dissolves into the liquid phase. There being a continuous transformation from solid to liquid phase, total loading of *B* in the slurry, both dissolved in solution and that present as particles, is incorporated in writing the material-balance equations for estimation of conversion of component *B* with the propagation of reaction time. The expressions for evaluation of performance of the *slurry-foam reactor* remain the same as those used for a slurry reactor, except that in the former case the total loading of component *B* and the instantaneous values of particle diameters have to be estimated by considering the conversions in both the sections, i.e. storage and foam simultaneously. For evaluation of performance of the slurry-foam reactor, component *A* balances in foam and storage sections, component *B* balance over the storage section, and the mass balance of particles over the storage section are written. Again for writing the component *A* balance over the storage section, the instantaneous concentration of component *A* in the liquid stream, for this moderately fast reaction, draining from the foam to the storage section is needed. This concentration is obtained by writing a pseudo-steady state material balance for component *A* over the foam section. Simultaneous solution of these material-balance equations also needs an expression for the instantaneous volume of particles in the drainage stream from foam section expressed in terms of that in the storage section. For this purpose a mass-balance equation is written assuming that the rate of dissolution of particles in the foam section equals that reacted in this section, so that the concentration of dissolved calcium hydroxide in the liquid entering the foam section and that in the drainage stream from this section are the same, conforming to the pseudo-first order reaction with respect to *A* in the foam section.

In order to validate the models developed, experiments on carbonation of hydrated lime in slurry with lean carbon-dioxide gas, 10 to 50 percent by volume, were performed in a short slurry bubble column reactor, without any surfactant added to the slurry as well as in a foam-bed reactor using different types of surfactants, cationic: cetyl trimethyl ammonium bromide, anionic: sodium dodecyl sulphate, and non-ionic: Triton X-100 as the foaming agents.

Under identical conditions of experiments, after 20 minutes of the reactor operation, a higher conversion, about 18 to 42 percent higher than that in a slurry reactor, was obtained in the foam reactor using a cationic or an anionic surfactant as the foaming agent. The variables and parameters studied include, nature of surfactant used in generating stable foam, initial loading of hydrated lime in slurry, superficial velocity of gas, height of foam column, volume of slurry charged into the reactor, initial size distribution of lime particles (samples received from different manufacturers), concentration of each of the surfactants mentioned above, and, concentration of CO_2 in the feed gas. Other essential or supplementary experiments performed are (i) particle-size distribution analysis of calcium-hydroxide samples used as reactant as well as that of the product $CaCO_3$ (ii) chemical analysis of hydrated lime samples received from different manufacturers and used in the experiments (iii) liquid hold-up measurements in the foam column for all the experimental conditions used in obtaining the different sets of data (iv) Thermo-gravimetric Analysis (TGA) and X-ray diffraction (XRD) studies of calcium hydroxide samples received from different suppliers and that of product calcium carbonate obtained after complete carbonation of lime samples and (v) Scanning Electron Micrograph (SEM) analysis of calcium hydroxide samples and product calcium carbonate particles.

Percentage of lime present in samples was found, through chemical analyses, to vary from 94.76 to 95.27 percent. XRD analyses indicate that major impurity is $CaCO_3$. Particle-size distributions (PSDs) of reactant $Ca(OH)_2$ have been measured using CILAS-940 and MALVERN MASTERSIZER 2000E particle-size analyzers. These play a significant role in governing the reactor performance and incorporated in the models. For

simulation purposes, the total amount of lime sample taken in an experiment was divided into twelve volume fractions.

For slow to moderately fast reactions, liquid hold-up is known to govern the performance of a foam-bed reactor. In the present investigation, it has been measured at different heights of the foam column, for all the experimental conditions used, by suction of foam into an evacuated glass bulb of a known volume. Average value of the liquid hold-up over foam column height is then estimated from the knowledge of volume of bulb, the extent of vacuum in the bulb, and the volume of slurry obtained from the condensed foam.

Conversions obtained in the **slurry-foam reactor** with ionic surfactants used as foaming agents after 10 minutes of reactor operation are found to be about 7 to 17 per cent higher than those obtained with non-ionic surfactants. The higher conversions obtained with ionic surfactants over those with a non-ionic surfactant are attributed to the higher gas-liquid interfacial areas and liquid hold-up values obtained experimentally. With an increase in the **initial solids loading,** solid-liquid interfacial area increases and results in increased rates of solid dissolution and rate of reaction. However, conversion of lime reduces because initial solids loading appearing in the denominator in the conversion calculation. **Superficial velocity of gas** is observed to be the second most important variable which bring about maximum variation in the conversion of lime. Increase in the superficial velocity of gas causes higher liquid hold-up, higher drainage rate within the foam column, and an increased turbulence intensity in the storage section. These result in higher rates of mass transfer and of conversion of the two reactants. With an increase in **the height of slurry-foam column,** the total gas-liquid interfacial area for gas absorption in the foam section, gas-liquid contact time, and the total amount of liquid in the foam section increase. These factors together contribute to higher conversion of lime. With increased **volume of feed slurry** at constant values of slurry concentration and other variables, a reduction in the conversion of lime is observed. With an increase in the volume of slurry, at constant gas-flow rate and other variables, the intensity of agitation in the storage section reduces with the consequent reduction in the mass-transfer coefficient. The rates of dissolution of solids and that of absorption of gas in the liquid reduce.

Besides, solids loading being constant, the total amount of solids present is more in a larger volume of slurry, and the calculated values of conversion is found to reduce primarily because of the definition used for its calculation. With an **increase in the concentration of surfactants**, viz. SDS; CTAB and Triton X-100; at constant values of all other variables, the conversion of lime is seen first to increase and then to reduce at still higher concentrations. Increased surfactant concentration render the foam to be more stable and thus liquid hold-up in the foam column increases. The total volume of liquid in the storage section reduces with the consequent increase in turbulence. These beneficial effects, along with the larger interfacial area in the foam section for the reasons cited earlier, off set any retarding effect the surface resistance may have on gas absorption, and a small increase in the conversion is thus obtained. However, at higher concentration levels of the surfactant, the particle surfaces get appreciably covered with the surfactant molecules (Stangle and Mahalingam, 1990), reducing the rate of dissolution of solids. These phenomena, therefore, cause a decrease in the conversion of lime at higher surfactant concentrations. **Effect of initial particle-size distribution of lime particles** on conversion of lime has also been studied maintaining all other parameters at constant values. For a given solids loading, the sample of solids having a larger population of finer particles would have a larger interfacial area per unit volume of slurry. The dissolution rate of solid particles being proportional to solid-liquid interfacial area, samples of hydrated lime with higher population of finer particles results in higher conversion of lime. The model also predicts the effect.

Effect of concentration of CO_2 gas on conversion of lime has been studied by varying the CO_2 concentration from 10 to 50 percent by volume. Rates of absorption of CO_2 gas in hydrated lime slurry and the reaction rates are enhanced significantly with the increase in concentration of CO_2 in the feed gas mixture, the equilibrium interface concentration of dissolved CO_2 being increased. For a given value of particle loading and at a given temperature, total solid-liquid interfacial area and interface concentration C_B^* remains invariant. Rate of dissolution of lime is enhanced for the reaction to proceed at a higher rate as CO_2 concentration in the feed gas is increased. This is possible only if solid-liquid mass-transfer coefficient value is increased. A dimensionless correlation has been developed using the experimental data collected for carbonation of hydrated lime slurry

as functions of concentration of carbon-dioxide gas and other variables/parameters pertinent to the experiments performed.

CONTENTS

LIST OF FIGURES

LIST OF TABLES

Chapter 1

INTRODUCTION

The state-of-the-art designs of Chemical Process Industries aim at producing highest quality products at a minimum cost with a zero discharge of pollutants. The most important requirement to achieve this target is that the existing chemical reactors be retrofitted for improving its performance and/or new efficient reactors developed. While conventional chemical-reactor configurations have been studied extensively for various gas-liquid and gas-liquid-solid reactions and ample information is available in the literature, in recent years, researchers working in chemical engineering and allied areas have turned their attention in developing novel contactors. Large gas-liquid interfacial areas, high values of mass-transfer coefficient and gas holdup, long gas-liquid contact times and low gas-phase pressure drops are some of the important parameters desired for a high performance gas-liquid contactor for mass transfer with chemical reaction. A foam-bed reactor has been claimed by numerous authors to possess the above features and especially advantageous for a precipitation reaction. In the latter case, recirculation of the solvent and that of the unreacted gas help in controlling the discharge to sewer/ atmosphere and also in reducing the product cost. A number of reactions have been studied by various authors in this reactor configuration. Of these, two important reactions studied in this reactor, one for a gas-liquid system: absorption of carbon dioxide gas in NaOH solution and the other for a gas-liquid-solid system: carbonation of hydrated lime slurry using lean carbon-dioxide gas have been chosen in the present work for re-analysis of the reported experimental findings and modeling/ parameter estimation aspects.

Foams, occupying more than 90 percent by volume of a foam-bed reactor, has been reported to create severe problems in large number of chemical process operations involving gas-liquid/ gas-liquid-solid systems. These include numerous unit operations and unit processes in chemical, biochemical and food industries including oil-well drilling, fermentation as well as in the manufacture of surfactants itself, viz., detergents, glycol antifreeze etc. These are agglomerates of gas bubbles separated from each other by thin liquid films. While froth bubbles are nearly spherical and small in size, foam bubbles are larger and polyhedral or deformed. Liquid content in foam is much lower ($\bar{\varepsilon}_l \leq 0.1$) than that in froth ($\bar{\varepsilon}_l \approx 0.5$).

Large volume of work has been reported in the literature on foams which aim at avoiding its formation in some of the process operations, while in some others the purpose is to stabilize the foams for the reasons cited above. Researchers and

particularly those in R&D organizations of industries perform rigorous studies on foams with the objective of producing better quality products and these studies include physico-chemical properties, structure, hydrodynamics, stability considerations as well as its specific usefulness in applications of mass transfer with or without chemical reaction.

For the purposes of gas absorption and various gas-liquid and gas-liquid-solid reactions, conventional chemical-reactor configurations have been studied extensively and immense information is available in the literature. It is desired in this work to focus on a novel reactor called a **foam-bed reactor**, for **gas–liquid** and **gas-liquid-solid reactions** which have not been extensively studied earlier and therefore not yet established on firm footing.

A foam-bed contactor is a device containing a shallow pool of liquid in which a reactive gas/ mixture of gases is brought into intimate contact with the liquid solvent or a solution containing a reactive species, the liquid being self-foaming or containing a surfactant for generation of stable foam, in which mass transfer occurs with or without a chemical reaction.

A foam-bed reactor has the following important features:

i. Gas-liquid contact time is sufficiently higher compared to other type of contactor

ii. This being a gas-liquid contacting device, can be operated in various modes: semi-batch, continuous flow, recycled, co-current, and countercurrent

iii. It can be conveniently used as a slurry reactor and fouling problem is less even with a sticky material because of presence of surfactant in the liquid

iv. A large amount of gas can be contacted with a small amount of liquid

v. Gas-liquid interfacial area and gas hold-up are higher than in any other type of contactor

vi. Gas pressure drop for flow through the reactor is low to moderate

vii. Only a marginal cost is incurred for the surfactant used in generation of a stable foam column for performing precipitation reactions, as the solvent can be completely recycled back into the reactor after separation of product solid.

The performance of a foam-bed reactor, under certain conditions, has been reported (Helsby and Birt, 1955; Metzner and Brown, 1956) to be far superior compared to that of the conventional contactors. Ponter et al. (1976) reported significant improvement in the efficiency of separation when surfactant was added to the distillation column of surface tension negative binary mixtures. This improvement was attributed to the increased interfacial area to mass transfer caused by the stabilization of the liquid film. Presence of proteins in the liquid in a fermentor lead to stabilization of foams and increased rates of mass transfer while simultaneously cause pumping problems and lead to improper detection of liquid level through sight glass. The above observations have led the researchers to find appropriate techniques to generate and stabilize or to destroy foams inevitably generated in various process operations.

Manufacture of precipitated calcium carbonate (PCC) through carbonation of hydrated lime is an industrially important reaction and has been chosen here for studies using a novel contactor. In the conventional process, a bubble column slurry reactor is employed for its production. PCC can also be produced by a liquid-phase reaction between calcium hydroxide and sodium carbonate in an aqueous solution. But crystal sizes of calcium carbonate obtained by these two alternative routs are different.

PCC is used as a raw material or filler, e.g. in the manufacture of paints, PVC, paper, rubber, medicines, cosmetics, etc. Major consumer of PCC is the paper industry. It is used as an additive in PVC to increase its impact strength. PCC surface is activated to match its surface properties with that of the compounds, e.g. thermoplastics, in which they are incorporated. Due to the specific shape of its particles, PCC is incorporated in paints to improve their hiding power and this reduces the quantity of titanium-dioxide fillers. It enhances the optical properties and printing quality of paper products. Calcium-based antacid tablets, multi-vitamin/mineral tablets, etc is produced using medicine-grade PCC which is normally produced from oysters. Calcium carbonate slurry obtained from the carbonating tower is used to produce activated calcium carbonate by adding stearic acid to it and by application of heat at the required temperature. Nano PCCs, less than 0.1 μm in size, control viscosity and sag in automotive and construction sealants such as poly-sulfides, urethanes, and silicones. Nano PCC is also used as an additive to printing ink.

Early studies on usage of foams for process studies were mostly focused on physical absorption of gases, or, on removal of dust particles from dust-laden exhaust gases (Luchinsky, 1939; Helsby and Birt, 1955; Jackson, 1963; Weissman and Calvert, 1965; Plevan and Quinn, 1966; Maminov and Usmanova, 1968; Onda et al., 1969; Kaldor and Phillips, 1976). Later, foam columns were utilized for studies of mass transfer with chemical reaction for a number of different reaction systems, the most important of which is possibly the carbonation of hydrated lime using CO_2 gas. Using dilute carbon-dioxide gas (1-10%), this reaction was studied mostly for the crystallization of calcium carbonate in different types of reactors (Maruscak et al. (1971), Reddy and Nancollas (1971), Tsuge et al. (1987), Kotaki and Tsuge (1990), Wachi and Jones (1991), Jones et al. (1992) and many others). During the last three decades, many important experimental studies on gas absorption with chemical reaction in foam reactors and predictions of reactor performance have also been published (Biswas and Kumar, 1981; Bhaskarwar and Kumar, 1984; Shah and Mahalingam, 1984; Bhaskarwar and Kumar, 1986; Bhaskarwar, 1987; Bhaskarwar et al., 1987; Biswas et al. 1987; Stangle and Mahalingam, 1989; Bhaskarwar and Kumar, 1995; Reddy and Bhaskarwar, 2000, and Gaikwad et. al., 2010).

Biswas and Kumar (1981) and Asolekar et al. (1988) studied gas-liquid and gas-liquid-solid reactions in semi-batch operated foam-bed reactors. Experimental conditions used by these authors indicate that only about 14 to 15% of the total liquid fed to the reactor constitutes the foam section. However, in the reactor model contribution of the storage section towards gas absorption and chemical reaction was considered negligible in comparison to that in the foam section although it contains about 85 to 86 percent of the total liquid feed. Therefore, although rigorous models of foam-bed reactors for carrying out above reactions have been put forward by several investigators (Biswas and Kumar, 1981; Asolekar et al., 1988), it appears essential, on review of literature (Jana and Bhaskarwar, 2010), that the experimental findings and models be reanalyzed and revised experimental findings and models proposed.

Lean CO_2 gas is vented to atmosphere from many process industries which can be usefully absorbed using a foam-bed reactor, as one is able to contact large quantity of gas with a relatively small amount of liquid in this type of contactor, and help approach the zero-discharge goal with respect to the "greenhouse" gas. Presence of surfactant may protect the equipment from fouling due to the highly sticky hydrated

lime in slurry and also help in easier cleaning of the equipment. The density of the solid product being much higher than that of the solvent, the product separates out by sedimentation rapidly and the solvent containing the surfactant can be recycled after filtration of the product. It therefore requires no discharge to water bodies and the fresh water requirement is minimized.

Mathematical model of a reactor provides a deep insight into the various physico-chemical phenomena occurring within it. Biswas and Kumar (1981) and later Bhaskarwar and Kumar (1984) made significant attempts in developing realistic models of a foam-bed contactor for gas-liquid systems, based on the regular pentagonal dodecahedral structure of foam bubbles. This idealized shape of foam bubbles is observed at relatively low gas velocities used for generation of stable foam column. Some investigators also studied gas-liquid-solid reactions incorporating either reactive or catalyst particles into the foam liquid (Bhaskarwar and Kumar, 1986; Asolekar et al., 1988). Carbonation of hydrated lime slurry using lean carbon-dioxide gas had been studied (Asolekar et al., 1988) earlier in a foam-bed reactor for which the conversion in the storage section had been found to be negligible although the storage constitutes more than 85 percent of the slurry charged into it. In all probability, the storage section would also contribute significantly towards the absorption of gas and conversion of reactants for this fast reaction. Under such conditions it appears justified to reproduce experimental data, reanalyze and if the findings are different from that reported in the literature, develop a new model depicting the actual phenomena occurring in the reactor.

In the present work, it is intended to reanalyze the reported mathematical model of a foam-bed reactor for a fast gas-liquid reaction through experimental verification of the contributions of the two sections of the reactor and that of a slurry-foam reactor for a moderately fast reaction. While for the former case reaction occurs in a reaction zone close to the gas-liquid interface and liquid hold-up is unimportant, the latter reaction occurs in the bulk of the liquid because of the sparingly soluble nature of $Ca(OH)_2$ and liquid hold-up is important. The two systems chosen are absorption of CO_2 in NaOH solution and carbonation of hydrated-lime slurry using lean carbon-dioxide gas. Studies on the gas-liquid system primarily aim at regenerating the experimental data for conversions separately for the two different sections of the reactor, reanalyze and propose a new model based on it, if required. With the gas-liquid-solid system, it is

also intended to generate new experimental data in the novel contactor, demonstrate the advantages for carrying our such precipitation reactions in a foam-bed reactor and propose a new and simplified model for the reactor. The variables to be studied are superficial velocity of gas, volume of solution/ slurry charged into the reactor, concentration CO_2 in the feed gas, concentration of NaOH / solids loading in the liquid feed to the reactor; and additionally for the slurry reactor, nature of surfactant used in generating stable foam, height of foam column, variation of concentration of each of the surfactants (i.e., cationic, anionic, and non-ionic) in slurry, and the initial particle-size distribution of lime particles in slurry. It is also proposed to compare its performance with a conventional slurry bubble-column reactor and to later develop mathematical models for both the bubble- and foam column reactors, taking into consideration the contributions of both the storage and foam-sections of the latter.

Reaction rate increases with an increase in the concentration of CO_2 gas and this requires availability of larger amount of dissolved lime in solution per unit time. The rate of dissolution of lime particles is therefore augmented to supply the necessary $Ca(OH)_2$ to the solution phase in the slurry reactor. It is therefore proposed to obtain a correlation for solid-liquid mass-transfer coefficient as functions of   concentration of CO_2 in the gas phase and the other important variables and parameters used in the experimental studies.

In the present thesis, Chapter 2 encompasses a brief introduction viz. structure of foam, types of surfactant, foam breaking agents, commercial production and applications of both sodium carbonate and calcium carbonate have been described. This follows a detailed review of literature covering the physico-chemical properties of foams and froths, hydrodynamic studies of foam columns, studies of mass transfer with or without chemical reaction in bubble column and foam bed reactors, two/three - phase foam contactors and evolution of mathematical models developed by the previous investigators. Chapter 3 describes the theoretical consideration of gas-liquid and gas-liquid-solid foam contactors. New mathematical models for gas-liquid and gas-liquid-solid bubble column foam-bed contactors, developed in the present work have been presented. Chapter 4 describes the material, experimental setup and experimental methods used for the study of performance of gas-liquid and gas-liquid-solid foam contactors. Experimental setup and methodology for liquid hold up and surface transfer coefficient measurement have also been described in this chapter.

Sample calculations for carbonation of sodium hydroxide and that of calcium hydroxide have been reported. Chapter 5 describes experimental as well as simulated results for gas-liquid and gas-liquid-solid bubble column and foam-bed contactors. Appendices 5A to 5E contain the experimental method calibration of rotameters, sample calculations, and, experimental data and simulated results of gas-liquid and gas-liquid-solid bubble column and foam-bed contactors. Chapter 6 presents conclusions and recommendations for future work.

Chapter 2

LITERATURE SURVEY

During the past three decades, many important experimental studies on gas absorption with/ without chemical reaction and reactor models for predicting foam-reactor performance have been published in the literature (Biswas and Kumar, 1981; Bhaskarwar and Kumar, 1984; Asolekar et al., 1988; Stangle and Mahalingam, 1990; Sharma et al., 2005; Jana and Bhaskarwar, 2010; to name a few). These include, removal of particles from exhaust gases, separation of gaseous mixtures by absorption in liquid and that of protein from its mixture with other substances, gas absorption accompanied by chemical reaction with the liquid phase component or with the fine reactive particles suspended in it. For critical analysis and modeling of this reactor for diverse situations, knowledge of hydrodynamic and physico-chemical parameters are required. These aspects are known to have significant effect on the performance of the reactor and have been studied by many investigators (Rodionov et al., 1966; Sharma and Dankwerts, 1970; Akita and Yoshida, 1973; Lee et al., 1999; Shimizu et al., 2000 and Kumar et al., 2009).

Some studies performed in foam-bed reactors for precipitation reactions, foam separations of proteins and other surface active substances, treatment of dust laden exhaust gases, etc have been reported in the literature. A comprehensive review of literature focusing on the following aspects is presented below. Gas and foam bubbles being intimately connected with the present studies, a brief account is presented in Appendix 2A. The review cited here incorporates experimental information, empirical correlations, mathematical models and design data.

Review of literature on foam-bed reactors may be broadly classified into the following:

1. Physico-chemical and hydrodynamic parameters, viz., Specific interfacial area, foam height, pressure drop, liquid holdup, foam drainage, foam stability, and, shape and size distribution of foam bubbles.

2. Foam separations and mass transfer with/ without chemical reaction in foam reactors.

In the present context, it appears highly appropriate to present a brief review on *foams in separation processes*.

Evolution of mathematical models of a foam-bed reactor has been presented in brief as the present work is a combination of both experimental and theoretical studies. It is

also considered reasonable to demonstrate the merits of a foam reactor for the system studied in the present work over conventional reactors. Hence a brief review of carbonation of lime slurry in conventional reactors studied earlier by various investigators, is presented first.

2.1 Carbonation of hydrated lime in conventional reactors

Studies reported in the literature on carbonation of hydrated lime in different types of reactors are found to follow three methods: (i) Wet process, (ii) Dry process, and, (iii) Semi dry process. While in most cases pure carbon-dioxide gas has been used (Weber and Nilsson, 1926; Ramachandran and Sharma, 1969; Sada et al., 1977; Sada et al., 1985; Kojima et al., 1989; Wei et al., 1997), for studies of reaction kinetics, reactor performances and reaction mechanism, use of lean CO_2 gas mixture are not uncommon (Juvekar and Sharma, 1973; Sada et al., 1984; Capuder and Koloini, 1984). Different types of reactors, viz., bubble column, mechanically agitated reactor and stirred-tank reactor with plane gas-liquid interface have been used for studies by wet process. While, Weber and Nelson (1926) studied carbonation reaction of lime in a mechanically agitated reactor, Tadaki and Maeda (1963) used a wetted wall column. These authors, however, did not give any clear picture about the mechanism of the reaction. Morris and Woodburn (1967) studied carbonation reaction of lime in a mechanically agitated reactor and concluded that the controlling resistance for the reaction lies on the gas side. Juvekar and Sharma (1973), however, reported a different opinion and presented the following reaction steps for carbonation of hydrated lime in aqueous slurry:

$$Ca(OH)_2 \ (s) \leftrightarrow Ca^{2+} \ (aq) + 2 \ OH^- \ (aq) \tag{2.1.i}$$

$$CO_2 \ (g) \ \leftrightarrow CO_2 \ (aq) \tag{2.1.ii}$$

$$CO_2 \ (aq) + OH^- \ (aq) \rightarrow HCO_3^- \ (aq) \tag{2.1.iii}$$

$$HCO_3^- \ (aq) + OH^- \ (aq) \rightarrow H_2O + CO_3^{2-} \ (aq) \tag{2.1.iv}$$

$$Ca^{2+} \ (aq) + CO_3^{2-} \ (aq) \rightarrow CaCO_3 \ (s) \tag{2.1.v}$$
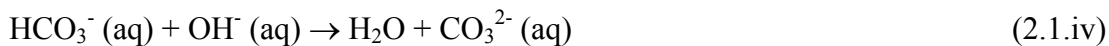
The overall reaction is

$$Ca(OH)_2 + CO_2 \rightarrow CaCO_3 + H_2O$$
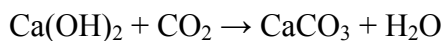
The above authors argued that steps (iv) and (v) are instantaneous and the rate-controlling step(s) could be the dissolution of solid (step i) and / or simultaneous

absorption and reaction of carbon-dioxide gas (steps ii and iii). The controlling resistance, therefore, lies on the liquid side and not on the gas side as proposed by Morris and Woodburn (1967).

While most of the studies reported in the literature follow a wet process, a dry process was used by Shih et al. (1999) for studies of kinetics of the reaction of calcium hydroxide powder with carbon-dioxide gas admixed with water vapor and nitrogen at low temperature (60-90˚C). A semi dry process was developed by Nakazato et al. (2002) for production of $CaCO_3$ in a "Powder-Particle Spouted Bed (PPSB)". The detailed studies of wet, dry and semi-dry processes are briefly discussed below.

2.1.1 Wet process

Wet process using pure carbon-dioxide gas

Ramachandran and Sharma (1969) presented analytical expressions for absorption of CO_2 gas with a fast chemical reaction into a slurry containing sparingly soluble fine particles. The authors concluded that when the diameter of the reactive particles in a slurry is greater than five times the liquid film thickness, solids dissolution and chemical reaction occur in series. The reaction scheme for this case is:

    a. Diffusion of the gaseous species *A* through the gas film.
    b. Dissolution of the solid species *B*
    c. Diffusion and simultaneous chemical reaction of the absorbed gas in the liquid film with the dissolved species *B* near the gas- liquid interface.

Whereas, if the average diameter of the particles is less than or of the order of one tenth of the film thickness, solids dissolution and chemical-reaction processes occur in parallel. Simultaneous dissolution of solid particles within the film and instantaneous reaction with the dissolved gas shift the reaction plane closer to the gas-liquid interface and cause a steeper concentration gradient of the dissolving gas. These phenomena cause increased rates of gas absorption and reaction.

Sada et al. (1977) made a comparative study of the models developed by Uchida et al. (1975) with that of Ramachandran and Sharma (1969) and argued that the model of Uchida et al. (1975) was more accurate in predicting the experimental data. A stirred tank with a plane gas-liquid interface was used by Sada et al. (1985) for studies on the absorption of carbon dioxide into concentrated slurries of calcium hydroxide. Their

observed rates of gas absorption were lower than their theoretical predictions in which they assumed identical population of particles in the bulk liquid phase as that in the liquid film. Based on this finding, they proposed a model which included an inert region in the vicinity of the gas-liquid interface to explain their experimental data.

While Sada et al. (1983) proposed a model for carbonation of a slurry containing high concentration of suspended particles and assumed the bulk concentration of dissolved gas to fall to zero, Kojima et al. (1989) used very low concentrations of the suspended solid particles and hence the dissolved gas concentration in the liquid bulk was assumed not to fall to zero. They measured the specific interfacial areas and volumetric mass-transfer coefficients and proposed a film-theory based model.

Wei et al. (1997) studied the effects of slurry concentration, gas flow rate and surfactant as an additive on the surface area (ranging from 10-70 m^2/g) and pore volume of precipitated calcium carbonate (PCC) obtained by injecting carbon-dioxide gas through a suspension of hydrated lime. They observed substantially higher reactivity of PCC towards sulfur dioxide which were correlated to the surface area and pore volume of the particles.

Wet process using lean carbon-dioxide gas

Juvekar and Sharma (1973) studied the absorption of carbon-dioxide gas *from a gaseous mixture* into lime slurry in a bubble column and in a mechanically agitated reactor. The authors reanalyzed the mechanism of carbonation reaction reported in literature and proposed a film model. They concluded that the reaction is liquid-film controlled and not gas-film controlled as it was claimed earlier by Morris and Woodburn (1967).

Sada et al. (1983) studied absorption of 5 volume-percent carbon dioxide from its mixture with nitrogen in a concentrated slurry of calcium hydroxide in a bubble column. They determined the volumetric mass-transfer coefficient and effective interfacial area experimentally. Maximum rate of absorption was found at the calcium-hydroxide concentration of about three weight percent.

Capuder and Koloini (1984) measured the gas hold-up and interfacial area in a bubble column for carbonation of hydrated-lime slurry using lean carbon-dioxide gas. They found gas hold-up and interfacial area to decrease substantially with an increase in the

concentration of solids in the suspension. The three-phase system was considered as a two-phase system and the slurry a non-Newtonian fluid. The existing correlations for Newtonian fluids were modified to obtain new correlations and the same were found to agree well with their experimental data. Concentration of CO_2 in the inlet gas mixture was 5-10% by volume for carbonation of 5 % $Ca(OH)_2$ suspension. They proposed the following correlation for interfacial area estimation:

$$aD = 1.67 \left(\frac{gD^2 \rho_l}{\sigma} \right)^{0.5} \left(\frac{gD^3 \rho_l^2}{\eta_{eff}^2} \right)^{0.021} \varepsilon^{1.13}$$ (2.2)

In equation (2.2), a is the interfacial area, m²/m³; D is the vessel diameter, m; ρ_l, the density of liquid suspension; ε, the gas hold-up; σ, the surface tension of liquid. η_{eff} is the effective viscosity of slurry, expressed by the following relation:

$$\eta_{eff} = K \left(40 V_G \right)^{n-1}$$ (2.3)

K and n in eqn. (2.3) are constants.

2.1.2 Dry process

Using a dry process, Shih et al. (1999) studied kinetics of the reaction of calcium hydroxide powder with carbon-dioxide gas admixed with water vapor and nitrogen at low temperature (60-90˚C). The gaseous mixture was passed through a perforated quartz sample pan in which hydrated lime powder was kept dispersed in quartz wool. Effects of particle size, relative humidity, BET surface area, temperature of gas and carbon-dioxide concentration in the feed gas were studied. Importantly, the reaction was found to occur only above a critical humidity of eight percent. They assumed, in their kinetic model that the rate was controlled by surface reaction and that the observed decrease in the reaction rate was due to surface coverage by the product layer.

2.1.3 Semi-dry process

Semi-dry process using pure carbon-dioxide gas

Chen et al. (2000) developed "High Gravity Reactive Precipitation (HGRP)" process for the synthesis of nanoparticles of $CaCO_3$ for high volume production at low cost.

Acceleration higher than the gravitational acceleration on earth (High Gravity) was generated by rotating the packed bed reactor. $Ca(OH)_2$ slurry was pumped to the top of the packed bed and the $Ca(OH)_2/CaCO_3$ slurry was recirculated till completion of carbonation reaction (pH = 7). They controlled the size of $CaCO_3$ particles in the size range 17-36 nm by changing the levels of high gravity, concentration of lime in the suspension and flow rate of carbon-dioxide gas. The initial concentration of $Ca(OH)_2$ was changed from 34.5 to 84.0 kg/m^3. There is however no mention of the initial particle size of $Ca(OH)_2$ in the feed slurry.

Semi-dry process using lean carbon-dioxide gas

Nakazato et al. (2002) developed a "Powder-Particle Spouted Bed (PPSB)" for the production of $CaCO_3$. Coarse particles with films of $Ca(OH)_2$ slurry on their surfaces were fluidized with hot gas containing CO_2. Fine particles of $CaCO_3$ formed got dried and detached from the surface of larger particles. Average size of $CaCO_3$ particles produced was around 1 *μm*. They studied the effects of superficial velocity of gas, static bed height (before start of fluidization) of coarse particles, concentration of carbon-dioxide gas in the feed gas on the conversion of calcium hydroxide and that of slurry concentration on the average particle-size of product.

2.2 Hydrodynamics of gas-liquid and gas-liquid-solid bubble column reactors: flow regimes

Bubble diameter (d_{b0}), the most important of the hydrodynamic parameters in a bubble column contactor, strongly affects the values of the mass transfer parameters, viz., mass transfer coefficient (k_l), specific gas-liquid interfacial area (a_b), residence time of gas in the column etc., and therefore governs its mass transfer performance (Deshpande et al., 1995; Kantarci, et al., 2005; Mena et al., 2005; Gourich et al., 2006; Lemoine et al., 2008). Bubble diameter, d_{b0}, in turn depends on the flow regimes in a bubble column contactor. While gas bubbles are of uniform size in a particular flow regime, there exists a wide distribution of bubble size in the other and the specific interfacial area is therefore calculated accordingly depending on the flow regime. For the cases of wide distribution of bubble size, bubble residence time in the dispersion also varies widely. Flow regimes in a bubble column are typically divided into four

types and specified in terms of the superficial velocity of gas (V_G) and column
diameter (d_c) as shown in Table 2.1.

Table 2.1 Flow regimes in a bubble column.

S. N.	Flow regime	Range of V_G or d_c	Remarks
1.	Homogeneous or, bubbly flow	V_G <0.05 m/s, d_c is not important.gas is uniformly distributed using multi-orifice nozzles. Constant bubble residence time.	Uniform bubble size or having a very narrow distribution, uniform distribution (no radial and axial gradients) of gas holdup. Mass transfer parameters are determined on a single bubble size.
2.	Transition regime	V_G depends on d_c, h_d, d_0 and physical properties of gas and liquid.	Critical gas hold-up depends on h_d / d_c and d_0.
3.	Heterogeneous or churn-turbulent flow	V_G > 0.05 m/s, d_c > 0.15 m; residence time of bubbles of different size are different in the dispersion. Residence time of bubbles, etc are determined on the assumption of two distinct bubble classes.	Radial gas-holdup profile with maxima at the center (density of dispersion being less than that at the wall) creates strong circulation and back mixing. Coalescence and bubble break up generates wide distribution of bubbles size and ***the mass transfer rate is governed by the latter.***
4.	Slug flow	d_c < 0.15 m; V_G >0.05 m/s. With increasing gas velocity, large gas bubbles in the form of slugs are formed.	Wall effect is important. Large bubbles are stabilized by the column and mixing is poor. Strongly affects mass transfer parameters.

Meikap et al. (2002) used a multi-stage bubble column scrubber for removal of SO_2 from wet flue gas. They observed 100 percent removal efficiency by water without any additive. Bandopadhyaya and Biswas (2011) studied hydrodynamics of a tapered bubble column using an air-water two phase system. The gas flow rate was found to exert a subtle effect on pressure drop due to the dynamic pressure recovery resulting from the increase in flow area in the axial direction. For scrubbing of fly ash or SO_2, performance of tapered column was found to be better than the conventional columns. Sathe et al. (2013) reported the characterization of turbulence in both the homogeneous and heterogeneous regimes of operation in a rectangular bubble column using particle image velocimetry (PIV) measurements.

2.3 Foam-bed reactors

A foam-bed reactor is known to offer favorable conditions, considered to be important for a gas-liquid/ gas-liquid-solid mass transfer device. These include high gas hold-up, long contact time, large gas-liquid interfacial area and low to moderate pressure drops. A comparison of a foam-bed reactor with other gas-liquid reactors in respect of the above parameters is presented in Table 2.2. A surface-active agent is usually added in small concentration to the liquid in foam reactors for the generation of stable foam. Therefore, a foam-bed reactor is particularly suitable when the solvent containing the surfactant is recycled back to the reactor so that pollution of water caused by its drainage to public sewer and the cost of surfactant used is minimized. This minimizes the need for fresh water too. Gas absorption with a precipitation reaction, particularly carbonation of hydrated lime using lean carbon-dioxide gas, is a good example of such a reaction and can be conveniently carried out in a foam-bed reactor. The solution containing the surfactant and unreacted gas can be recycled back to the reactor after separation of the product solid. The other advantages derived from such a process are that hydrated lime in slurry being highly sticky, presence of surfactant protects the equipment from fouling and cleaning of the equipment becomes easier. A foam-bed reactor has also been reported to be beneficial for the treatment of large quantities of dust laden exhaust gases with a relatively small amount of liquid (Jackson, 1963).

Table 2.2 Comparison of physico-chemical parameters of a foam-bed reactor with few selected conventional reactors

Type of reactor	Sp.interfacial area, 'a_b',m^2/m^3	Time of contact, 't, t_c', s	Liquid hold-up, '$\bar{\varepsilon_l}$'	Pressure drop, 'Δp', (N/m^2)/m	'$k_l a_b$' (s^{-1}) x 10^2	System used for estimation of 'a_b' and '$k_l a_b$'
Foam-bed reactor	1105-2645 [Shah and Mahalingam, 1984]	20-55 [Shah and Mahalingam, 1984]	<0.06 [Shah and Mahalingam, 1984]	100-480 [Shah and Mahalingam, 1984]	4-23 [Shah and Mahalingam, 1984]	CO_2-Na_2CO_3+ $NaHCO_3$ and CO_2 -NaOH [Shah and Mahalingam, 1984]
Bubble column	100-1000 [Sharma and Danckwerts, 1970]	22-36 [b] [Akita and Yoshida, 1973], [Perry, 1987]	0.72-0.98 [Shih et.al., 1999]	626-2217 [Lee et. al., 1999]	3.5-16 [Mashelkar, 1970]	CO_2- NaOH/ KOH/ aq. amine and O_2 -dithionite soln. [Sharma and Danckwerts, 1970], $SO_3^=$ oxid[n] in aq. soln.[Mashelkar, 1970]
Packed column (counter)	20-350 [Sharma and Gupta, 1967]	2.9-7.9[b] [Perrin et. al., 2002]	0.08 [Westerterp et. al., 1963]	200-400 [Tsuge, et.al.,1987]	0.11-11.1 [Zurakowski and Glaser, 1965]	CO_2-NaOH/KOH/MEA, O_2-aq. dithionite [Sharma and Gupta, 1967],CO_2-NaOH [Zurakowski and Glaser, 1965]
Mechanic	314-1810	0.70-1.92[b]	0.78-0.93	-----------	7.17-25.3	O_2 desorption

ally agitated bubble reactor	[Robinson and Wilke, 1974], 70-2300 [Xie et. al., 2004]	[Calderbank,1958]	[Kawecki et. al.,1967]		[Robinson and Wilke, 1974]	and CO_2 absorption in KOH-K_2CO_3 [Robinson and Wilke, 1974], CO_2-NaOH in aq. glycerine [Xie et. al., 2004]

It is thought appropriate to document the important aspects of foams and brief review of its advantageous/ deleterious effects in process operations followed by the detailed review of all the important parameters governing the performance of a foam-bed reactor. A concise review of the mathematical models reported in the literature is also desired. These are presented below.

2.4 FOAMS

2.4.1 Importance of Foams in Industrial Process Operations

Neither pure liquids nor saturated solutions can be made to produce foams. By virtue of its large surface area and low density; optical, mechanical, thermal and surface properties, liquid foams are known to be used for numerous applications. These include gas absorption operations with/without chemical reactions, separation of valuable ores into concentrate and gangue, fire fighting, waste water treatment, instrumentation, e.g., soap-bubble meter, and chemical analysis. An example of the latter application is that CO_2 liberated by decomposition of $MgCO_3.(NH_4)_2CO_3.4H_2O$ with H_2SO_4 in presence of albumin is immobilized in foam. The gas volume is calculated through measurement of foam volume and that of the condensate obtained from it. On the other hand, in many industrial situations foams seriously affect process operations and reduce energy/ production efficiency substantially. Thus, while in some process operations specific surface active agents are added to the liquid phase in desired quantity to produce stable foams, in others, foams are broken mechanically or some anti-foaming agents added to the liquid to avoid its generation, else, to destroy it in order to maintain trouble free operation.

2.4.2 Foam rheology

Foams are heterogeneous dispersions and found to possess a yield stress (τ_0) and that the shear characteristics ($-dv_y/dx$ vs τ) are non-linear. During its upward flow through a pipe, the wall gets coated with a liquid rich layer which generates an effect of slip and the layer is idealized as a lubricating layer of pure liquid that separates the foam from the pipe wall. The yield stress and shear characteristics are reported to be strong functions of surface tension of the liquid and that of the foam bubble size. The following factors are considered (Heller and Kuntamukkulla, 1987; Calvert, J. R., 1990; Deshpande and Barigou, 2000) important in governing the flow behavior of foams and design of the relevant experiments: (i) ratio of mean bubble size to flow channel size, (ii) concentration of foamant (iii) foamant-channel wall interactions (slip, adsorption etc) (iv) quality of foam (volume fraction of dispersed phase) (v) physico-chemical properties of foamant (vi) size distribution of bubbles (vii) absolute pressure and (viii) properties of the two fluid phases.

2.4.3 Foam generation: Excess concentration of surface active substances & work required

Excess Concentration

The excess concentration of soluble substances that have a strong tendency to concentrate at the surface layer, reduces the surface tension of water. It is quantitatively expressed by the Gibbs' adsorption isotherm

$$E_{cs} = \left(\frac{-C}{RT}\right)\left(\frac{d\gamma}{dc}\right) \tag{2.4}$$

Where, E_{cs} is the excess concentration at the surface, C is the bulk concentration of solute and $d\gamma/dc$ is the change of surface tension with concentration of solute.

Work required for foam generation

To create foam, work (W) is needed to increase the surface area (ΔA):

$$W = (\gamma(\Delta A)) \tag{2.5}$$

Where, γ is the surface tension of the liquid.

Excess pressure in a foam bubble

Gas is confined in a bubble under a pressure greater than that outside and described by the thermodynamic equation

$$\Delta P = \frac{2\gamma}{r_{b0}}$$

(2.6)

Where, ΔP is the excess pressure, γ is the surface tension of the liquid in the bubble wall and r_{b0} is the radius of the bubble. The pressure is therefore inversely proportional to the bubble size. In a foam matrix, where γ is the same for every bubble, the gas inside the smaller bubbles is at a higher pressure than the gas inside the larger bubbles. When the bubble wall becomes substantially thin, say through drainage and become permeable, the gas from the smaller bubbles diffuses into adjacent larger bubbles to equalize the pressure.

2.4.4 Foam stabilization and foam breaking

A foam consists of spherical or polyhedral cells each containing a gas at an excess pressure corresponding to the radius of curvature of its equivalent sphere (Nishioka and Ross, 1981).

Foam instability is caused by two major reasons, drainage of liquid from the lamellae and the other by inter bubble diffusion of gas resulting in the expansion of larger bubbles at the expense of the smaller ones present in the foam. Foam instability is also observed to increase over a narrow range of increase in temperature possibly due to increase in drainage rate which may be related to variation in surface viscosity and surface tension. At higher temperatures, rate of increase in instability has been found to be smaller.

Foam stability is enhanced by adding a water insoluble co-surfactant that results in an increase of surface viscosity and surface elasticity reducing both the rate of drainage and rate of inter bubble diffusion. It has also been reported that addition of water-soluble polymers, e.g., 0.75 wt% sodium carboxy methyl cellulose (SCMC) enhances foam stability by about 10 fold (Sarma et al., 1987; Pradhan et al., 1990). The drainage rate is retarded due to the increase in bulk viscosity of liquid phase while the

gas diffusion rate is retarded due to decrease in diffusivity and solubility of gas in the liquid phase.

Foam stability is measured by (i) static drainage (ii) surface decay (iii) half life of foam and (iv) half life of drainage. Ross-Miles method, Bikerman method, photographic technique etc.

Several steps to increase foam stability have been proposed (Perry and Green, 1987): (i) reduction of liquid surface tension, ii) maintaining high lamella thickness through use of high liquid to gas ratio, iii) increasing surface concentration of foaming agent, iv) preventing liquid evaporation, v) increase of bulk-liquid viscosity, and vi) increase of surface viscosity. Higher superficial velocity of gas, presence of certain finely divided solid particles increase foam stability through reduction of film drainage. When foam is generated from a surfactant solution using moderate superficial velocity of gas, the shape of the bubbles formed is idealized as pentagonal dodecahedral. Gas bubbles in the foam column are packed in such a way that three pentagonal faces meet along an edge at an angle of approximately 120° between any two films. *These edges are called Plateau borders.* The Plateau borders form a network. Plateau borders being curved with higher cross-sectional area than those of the liquid films, liquid drains from the films into the Plateau borders because of capillary force from where it drains down due to gravity through the network of Plateau borders.

Stabilizing factor: The Marangoni effect

Any stress that tends to create local thinning and stretching of the films surrounding a foam bubble must rapidly produce counter balanced restoring forces during the initial displacement of the material of the film for a foam bubble to be stable. This elasticity exists in a film if a surface active solute is present in it. It is postulated that due to stretching of the film, local surface area as well as local surface tension increases and a gradient of tension is set up. Liquid from the thicker regions along with the surface elements flows to the thinned spot. The increase in surface tension with time is known as the ***Marangoni effect*** (Rosen, M. J., 1978), while its increase with concentration of surfactant as the ***Gibbs effect***.

On a foam bubble, the liquid film is flat at one place and curved convexly at the Plateau border. Cross-sectional area at the curved region is much larger than that at

the flat region. The pressure being lower at the higher cross-sectional area than that at the lower, the convex curvature creates a capillary force that sucks liquid out of the flat part of the foam films. This **internal flow** is called **Laplace effects**. Thus, internal liquid flows constantly from the flatter (films) to the more curved parts (Plateau borders) of the films. Thereafter, liquid from the Plateau borders drains out by gravity. Sometimes Marangoni effect is also explained in the following way. As the liquid flows, the films are stretched and new surface of higher tension is created. A counter flow **across the surface** is generated to restore the thinned out parts of the films. This is called **Marangoni effect**. Pure liquids cannot foam because of the absence of a Marangoni effect. The primary stabilizing factor in foam is the resilience of the film provided by the Managoni effect.
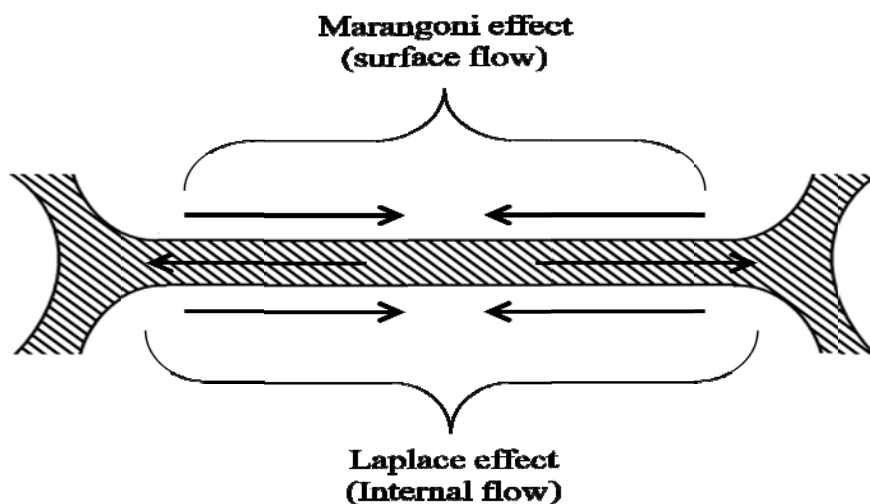
Figure 2.1 Marangoni effect

2.4.5 Stabilization of foams made for diverse applications

Diverse applications necessitate foams of varied stability. Foams for ore flotation or other foam flotation operations need to be moderately stable, these being required to be condensed later for separating the ore. Moderately stable foams are also required for tall slurry-foam columns used as foam reactors for increased rate of dissolution of gas and consequent high rate of reaction. Fire fighting foams, one variant of which is

produced from sodium bicarbonate, aluminum sulfate along with foaming agent, need to be highly stable. Thermal insulation of fuel storage tanks for protection from radiation due to fires, and, lubrication of airport runways for emergency landing etc, medium to highly stable foams are desired.

Certain surface active additives, when *added in small quantity to solution of another surfactant*, the elasticity of surface films increases. The foam stability is thereby increased and the surfactant causing enhancement of foam stability is called a co-surfactant. The most effective co-surfactants added to a surfactant solution for increasing its stability are generally water insoluble, polar components with long straight chain hydrocarbon groups closely resembling the hydrophobic group of the surfactant and, that lower the CMC of the surfactant solution considerably. The order of ability to stabilize foams of various types of anionic surfactants has been reported (Sawyer and Fowkes, 195*8*) as: primary alkyl sulfates> 2-n-alkanesulfonates> secondary alkyl sulfates> n-alkyl benzene sulfonates > branched-chain alkyl benzene sulfonates. A somewhat different explanation of foam stability put forward by many investigators is as follows: surfactant molecules that are widely spaced in the surface because of the mutual repulsion of the oriented polar heads make the films mechanically weak and non-viscous. Liquid, therefore, drains rapidly from the lamellae rendering it unstable. It is believed that the molecules of co-surfactant (Table 2.3) penetrate into the surface film of the existing surfactant molecules, orient themselves among these members and form a close packed layer with higher surface viscosity. This reduces drainage rate and increases foam stability. On the other hand, substances that decrease film elasticity through an increase in the rate of attainment of surface tension equilibrium are known to be foam inhibitors.

Table 2.3 Typical **surfactant and co-surfactant pairs**

Surfactant	Co-surfactant	Reference
Sodium dodecyl sulphate	(i) Lauryl alcohol	Sharma et al. (1988)
Dodecyl Benzene sulfonate	N,N- bis (hydroxyethyl) lauramide	Rosen, M. J. (1978)
	N,N dimethyl dodecyl amine oxide	
Potasium laurate	Lauric acid	

2.4.6. Foam breaking

Various thermal, mechanical, electrical and chemical methods have been adopted for destroying foam during process operations. Heating the foam along with the application of mechanical force with a revolving paddle has been found to be very useful. Heating foams above a critical temperature substantially reduces the surface viscosity of the film and the drainage rate is thereby increased. Foam bubbles get expanded and strain is incorporated, increased evaporation rate makes the films thinner. Combined effect of all these contribute to foam breakage.

Chemical de-foaming techniques are of two types. In one method, a substance that stabilize foam is desorbed from the interface by displacing it with a more surface-active but non-stabilizing compound. For example, foams stabilized with an ionic surfactant say, SDS, can be broken by the addition of silicone oil in ppm level. In the other method, chemical changes in the absorption layer are brought about leading to formation of a non-stabilizing structure.

2.4.7 Froths

Froth bubbles are spherical and small in size and liquid content in froth≈0.5 (Valentine, 1967). The gas–phase controlled mass transfer in a co-current froth flow was investigated by Huess et al. (1965) by absorbing ammonia in water flowing in a 4-ft.-long Lucite test section of 1-in. I. D. Under the stated conditions of their experiments, the bubble could be regarded as spherical. They explained the absorption data by using the model of an unsteady state mass transfer in a stagnant sphere. Average bubble size calculated from the mass transfer data using this model were found to be in agreement with a prediction made from the data of James and Silberman (1956), the only data then available on bubble size and distribution in froth flow.

Mutriskov et al. (1975) reported the absorption of CO_2 in sodium hydroxide solution under frothing conditions. Effects of initial concentration of NaOH, flow rate of feed gas, temperature of feed solution and foam expansion ratio on rate of reaction and mass-transfer coefficient were studied. They observed the mass transfer coefficient to increase with an increase in the concentration of sodium hydroxide. The authors also observed the mass transfer coefficient to decrease with an increase in the gas flow

rate, the opposite trend was, however, reported by Bogatykh (1964), Zurakowski and Glaser (1965), Shah and Mahalingam (1984).

An empirical correlation was proposed by Manvelyan et al. (1967a) for the degree of absorption of CO_2 as a function of gas velocity and froth height on absorption of sodium metasilicate in a column of froth in a sieve-tray column.

Galkina and Gertsen (1969) studied the kinetics of absorption of hydrogen fluoride in water from a dilute gaseous mixture in a froth absorber. The authors obtained a very high degree of separation which under optimum conditions reached 98 percent. The observed value of the mass transfer coefficient was 14500 m/hr. They observed the optimum diameter of orifices on the grid plate to be 0.003 m and pitch 0.006 m. For very high separation efficiency, recirculation of liquid was recommended, provided the concentration of HF in the sorbate does not exceed 1 percent.

Reddy and Bhaskarwar (2000) presented a brief account of the differences between foams and froths with reference to shape and size of bubbles as demonstrated by Rennie and Evans (1962). The authors (Reddy and Bhaskarwar, 2000) developed a model to predict conversion in a froth-bed reactor. The most important difference in formulating the model of a froth-bed reactor and that of a foam-bed reactor was that the foam bubbles were regular pentagonal dodecahedral in shape whereas the froth bubbles were assumed to be spherical. For the mass balance, the diffusion equation in the froth-bed reactor model was written in terms of spherical coordinates while that for the foam-bed model, Cartesian coordinate was used. For a froth bubble, the volume of gas pocket available for absorption was taken as the bubble volume, V_b, whereas for a single pentagonal film of a foam bubble the volume of gas pocket available was assumed to be $V_b/12$. Model predictions were found to agree well with the experimental data of Bhaskarwar and Kumar (1984) for oxidation of sodium sulfide in a foam-bed reactor.

2.5 Foam separations

Differences in surface activity of components, in very dilute aqueous solutions/ suspensions, form the basis of foam separation of the components of a solution. On the other hand, substantial difference in the wetting ability, a surface chemical property of the solids, is the basis of separation of mineral ores by foam flotation

which are not naturally floatable. While frothers produce stable foam bubbles, modifiers are used to make a mineral surface amenable to collector coating, control pH, assist in selectivity or stop unwanted materials from floating. Na_2S, strong acids and bases, calcium cyanide, sodium ferrocyanide, etc are some examples of modifiers, choices being dependent on the specific cases. Promoters, also variously known as collectors, provide a water-repellant air-avid coating that adheres to an air bubble. For flotation of metallic sulfides, xanthates and dithiophosphates (Perry and Green, 1987) are the commonly used collectors.

Foam separations are broadly classified into two types: foam fractionation and foam flotation. The latter in turn is sub-divided into ore flotation, macro flotation, micro flotation, precipitate flotation, ion flotation, molecular flotation and adsorbing colloid flotation. While foam fractionation, in general, refers to the removal of dissolved material from a solution, flotation refers to the removal of solid particulate material. Ore flotation being not a transfer process on molecular level, details of this is not included in this work.

2.5.1 Foam fractionation

Concentrating a particular ingredient from a solution containing two or more components into the foams produced by the use of a surface active material which is already present in the solution or added for the purpose is termed as foam fractionation. This separation is based on the differences in surface activity of the components to be separated. This adsorptive bubble separation process has the advantage that no extraneous solvent is added, instead only air or an inert gas when there remains the possibility of oxidative degradation, is used. This is useful for the separation of surfactants, proteins from fermentation broths, enzymes, ions from metal extraction units etc and especially useful for separation of substances sensitive to heat and extreme pH values.

2.5.2 Foam flotation: Foam flotation being not a molecular phenomena, its detailed discussion is not included here.

2.6 Gas absorption in foam-bed reactors

During the past three decades, quite a few foam reactor models have been reported in the literature. These models provide an insight into the various aspects of gas

absorption with/ without chemical reaction closely approximating the practical situation in a foam column. It is however observed that the reactions considered are primarily those with zero- and pseudo-first order reaction kinetics. Various systems for which models have been reported are: NaOH-CO_2 (Biswas and Kumar, 1981); O_2-Na_2S (Bhaskarwar and Kumar, 1984); BaS-CO_2 (Gaikwad et al., 2010); O_2-$Na_2S_2O_6$ (Varshney et al., 2003); $Ca(OH)_2$-CO_2 (Jana and Bhaskarwar, 2010); etc. In these studies, CTAB, HDTMAB, SDS, Triton X-100 and Teepol were almost exclusively used for the generation of stable foam. *The reported models are found to be much involved but interesting to the same extent as well*. A foam reactor invariably consists of two parts: a storage section containing a shallow pool of liquid with a surfactant dissolved in it and a tall column of foam above the storage section, called the foam section. The storage section is assumed to be well stirred with the rising gas bubbles and the column of foam in the foam section to be in plug flow. As the gas bubbles exit from the storage section, these are transformed into foam bubbles. Concentration of absorbing/ reacting species is therefore taken as uniform at a given any instant of time in the storage section but in the foam section it is different at different locations in the column due to incessant mass transfer from gas contained within the rising bubble to the surrounding liquid film. For determination of unsteady state concentration distribution of the reacting species *A* as a function of time and position within a foam film, its concentration in the liquid contained in a foam film leaving the storage section, same as that entering the foam section, is taken as the initial (at *t*=0) concentration of the species and no flux through the central plane of the film, the latter being symmetrical and same interfacial concentration of *A* on either side of the film. Mass transfer and reaction rates are therefore written accordingly for the two sections. For slow to moderately fast reactions, conversion being small in a foam reactor, it is generally operated in a semi-batch mode and for obtaining high conversions, foam reactors are required to be operated in series (Jana and Bhaskarwar, 2011).

A model for gas absorption in a froth-bed reactor was developed by Reddy and Bhaskarwar (2000) to predict conversion of Na_2S. The froth bubbles were assumed to be spherical in contrast to the regular pentagonal dodecahedral shape conventionally assumed for a foam bubble. For the mass-balance, the diffusion equation was accordingly written in terms of spherical coordinates instead of the Cartesian coordinates used for writing the foam reactor model.

2.6.1 Hydrodynamic and physico-chemical parameters

One of the major motivations for research in the areas of foams being to avoid its formation in some of the process operations, while in some others the purpose is to stabilize the foam. This involved in-depth research on various aspects of foam which include its structure, physico-chemical properties, hydrodynamics, stability considerations as well as its usefulness in applications of mass transfer with or without chemical reaction.

Semi-theoretical correlations for the estimation of hydrodynamic, physico-chemical and other parameters in foam columns have been proposed by a large number of investigators. The pertinent parameters include liquid holdup, pressure drop, specific interfacial area, variation of foam height with surfactant concentration, shape and size distribution of bubbles in the foam column, etc. A brief discussion of these aspects is narrated in the following paragraphs.

Rate of physical absorption of gas, or, that of gas absorption with a finite rate of chemical reaction, increases substantially with an increase in the liquid holdup in the foam column. Liquid holdup increases with the superficial velocity of gas and viscosity of liquid while it reduces with an increase of the foam height, density of liquid and bubble diameter. Liquid hold-up values in foam columns have been studied by a number of investigators (Biswas and Kumar, 1981; Houghton et al., 1957; Rubin et al., 1967; Hoffer and Rubin, 1969; Shih and Lemlich, 1971; Hartland and Barber, 1974; Steiner et al, 1977) and diverse techniques have been used for its measurements.

2.6.1.1 Drainage rate

Drainage rate is one of the parameters governing the stability of foams. Higher drainage rate reduces foam height. It, therefore, depends on all such parameters that stabilize foams or increase foam height. While in most of the process operations in which foam is a desired substance, only low to moderately stable foams are useful. In a foam column, liquid from the films flows into the plateau borders from where it flows down by gravity. The other important parameter of foam stability is the rate at which the body of the foam breaks down. In the case of very unstable foams, most of the liquid drainage is due to the liquid released by the rupture of bubbles. On the other hand, stable foam bubbles rupture only after most of the gravity drainage of the liquid has taken place and after the films have become critically thin. In case the of mass-

transfer operations, maintaining larger thickness of liquid films through reduction of drainage rate over the gas-liquid contact period is important as this enhances the rate of mass transfer. Extensive work, both theoretical and experimental, on foam drainage phenomena has been reported in the literature. Some of the authors (Miles et al., 1945) have considered the foam-drainage to be similar to that from a series of capillary tubes while others considered the drainage to be like that of the liquid confined between two parallel plates. The separation between the plates reduces with the progress of drainage. Kruglyakov and Taube (1965) proposed a simple empirical correlation for estimation of the drainage rate in absence of bubble breakage:

$$\frac{V_d}{V_{f0}} = 1 - e^{-c_1 t_d} \qquad (2.7)$$

, where c_1 is an empirical constant. V_d and V_{f0} are the liquid drained in time t_d and the initial total volume of liquid contained in foam, respectively.

Miles et al. (1945) proposed an equation with three constants. It takes into account the height of the liquid in the capillary tube in excess of the equilibrium capillary height and the viscosity of the liquid:

$$(V_{f0} - V_d) - c_2 . \log(V_{f0} - V_d) + c_3 = c_4 . t_d \qquad (2.8)$$

Jacobi et al. (1956) proposed an equation with two constants in the form:

$$V_d = \frac{2c_6}{c_5}[1 - (c_5 t_d + 1)^{-0.5}] \qquad (2.9)$$

It is observed that when $t_d \to \infty$, $(c_5 t_d + 1)^{-0.5} = 0$ and $V_d = V_{f0}$. Thus, $\frac{2c_6}{c_5} = V_{f0}$

The above equation, therefore, reduces to the one-parameter equation as:

$$V_d = V_{f0}[1 - (c_5 t_d + 1)^{-0.5}] \qquad (2.10)$$

Many more articles have been published in literature addressing the drainage rates from foam (Brady and Ross, 1944; Haas and Johnson, 1967; Shih and Lemlich, 1971, to name a few).

Bikerman (1956) proposed correlations for estimation of film thickness, '2*a*', at a depth H_T from the top of the foam column after time t_d seconds of the start of drainage

$$2a = 4\mu_l H_T / g\rho_l\, t_d \qquad\qquad (2.11)$$

This equation shows that film thickness reduces from bottom to the top of a foam column due to drainage of liquid.

Haas and Johnson (1967) presented a model and experimental results for drainage of solution between foam bubbles. They concluded from their study that the drainage of solution between foam bubbles is principally through the Plateau borders. The relationships among the experimental variables: superficial liquid velocity, superficial gas velocity, foam bubble diameter, fractional volume of liquid in the foam, time of operation and configuration of reactor, were found to be in excellent agreement with the model predictions reported by the authors.

2.6.1.2 Pressure drop

 Pressure drop over foam columns have been measured by various investigators for flow through tubes of different lengths and made of different materials (Calvert, J. R., 1990; Thondavadi and Lemlich, 1985). Foam was generated using solutions and slurries made of coal, sand and surfactants. Measured values of pressure drop are reported to be low to medium and considered to be an advantage for foam reactors over other reactors. Correlations for its estimation has been proposed by a number researchers (Jackson, J., 1963; Hoffer and Rubin, 1969; Barigou and Davidson, 1996; Deshpande and Barigou, 2000).

Metzner and Brown (1956) measured the pressure drop per unit height of foam column as a function of gas flow rate. They observed two distinct regions at low gas rates in which pressure drop decreases with an increase in the gas rate, and, a region at higher gas flow rates in which the pressure drop increases with an increase in the flow rate of gas. These two regions were marked as quiet and turbulent foaming regions. The bubbles were observed to be uniformly distributed in the quiet region and moved up the column smoothly. However, in the turbulent region, considerable swirling of the foam was observed. In the quiet region, the amount of gas in the foam increased

with an increase in the gas rate and the foam was recognized as dry foam and hence the foam density decreased. In the turbulent region, the mechanical action acted upon the gas to break up the foam progressively became more efficient and rupture of groups of bubbles increased substantially with an increase in the gas flow rate. This caused violent swirling and breakup of foams and higher density of foam.

Mersmann (1962) studied pressure drop for flow of air through the liquid layer on a sieve tray. According to him, the total pressure drop comprises of three parts: drop in pressure required to overcome the resistance of the dry plate, the hydraulic pressure of the liquid and that required to produce bubbles.

A venturi type scrubber was used by Jackson (1963) for cleaning of dust-laden gases in foam column. Highly soluble gases, e.g., NH_3, HCl etc. and CO_2 were used for generation of stable foam column. Correlations were proposed for estimation of pressure drop in the foam column:

Dry plate pressure drop (Δp_1):

$$\Delta p_1 = 1.45 k_c \left(\rho_G u_0^2 / 2g \right) \tag{2.12}$$

where k_c is a coefficient, a function of plate thickness; u_0 = gas velocity through orifices, m/s; ρ_G = gas density, kg/m^3.

Foam column pressure drop (Δp_2):

$$\Delta p_2 = 0.85 h_0 \rho_l + 0.2 \sigma_l \left(10^4 \right) \tag{2.13}$$

where ρ_l = liquid density, kg/m^3

Hoffer and Rubin (1969) studied pressure drop for flow of foam through a vertical column operated under steady state conditions. The plots of static pressure vs foam height were found to produce a region of varying slope at low foam heights which was attributed to the fast variation in the liquid holdup in this region of the tower and a flat velocity profile at higher heights of the column, liquid holdup remaining almost constant in this region.

Thondavadi and Lemlich (1985) measured pressure drop for flow of foam made of aqueous solutions of hexadecyl dimethyl ammonium bromide through acrylic and galvanized steel pipes. Significant variation in the pressure drop was observed as the Sauter mean bubble diameter was varied from 0.1×10^{-3} m to 1×10^{-3} m and the foam quality from 0.88 to 0.99. Use of slurry made from fine coal and sand particles up to 30 weight percent produced similar results.

Calvert (1990) reported the results of pressure drop measurement for flow of 3% aqueous solution of a detergent through polyethylene tubing of different lengths and diameters. The measured values of the pressure drop were found to be about 92 times larger than that calculated using the Lockhart- Martinelli two-phase flow pressure drop correlation. As the foam-flow rate was varied from 1.67×10^{-6} to 1.0×10^{-4} m^3/s, pressure-drop values were observed to vary from 22 to 160 kPa.

2.6.1.3 Specific interfacial area

Specific interfacial area, a very useful property of foams, is the most important reason for high rates of mass transfer in foam reactors. This is inversely proportional to the bubble sizes and in a foam column its value lies in the range 1105 to 2645 m^2 m^{-3}. This parameter has been studied and reported by several investigators (Steiner et al., 1977; Rodionov et al., 1966; Gestrich and Krauss, 1976). Efficiency of bubble separation processes and mass transfer with/ without chemical reaction increases with an increase in the interfacial area. Large specific interfacial area with small foam bubbles can be produced using high gas velocity and with small diameter orifices on gas distributor plates.

$$a_b = \left(6\overline{\varepsilon_G} \right) / d_{b0} \qquad (2.14)$$

Where,

$$\overline{\varepsilon_G} = 1 - \left(\rho_f \big/ \rho_l \right)$$

Gestrich and Krauss (1976) used 223 sets of experimental data from literature to obtain correlations for specific interfacial area. It was found to be proportional to the average gas holdup and $(h_0/d_c)^{-0.3}$. They also analyzed the applicability of the other correlations on foams available in the literature.

Shah and Mahalingam (1984) obtained interfacial area in a foam-bed reactor experimentally. It was found to depend strongly on the mesh size but independent of the gas velocity in the range they studied.

Stangle and Mahalingam (1990) determined specific solid-liquid interfacial area, a_p, and gas-liquid interfacial area, a_b, in a slurry foam column. a_p was calculated using the relation $a_p = \dfrac{6w}{\rho_B d_p}$, where w is the total mass of hydrated lime present as particles per unit volume of slurry, and ρ_B and d_p the density of hydrated lime and average diameter of lime particles present in slurry, respectively. Initial value of d_p in the slurry was determined by taking into account the decrease in size of the suspended particles in its saturated solution. The expression for a_p is obtained as follows:

$$a_p = \pi \, d_p^{\,2} \qquad\qquad\qquad\qquad 2.15\,(i)$$

$$v_p = \frac{w}{\rho_p} = \frac{\pi \, d_p^{\,3}}{6} = \frac{\left(\pi d_p^{\,2}\right) d_p}{6} = \frac{a_p d_p}{6} \qquad\qquad 2.15\,(ii)$$

Rearranging 2.15 (ii), one gets

$$w = \frac{a_p d_p \rho_p}{6} \qquad\qquad\qquad\qquad 2.15\,(iii)$$

Or,

$$a_p = \frac{6w}{d_p \rho_p} \qquad\qquad\qquad\qquad 2.15(iv)$$

For estimation of gas-liquid interfacial area, they measured the distribution of foam-bubble sizes using a photographic technique. For each size of wire mesh they used for generation of foam column, average foam-bubble size was obtained. Specific interfacial area was then obtained as, $a_b = \dfrac{6\bar{\varepsilon}_G}{d_s}$, where d_s = the Sauter mean bubble diameter. d_s was calculated using the relation

$$d_s = \frac{\displaystyle\sum_{j=1}^{n} N_j (d_{b_j})^3}{\displaystyle\sum_{j=1}^{n} N_j (d_{b_j})^2} \qquad\qquad\qquad\qquad (2.16)$$

, d_{b_j} = the average diameter of foam bubbles of the jth (j= 1 to n) size interval and N_j = the number of bubbles in this size interval.

The gas hold-up, $\bar{\varepsilon}_G$, in the foam column was determined using the relation

$$\bar{\varepsilon}_G = (E-1)/E \qquad\qquad (2.17)$$

, where E = foam-expansion ratio defined as the ratio of total volume of foam to the total volume of liquid in the foam.

2.6.1.4 Foam height

Foam height, in a gas-liquid or gas-liquid-solid reactor, is a measure of time of contact between the phases and that of the total gas-liquid interfacial area available for mass transfer in the column. Although foams are produced when a gas or a vapor flows through a liquid and its height normally fluctuates during process operations, a particular foam height can be maintained by breaking foams mechanically or chemically at the desired foam height. Foam column heights depend on the superficial velocity of gas, initial concentration of surface active agents and presence of certain finely divided solid particles, co-surfactants, electrolytes in the liquid or such other parameters that stabilize foams.

Mersmann (1962) measured foam height on sieve plates for pure and binary liquid mixtures as functions of gas flow rates, and, those of viscosity and surface tension of the liquid. While for pure liquid, foam height varied significantly with all these variables, for binary mixtures it was invariant to viscosity and surface tension of the liquid but affected due to accumulation of lower surface tension liquid at the surface.

Pozin et al (1964) studied the height of foam layers in sieve-plate and overflow type absorbers with gas (CO_2 and air) and liquid (monoethanol amine and water) in counter flow and cross flow patterns, respectively. The height of foam layer on sieve plate increased continuously with the gas and liquid flow rates. In the case of over flow plates, the height of foam layer decreased continuously with increasing air velocities and this decrease was more for monoethanol amine foam than with the water foam. They proposed correlations for calculation of initial height of foam layer for the two types of absorbers for different dimensions and types of plates, flow rates of gas etc.

Manvelyan et al. (1967b) studied the effects of initial height of liquid (h_0), superficial velocity of gas, temperature, liquid-feed rate and composition of solutions on the height of froth (H_f) formed in a 0.06 m diameter vertical column for carbonation of sodium-metasilicate solution using lean carbon-dioxide gas. The ranges of variables studied were: superficial velocity of gas: 0.5 to 2.0 m/s, H_f/h_0 : 2-10, concentration of sodium metasilicate solution 200-600 kg/m^{3}and initial height of liquid: 0.02-0.10 m. Empirical equations were proposed for estimation of H_f in terms of the above variables.

Grishina et al. (1971) studied the effects of initial height of liquid (h_0) and surface tension (σ_l) on the degree of foaming, viz., the height of foam/ initial height of liquid. Foam was generated by blowing air through surfactant solutions. They proposed a correlation for foam height for 0.0025 to 0.01 percent solution of sulfanol as,

$$H_f = 7.85 h_0^{0.12} \exp\left[-3.85 h_0 - 104\left(\sigma_l - 0.08\right)^2\right]$$
(2.18)

Dilman and Gazizulin (1984) proposed a correlation for estimation of foam height as functions of superficial velocity of gas and liquid flow rates for absorption of chlorine gas in monoethanol amine solution.

2.6.1.5 Shape and size distribution of bubbles

Structure of foams and measurement of foam bubble sizes have been studied and reported by many investigators (Calderbank and Rennie, 1962; Thomas et al., 1995; Lipping et al., 2003). These studies have proved useful in the theoretical investigation on foam drainage phenomena. It is reported that (Deshpande and Barigou, 2000) at low gas velocities foams form with a polyhedral structure while at substantially higher gas velocities foam bubbles formed are spherical in shape. Shapes of bubbles have been correlated with liquid content by Leonard and Lemlich (1965). Foams with high liquid content are called wet foams and possess spherical bubbles while polyhedral bubbles are formed with low liquid content when foams are termed as wet foams. With low to moderate viscosity liquids and also when foam bubble sizes are not very small, the foam bubbles at distances higher than about one bubble diameter above the liquid pool are polyhedral. These polyhedral bubbles have been idealized by a regular pentagonal dodecahedral shape (Figure 2.2 (a) and 2.2 (b)).
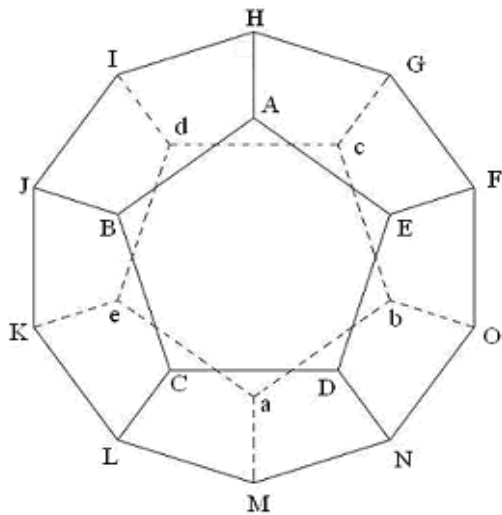
Figure 2.2 (a) An idealized pentagonal dodecahedral foam bubble
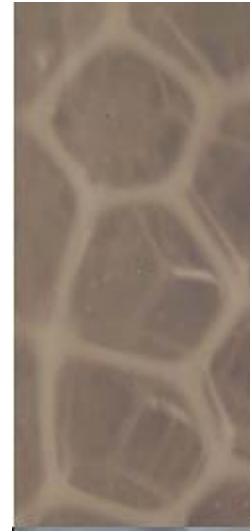
Figure 2.2 (b) Photograph of a set of three nos of pentagonal foam bubbles in a foam-bed reactor operated at low gas velocity

Shape and size distribution of bubbles in the foam columns have been studied by many investigators by photographic technique and image analysis (Calderbank and Rennie, 1962; Xie et al., 2004; Thomas et al., 1995). A large number of investigators have reported mathematical models of foam-bed reactors based on the pentagonal dodecahedral shape of foam bubbles (Biswas and Kumar, 1981; Bhaskarwar and Kumar, 1984; Jana and Bhaskarwar, 2010)**.**

Calderbank and Rennie (1962) measured Sauter mean bubble diameter of foam bubbles formed on sieve-plates having 1/8 in. diameter holes and produced using air and water in a rectangular perspex column. The range of superficial velocities of gas and liquid flows were 0.15 to 0.76 m/s and 0.015 to 0.6 m^3/s, respectively. Froth was formed at higher gas velocities. The bubbles were photographed and Sauter mean bubble diameters were estimated using the "pin-dropping technique". The bubble diameters estimated using the above method in the cellular-foam region were found to be much larger than those obtained from optical reflectivity and γ-ray transmission measurements.

Shah and Mahalingam (1984) experimentally determined the foam-bubble size using a photographic technique. For the three wire mesh sizes 20, 60, and 100 used by them,

the corresponding Sauter mean bubble diameters were found to be 5.4 x10^{-3} m, 2.85 x10^{-3} m and 2.2 x10^{-3} m, respectively.

Lipping et al. (2003) used a capillary probe fitted with photoelectric sensor to measure the variation of bubble-size distribution in a protein-foam fractionation column. It is reported that the size distributions of foam bubbles were affected by the column wall. The protein-concentration distribution along the cross-section of the column was found to be nearly constant during the steady-state operation of the column. It is indicative of the fact that the bubble-flow distribution attained a flat profile across the height of the column.

Xie et al. (2004) measured liquid hold-up and condensate of the overflowing foams in a vertical foam column and thus obtained the average size of foam bubbles. The experiments were performed with different orifice diameters, gas-flow rates and sodium dodecyl sulphate concentrations. They observed an increased coalescence of bubbles and a decreased flow rate of foam condensate with the use of smaller diameter orifices. They also performed image analysis to determine the size of foam bubbles in the column.

2.6.1.6 Liquid hold-up

Liquid hold-up in a foam column has been determined experimentally by different methods by various investigators, e.g., through measurement of pressure-drop data using a manometer connected to a foam column (Houghton et al., 1957); that of linear foam velocity and flow rate of foamate in a foam column (Rubin et al., 1967), collecting the foam overflowing through the column exit (Hoffer and Rubin, 1969), finding the electrical conductivity of foam using platinum electrodes inserted into the foam column at different foam heights (Shih and Lemlich, 1971); incorporating a radio-active tracer (^{22}NaCl) to the liquid and measuring the γ-radiation (Hartland and Barber, 1974); drawing foam through application of vacuum into a bulb from a given height of a foam column, and measurement of the volume of liquid after collapse of the foam (Biswas and Kumar, 1981), and using fixed γ-ray absorption densitometer (Steiner et al. 1977, Desai and Kumar,1983,1985).

Houghton et al. (1957) estimated liquid hold-up value in the foam column using the manometer readings collected for pressure drop measurement. Water, various organic

solvents and aqueous solutions along with nitrogen, oxygen, and carbon-dioxide gases were used for the generation of foam.

The following force-balance equation was used for estimation of liquid holdup:

$$\rho_f H_f g = \rho_m h_m g \qquad (2.19)$$

it follows that

$$\rho_f = \frac{\rho_m h_m}{H_f} \qquad (2.20)$$

where ρ_f and H_f are the mass density and height of the foam, and ρ_m and h_m are the mass density of the manometer liquid and the differential height in the manometer, respectively.

ρ_f can be taken as the liquid hold-up in the foam column as $\rho_G << \rho_l$. They found that the bubble diameter increased as the superficial gas velocity was increased. Foam columns were found to be more sensitive to the number, size, and distribution of pores in the gas-distributor plate than that observed in fluidized beds.

Ambulgekar et. al. (2004) calculated the liquid holdup by measuring the hydrostatic head of liquid contained in the foam as detected by a micro manometer and with the knowledge of foam height at different times of process operation. The foam density ρ_f is determined from equation (2.20) and (2.21) and is used for the calculation of liquid holdup.

$$\rho_f = \frac{h_m \rho_m}{H_f} \qquad (2.21)$$

Also $\rho_f = \overline{\varepsilon_l} \rho_l + \overline{\varepsilon_G} \rho_G \qquad (2.22)$

Since $\overline{\varepsilon_G} \rho_G <<< \overline{\varepsilon_l} \rho_l$

Therefore $\qquad \rho_f = \overline{\varepsilon_l} \rho_l \qquad (2.23)$

So liquid hold up

$$\overline{\varepsilon_l} = \frac{\rho_f}{\rho_l} \qquad (2.24)$$

2.6.1.7 Mass transfer coefficient

Mass-transfer coefficient values are reported to be higher in a foam-bed reactor over that in a bubble column reactor under otherwise identical operating conditions. Values of this parameter has been reported to be dependent on initial heights of liquid in the storage section, height of foam in the column, superficial velocity of gas, radius of foam bubbles and viscosities of gas and liquid. Details of correlations proposed by various investigators are enumerated below.

Helsby and Birt (1955) observed larger values of the overall gas phase mass-transfer coefficient, K_{Gab}, in a foam reactor than in a conventional packed tower and extent of absorption in ¾ cu. ft of foam was found to be more than that in a 4 cu. ft packed volume. These authors have demonstrated that a foam column is more efficient than a conventional packed tower for the absorption of CO_2 gas from its mixture with air in monoethanol amine (MEA) and caustic soda (NaOH). For the same system, NaOH-CO_2, a different group of investigators (Maminov and Mutriskov, 1969) proposed a correlation for liquid phase mass-transfer coefficient in a continuously operated foam column:

$$k_l = 5.35x10^3 H_f^{-0.7} \left[\frac{D_A.W_r}{r_{b0}} \right]^{0.7} \left(1 + \left(\frac{\mu_G}{\mu_l} \right) \right)^{-0.5} \tag{2.25}$$

Where, W_r is the difference in flow rates of gas and liquid, r_{b0} the bubble radius and H_f the foam height.

CO_2 absorption in aqueous glycerol and cane-sugar solutions in a foam column was reported by Onda et al. (1969) and that in sodium hydroxide solution by Mutriskov et al. (1964). While the former group of authors proposed correlations for the temperature dependence of mass-transfer coefficient, the latter group obtained the relation, $Sh = 0.7 \, Re^{0.9} Sc^{0.5}$ for estimation of the mass-transfer coefficient, k_l. The values of volumetric mass-transfer coefficients in a foam column were found to be several times larger than those in a packed column, but smaller than those in a bubble column.

Rukhadze et al. (1990) studied CO_2 absorption in barium-sulfide solution in a continuous foam-bed reactor for precipitation of barium carbonate. They determined optimum conditions for maximum yield of $BaCO_3$ (99.9%). This was obtained for a

BaS concentration of 46 kg/m^3, carbon dioxide concentration of 57 volume percent, temperature 60 °C, and solution-feed rate of 1.67 x 10^{-7} m^3/s (10 ml/min). Desorption of CO_2, a liquid-phase controlled process, from stable aqueous foams using water-saturated air has also been reported (Weissman and Calvert, 1965) with a critical analysis of the experimental data.

Shabel'nikov and Mukhlenov (1963) reported absorption of SO_2 and Cl_2, the two gases moderately soluble in water, from their mixtures with air at 16 °C and 7 °C, respectively. The authors studied the effects of various operating parameters viz. foam height (H_f), initial height of liquid in the storage section (h_0), superficial velocity of gas (V_G), flowrate of liquid (Q) and proposed a correlation for estimation of the values of mass-transfer coefficient

$$k_l = B_1 H_f^{0.33} h_0^{0.02} V_G^{0.8} Q^{0.4} \tag{2.26}$$

The values of the constant B_1 are 9.2 for SO_2 and 4.3 for Cl_2.

Shah and Mahalingam (1984) studied mass transfer with chemical reaction in a foam reactor using lean carbon dioxide gas. Nonionic and cationic surfactants, Triton X-100 and hexadecyl trimethyl ammonium bromide (HDTMAB), respectively, were used for generating stable foam. The variables studied were gas flow rate, wire mesh size and nature of surfactant. The gas holdup and interfacial area were determined experimentally. The liquid-side mass-transfer coefficient and modified interfacial mass-transfer coefficient were determined semi-theoretically.

2.6.1.8 Surface coefficient

In most of the studies on foam reactors, a surface-active agent has been used in small amounts, generally sufficient to produce stable foam. Though, it has often been found that *the addition of a surfactant reduces the rate of interphase mass transfer, instances of enhancement in mass-transfer rate are not uncommon*. Two mechanisms have been proposed to explain the reduction in mass-transfer rate, viz. the hydrodynamic mechanism (Llorens et al., 1988), and the barrier mechanism (Goodridge and Bricknell, 1962). According to the hydrodynamic mechanism, the hydrodynamics of a flow system changes due to the presence of a surfactant and that this is the principal cause of the reduction in the rate of mass-transfer. The barrier mechanism, on the

other hand, postulates that in addition to the hydrodynamic effect, the surface-active agents physically block the interface, and thus the rate of mass transfer is reduced.

The effect of surface-active agents on mass transfer in gas-liquid systems have been studied by various investigators using wetted-wall column (Ternovskaya and Belopolskii, 1950; Emmert and Pigford, 1954); modified wetted-wall column (a thin film running down a sphere, Cullen and Davidson, 1956); manometric apparatus (Blank and Roughton, 1960); stirred vessel (Goodridge and Bricknell, 1962) and liquid laminar jet (Caskey and Barlage, 1972).

Jana and Bhaskarwar (2012) proposed a model for estimation of surface transfer coefficient for absorption of pure CO_2 gas in saturated lime solutions. Experiments were performed in a modified manometric apparatus. Three types of surfactants, Triton X- 100, SDS and CTAB: cationic, anionic and non-ionic, respectively were used for these studies. Volume of gas absorbed was calculated using the model developed along with the manometer reading obtained from experiments of gas absorption in lime solution with and without addition of surfactant to it. The measured values of surface transfer coefficient varied from 0.350×10^{-4} to 1.068×10^{-4} m/s.

Surface resistance to mass transfer in liquid-liquid systems have been measured using two methods, viz. by measuring the rate of mass transfer to and from a drop moving through a stagnant liquid, and in the second method by measuring that across an interface between stirred liquids.

2.7 Absorption with/ without chemical reaction in foam-bed reactors

2.7.1 Gas-liquid-solid foam-bed reactors

Precipitated calcium carbonate (PCC) and sodium dodecyl sulfate are used for the manufacture of tooth paste (e.g., Colgate). PCC and CTAB (an antifungal agent) are mixed with hydrated magnesium silicate and other ingredients for the manufacture of face powder. PCC can, therefore, be produced in a slurry-foam reactor using SDS or CTAB depending on its usage and preferably with a thermal or mechanical method of foam breaking for maintaining the desired foam column height.

Usually, a small but known amount of a surface-active agent is added to the liquid in foam reactors for the generation of stable foam. Usage of a foam-bed reactor (Fig. 2.3)

is, therefore, especially suitable when the surfactant solution is recycled back to the reactor so that the recurring cost of surfactant and the pollution of water due to its discharge to water bodies can be minimized. This reduces the need for fresh water as well. Gas absorption with a precipitation reaction, e.g., carbonation of hydrated lime using carbon-dioxide gas, is a typical example of such a reaction and can be advantageously carried out in a foam-bed reactor such that the unreacted gas, if any, and the solution containing the surfactant can be recycled back to the reactor after separation of the product solid. Presence of surfactant in the reaction medium protects the equipment from fouling arising due to the highly sticky hydrated lime present in slurry and also helps in easier cleaning of the equipment.

Asolekar et al. (1988) studied the absorption of lean carbon-dioxide gas in slurries of hydrated lime. The authors developed a mathematical model for a semi-batch foam-bed reactor based on the idealized pentagonal dodecahedral structure of cellular foam and verified it using their experimental data. Although the storage constituted about 85 percent of the total liquid charged into the reactor, the authors assumed the extent of gas absorption in the storage section to be negligible. The diffusion equation for species '*A*' was written only for absorption in the pentagonal slurry-foam films in the foam section. The effects of time of reaction, composition of slurry, and nature of surfactant on the rate of consumption of calcium hydroxide were investigated. The plots of calcium hydroxide consumed versus time were observed to consist of a constant-rate period and a falling-rate period. The reaction between the dissolved solid species '*B*' with the absorbed gaseous component '*A*' occurring in the foam films was assumed to be pseudo-first order. The authors found the model to agree well with the experimental data when distribution of particle-size instead of the average particle size was incorporated in the model.

Stangle and Mahalingam (1990) used two glass columns of 0.86 m and 0.41 m length to study the absorption with chemical reaction of lean carbon-dioxide gas in slurry-foam reactors operated under steady-state conditions. The effects of solids loading, gas-flow rate, wire-mesh size, height of foam column, and type of surfactant on the stability of foams, rates of gas absorption, and dissolution of solids on the reactor performance were investigated. Using the experimental data, they evaluated the solid-liquid mass-transfer coefficient, average gas-absorption rate, pressure drop, gas-liquid interfacial area, foam-bubble size, solid-liquid interfacial area and gas hold-up.

The authors derived analytical equations to predict the effect of solids dissolution on the specific rate of absorption of carbon-dioxide gas in the stable-foam stage of the foam reactor. Solids loading, gas-liquid interfacial area and foam-flow rate were the three significant parameters shown to affect the performance of a three-phase slurry-foam reactor.

Jana and Bhaskarwar (2010) reported their studies on absorption of pure carbon-dioxide gas in lime slurry in a foam-bed reactor. The authors emphasized that the diverse foam-bed reactor models, published in the literature for the cases of negligible conversion in the storage section of a foam reactor, need to be re-examined for the reason that storage section contains 60 to 85% of the reaction mass and therefore its contribution towards total conversion can not be neglected. They reported a composite model for a slurry-foam reactor taking into account the contributions of both the sections of the reactor towards gas absorption, solid dissolution and reaction incorporating sparingly soluble fine particles. In this case, since the reaction occurs in the liquid phase, concentration of component *B* (present as particles and also dissolved in the solution) in the liquid phase reduces due to reaction while simultaneously increases because of continuous dissolution of suspended particles. Therefore, the instantaneous concentration of *B* required for calculation of reaction rate and the total loading required for the calculation of conversion, can't be written in the conventional way. The authors (Jana and Bhaskarwar, 2010) reported the pertinent mass-balance equation for this special case for the calculation of the instantaneous concentration of component *B* in solution and its total loading in the reactant slurry.

2.7.2 Gas-liquid foam-bed reactors

Since the year 1939 a large number of studies on gas absorption in gas-liquid foam reactors have been reported in the literature. Early studies on foam reactors were mostly focused on development of empirical correlations for mass-transfer coefficients, gas-liquid interfacial areas, drainage rates of foams etc, or on removal of dust particles from dust laden exhaust gases. (Luchinsky, 1939; Helsby and Birt, 1955; Jackson, 1963; Weissman and Calvert, 1965; Plevan and Quinn, 1966; Maminov and Usmanova, 1968; Onda et al., 1969; Kaldor and Phillips, 1976; to name a few). Starting from nineties, quite a few models on gas-liquid foam-bed reactors depicting more insight of the physical phenomena have appeared in the literature

(Biswas and Kumar, 1981; Bhaskarwar and Kumar, 1984; Shah and Mahalingam, 1984; Bhaskarwar and Kumar, 1986; Bhaskarwar, 1987; Bhaskarwar et al., 1987; Biswas et al. 1987; Stangle and Mahalingam, 1989; Bhaskarwar et al., 1990; Sree, 1993; Bhaskarwar and Kumar, 1995; Bhattacharhee et al., 1997; Subramanyam et al., 1999; Reddy and Bhaskarwar, 2000; Bhattacharhee et al., 2001; Varshney et al., 2003 and Sharma et al., 2005).

Conflicting reports of the effects of foams on the performances of strippers, absorption and distillation columns, fermentation broths, and, operational problems in the paper, sugar, beer and many other manufacturing units has been cited in the literature. While many investigators (Chen et al., 2007) observed increased rates of mass transfer in fermentation broths and absorption or distillation columns for its operation in the frothing region, others (Kister, H.Z., 2003) reported a decrease in the performance of these contactors. In the following paragraphs, observed effects of foams on performances of gas absorption have been presented.

The first attempt to discover the potential of a foam-bed reactor as an efficient mass-transfer device was made by Luchinsky, 1939. Weissman and Calvert (1965) studied desorption of CO_2 and NH_3 from aqueous foams flowing through a pipe placed horizontally. These two systems are liquid-phase controlled and gas-phase controlled, respectively. The authors used the number of transfer units approach to analyze their experimental data. Two correction factors were incorporated in the expressions for number of transfer units.

Biswas and Kumar (1981) proposed a new model of a foam-bed reactor incorporating idealized dodecahedral structure of a foam bubble. Bhaskarwar and Kumar (1984) modified this single stage model for application to a gas-liquid foam-bed reactor. The reaction was assumed to be pseudo-first order. Effects of initial concentration of sodium sulphide, catalyst loading and average liquid hold-up on conversion of sodium sulfide were studied in a 1.5 m tall foam column. Predictions of the model agreed well with the experimental data.

Bhaskarwar and Kumar (1986) presented a modification of the single stage model over their previous model (Bhaskarwar and Kumar, 1984) for oxidation of sodium sulfide by air in presence of activated carbon as the catalyst. The details of the model

proposed by Biswas and Kumar (1981) and modifications of this model by various investigators have been discussed in detail later in this chapter.

Table 2.4 Reported correlations for estimation of parameter values in a foam-bed reactor

S. No.	Parameter	Correlations Reported	Reference
1	Film Thickness	$2a = 4\mu_l H_T / g\rho_l t_d$	Bikerman, J. J., (1956)
2	Pressure drop	$\Delta p_1 = 1.45\ K_c\ (\rho_G u_o^2/2g)$; $\Delta p_2 = 0.85\ h_o \rho_l + 0.2\ \sigma_l\ (10^4)$	Jackson, J. (1963)
3	Foam height	$H_f = 4.35 \times 10^{-5}\ (h_o^{0.6}\ V_G^{0.5} / (\sigma_l^{1.3}\ V_l^{0.25})$	Jackson, J. (1963)
4	Mass-transfer coefficient, k_l	$k_l = B_l H_f^{0.33}\ h_0^{0.02}\ V_G^{0.8}\ Q^{0.4}$	Shabel'nikov and Mukhlenov, (1963)
5	Drainage rate	$V_d / V_{f0} = 1 - e^{-c_l t_d}$	Kruglyakov and Taube,(1965)
6.	Specific interfacial area	$a_b = (6\bar{\varepsilon}_G / d_b)$; $\bar{\varepsilon}_G = 1 - (\rho_f / \rho_l)$	Rodionov et al. (1966)
7.	Liquid holdup	$\varepsilon_l = 2.34 \dfrac{(\mu_l V_G)^{5/7} d_b^{2/7}}{(\rho_l g)^{1/7}(\sigma_l H_f)^{4/7}} + 520 \dfrac{(\mu_l V_G)^{6/7}}{(\rho_l g)^{4/7}(\sigma_l H_f)^{2/7} d_b^{6/7}}$	Hartland and Barber (1974)

Bhaskarwar et al. (1987) presented a theoretical analysis of mass transfer with chemical reaction in an oil-in-water type emulsion foam-bed reactor. The authors studied the mechanisms of mass transfer in this modified system and developed a mathematical model through extension of the single-stage model proposed by Bhaskarwar and Kumar (1984). Species *A* in the gas phase was assumed to be the limiting component and surface resistance offered by the surfactant was neglected. The effects of distribution coefficient of organic phases, the size of droplets and volume fraction of organic phase on the fractional rate of gas absorption were studied. A model for simultaneous mass transfer to both aqueous and organic phases was also developed. A finite-difference method was used for simultaneous solution of the two partial- differential equations.

Biswas et al. (1987) presented a modified model over that reported by Biswas and Kumar (1981) by incorporating surface resistance for absorption of carbon-dioxide gas in sodium- hydroxide solution containing a surfactant in a foam bed reactor.

Bhaskarwar et al. (1990) developed a general model of foam-bed reactor. Depending on the specific cases, the model could be reduced to one of negligible conversion in the storage section or that in the foam section. Variation of concentration of component *A* in the gas phase, and that of component *B* in solution and of dissolved species *A* in the liquid with time could be predicted using the model. A good agreement was found between the model predictions and the previously reported experimental data by Bhaskarwar and Kumar (1984) for the oxidation of sodium sulphide in a semi-batch foam-bed reactor.

Sree (1993) used a sub-model for prediction of mass transfer from the adjacent gas pockets into the micro-emulsion foam film. Simulation results of the effects of average velocity of foam bubbles, thickness of foam films, volume fraction of dispersed phase in the micro emulsion, reaction velocity constant, surface area of micro emulsion film, distribution coefficient of reactant between aqueous and organic phase and time of absorption on the extent of absorption of gas in the foam film were presented. The methodology adopted was reported to be more effective for slow reaction.

Bhattacharjee et al. (1997) studied the phenomena of concentrating protein using casein and bovine serum albumin (BSA) solutions in a batch foam columns. A larger height of liquid pool and a higher drainage time produced better protein separation. The most important phenomena for separation of protein from solution in the foam column were identified as adsorption of protein at the gas-liquid interface on the film surface and drainage of liquid from the foam film. The authors proposed a model for predicting separation factor and the model predictions agreed well with the experimental data.

Varshney et. al. (2003) studied gas absorption under pseudo-zero order reaction system for oxidation of aqueous solution of sodium dithionite using air in a foam bed reactor. Triton X-100 was used for generating stable foam and the experiments were carried out at 30° C temperature and at atmospheric pressure. The variables studied were superficial gas velocity and initial liquid phase concentration of reactant on conversion. Conversion of dithionite was found to increase with the increase in its

initial concentration in solution and with the superficial velocity of gas. The simulated results were presented for the effects of gas flow rates, reaction rates and time of contact. The simulated results agreed well with the experimental data.

Sharma et al. (2005) developed a mathematical model of a foam-bed reactor for simultaneous absorption, reaction and desorption of gas in a foam reactor. This model incorporates the gas-phase and surface resistances, which were not taken into account in most of the published models of foam-bed reactors. The model incorporates all the coupled processes in the reactor. The authors used a modular approach to find out the transient concentration profiles of the gas-phase reactant *A* and that of the product inside the surface element of a single foam film with the help of a sub-model. Effects of kinetic, physicochemical and system parameters on fractional gas absorption were analyzed.

Depth of liquid in the storage section being low and gas-liquid contact time small, extent of gas absorption or conversion of reactants in a single column remains low for a once through gas-liquid contact and therefore, a single reactor cannot be used for continuous operation to obtain high conversion. Either semi-batch operation of single reactor with provision for foam breaking, recirculation of condensate, or, reactors in series (Jana and Bhaskarwar, 2010) are essentially required for obtaining high conversion.
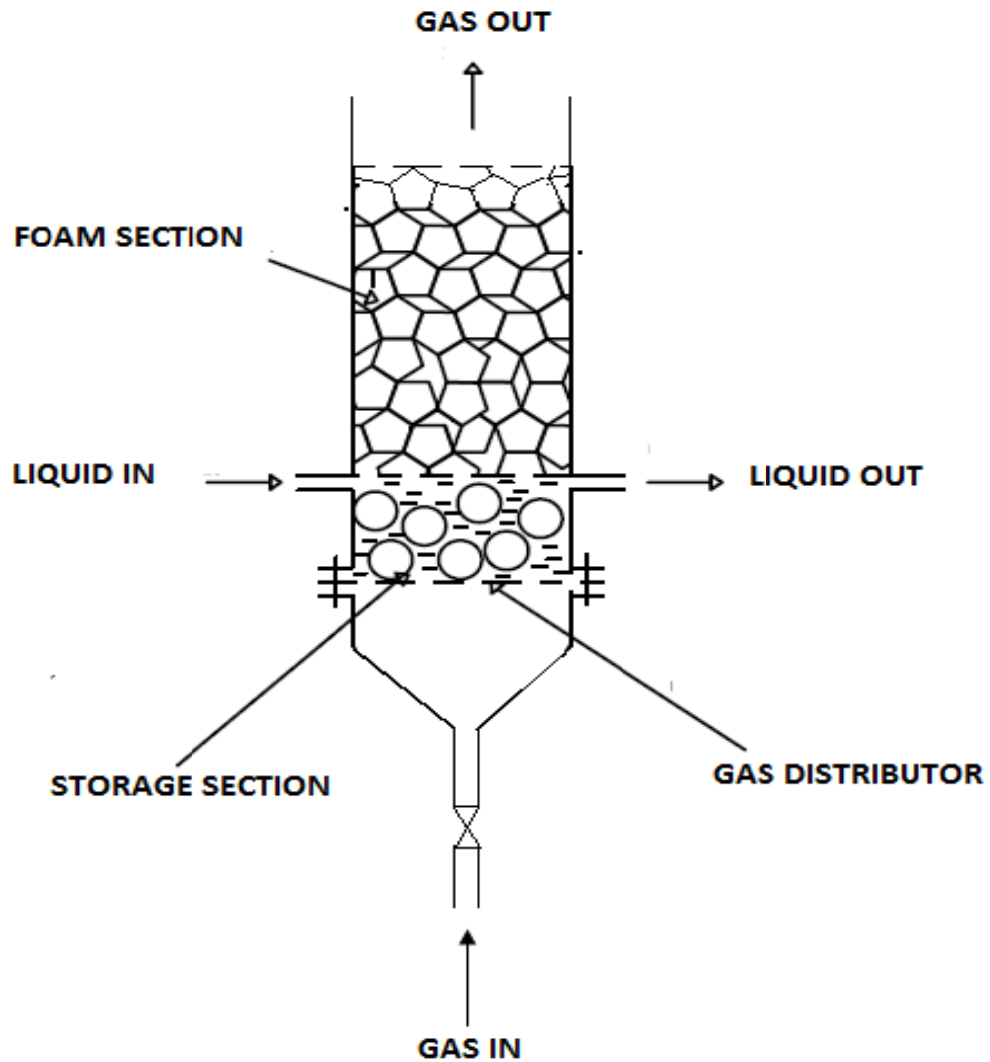
Figure 2.3   A schematic diagram of a foam-bed reactor

2.8 Foam-bed reactor models

In the early models to interpret the experimental data on gas absorption with/ without chemical reaction in foam columns, all the investigators considered the bubbles to be spherical. However, this is not true under all operating conditions. The foam bubbles are polyhedral in shape (Deshpande and Barigou, 2000) and this is especially true in the range of low gas velocities normally used for the operation of foam-bed reactors. The bubbles in foam columns are idealized in accordance with the laws of foam structure (Plateau, 1873) as regular pentagonal dodecahedrons (Fig. 2.2).

2.8.1 Multistage model of foam-bed reactor: The first attempt to develop a realistic model of a foam reactor was made by Biswas and Kumar (1981). However, in the development of the model to predict the performance of the reactor, they considered

the contribution of only the foam section towards the conversion of reactants as they found the extent of gas absorption in the storage section to be less than 5 percent of the total. This aspect has been analyzed at length in this work.

For the absorption of CO_2 in NaOH solution, the experimental conditions maintained were such that the reaction kinetics conforms to fast pseudo-first order reaction. Calculations from experimental conditions: $r_c = 0.0385$ m, $V_l = 1.0 \times 10^{-4}$ m^3 and the variables: $H_f = 0.05$ m, $\overline{\varepsilon_l} = 0.017$ for set I; $H_f = 0.26$ m, $\overline{\varepsilon_l} = 0.085$ for set II used by these authors (Biswas and Kumar, 1981) show that only about 4 to 10 percent by volume of the total liquid charged into the reactor constitutes the foam section. However, for the development of their model, the authors (Biswas and Kumar, 1981) assumed the entire phenomenon of mass transfer accompanied by a fast pseudo-first order reaction to occur within this limited volume of liquid in the foam section. Although, the storage section liquid has been assumed well stirred ($h_l = 1.93 \times 10^{-2}$ to 2.06×10^{-2} m, $V_G = 8.1 \times 10^{-2}$ to 22.5×10^{-2} m s^{-1}) but its contribution to the absorption of gas and the overall rate of reaction has been assumed negligible in comparison to that in the foam section where gas absorption occurs exclusively by molecular diffusion. To emphasize this, gas inlet has been shown to the foam section and not to the storage section.

On the whole, this model (Biswas and Kumar, 1981) has an invaluable contribution to serve as a starting point to develop superior models for such systems and impart a deep insight into the absorption-reaction phenomena occurring in this novel reactor. This rigorous model being the first of its kind, the pertinent differential equations, boundary- and initial conditions and the final solutions are cited here, although the detailed analytical solution and the calculations are highly involved.

The material-balance equations (Biswas and Kumar, 1981) for liquid-phase component B in the storage and foam sections are as follows (Fig. 2.4).

Storage section:

$$-V_l \frac{dC_{Bs}}{dt} = (Q_d + Q)C_{Bs} - QC_{B0} - Q_d C_{Bd} \tag{2.27}$$

Foam section:

$$Q_d C_{Bd} = \sum_{i=1}^{m} q_i C_{B,i} \tag{2.28}$$

,where

$$Q_d = \sum_{i=1}^{m} q_i \tag{2.29}$$

The unsteady state diffusion of component *A* with pseudo-first order reaction in the pentagonal films of dodecahedral bubbles are written as

$$\frac{\partial C_A^{/}}{\partial t_c} = D_A \frac{\partial^2 C_A^{/}}{\partial x^2} - \lambda C_A^{/} \tag{2.30}$$

, where $C_A^{/}$ is the concentration of reactant *A* in the foam film at position *x* and contact time t_c, and $\lambda = k_2 C_B$.

The initial and boundary conditions for the solution of equation (2.30) are described below.

The simplifying assumption that the liquid films surrounding a bubble leaving the storage and entering the foam section do not contain any dissolved reactant *A*, was used to signify that the storage neither contributes to absorption nor to reaction. The initial condition was therefore written as

$$At \ t_c = 0, \quad -a \leq x \leq a, \quad C_A^{/} = 0 \tag{2.31}$$

The boundary condition was obtained by writing mass balance for component *A* over a half-film/ gas-pocket (one-twelfth of the volume of gas in a bubble) system considering that the rate of decrease of component *A* in the gas pocket was equal to its rate of increase in the liquid half-film by its absorption:

$$At \ t_c > 0, \quad x = \pm a; \quad -(\frac{V_b}{12})(L)\frac{\partial C_{AG}}{\partial t_c} = \pm(S)D_A \frac{\partial C_A^{/}}{\partial x} \tag{2.32}$$

, where $\quad L = \dfrac{V_b}{12.k_e.S} \quad$ and $\quad C_A^{/} = k_e C_{AG}$

To account for the variation in the liquid hold-up values in the foam column, the foam height was divided into a number of sub-sections, *m*, each with a height equal to one bubble diameter and having different liquid hold-up values, $\bar{\varepsilon}_{l,i}\,(i=1,2,...,m)$.

For the special case of semi-batch operation of a reactor (Q=0), the solution of equation (2.27) for transient concentration of component *B* in the storage section was obtained (Biswas and Kumar, 1981) as,

$$C_{Bs} = C_{B0} - \frac{1}{V}[\frac{2R_{BA}Q_dM_1}{V_1} + \frac{2R_{BA}(Q_d-q_1)(M_2-M_1)}{V_2} \quad +....$$
$$+ \frac{2R_{BA}(Q_d-(q_1+q_2+...+q_{m-1}))(M_m-M_{m-1})}{V_m}](t)$$

(2.33)

The above model, developed for gas absorption accompanied by a fast chemical reaction, does not take into account the surface resistance arising due to the presence of surfactant in the liquid, especially important for a fast reaction, because the authors did not use any surfactant in their experiments. Gas-phase resistance for absorption of a component from a lean gaseous mixture known to be important for very fast reactions is not seen to be included in the model. Most importantly, the assumption that all the gas absorbed got reacted then and there in the different sub-sections of the foam column necessitated the use of local liquid hold-up values and increased the complexity of calculations.

2.8.2 Simplification of the multistage model of foam-bed reactor

A simplified version of the model proposed by Biswas and Kumar (1981) was developed by Bhaskarwar and Kumar (1984) with the objective of validating their experimental data on oxidation of sodium sulfide in a foam-bed reactor. They assumed the entire foam column to be a single section with a constant average liquid hold-up ($\bar{\varepsilon}_l$), based on the findings of Desai and Kumar (1983) that within about 3 x 10^{-2} to 4 x 10^{-2} m from the liquid-foam interface, the liquid hold-up in a foam bed decreased upwards very rapidly and thereafter remained almost constant at higher heights of the foam column. The constituent equations and the analytical solution obtained were therefore simpler and eliminated the need for calculation of individual bubble volumes, drainage rates, gas-liquid contact times, half-film thicknesses etc for every sub-section of the foam column without appreciable loss of accuracy in the

prediction of the reactor performance. However, the contribution of storage section towards the overall conversion in the reactor was not incorporated in this model also as they found negligible conversion in the storage section.

The assumption of negligible extent of gas absorption and conversion in the storage section and the concept of the single-stage model developed by Bhaskarwar and Kumar (1984) were adopted by Asolekar et al. (1988) to develop a model for a slurry-foam reactor. However, in this case, the effect of surface resistance due to the presence of surfactant at the gas-liquid interface in the foam section was taken into account in the diffusion equation for component *A* written for the foam section. The entry of the lean gaseous mixture was shown into the storage section and not into the foam section as it was done for the models developed by Biswas and Kumar (1981) and also that by Bhaskarwar and Kumar (1984). However, the concentrations of component *A* were shown to be $C_{AG}{}^{0}$ both in the inlet as well as in the exit streams from the storage section. This was done to emphasize that the extent of gas absorption in the storage section was negligible and to be specific, 'zero' as with all the other cases.

Very similar concept is found to be applied for the development of a model by Stangle and Mahalingam (1990) for a *continuously operated slurry-foam reactor* for carbonation of lime in aqueous slurry using lean carbon-dioxide gas. The initial gas composition, solids loading and size of suspended particles have been measured at the inlet and exit of the reactor, whereas the differential equation representing the material balance equation has been integrated numerically from bottom to top of the stable foam stage, excluding the 'foam generation section' located below the 'stable foam stage' for comparing the computed values of the exit gas composition with those of the experimental data and thereby estimating the unknown value of k_{sl} iteratively. The contribution of the 'foam generation section' towards gas absorption, solid dissolution and overall rate of reaction was therefore neglected. It may be observed that the gas concentration and average particle size has been determined upstream of the foam generation section constituting the well-stirred pool of slurry with the feed gas.
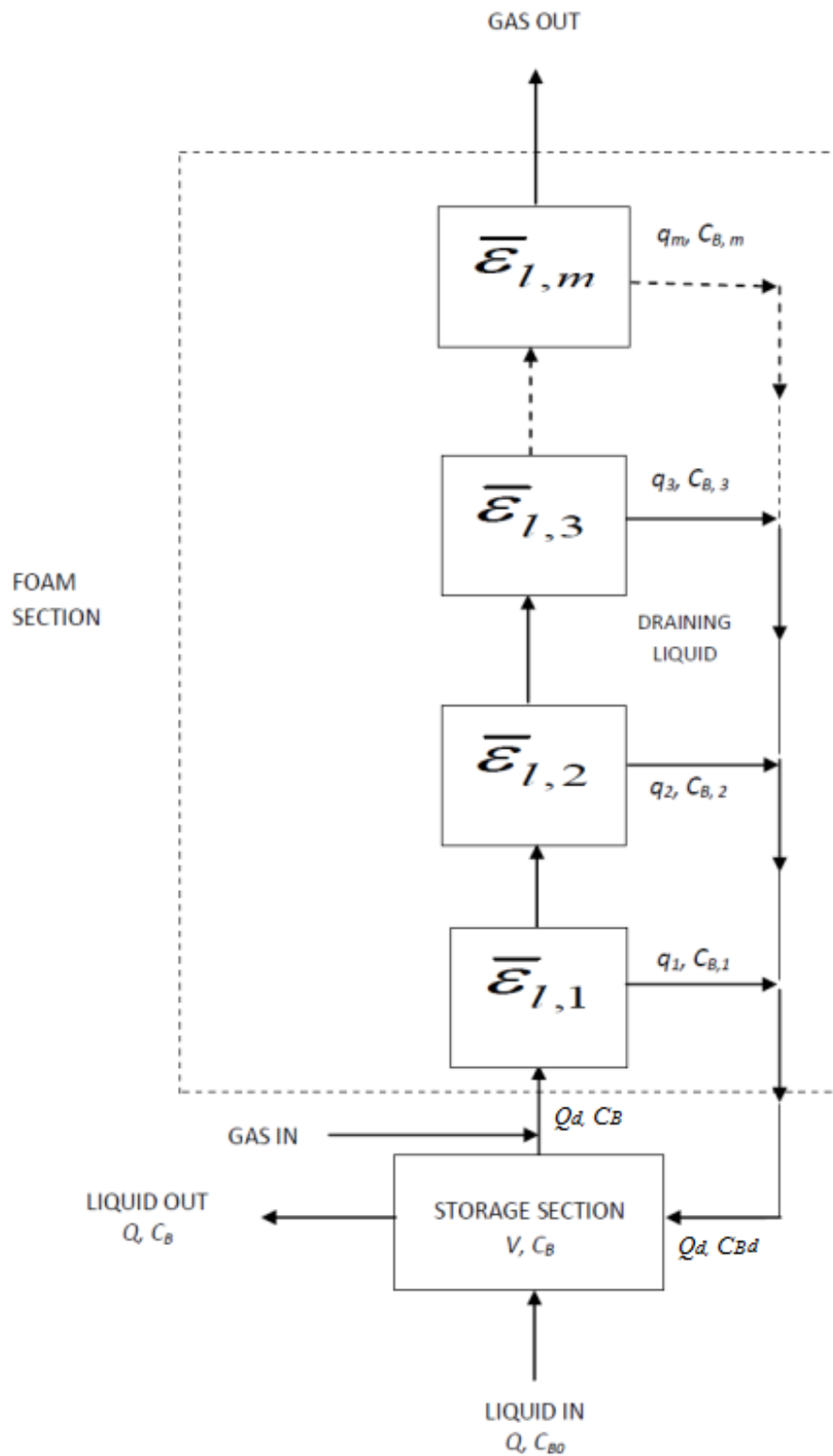
Figure 2.4 Model representation of a foam-bed reactor (Biswas and Kumar, 1981)

Gaikwad and Bhaskarwar (2007) reported the removal of CO_2 gas by treating it with aqueous barium sulphide (BaS) solution in a semi-batch foam-bed reactor. The system studied comprises of simultaneous gas absorption, chemical reaction and desorption. The variables studied were height of foam bed, initial concentration of barium sulfide in aqueous solution, gas flow rate, concentration of carbon dioxide in the feed gas diluted with nitrogen, volume of the barium-sulfide solution charged into the reactor, surfactant concentration in the aqueous solution, and the nature of surfactant. Effect of other parameters like temperature and addition of different concentrations sodium chloride were also studied.

Gaikwad et al. (2010) studied the performance of a foam-bed reactor for carbonation of barium sulfide using lean CO_2. Reactant solution was prepared by dissolving commercial barium sulfide containing about 60% BaS. The variables studied are height of foam bed, initial concentration of barium sulfide in aqueous solution, gas flow rate, concentration of carbon dioxide, volume of barium sulfide solution charged into the rector and the surfactant type and its concentration in aqueous solution. Maximum conversion of barium sulfide was obtained at a foam height of 0.4 m beyond which, the conversion decreased as the reverse diffusional flux of desorbing hydrogen-sulfide gas dominated the advantages of larger interfacial areas and contact times. Conversion increased almost by a factor of 2.5 to 3.0 with an increase in the air flow rate in the range 4.17 x 10^{-5} m^3/s to 12.5 x 10^{-5} m^3/s. Conversion also increased with an increase in the concentration of CO_2 gas. However, it was observed to decrease with an increase in the concentration of BaS in the feed solution, concentration of surfactant and volume of solution charged to the reactor. The authors proposed a model for the system studied and verified it with their experimental data.

2.8.3 Composite model: The above analysis that all the reported models have been developed considering negligible conversion in the storage section although it constitutes 65 to 96 percent of the total volume of liquid / slurry charged into the reactor, led Jana (2007) to confirm this aspect by performing experiments in conventional bubble column- and foam-bed slurry reactors for carbonation of hydrated lime slurry using pure carbon-dioxide gas under otherwise identical conditions. *Contrary to all previous findings*, storage section was found to be the main section governing the performance of the foam-bed slurry reactor. Accordingly, a composite model for a semi-batch foam-bed slurry reactor was developed by combining the

contributions of the storage and foam sections towards the overall conversions of the reactants. This new model was found to produce good agreement with the experimental data. Being the most realistic model of a foam-bed reactor published so far, a brief discussion of the model is presented below.

Estimation of the instantaneous value of conversion of $Ca(OH)_2$, referred as component B here, needs its initial total mass $m_{B(0)}{}^T$ and its total unreacted amount, as a function of time $m_{B(t)}{}^T$. Amount of $Ca(OH)_2$ being reduced in solution due its consumption by reaction with CO_2, referred as component A here, and increased in solution due to dissolution of its sparingly soluble fine particles, total mass of B in the slurry $m_{B(t)}{}^T$ is determined by summing up the mass of B present in solution and that as suspended particles. Simultaneous solution of transient mass balance equations for components A and B in solution and those of the suspended particles, as shown below, are therefore performed to obtain $m_{B(t)}{}^T$. Detailed derivation of the material balance equations have been described elsewhere (Jana and Bhaskarwar, 2010).

$$\frac{dC_{As}}{dt} = (k_l^0 a_b)(C_{Ai} - C_{As})E_a + \frac{V_{b(0)} - V_{b(t_c^*)}}{V_{MG}.V_l}.\frac{Q_G}{V_{b(0)}} -$$

$$\frac{(\sum_{k=1}^{z} n_{pk} \pi d_{pk}{}^2)k_{sl}(C_{Bi} - C_{Bs}).V_l{}^{foam}}{V_l R_{BA}} - 2k_2 C_{As} C_{Bs} \tag{2.34}$$

$$\frac{dC_{Bs}}{dt} = \sum_{k=1}^{z}(n_{pk}\pi d_{pk}{}^2)(k_{Sl})(C_{Bi} - C_{Bs})\frac{V_{sl}}{V_l} - 2R_{BA}k_2 C_{As} C_{Bs} \tag{2.35}$$

$$\frac{d(\sum_{k=1}^{z} n_{pk} v_{pk})\rho_B}{dt} = [(Q_f.t_c^*/V_{sl})+1][-(\sum_{k=1}^{z} n_{pk}\pi d_{pk}{}^2)(k_{SL})(C_{Bi} - C_{Bs})M_B] \tag{2.36}$$

The initial conditions for solution of the ordinary differential eqns. (2.33) to (2.35) are:

At $t = 0; C_{As} = 0; C_{Bs} = C_{Bi}; v_{pk} = v_{pk(0)}$ \hfill (2.37)

The diameter of the suspended particles reduces with time, thereby reducing the availability of solid-liquid interfacial area for dissolution. Particle diameters in lime samples have been observed to vary widely, say 0.5 to 45 μm in some of the samples used by the authors (Jana and Bhaskarwar, 2010). These are conveniently divided into

smaller volume fractions to obtain a meaningful average size and the corresponding specific surface area for estimation of instantaneous rate of dissolution of particles. The subscript '*k*' indicates the different volume fractions of solid present in slurry. Each fraction comprises of particles of a sufficiently narrow size range and $d_{pk(t)}$ in the above equations is the average size of particles in k^{th} volume fraction of solid present in the slurry at any time '*t*' during an experimental run.

Total molar loading of component *B*, required for conversion calculation, was obtained by writing a mass balance equation for the component present as dissolved *B* in solution as well as particles of reduced size at any instant of time.

2.9 Foam-bed reactors in series: continuous operation

A laboratory scale foam-bed reactor consists of a small pool of solvent or a reactant solution/ slurry and a tall column of foam above it. Hence, for production on an industrial scale, using a continuous foam reactor, the volumetric flow rate of the liquid phase being high, the conversion obtainable in a single reactor is likely to be small. For achieving high conversion or high separation efficiency in a given volume of solvent, it is therefore required to use multiple foam reactors, either in series or in parallel. It has been suggested that reactors arranged in series are more convenient as it obviates the need for recirculation of partially converted reactant or partially saturated solvent.

Subramanyam et al. (1999) used the single-stage model of Bhaskarwar and Kumar (1984) for gas absorption accompanied by a pseudo-first order reaction in continuous operation and developed the performance equation for several foam reactors in series for treatment of the effluent from Kraft paper mills. The predictions from the model were presented in graphical form. It was suggested that similar charts may be prepared for other reaction kinetics. Based on an assumed value of the aspect ratio of the column, number of reactors in series may be determined for desired value of the operating conditions and liquid holdup in the column.

Gaikwad and Bhaskarwar (2010) studied the design of a continuous foam-bed reactor system for CO_2 removal from Power Plant Exhausts using BaS solution. They used the single stage model (Gaikwad and Bhaskarwar, 2007) to a system of N foam-bed reactors in series, equal in size, operated continuously. The reaction product

consisted of particles of $BaCO_3$ and H_2S gas. The specifications used for the design problem are, effluent flow rate: 100 tons/day; concentration of BaS solution in the feed stream: 0.56 kmol/m³; concentration of CO_2 in the feed stream: 1 x 10⁻² kmol/ m³; gas flow rate: 8 x 10⁻³ m³/s; desired conversion: 95 percent and above. The simulation was performed for different values of reaction velocity. A design chart was proposed for the estimation of number of reactors in series as a function of liquid hold-up in the column and aspect ratio as the parameters required for a given plant capacity

Jana and Bhaskarwar (2011) extended the model of a semi-batch slurry-foam reactor for carbonation of hydrated lime reported by them (Jana and Bhaskarwar, 2010) to the design of N_r continuous slurry-foam reactors in series for the manufacture of 50 tons of precipitated calcium carbonate per day using hydrated lime and pure carbon-dioxide gas as the raw materials and Triton X-100 as the surface active agent. Details of design data for slurry-foam reactors in series used by Jana and Bhaskarwar (2011) are given below.

Rate of production of PCC: 50 tons/day; Purity of hydrated lime: 92.28 percent hydrated lime, 7.72 percent $CaCO_3$; Slurry flow rate: 3.0784 x 10⁻³ m³/s: Slurry concentration : 150 kg hydrated lime/m³ solvent: Concentration of surfactant (Triton X-100): 1.64 kg/m³; Surface coefficient: 0.57 x 10⁻⁴ m/s; Desired conversion of lime: 99 percent. The following performance equations were proposed.

The conversion, X, in the yth reactor, any reactor in the series, at the end of reactor operation time t with a step size Δt was given by:

$$X = \frac{V_l.C_B^T(0) + [\sum(Q.(\frac{V_l}{V_{sl}})\Delta t).C_B^T{}_{(y-1)}] - V_l.C_B^T{}_{(p)} - [\sum(Q(\frac{V_l}{V_{sl}})\Delta t).C_B^T{}_{(y)}]}{V_l.C_B^T(0) + [\sum(Q.(\frac{V_l}{V_{sl}}).\Delta t.)C_B^T{}_{(y-1)}]} \quad (2.38)$$

During time period t, conversion obtainable in N_r reactors in series was obtained as:

$$X = \frac{N_r.V_l.C_B^T(0) + t.Q.(\frac{V_l}{V_{sl}}).C_B^T(0) - \sum_{y=1}^{N_r}V_l.C_B^T{}_{(y)} - \sum(Q(\frac{V_l}{V_{sl}})\Delta t.)C_B^T{}_{(N_r)})}{N_r.V_l.C_B^T(0) + t.Q.(\frac{V_l}{V_{sl}}).C_B^T(0)} \quad (2.39)$$

In equation (2.39), the first term in the numerator signifies the amount of component *B* (k mol) in the slurry filled in all the N_r reactors before the reactors start operating. The second term indicates kmol of *B* entering the first reactor in the series that moves through the successive reactors over the time period *t*. The third and fourth terms indicate total moles of *B* left out in all the reactors after time *t* and discharged from $N_r{}^{th}$ reactor during the reactor operation time *t,* respectively.

It is interesting that a model developed for a semi-batch reactor operation was extended to each of the N_r reactors in the series operating in a continuous mode. Considering the yth reactor in the series, volume of slurry ($Q.(V_l/V_{sl}).\Delta t$) which would have entered a reactor during a small time step Δt, (the entire quantity) is assumed to enter the reactor at the beginning of the time step itself. The volume-averaged concentrations and volumes of particles of each size are calculated using the mixing rule (Jana and Bhaskarwar, 2011). These concentrations are used at the start of a time step Δt for calculation of new concentrations and volumes at the end of time step, viz., $C_{A_{(y),k}}$, $C_{B_{(y),k}}$ and $v_{pi_{(y),k}}$ in reactor *p* using equations 2.33 to 2.35. $C_B{}^T{}_{(y)}$ is calculated from a material balance equation written for total loading of component *B* and *X* is predicted using equation 2.38. The above procedure is repeated for the subsequent Δt's.

2.10 <u>Remarks on scope for work: problem identification</u>

The detailed survey of literature indicates that there are ample opportunities for further studies both in the experimental as well as in the modeling areas on a foam reactor.

(1) Quite a few models on gas-liquid and gas-liquid-solid reactions in a foam-bed reactor have been reported in the literature. Some of the models for absorption of lean carbon-dioxide gas in NaOH solution assume negligible conversion in the storage section although the storage constitutes more than 90 percent of the total reactant solution charged into it. *It is proposed to reexamine this assumption experimentally and develop a composite model incorporating contributions of the storage section as well if conversion in this section is observed to be significant.*

(2) Experimental data reported in the literature on carbonation of hydrated lime slurry using lean CO_2 gas in foam-bed reactor were obtained by analysis of product slurry

drawn directly from the reactor at regular time intervals. While there are also reports in connection with the product analysis of carbonation of hydrated lime using pure CO_2 gas that the slurry being anisotropic, analysis of entire volume of product slurry is essential. *It is, therefore, decided to generate new experimental data for the carbonation reaction using lean CO_2 gas.*

(3) Rates of absorption of CO_2 gas in hydrated lime slurry and the reaction rates are enhanced significantly with the increase in concentration of CO_2 in the feed gas mixture, the equilibrium interface concentration of dissolved CO_2 being increased. For a given value of particle loading and at a given temperature, total solid-liquid interfacial area and interface concentration C_B^* remains invariant. Rate of dissolution of lime is enhanced for the reaction to proceed at a higher rate with an increase in concentration of CO_2 in the feed gas. This is possible only if solid-liquid mass-transfer coefficient value is increased. *In this work, it is intended to obtain a dimensionless correlation for the solid-liquid mass-transfer coefficient as functions of concentration of CO_2 in the gas phase and other significant variables used for collection of experimental data.*

Chapter 3

THEORETICAL CONSIDERTION

Mathematical models provide an insight into the different aspects of the system in regard to transient behaviour of a system, reaction mechanism involved, effects of operating variables and parameters on the system performance etc. In this chapter, mathematical models for the two reaction systems performed in two different types of reactors have been presented. Treatment of *gas-liquid system* being simpler than the three phase system, models for the former is treated first followed by the latter.

3.1 Mathematical model for gas-liquid contactor: Absorption of CO_2 in NaOH solution

Models have been developed for absorption of lean carbon dioxide gas, 0.22% to 0.49% by volume, from its mixture with air in sodium hydroxide solution, 0.23 to 0.87 (N), in semi-batch bubble column- and foam-bed reactors. The foam-bed reactor comprises of a storage section and a foam section. The storage section is a pool of gas-liquid dispersion and assumed to be well stirred with the rising gas bubbles. Mass transfer with chemical reaction is treated using the principle of absorption into agitated liquids for the development of models for this section. In the foam section, on the other hand, mass transfer occurs into the foam films primarily by molecular diffusion and the model is developed using the theories of absorption into quiescent liquids. This section comprises of a column of rising foam bubbles. The theories involved in the mass-transfer with chemical reaction in a ***bubble column being simpler*** than that in the foam-bed reactor, bubble column reactor is treated first followed by the foam-bed reactor.

3.1.1 Mathematical model for a gas-liquid bubble-column reactor

The transient conversion of reactant *B*, i.e. NaOH in solution in a semi-batch reactor can be calculated using the expression:

$$X = \frac{C_{B(0)} - C_{B(t)}}{C_{B(0)}} \times 100 \tag{3.1}$$

where, $C_{B(0)}$ and $C_{B(t)}$ are the initial and transient concentrations of NaOH in the semi-batch reactor. However, as component *B* is consumed by reaction with *A*, its instantaneous concentration, $C_{B(t)}$ is calculated by using the reaction stoichiometry and the material balance equation for component *B*. Rate of consumption of component *A*

required for this is obtained by solution of diffusion-reaction equation for component *A*.

The reaction between dissolved carbon-dioxide and OH⁻ ions have been reported (Danckwerts, 1970) to follow the second-order reaction kinetics. The reaction occurs in the liquid close to the gas liquid interface. For this irreversible reaction, bulk concentration of dissolved gas, component *A* here, is considered to be zero (Danckwerts, 1970). Concentration distribution of component *A* in the liquid film ***close to the gas-liquid interface*** may be obtained from the diffusion-reaction equation:

$$\frac{\partial C_A}{\partial t} = D_A \frac{\partial^2 C_A}{\partial x^2} - k_2 C_A C_B \qquad (3.2)$$

However, the experimental conditions in the present work was maintained to satisfy the necessary conditions for the reaction between dissolved CO_2 and OH⁻ ions to follow the *fast pseudo-first order reaction kinetics*. These conditions have been taken from the published work of Biswas and Kumar (1981) as well as verified further in this work following Danckwerts (1970).

For this special case, when the concentration of reactant *B* in the bulk of the liquid is maintained substantially high compared to a low concentration of dissolved CO_2 i.e., C_A^* corresponding to a very low partial pressure of CO_2 in the gas phase, reactant *B* diffuses from the bulk of liquid to the reaction zone located close to the gas-liquid interface to nullify its (that of *B*) depletion by reaction and maintain the same concentration of *B* as that existed in the bulk liquid. For this case, eqn. (3.2) reduces to

$$\frac{\partial C_A}{\partial t} = D_A \frac{\partial^2 C_A}{\partial x^2} - \lambda C_A \qquad (3.3)$$

where, $\lambda = k_2 C_B$, the pseudo-first order reaction rate constant and C_B, the concentration of *B* in the liquid film, virtually same as that existing in the bulk liquid, C_{Bs} (Fig. 3.1). Although the following B.Cs. show only the concentration of *A* as a function of time and position, λ contains C_B (= C_{Bs}), value of which reduces with propagation of reaction. This new value of C_{Bs} is calculated from reaction stoichiometry and used for calculation of new value of λ. The progress of reactor simulation continue to follow the procedure.

The initial and boundary conditions for solution of equation (3.3) are,

$$C_A = 0, \qquad x \rangle 0, \qquad t = 0 \qquad \text{(i)}$$
$$C_A = C_A^*, \qquad x = 0, \qquad t \rangle 0 \qquad \text{(ii)} \quad \text{(3.4)}$$
$$C_A = 0, \qquad x = \infty, \qquad t \rangle 0 \qquad \text{(iii)}$$
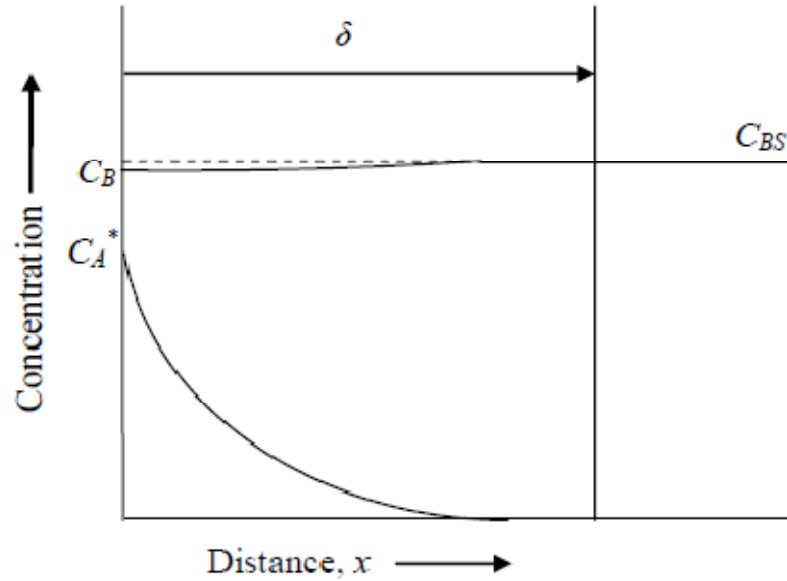
Figure 3.1 Concentration profiles for absorption with pseudo-first order reaction (NaOH-lean CO₂)

It is important that B. C. (3.4) can be used for solution of eqn. (3.3) only for a small time interval Δt, because along with the progress of reaction, B is consumed and concentration of component B reduces. This new concentration having a lower value than the previous C_{Bs} value becomes the new value of C_{Bs}. This new concentration of B after a small time step Δt is calculated and assumed to have this same value in the bulk liquid and that close to the gas liquid interface, and, eqn. (3.3) subject to B.C. (3.4) is executed repeatedly following this procedure for the entire period of reaction.

The average concentration of A at x, averaged over the various elements constituting the surface is defined following the surface renewal theory as,

$$\overline{C}_A = s \int_0^\infty C_A(x, \theta) e^{-s\theta} d\theta \qquad \text{(3.5)}$$

Equation (3.3) and the boundary conditions (3.4) may be rewritten applying Laplace Transformation as,

$$D_A \frac{\partial^2 \overline{C}_A}{\partial x^2} = \overline{C}_A (\lambda + s) \tag{3.6}$$

and

$$\begin{aligned} \overline{C}_A &= C_A^*, \quad x = 0 \\ \overline{C}_A &= 0, \qquad x = \infty \end{aligned} \tag{3.7}$$

Solution of equation (3.6) subject to conditions (3.7) for $\overline{C}_A$ has been obtained (Danckwerts, 1970) as,

$$\overline{C}_A = C_A^* \exp[-\frac{xk_l}{D_A}\sqrt{(1+\frac{\lambda}{s})}] \tag{3.8}$$

The quantity 's' in equation (3.8) is substituted, using the expression, $k_l = \sqrt{D_A s}$ to obtain the average concentration of dissolved gas at a distance x from the gas-liquid interface:

$$\overline{C}_A = C_A^* \exp[-\frac{xk_l}{D_A}\sqrt{(1+\frac{D_A \lambda}{k_l^2})} \tag{3.9}$$

The average value of molar flux, moles of component *A* absorbed per unit gas-liquid interfacial area per unit time, is obtained as:

$$\overline{N}_A = s\int_0^\infty N_A(x,\theta)\, e^{-s\theta} d\theta \tag{3.10}$$

Substituting the expression for N_A one obtains,

$$\overline{N}_A = s\int_0^\infty - D_A (\frac{dC_A}{dx})_{x=0} e^{-s\theta} d\theta$$

$$= -D_A s[\frac{d}{dx}\int_0^\infty C_A e^{-s\theta} d\theta]_{x=0} \tag{3.11}$$

Making use of equation (3.5), eqn. (3.11) is rewritten as,

$$\overline{N}_A = -D_A(\frac{d\overline{C}_A}{dx})_{x=0} \tag{3.12}$$

Substituting for $\overline{C}_A$ from eqn. (3.9) into eqn. (3.12) one obtains,

$$\overline{N}_A = -D_A(\frac{d}{dx} C_A^* \exp[-\frac{xk_l}{D_A}\sqrt{(1+\frac{D_A\lambda}{k_l^2})}]_{x=0}) \tag{3.13}$$

Or, $\quad \overline{N}_A = -D_A C_A^*(\frac{d}{dx}\exp[-\frac{xk_l}{D_A}\sqrt{(1+\frac{D_A\lambda}{k_l^2})}]_{x=0})$

Substituting $m = \frac{k_l}{D_A}\sqrt{(1+\frac{D_A\lambda}{k_l^2})}]$ and performing the required differentiation one

obtains,

$$\overline{N}_A = -D_A C_A^*\{(-m)\, e[-mx]_{x=0})\}$$

On simplification, the final expression for estimation of average flux is obtained as

$$\overline{N}_A = k_l C_A^*\sqrt{(1+\frac{D_A\lambda}{k_l^2})} \tag{3.14}$$

Rate of consumption of B, i.e., total moles of B reacted over contact time Δt, by this
fast pseudo-first order reaction, occurring in a zone close to the gas-liquid interface
is therefore obtained as,

$$(W_B)_{storage,\ \Delta t} = (R_{BA})\{k_l C_A^*\sqrt{(1+\frac{D_A\lambda}{k_l^2})}\}(a_s)(V_l)(\Delta t) \tag{3.15}$$

Concentration of B in the storage section after time step Δt is therefore obtained as,

$$C_B^{i+1} = C_B^i - [\frac{1}{V_l}(R_{BA})\{k_l C_A^*\sqrt{(1+\frac{D_A\lambda}{k_l^2})}\}(a_s)(V_l)(\Delta t)]$$

where, a_s is the interfacial area per unit volume of gas-liquid dispersion.

Or, $C_B^{i+1} = C_B^i - (R_{BA})\{k_l C_A^*\sqrt{(1+\frac{D_A\lambda}{k_l^2})}\}(a_s)(\Delta t)]$ (3.16)

Conversion is calculated using eqn. (3.1) and the required transient values of C_B are obtained from eqn. (3.16).

It may be observed that surface renewal theory has been used for the estimation of transient concentration of B in the reactor. However, in the following development, Higbi's penetration theory or film theory has been used. This has been done so considering some important findings by Danckwerts (1970). Absorption of CO_2 into alkaline solutions was studied by Danckwerts et al. (1963) and the results were reported to be consistent with both the Higbie and Danckwerts surface renewal model. That the three models can be regarded as interchangeable for many purposes and one of these can be chosen based on convenience, has been suggested by Danckwerts (1970). These authors (Danckwerts, 1970) also argued that the differences between the predicted values are expected to be less than the uncertainties considering the values of the physico-chemical parameters used in the calculations.

Prediction of parameter values

(i) *Estimation of* $C_A{}^*$

Solubility of CO_2 gas in water being substantially low, liquid phase ***resistance*** is considered to be much higher as compared to that in gas phase. Even though lean gaseous mixture has been used in the present studies, temperature of reaction is a bit high, 30°C. It is known that gas phase diffusion coefficient increases by $T^{1.5}$ while that in the liquid phase by $T^{1.0}$. The partial pressure-solubility relationship of CO_2 in air-water system at 30 °C is known to be, $P_{Ai} = (36)(C_{Ai})$ and the value of the corresponding Henry's law coefficient, H, comes out to be 36 $(m^3)(atm)/kmol$. Hence, it is assumed that interfacial resistance in the gas phase in the *well-stirred storage section* is negligible compared to that in the liquid phase.

The gaseous mixture used in the experiments being very lean, *percentage reduction* in the concentration of solute gas at the exit of the reactor is likely to be substantial in comparison to its concentration at the reactor inlet. Use of the average interfacial pressure at the gas-liquid interface of those at the reactor inlet and that at the exit of the reactor, is therefore considered to be more appropriate instead of interfacial partial pressure at the inlet to the reactor alone. The average interfacial partial pressure of

component A in the reactor for diverse operating conditions can therefore be obtained as,

$$P_{Ai} = (P_{Ai,inlet} + P_{Ai,exit})/2 \qquad (3.17)$$

The bubble column or the storage section of the foam reactor is considered to be fully stirred for which exit concentration of A in the gas is used for reactor performance (Danckwerts, 1970). However, considering the above arguments, arithmetic mean partial pressure was used for the reason that bubble column is very short, approximately 3.0×10^{-2} m. Instead of arithmetic mean, log mean partial pressure could also be used. For a typical experimental run, the partial pressures of CO_2 at the inlet to- and exit from the bubble column reactor are 3.5885×10^{-3} and 2.1195×10^{-3} atm., respectively. The arithmetic mean and log mean partial pressures comes out to be 2.854×10^{-3} and 2.7898×10^{-3} atm. The latter is found to be about 2 percent lower than the former and the error is considered negligible.

Solubility of carbon-dioxide gas in NaOH solution, C_A^*, has been calculated using Henry's law:

$$C_A^* = C_{Ai} = H\,P_{Ai} \qquad (3.18)$$

Where, H is the Henry's law solubility coefficient for solution containing ions and P_{Ai} has been defined by equation (3.21) subject to assumptions mentioned above.

H is related to its value in water, H_{w0} by the empirical equation (Danckwerts & Sharma, 1966).

$$\log\frac{H}{H_{w0}} = -hI \qquad (3.19)$$

Where, I is the ionic strength, calculated using the equation,

$$I = \frac{1}{2}\sum z_i^2 C_i \qquad (3.20)$$

And h is a constant for ions calculated (Sherwood et al., 1975) as,

$$h = h_+ + h_- + h_G \qquad (3.21)$$

H_{w0} by the empirical equation (Haq,1982)

$$\log H_{w0}: 4.117 - 0.059\,T + 7.885 \times 10\text{-}5\,T^2 \tag{3.22}$$

(ii) k_2 , k_l^0 , D_A

Reaction rate constant k_2 for the reaction between carbon dioxide and hydroxyl ions at infinite dilution is estimated following Astarita (1967):

$$\log_{10} k_2 = 13.635 - \frac{2895}{T} + 0.13I \tag{3.23}$$

At 30°C (303 K) and in a 0.5 molar solution of NaOH, values of k_2 comes out to be 1.398×10^4 (lit)/(g mole) (s).

For a bubble column reactor, the average value of the liquid-phase mass-transfer coefficient for physical absorption is calculated using the expression given by Higbie et al. (1935) as:

$$k_l^0 = 2.0 \text{ x } \sqrt{\frac{D_A}{\pi t_c}} \tag{3.24}$$

The diffusivity of carbon-dioxide in water, D_A, has been obtained using the correlation reported by Haq (1982):

$$\log_{10}(D_A) = -4.1764 + \frac{712.5}{T} - \frac{2.59 x 10^5}{T^2} \tag{3.25}$$

This data has been used for the present system consisting of an electrolyte solution, in absence of more accurate correlation, and the error is expected to be ~1% (Stangle and Mahalingam, 1990).

In the present studies, swarms of bubbles rise through the column. The free rise velocity is therefore hindered and actual velocity of bubble rise is smaller. Therefore, it does not appear justified to use free rise velocity for calculation of k_l^0. The contact time of gas required for solution of eqn. (3.24) is calculated using the bubble swarm velocity as given by equation (3.26) and the residence time of a bubble within the

dispersion by eqn. (3.36). Value of t_c being increased, k_l^0 calculated with u_{swarm} is proportionately higher than that calculated with u_{single}.

$$t_c = \frac{d_{b0}}{u_{swarm}} \tag{3.26}$$

The bubbles rising through the liquid pool in the storage section are assumed to be spherical and remain so during the entire rise period. The initial bubble diameter is given by:

$$d_{b0} = 2.(r_{b0}) = (2).\left(\frac{3V_{b0}}{4\pi}\right)^{0.3333} \tag{3.27}$$

The initial bubble volume, V_{b0} in turn is calculated using the correlation of Kumar and Kuloor (1970)

$$V_{b0} = (0.976).\left(\frac{Q_G}{H_N}\right)^{1.2} \bigg/ g^{0.6} \tag{3.28}$$

Velocity of swarms of bubbles, u_{swarm}, rising through a column of liquid has been given by Marrucci (1965) as:

$$u_{swarm} = u_{single} \frac{(1-\bar{\varepsilon}_G)^2}{1-\bar{\varepsilon}_G^{5/3}} \tag{3.29}$$

The rise velocity of single bubble, in turn, is calculated following the correlation given by Clift et al. (1978):

$$u_{single} = \sqrt{\frac{(2.14\sigma_1)}{(\rho_l d_{b0})} + 0.505 g d_{b0}} \tag{3.30}$$

(iii) Specific interfacial area, a_s

The specific interfacial area, a_s, available for mass transfer in the bubble column is calculated using the equation:

$$a_s = \frac{a^t_{bc}}{V_l} \tag{3.31}$$

Where, $a^t{}_{bc}$ is the total interfacial area in the bubble column and obtained as follows:

$$a^t{}_{bc} = (number\ of\ bubbles\ in\ the\ dispersion\ at\ any\ time\ in\ bubble\ column)\left(\frac{area}{bubble}\right)$$

or, $\qquad a^t{}_{bc} = (n_{bc})(a_b)$ \hfill (3.32)

The residence time that **each bubble remains within the dispersion** in the storage section after its formation, i.e., the gas-liquid contact time, t_{bc}, in the dispersion of the bubble column is given by,

$$t_{bc} = \frac{h_d}{u_{swarm}}.$$ \hfill (3.33)

where, h_d is the height of dispersion and calculated as, $h_d = \dfrac{V_d}{a_c}$ \hfill (3.34)

V_d is the total volume of dispersion in the bubble column and a_c, the cross-sectional area of the column.

Total volume of dispersion, $V_d = V_l + V_g$ \hfill (3.35)

Total volume of gas in the dispersion can be obtained from the expression,

$$V_g = (vol\ of\ dispersion)(gas\ holdup) = (\frac{V_l}{\overline{\varepsilon_l}})(\overline{\varepsilon_G}) = \frac{V_l}{(1-\overline{\varepsilon_G})}\left(\overline{\varepsilon_G}\right)$$ \hfill (3.36)

Gas holdup in bubble column required for solution of equation (3.36) is obtained using the experimental data proposed by Shulman and Molstad (1950) and cited by Kumar et al. (1976).

Total number of bubbles at any time in the dispersion in the bubble column available for gas absorption is obtained as

$$n_{bc} = (\frac{Q_G}{V_{b0}})(\frac{h_d}{u_{swarm}})$$ \hfill (3.37)

Interfacial area per unit volume of solvent is therefore obtained as,

$$a_s = \frac{Q_G}{V_{b0}} \frac{h_d}{u_{swarm}} \frac{1}{V_l} \qquad (3.38)$$

Condition for pseudo-first order reaction

Conditions to be satisfied for pseudo-first order reaction for a gas-liquid system (Kucka et al., 2002; Suresh, A. K., Lecture notes: NPTEL)

$Ha > 2$ (i)

$E_a/ Ha > 5$ (ii)

And, $\dfrac{k_l a}{k_2 C_{B0}} <<1$ (iii)

Physico-chemical data

D_A = 2.2595 x 10^{-5} cm^2/s or 2.2595 x 10^{-9} m^2/s at 30°C

k_2 = 1.3981x10^7 cm^3/g mole. s

C_{B0} = 0.44136 x 10^{-3} g moles/ cm^3

D_B =1.7979 x 10^{-5} cm^2/s

z=2.0

$C_A{}^*$ = 0.6914 x 10^{-7} g moles cm^{-3}

$$\text{(i)} \qquad Ha = \frac{\sqrt{k_2 C_{OH^-} D_{AB}}}{k_l} \qquad (3.39)$$

$$= \frac{\sqrt{(1.398x10^7\, cm^3 / gmol.s)(0.44136x10^{-3}\, gmol / cm^3)(2.2595x10^{-5}\, cm^2 / s)}}{0.0261(cm / s)}$$

=14.30

$$\text{(ii)} \qquad \frac{E_a}{H_a} > 5$$

$$\frac{E_a}{H_a} = \left(1 + \frac{D_B C_{B0}}{z D_A C_A^{*}}\right) \Big/ \frac{\sqrt{k_2 C_{OH^-} D_{AB}}}{k_l} \tag{3.40}$$

$$= [1 + \frac{(1.7979 \times 10^{-5})(0.44136 \times 10^{-3})}{(2)(2.2595 \times 10^{-5})(0.6914 \times 10^{-7})}]/14.30$$

$$= [1 + (0.2539 \times 10^4)]/ \ 14.30$$

$$= 2540/ \ 14.30$$

$$= 177.6$$

And, (iii) $\quad \dfrac{k_l a}{k_2 C_{B0}} \ll 1 \tag{3.41}$

Condition (iii) may be obtained as follows. When the bulk liquid is in quasi-stationary state,

$$V_l k_l a (C_A^{*} - C_{Ab}) = V_l (K_2 C_{AB} C_{Bb})$$

$$\text{Or, } k_l a C_A^{*} = C_{Ab}(a k_l + k_2 C_{Bb})$$

$$\frac{C_{Ab}}{C_A^{*}} = \frac{k_l a}{k_l a + k_2 C_{Bb}} = \frac{1}{1 + \dfrac{k_2 C_{Bb}}{k_l a}} = \frac{1}{1 + P}$$

For a fast gas-liquid reaction, the dissolved gas gets completely reacted within the film and the bulk concentration $C_{Ab} \to 0$.

Therefore, $\quad \dfrac{1}{1 + P} \to 0$

And hence, $P \gg 1$

Hence, a condition for pseudo-first order reaction is obtained as, $\dfrac{k_l a}{k_2 C_{Bb}} \ll 1$.

$$\frac{k_l a}{k_2 C_{B0}}$$

$$= \frac{(0.0261)(0.9699)}{(1.398 x 10^7)(0.44136 x 10^{-3})}$$

$$= 4.103 x 10^{-6}$$

Ha being much larger than 2, $E_a/$ *Ha* much larger than 5 and $\dfrac{k_1 a}{k_2 C_{Bb}} \ll 1$, the reaction is pseudo- first order.

The present experimental conditions therefore satisfy the requirement of pseudo-first order reaction.

3.1.2 Mathematical model for a gas-liquid foam-bed reactor

A foam-bed reactor consists of a shallow pool of liquid well agitated with gas bubbles and a column of rising foam above it. The mathematical model for the storage section is developed considering gas absorption into agitated liquids as it was done for the bubble column. In the foam section, on the other hand, the foam moves upward in a plug flow manner and the absorption of gas from the gas pockets into the foam films occur by molecular diffusion. Gas absorption phenomena in this section have been treated as that into quiescent liquid.

The following simplifying assumptions have been made in the development of the model:

1. The reaction system consists of two sections: storage and foam sections. The contribution of both the sections towards gas absorption and chemical reaction are considered to be important.

2. The superficial velocity of gas being substantially high, it is assumed that bubbles in both the sections are spherical and not polyhedral in foam section as reported by previous investigators observed specially at low gas velocities.

3. The storage section liquid is assumed to be well-stirred.

4. Change in bubble size with foam height is assumed to be negligible as the feed gas mixture contains more than 99 percent inert.

5. The reaction conditions maintained for the gas-liquid system are such that the reaction kinetics conforms to an irreversible fast pseudo-first order reaction kinetics.

6. Concentration of surfactant being very small, the resistance to mass transfer due to the presence of surfactant is neglected. This simplifies the model greatly.

Transient values of conversion in the reactor are calculated using the expression:

$$X(t) = \frac{C_B(0) - C_{Bm}(t)}{C_B(0)} \times 100 \qquad (3.42)$$
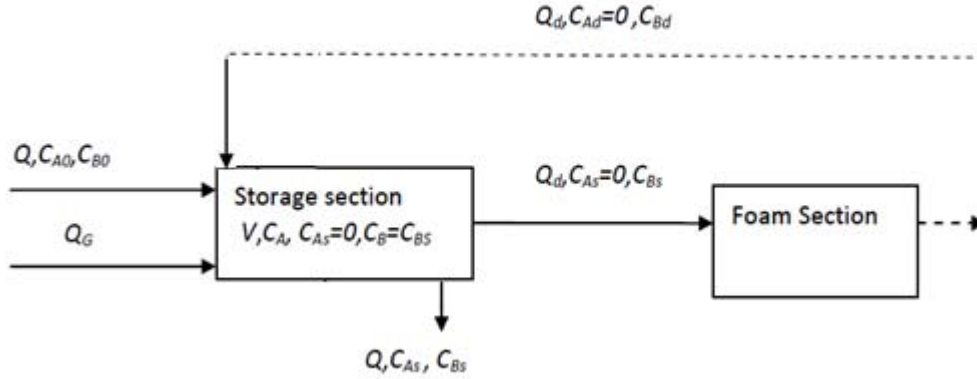
Figure 3.2 Single stage model of a foam bed reactor for gas-liquid system

$C_{Bm}(t)$ has been defined in equation (3.61)

(i) Gas absorption in the storage section

Rate of consumption of sodium hydroxide in the storage section of the foam-bed reactor can be calculated using the same equation as that used for the bubble column described above.

However, as part of the reactant solution constitutes the foam section, for identical operating conditions, volume of liquid phase reactant in the storage section is reduced and the calculations for the rates of consumption of sodium hydroxide are performed considering the appropriate values of the variables and parameters, viz., V_{ls}, h_d, etc in the storage section.

Volume of liquid in the storage section, $V_{l,store}$, is obtained using the expression,

$$V_{l,store} = V_l - \left(H_f\right)\left(a_c\right)\left(\overline{\varepsilon_l}\right) \qquad (3.43)$$

Concentration of B in the storage section after time step Δt is obtained using equation (3.16) for this case also but conversion of B in the storage section alone after a given time of reactor operation is expected to be less compared to the bubble column

because of the reduced volume of liquid and thus lower volume of total gas-liquid interfacial area in the dispersion.

$$C_{Bs}{}^{i+1} = C_{Bs}{}^{i} - [(R_{BA})\{k_l C_A{}^{*} \sqrt{(1 + \frac{D_A \lambda}{k_l{}^2})}\}(a^t{}_{storage})(\Delta t)] \qquad (3.44)$$

$$\text{where, } a^t{}_{storage} = (n_{storage})(a_b) \qquad (3.45)$$

(ii) Gas absorption in the foam section

The rate of gas absorption in the foam section is entirely by molecular diffusion from a very low concentration of CO_2 in air. The column of foam immediately above the liquid surface of the storage section is pushed up by the new foam bubbles generated subsequently. The column of foam moves upwards in a plug flow manner and gas absorption occurs from the limited gas pockets into the adjacent foam films. Hence, the mechanism of gas absorption from bubbles into foam films is approximated, for development of models, as *absorption into quiescent liquids*. For a reasonably high concentration of NaOH in solution, its reaction with CO_2 has been shown to be fast pseudo-first order (Biswas and Kumar, 1981). For the experimental conditions used in the present study this has been shown to be perfectly applicable as well (Appendix 3A). Concentration of CO_2 in the feed gas being less than 1% and the fast reaction occurs in a zone close to the gas-liquid interface, it is assumed that all the absorbed CO_2 reacts then and there with the NaOH in solution and its concentration in the drainage stream, C_{Ad}, is zero.

Pseudo-steady state material balance over a small time interval *Δt* for component *B* arround the foam section

$$0 = \begin{Bmatrix} Rate\,of\,B\,into\,the\,foam\,section \\ from\,storage \end{Bmatrix} + \begin{Bmatrix} Rate\,of\,B\,generated\,in\,foam \\ section \end{Bmatrix}$$
$$- \begin{Bmatrix} Rate\,of\,B\,draining\,out\,of\,the\,foam \\ section\,and\,entering\,into\,the\,storage \end{Bmatrix} - \{Rate\,of\,B\,reacted\,in\,the\,foam\,section\}$$

$$(3.46)$$

(i) *Moles of B reacted in the foam section per unit time may be calculated as follows:*

A pseudo-steady state material balance for component *A* in the foam section over a small time step Δt is written to obtain *the rate of absorption of A in the foam section.*

Moles A absorbed per unit time =

$$\left\{\frac{area}{bubble}\right\}\{no\ of\ bubbles\ \}\left\{\frac{moles\quad A\ absorbed}{(time\ )(area\ )}\right\} \tag{3.47}$$

$$n_{A,abs} = \left\{4\pi r_{b0}^2\right\}\left\{a_c\ H_f\ \overline{\varepsilon_G}\ /V_{b0}\right\}\left(-D_A\ \frac{dC_A}{dx}\right)_{x=0} \tag{3.48}$$

Moles of *B* reacted in the foam section per unit time is therefore obtained, considering the assumption that all the CO_2 absorbed in the foam section reacts then and there, as

$$n_{B,abs} = (R_{BA})\left\{4\pi r_{b0}^2\right\}\left\{a_c\ H_f\ \overline{\varepsilon_G}\ /V_{b0}\right\}\left(-D_A\ \frac{dC_A}{dx}\right)_{x=0} \tag{3.49}$$

There being no *B* generated in the foam section, equation (3.46) reduces to

$$Q_d.C_{Bd} = Q_d.C_{Bs} - R_{BA}\left[Q_d.C_{As} + (4\pi r_0^2)\left(-D_A\ \frac{dC_A}{dx}\right)_{x=0}\left(a_c.H_f\ \overline{\varepsilon_G}\ /V_{b0}\right)\right] \tag{3.50}$$

C_A in eqn. (3.46) implies concentration of absorbed *A* in the liquid film close to the gas-liquid interface while C_{As} that in the bulk. The quantity Q_dC_{As} in the second term on the rhs of equation (3.50) represents moles of *A* entering into the foam section from storage by flow in the form of dissolved CO_2 in the foam films and reacts with *B* leading to its depletion. As already stated, the reaction of dissolved CO_2 with OH^- ions, in the present work, follows fast pseudo-first order reaction kinetics. The reaction occurs entirely in a zone close to the interface and, under this condition it appears fairly accurate to assume that all the *A* absorbed in the storage section get reacted and none of it goes to foam section, i.e., $C_{As}=0$. The other quantity in the second term also indicates depletion of *B* by reaction with *A* absorbed in the foam section as indicated by equation (3.49).

With this simplification, rearrangement of equation (3.50) yields

$$C_{Bd} = C_{Bs} - (R_{BA}/Q_d)(4\pi r_{bo}^2)\left(-D_A \frac{dC_A}{dx}\right)_{x=0} \left(a_c.H_f \overline{\varepsilon_G}/V_{b0}\right)$$ (3.51)

(ii) An algebraic expression in place of $\left(-D_A \dfrac{dC_A}{dx}\right)_{x=0}$ *for substitution in equation*

(3.51)

An working equation for estimation of diffusive flux of component *A* is obtained by simultaneous solution of the diffusion reaction equations:

$$\frac{\partial C_A}{\partial t} = D_A \frac{\partial^2 C_A}{\partial x^2} - k_2 C_A C_B$$ (3.52)

$$\frac{\partial C_B}{\partial t} = D_B \frac{\partial^2 C_B}{\partial x^2} - R_{BA} k_2 C_A C_B$$ (3.53)

C_A and C_B are concentrations of *A* and *B*, respectively, in the liquid film. For the situation, when component *B* diffuses towards the surface fast enough to prevent its depletion by reaction, the concentration of *B* every where remains the same at C_B and the equations (3.52) and (3.53) reduce to

$$\frac{\partial C_A}{\partial t} = D_A \frac{\partial^2 C_A}{\partial x^2} - \lambda C_A$$ (3.54)

$$\frac{\partial C_B}{\partial t} = D_B \frac{\partial^2 C_B}{\partial x^2} - R_{BA} \lambda C_A$$ (3.55)

where, λ is the pseudo-first order reaction rate constant. That the reaction occurs as per pseudo-first order kinetics, has been stated in §3.1.1 through estimation of *Ha, Ea/Ha* and k_{la}/λ .

The initial and boundary conditions for solution of equations (3.54) and (3.56) are

$$
\begin{array}{llll}
C_A = C_{A0} = 0, & C_B = C_{Bs}, & x \rangle 0, & t = 0 \\[2mm]
C_A = C_A^*, & \dfrac{\partial C_B}{\partial x} = 0, & x = 0, & t \rangle 0 \\[2mm]
C_A = C_{A0} = 0, & C_B = C_{Bs}, & x = \infty, & t \rangle 0
\end{array}
$$ (3.56)

Concentration C_{Bs} shown in the B. C. (3.56) pertaining to that within the film and the latter considered identical to that in the liquid bulk remains valid for a small time

interval Δt and is used for solution of eqns. (3.54-3.55). After each time step, the new value of C_{Bs} is calculated using equation (3.60) which then becomes the new value for C_{Bs} in the B. C. (3.56) for solution of eqns. (3.54-3.55) and so on.

The rate of absorption of component A accompanied by chemical reaction according to pseudo-first order kinetics has been obtained by solution of equations (3.54) and (3.55) subject to conditions (3.56) as,

$$- D_A (\frac{dC_A}{dx})_{x=0} = C_A^* (\sqrt{D_A k_2 C_{Bs}})$$
(3.57)

Substituting this in equation (3.51), the concentration of B in the drainage stream is obtained as,

$$C_{Bd} = C_{Bs} - (\frac{R_{BA}}{Q_d})(4\pi r_{b0}^2) C_A^* (\sqrt{D_A k_2 C_{B0}})(\frac{a_c . H_f \overline{\varepsilon_G}}{V_{b0}})$$
(3.58)

Concentration of B in the drainage stream after a small time step Δt can therefore be obtained as,

$$C_{Bd}^{i+1} = C_{Bs}^i - (\frac{R_{BA}}{Q_d})(4\pi r_{b0}^2) C_A^* (\sqrt{D_A k_2 C_{B0}})(\frac{a_c . H_f \overline{\varepsilon_G}}{V_{b0}})(\Delta t)$$
(3.59)

where, C_{Bs}^i is the concentration of B in the storage section at time 't' that ***enters the foam section*** and C_{Bd}^{i+1} is the concentration of B draining from the foam section at the end of a time step Δt, i.e., at time $t + \Delta t$.

Concentration of B in the storage section at the end of a time step Δt is calculated using the material balance equation:

$$C_{Bm}^{i+1} = \frac{V_{l,store} C_{Bs}^{i+1} + [Q_d(\Delta t)] C_{Bd}^{i+1}}{V_{l,store} + Q_d(\Delta t)}$$
(3.60)

A volume of liquid in the storage, $V_{l,store}$ with concentration C_{Bs}^{i+1} get mixed up with $Q_d . \Delta t$ volume of draining liquid of concentration C_{Bd}^{i+1} to produce a total volume of $(V_{l,store} + Q_d . \Delta t)$ with the resultant concentration C_{Bm}^{i+1}. However, for estimation of conversion, X, in the foam-bed reactor, entire volume of reaction mixture is required to be included. Equation (3.56) should therefore be written as,

$$C_{Bm}^{\ i+1} = \frac{V_{l,store} C_{Bs}^{\ i+1} + V_l^{\ foam} C_{Bd}^{\ i+1}}{V_{l,store} + V_l^{\ foam}} \tag{3.61}$$

The entire volume of reaction mixture comprising of $V_{l,store}$ and $V_l^{\ foam}$ being assumed to mix after each time step, use of equation (3.60) leads to some error in the estimation of C_{Bm}, actual volume of liquid draining to the storage section in the small time step Δt being much less than the total volume of liquid contained in the foam section. However, maximum volume of liquid in the foam section being only about 14% of the total volume of liquid phase reactant and considering the difference of the total moles of *B* reacted in the two sections of the reactor in the time step Δt, error is considered to be negligible without significant loss in accuracy.

3.2 Mathematical model for gas-liquid-solid contactor- Absorption of CO_2 in hydrated lime slurry

3.2.1 Slurry Reactor: $Ca(OH)_2$ slurry-lean CO_2 system

Carbonation of hydrated lime for the manufacture of precipitated calcium carbonate is an industrially important process, chosen for the present studies. Carbon dioxide gas, when passed through calcium hydroxide slurry, precipitated calcium carbonate is produced. The overall process of carbonation of lime and the detailed reaction mechanism (Juvekar and Sharma, 1973) have been described in §2.1. Steps (iv) and (v) of eqn. (2.1) are instantaneous, and the rate controlling step could be the dissolution of solid, step (i) and / or simultaneous absorption and reaction of carbon dioxide gas, steps (ii) and (iii).

The slurry reactor in the present work is operated in a semi-batch mode. A batch of liquid is fed to the reactor and gas fed continuously. The feed slurry contains a saturated solution of hydrated lime (component *B*) in water and its particles remaining in suspension. Mixture of carbon-dioxide gas (component *A*) and air at different compositions for different experimental runs is fed continuously from the bottom of the reactor. A column of foam is generated and reaction occurs both in the pool of liquid (storage section) and in the liquid films surrounding the foam bubbles. Reaction between the lime present in solution and the dissolved gas is assumed to be of second order (Sada et al., 1977).
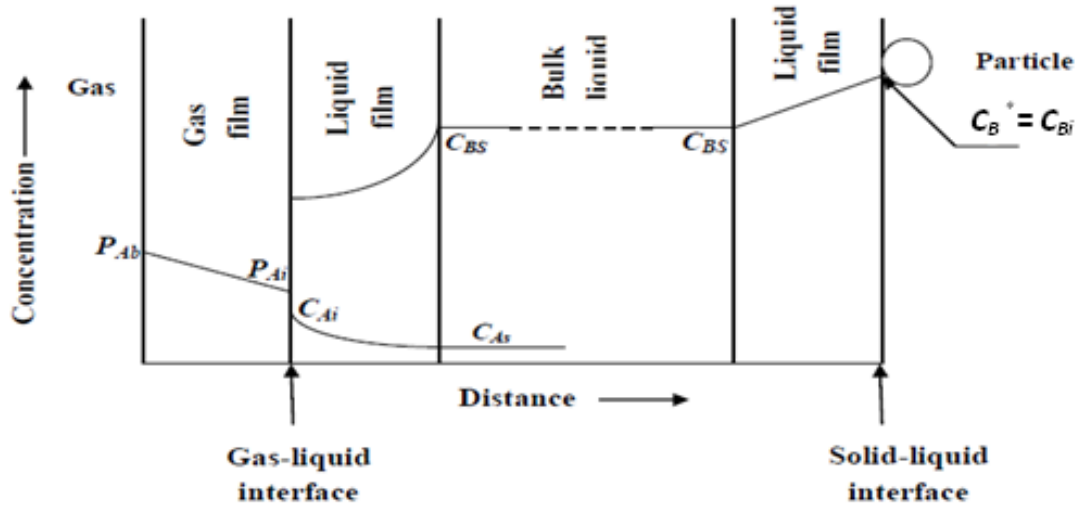
Figure 3.3 Concentration profiles of dissolved *A* & *B* in the bubble column-/foam-bed slurry reactors

Immediately after the reaction commences, the concentration of component *B* in the solution i.e. in the bulk liquid starts to drop below the saturation concentration (Figure 3.3). But, its concentration in the liquid at the particle surface corresponds to its solubility, C_B^* or C_{Bi}. As the reaction proceeds, this driving force causes transport of dissolved *B* from the solid-liquid interface to the bulk liquid. Consequently, with the propagation of reaction, more and more solids dissolution occurs as long as the solid particles are present in the liquid. Thus, a continuous supply of component *B* from solid to the solution is established and the above reaction proceeds at a sufficiently rapid rate. A detailed mathematical analysis is presented below.

The extent of time-dependent conversion of the reactants in a semi-batch reactor, for different values of the operating variables, is a measure of the performance of the reactor. For the case of carbonation of hydrated lime (*B*) slurry using carbon-dioxide (*A*) gas, percentage conversion (*X*) of the dissolved species *B* at any time '*t*' may be written as

$$X = \frac{m_B^T(0) - m_B^T(t)}{m_B^T(0)} \times 100 \tag{3.62}$$

$$= \frac{C_B^T(0) - C_B^T(t)}{C_B^T(0)} \times 100 \, ,$$

in mass and molar concentration units, respectively. Total loading of *B*, $C_B^{\ T}(t)$, is required for calculation of conversion as *B* remains both in liquid phase due to dissolution as well as suspended solid particles and there exists a continuous transfer of *B* from solid to liquid phase and depletion of *B* from solution by reaction. $C_B^{\ T}(t)$ in equation (3.62) is, therefore, calculated using an unsteady state material balance equation for component *B* in the slurry. The pertinent equation for a slurry reactor incorporating sparingly soluble fine reactive particles of component *B* has been reported by Jana and Bhaskarwar (2010). Instantaneous value of its total molar loading can be obtained as

$$C_B^{\ T}(t) \ = C_{Bs}(t) + \sum_{k=1}^{z} (n_{pk} \frac{\pi \, d_{pk}(t)^3}{6}) \frac{\rho_B}{M_B} \frac{V_{sl}}{V_l} \tag{3.63}$$

Molar concentration of dissolved *B* at any time in the storage is assumed to be equal to that in foam section (assumption 3, § 3.2.2), i.e., $C_{Bs}(t) = C_B^f(t)$. Number of particles, n_{pk}, is assumed to remain unchanged over the entire period of reactor operation.

The first term on the right hand side of Eqn. (3.63) indicates concentration of *B* dissolved in the liquid at any time 't' while the second one signifies the molar loadings of suspended particles of *B* at the same instant in the slurry. Instantaneous values of $C_B^{\ T}(t)$, $C_{Bs}(t)$, and $d_{pk}(t)$ can be calculated by solving the unsteady-state material-balance equations for components *A* and *B* in solution, and the mass balance for the suspended particles of component *B*, written for a semi-batch operation of the slurry or slurry-foam reactor.

Bubble column slurry reactor

For absorption of a lean gas in a liquid, the overall liquid-phase mass transfer coefficient can be estimated using the expression,

$$\frac{1}{K_l} = \frac{1}{k_l} + \frac{1}{H \ k_G} \tag{3.64}$$

In equation (3.64) the units of k_G and H are kmol m^{-2} s^{-1}(N/m^2)$^{-1}$ and (N/m^2) (kmol/ m^3)$^{-1}$, respectively. When applied to the lean CO_2-water system, solubility of CO_2 in water being substantially low, liquid phase mass-transfer ***resistance*** is much larger

than that in the gas phase, i.e., $(\dfrac{1}{k_l} >> \dfrac{1}{H\, k_G})$. It follows that, $K_l \approx k_l$ (Ramachandran and Sharma, 1969). For the gas-liquid-solid system, 10-50% CO_2 in air has been used for experimental studies. A detailed justification of neglecting gas phase resistance has been provided in § 3.1.1. The value of k_l has been calculated using the correlation given by Sada et al. (1985). *In the following treatment, however, concentration difference on only one side of the interface along with the film coefficient, k_l, has been used for establishing the material balance equations.*

The material-balance equation for the absorbed gas-phase component A (i.e. CO_2) can be written assuming the slurry in the reactor to be well mixed as:

$$V_l \frac{dC_{As}}{dt} = k_l^{0} a_b (C_{Ai} - C_{As})V_l E_a - k_2 C_{As} C_{OH^-} V_l \qquad (3.65)$$

The dissolution of one g mole of lime produces two g ions of hydroxide (OH⁻) ions. Equation (3.65) can therefore be rewritten as:

$$V_l \frac{dC_{As}}{dt} = k_l^{0} a_b (C_{Ai} - C_{As})V_l E_a - k_2 C_{As}(2C_{Bs})V_l \qquad (3.66)$$

The first term of equation (3.66) on its right hand side represents the molar rate of absorption of carbon-dioxide gas in the slurry, while the rate of loss of moles of absorbed carbon-dioxide by reaction with the hydroxide ions is represented by the second term. k_2 is the second-order reaction rate constant for the reaction between OH⁻ ions and absorbed carbon-dioxide in the liquid.

Equation (3.66) simplifies to:

$$\frac{dC_{As}}{dt} = k_l^{0} a_b (C_{Ai} - C_{As}) E_a - 2 k_2 C_{As} C_{Bs} \qquad (3.67)$$

Likewise, the material balance equation for component B dissolved in the liquid can be written as:

$$V_l \frac{dC_{Bs}}{dt} = k_{sl} a_p (C_{Bi} - C_{Bs})V_{sl} - R_{BA} k_2 C_{As}(2C_{Bs})V_l \qquad (3.68)$$

Equation (3.68) can be simplified as follows:

$$\frac{dC_{Bs}}{dt} = k_{sl} a_p (C_{Bi} - C_{Bs})(V_{sl}/V_l) - 2k_2 R_{BA} C_{As} C_{Bs} \tag{3.69}$$

R_{BA} is the stoichiometric factor for the overall reaction between the absorbed carbon-dioxide gas and dissolved hydrated lime (moles lime reacted/ mole of CO_2 gas).

Volume of particles is reduced due to its dissolution in slurry and the reduced solid-liquid interfacial area cause a decrease in the rate of its dissolution and thereby the rate of supply of component B to the solution. Rate of depletion in the concentration of component B due to its consumption by reaction is thereby reduced/ nullified. Rate of decrease in the volume of particles (presented here in terms of mass, density being constant) can be written as,

$$\frac{d(\sum_k n_{pk} v_{pk})\rho_B}{dt} = -\sum_{k=1}^{z} (n_{pk} \pi d_{pk}^2) k_{sl} (C_{Bi} - C_{Bs}) M_B \tag{3.70}$$

The initial conditions for solution of equation (3.67), (3.69) and (3.70) are,

$$At \quad t = 0, \quad C_{As} = 0, \quad C_{Bs} = C_{B0} = C_{Bi} \quad \& \quad v_{pk} = v_{pk0} \tag{3.71}$$

The ordinary differential equations (3.67), (3.69) & (3.70) are solved simultaneously using fourth-order Runge-Kutta method subject to initial conditions (3.71) to obtain C_{As}, C_{Bs} and v_{pk} as functions of time and conversion, X, is estimated using eqn. (3.62).

Estimation of parameter values

For a slurry reactor, the correlation for liquid-phase volumetric mass-transfer coefficient has been given by Sada et al. (1985) as

$$k_l^0 a_b = 0.022 (u_G)^{0.86} \tag{3.72}$$

Gas hold-up, $\bar{\varepsilon}_G$, for absorption of carbon-dioxide gas in lime slurry is obtained using the correlation given by Capuder and Koloini (1984)

$$\frac{\bar{\varepsilon}_G}{1 - \bar{\varepsilon}_G} = 0.083 \left(\frac{u_G^3 \rho_l^2}{\mu_{eff}(\rho_l - \rho_G)g}\right)^{0.25} \tag{3.73}$$

The value of μ_{eff}, required for solution of equation (3.73) is estimated using the following correlation:

$$\mu_{eff} = K\,(40\,u_G)^{n'-1} \tag{3.74}$$

The constants n' and K are estimated by fitting the experimental data of Capuder and Koloini (1984).

The instantaneous value of enhancement factor for the present system is written as:

$$E_i = \frac{k_{lr}}{k_l} = \sqrt{\frac{D_A\,\lambda}{D_A\,/\,\pi.t_{cs}}} = \sqrt{\pi\lambda t_{cs}} = \left(\sqrt{\pi\lambda d_{b0}\,/\,u_{swarm}}\right) \tag{3.75}$$

The average value of the enhancement factor, E_a, can therefore be obtained as

$$E_a = \frac{1}{t_{cs}}\int_0^{t_{cs}} E_i\,dt_{cs} = \frac{2}{3}\left(\sqrt{\pi\lambda\,d_{b0}\,/\,u_{swarm}}\right) \tag{3.76}$$

The other parameter values, *viz.*, d_{b0}, V_{b0} and u_{swarm} have been calculated using the equations (3.30) to (3.32), respectively.

3.2.2 Slurry-foam reactor: Ca(OH)$_2$ slurry-lean CO$_2$ system

Configuration of the Single stage model of a slurry-foam reactor has been shown in Fig. 3.4. The assumptions made in the development of the model are as follows:

1. Volume fraction of solids in slurry in the storage and foam sections is assumed to have the same value in both the sections.

2. Vaporization of liquid from the film surfaces is assumed to be negligible.

3. With the decrease in the concentration of OH$^-$ ions due its reaction with absorbed CO$_2$ in solution, more of lime gets dissolved in the liquid and the concentration of OH$^-$ ions in the liquid phase remains reasonably constant (quasi-stationary state). The reaction between OH$^-$ and CO$_2$ being fast and the dissolution rate of lime being small (stagnant foam films), it is assumed that all the lime dissolved in foam section gets reacted in this section such that the concentration of dissolved calcium hydroxide in the draining liquid from the foam section remains same as that entered into the foam

section (pseudo-first order reaction in the foam section, and quasi-stationary state, i.e. consequently, $C_{Bd} = C_{Bs}$).

4. The superficial velocity of gas being substantially high, it is assumed that bubbles in both the sections are nearly spherical and idealized as spherical bubbles. The bubbles are not considered polyhedral in foam section as reported by previous investigators at low gas velocities. This assumption simplifies the model without significant loss in accuracy.

5. The concentration of CO_2 gas being substantially low, the change in bubble size as it rises from bottom to top of the column is negligible.

6. Coalescence of bubbles both in the storage- and foam sections is assumed to be negligible.

7. The reaction is assumed to be pseudo-first order in the foam section. The reaction between A and B is treated as of second order in the storage section on account of the much higher time scale of reactor operation (Sada et al., 1977). The concentration profiles in the storage section are shown in Fig. 3.3.

As for the slurry reactor, the performance of the slurry-foam reactor can also be evaluated by conversion defined in equations (3.62 - 3.63). However, in this case C_{Bs} and d_{pk} are to be estimated by considering the conversions in both the storage and foam sections simultaneously.
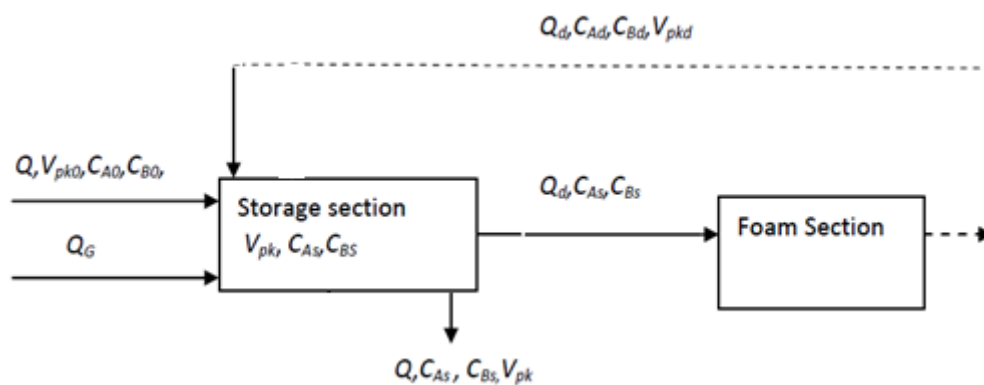
Figure 3.4: Single stage model of a slurry foam-bed reactor
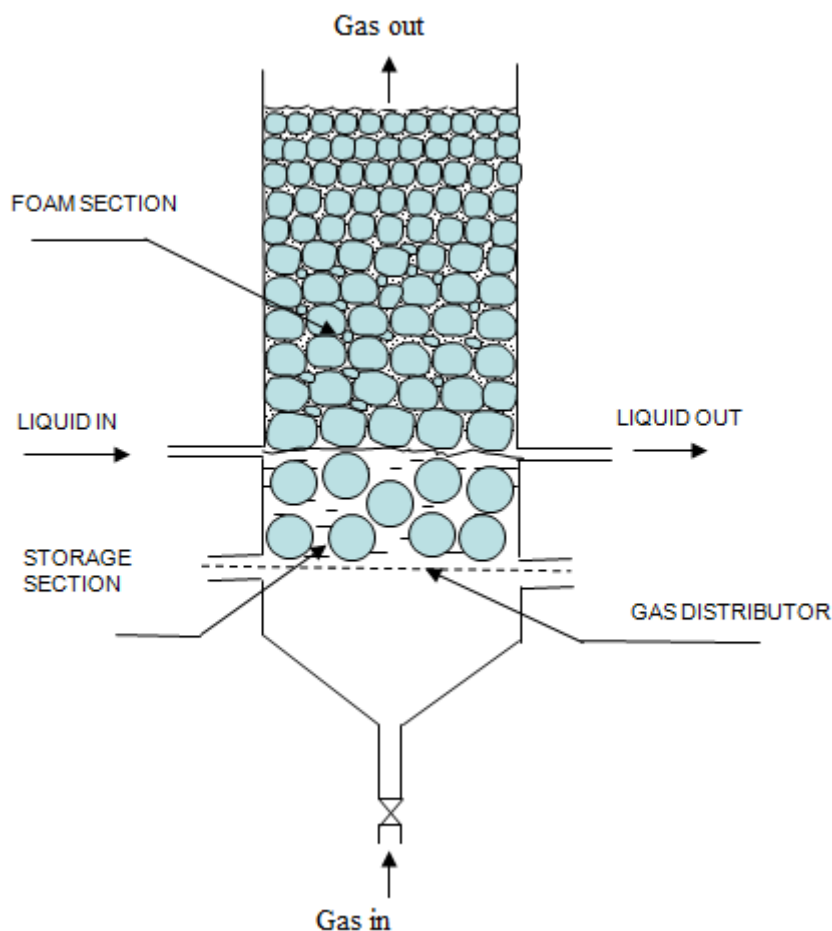
Figure 3.5: A sketch of foam bed reactor

The material-balance equations for the two components, A (CO_2) & B (hydrated lime), and mass balance equation for the particles in slurry in both the storage and foam sections are needed for the development of a slurry foam reactor model. The instantaneous concentration of component A in the drainage stream from the foam to the storage section is required for component A balance over the storage section as the exit stream from the foam section enters the storage section. Rate of reaction between $Ca(OH)_2$ & CO_2 depends on the rate of dissolution of lime or that of absorption of CO_2 and therefore a mass-transfer controlled process (Juvekar and Sharma, 1973). $Ca(OH)_2$ being sparingly soluble, concentration of OH^- in solution remains at low level and concentration of absorbed carbon-dioxide is therefore no longer considered negligible/ zero in the bulk of the liquid. The expression for instantaneous concentration of component A is obtained by writing a pseudo-steady state material balance equation for component A over the foam section (Fig. 3.4) as:

$$0 = \begin{Bmatrix} moles\ of\ dissolved\ A \\ in\ from\ storage\ into\ foam \\ sec\,tion\ per\ unit\ time \end{Bmatrix} + \begin{Bmatrix} moles\ of\ A\ absorbed\ in \\ foam\ per\ unit\ time \end{Bmatrix}$$

$$- \begin{Bmatrix} moles\ of\ dissolved\ A\ out \\ from\ foam\ to\ storage \\ sec\,tion\ per\ unit\ time \end{Bmatrix} - \begin{Bmatrix} moles\ of\ A\ reacted\ in \\ foam\ per\ unit\ time \end{Bmatrix}$$

(3.77)

Eqn. (3.77) can be rearranged to the following:

$$\begin{Bmatrix} moles\ of\ dissolved\ A\ out \\ from\ foam\ to\ storage \\ sec\,tion\ per\ unit\ time \end{Bmatrix} = \begin{Bmatrix} moles\ of\ dissolved\ A \\ in\ from\ storage\ into\ foam \\ sec\,tion\ per\ unit\ time \end{Bmatrix} + \begin{Bmatrix} moles\ of\ A\ absorbed\ in \\ foam\ per\ unit\ time \end{Bmatrix}$$

$$- \begin{Bmatrix} moles\ of\ A\ reacted\ in \\ foam\ per\ unit\ time \end{Bmatrix}$$

(3.78)

$$Q_d.C_{Ad} = Q_d.C_{As} + (\frac{k_c}{RT}\Delta p)(4\pi r_{b0}^2)(\pi r_c^2 H_f \overline{\varepsilon_G}\ /V_{b0}) - \frac{\left[\sum_{k=1}^{z} n_{pk}(v_{pk} - v_{pkd})\right]V_{foam}^l \rho_B}{M_B t_c^* R_{BA}}$$

(3.79)

where the quantities, $(\frac{k_c}{RT}\Delta p)(4\pi r_{b0}^2)$ and $\frac{\pi r_c^2 H_f \overline{\varepsilon_G}}{V_{b0}}$ in the second term on the right-

hand side of the above equation accounts for the moles of A absorbed per bubble per

unit time and number of bubbles in the foam column respectively. Average bubble

volume in the foam column has been assumed to be V_{b0} considering that the decrease

in bubble volume due to absorption of component A from the lean gaseous mixture

and its increase due to the reduction in the hydrostatic head as the bubbles rise through

the storage and foam sections are both substantially small and effect of one nullify that

of the other. In the third term, the quantity $\dfrac{(\sum_k n_{pk}V_{pk} - V_{pkd}))V_l^{foam}.\rho_B}{M_B}$ indicates

the moles of B reacted during the contact time t_c^* in foam section.

Rearranging equation (3.79), we obtain

$$C_{Ad} = C_{As} + k_c \left(\frac{\Delta p}{RT}\right)(4\pi r_{b0}^2)\frac{\pi r_c^2 H_f \overline{\varepsilon_G}}{Q_d V_{b0}} - \frac{(\sum\limits_{k=1}^{z} n_{pk}(v_{pk} - v_{pkd})).V_l^{\text{foam}}.\rho_B}{Q_d.M_B.t_c^* R_{BA}} \qquad (3.80)$$

Substituting the value of $k_c = \dfrac{3.29 D_G}{r_{b0}}$ (Bhaskarwar and Kumar, 1995) in equation (3.80), one obtains an expression for C_{Ad} as:

$$C_{Ad} = C_{As} + \left(\frac{3.29 \, D_G}{r_{b0}}\right)\frac{(\Delta p)}{RT}(4\pi r_{b0}^2)\frac{\pi r_c^2 H_f \overline{\varepsilon_G}}{Q_d V_{b0}} - \frac{(\sum\limits_{k=1}^{z} n_{pk}(v_{pk} - v_{pkd})).V_l^{\text{foam}}.\rho_B}{Q_d.M_B.t_c^* R_{BA}} \qquad (3.81)$$

(i) **Component *A* balance over the storage section** (Figure 3.4):

$$\frac{d(V_l C_{As})}{dt} = Q.C_{A0} + V_l(k_l^0 a_b)(C_{Ai} - C_{As})E_a + Q_d C_{Ad} - Q_d C_{As} - Q.C_{As} - k_2 C_{As}(2C_{Bs})V_l$$

$$(3.82)$$

For a semi-batch foam bed reactor, there being no inlet and exit streams, $Q = 0$ and equation (3.82) simplifies to:

$$\frac{d(C_{As})}{dt} = (k_l^0 a_b)(C_{Ai} - C_{As})E_a + (Q_d/V_l)(C_{Ad} - C_{As}) - 2k_2 C_{As} C_{Bs} \qquad (3.83)$$

(ii) **Component *B* balance over the storage section:**

A material balance equation for component *B* can be written similar to that of component *A*:

$$\frac{d(V_l C_{Bs})}{dt} = Q.C_{B0} + Q_d C_{Bd} - Q.C_{Bs} - Q_d C_{Bs} + V_{sl}\sum\limits_{k=1}^{z} n_{pk}(\pi d_{pk}^2)(k_{sl})(C_{Bi} - C_{Bs})$$

$$- 2R_{BA}k_2 C_{As} C_{Bs} V_l$$

$$(3.84)$$

From assumption 5 above the conditions, $C_{Bd} = C_{Bs}$ (quasi-stationary state) and $Q = 0$ (semi-batch reactor) are substituted in equation (3.84) to obtain:

$$\frac{d(C_{Bs})}{dt} = \sum\limits_{k=1}^{z} n_{pk}(\pi d_{pk}^2)(k_{Sl})(C_{Bi} - C_{Bs})\frac{V_{sl}}{V_l} - 2R_{BA}k_2 C_{As} C_{Bs} \qquad (3.85)$$

(iii) Mass balance of particles in slurry:

There being a continuous phase transfer of component B from solid to solution, mass balance for $Ca(OH)_2$ particles in the slurry is required to be written and included in simultaneous estimation of transient concentrations of components A and B followed by conversion of B. The desired mass balance equation for $Ca(OH)_2$ particles in the slurry can be written as:

$$\frac{d\sum_{k=1}^{z}(V_{sl}n_{pk}V_{pk})\rho_B}{dt} = \begin{bmatrix} Q\sum_{k=1}^{z}\left(n_{pk}V_{pk0}\right)+Q_d\sum_{k=1}^{z}\left(n_{pk}V_{pkd}\right)- \\ Q\sum_{k=1}^{z}\left(n_{pk}V_{pk}\right)-Q_d\sum_{k=1}^{z}\left(n_{pk}V_{pk}\right) \end{bmatrix}\rho_B$$
$$-V_{sl}\sum_{k=1}^{z}\left(n_{pk}\pi d_{pk}^{\ 2}\right)k_{sl}\left(C_{Bi}-C_{Bs}\right)M_B \qquad (3.86)$$

For a semi-batch foam reactor, $Q = 0$. Substituting this in equation (3.86) and simplifying one gets:

$$\frac{d\left(\sum_{k=1}^{z}n_{pk}V_{pk}\right)}{dt} = -\left(Q_d\big/V_{sl}\right)(\sum_{k=1}^{z}n_{pk}V_{pk}-\sum_{k=1}^{z}n_{pk}V_{pkd})-\sum_{k=1}^{z}\left(n_{pk}\pi d_{pk}^2\right)\left(k_{sl}\right)\left(C_{Bi}-C_{Bs}\right)\frac{M_B}{\rho_B}$$

$$(3.87)$$

iv) Estimation of V_{pkd} in terms of V_{pk}

As per the assumption at Sr No. 3 that all the lime dissolved in foam section gets reacted in this section such that the concentration of dissolved calcium hydroxide in the draining liquid from the foam section remains same as that entered into the foam section (pseudo-first order reaction, and quasi-stationary state, i.e. consequently, $C_{Bd} = C_{Bs}$). Equating the mass of lime dissolved in the foam section to that reacted in this section, one gets,

$$\sum_{k=1}^{z}V_{sl}^{foam}n_{pk}(V_{pk}-V_{pkd})\rho_B = (2k_2C_A'C_{Bs})(R_{BA}M_B)t_c^*.V_l^{foam} \qquad (3.88)$$

The values of C_A' & t_c^* have been calculated using the following expressions

$$C_A' = \left[\frac{C_{As}+C_{Ad}}{2}\right]. \qquad (3.89)$$

The value of t_c^* has been given by Biswas and Kumar (1981).

$$t_c^* = \frac{H_f \, \pi \, r_c^2 \, (1 - \overline{\varepsilon_l})}{Q_G}$$ (3.90)

A second equation, that obviates the need of a value of v_{pkd}, for estimation of C_{Ad} is written below for obtaining the value of $C_A^/$. With his objective, a pseudo-steady state material balance for component A over the foam section may be written as,

$$Q_d C_{Ad} = Q_d C_{As} + (H_f \pi r_c^2 \overline{\varepsilon_G})(4\pi r_{b0}^2)[k_c(P_{Ab} - P_{Ai})] - (2k_2 C_{As} C_{Bs})V_l^{foam}$$ (3.91)

The working equation for $C_A^/$ can be obtained using eqns. (3.89) and (3.91) along with the relation for $k_c = \dfrac{3.29 D_G}{RT}$:

$$C_A^{\,\prime} = C_{As} + \left[(H_f \pi r_c^2 \overline{\varepsilon_G} / V_{b0})(4\pi r_{b0}^2)[\frac{3.29 D_G}{RT}(P_{Ab} - P_{Ai})] - (2k_2 C_{As} C_{Bs})V_l^{foam} \right] / 2(Q_d)$$ (3.92)

Rearrangement of equation (3.88) yields

$$\sum_{k=1}^{z} n_{pk} V_{pkd} = \sum_{k=1}^{z} n_{pk} V_{pk} - \sum_{k=1}^{z} 2k_2 C_A^{\,\prime} C_{Bs} R_{BA} \frac{M_B}{\rho_B} t_c^* \cdot \left(\frac{V_l^{foam}}{V_{sl}^{foam}} \right)$$ (3.93)

Substituting for $\displaystyle\sum_{k=1}^{z} n_{pk} V_{pkd}$ from equation (3.93) into equation (3.87), we obtain

$$\frac{d\left(\displaystyle\sum_{k=1}^{z} n_{pk} V_{pk} \right)}{dt} = -\left(Q_d \Big/ V_{sl} \right) \sum_{k=1}^{z} \left[2k_2 C_A^{\,\prime} C_{Bs} R_{BA} \frac{M_B}{\rho_B} t_c^* \cdot \left(\frac{V_l^{foam}}{V_{sl}^{foam}} \right) \right] - \sum_{k=1}^{z} \left(n_{pk} \pi d_{pk}^2 \right)(k_{sl})(C_{Bi} - C_{Bs}) \frac{M_B}{\rho_B}$$

(3.94)

$C_A^/$ in equation (3.94) is to be evaluated using equation (3.92). For the special case of no foam in the column, t_c^* equals zero and equation (3.94) reduces to equation (3.70), i.e. to the mass balance for particles in a bubble column slurry reactor.

In a similar manner, substituting the expressions for C_{Ad} from equation (3.81) into equation (3.83) and simplifying one gets,

$$\frac{dC_{As}}{dt} = \left(k_l^0 . a_b\right)\left(C_{Ai} - C_{As}\right).E_a + \left(\frac{3.29\, D_G}{r_{b0}}\right)\frac{\Delta p}{RT}\left[\left(4\pi r_{b0}^2\right)\left(\frac{\pi r_c^2 H_f \bar{\varepsilon}_g}{V_{b0}}\right)\right]\frac{1}{V_l}$$

$$-\frac{\left(\sum_k n_{pk}\pi d_{pk}^2\right)k_{sl}\left(C_{Bi} - C_{Bs}\right).V_l^{foam}}{V_l.R_{BA}} - 2k_2 C_{As} C_{Bs}$$

$$(3.95)$$

The product, $(4\pi r_{b0}^2)(\frac{\pi r_c^2 H_f \bar{\varepsilon}_g}{V_{b0}})$, indicates total interfacial area available for absorption of carbon dioxide gas in the foam section. Entering gas bulk partial pressure, p_{Ab} being known, solubility of gas at the given temperature, C_{Ai} can be obtained from the literature. p_{Ai} therefore, can be obtained as C_{Ai}/H. The quantity Δp in eqn. (3.95) may then be obtained as, $\Delta p = p_{Ab} - p_{Ai}$. Only a small percentage of CO_2 of the total gas fed to the reactor being consumed in this slurry reactor, inlet concentration of gas is used for calculation of conversion which involves only a small error. Initial estimate of C_{As}, concentration of A within the gas bubbles, leaving the storage and entering the foam section is obtained from the conversion of $Ca(OH)_2$ in a bubble column slurry reactor under otherwise identical operating conditions and the volume of liquid in the storage section of the foam reactor.

Equations (3.85), (3.94), and (3.95) are solved simultaneously using fourth order Runge-Kutta algorithm for C_{As}, C_{Bs} and $v_{pk}(t)$, and, conversion of lime is calculated using equations (3.62) and (3.63).

Chapter 4

EXPERIMENTAL:

Materials and Methods

The present investigation is a combination of both theoretical and experimental studies. Theoretical developments for carbonation of NaOH solution using lean carbon-dioxide gas and that of hydrated lime slurry have been presented in Chapter 3. In this chapter, experimental studies of the performance of gas-liquid and gas-liquid-solid bubble column and foam-bed reactors in relation to different variables/parameters have been described to support the detailed theoretical analysis presented in Chapter 3.

In the following sections, the details of the experimental set-ups, materials used, experimental procedure for carbonation reactions for the two different systems used in the present studies, liquid hold-up in the foam reactor, surface-transfer coefficient measurement, methods of chemical analysis, mass balance verification for hydrated lime and sample calculations using the experimental data have been presented. The gas-liquid system is described first followed by the gas-liquid-solid system.

4.1 Gas-liquid system

4.1.1 Experiments Performed: The following experiments were performed to analyze the performance of the foam-bed reactor for absorption with reaction of CO_2 gas in NaOH solution, a gas-liquid reaction system and its comparison with that of the bubble column reactor.

A. Bubble column reactor: Effects of the following variables were studied for a comparison of the performance of this reactor with that of a foam-bed reactor.
  (i) Gas flow rate
  (ii) Concentration of sodium hydroxide in solution

B. Foam-bed reactor: Effects of the following variables on conversion of NaOH were studied.
  (i)   Gas flow rate
  (ii)   Concentration of sodium hydroxide in solution
  (iii)   Volume of sodium hydroxide solution charged into the reactor
  (iv)   Concentration of CO_2 gas in the feed gas mixture

4.1.2 Experimental set-up: The experimental set-up used in the present studies is shown schematically in Figure 4.1. It comprises of a glass column, a bubble flow meter, CO_2 cylinder, air compressor, rotameter for air, a mixer for CO_2 and air, and, an infrared (I.R.) lamp. The glass column, 0.74 m long and 10.5×10^{-2} m internal diameter is connected at the bottom to a glass cone with the help of flanges. A gas distributer plate, 2.0×10^{-3} m thick and made up of perspex is placed between the flanges. There are 31 holes of 1.0×10^{-3} m diameter and arranged in triangular pitch. The infrared lamp is used to heat the rear part of carbon-dioxide regulator to prevent the formation of dry ice and choking of the tube carrying gas to the rotameter. A rotameter is used for metering the air flow rate. A sieve plate made up of perspex and having 57 holes of 3.0×10^{-3} m diameter is connected to a thin copper rod. The plate is used for foam breaking to maintain the desired foam height.

Flow rates of carbon-dioxide used in the present experiments being substantially low, 1.6×10^{-6} to 3.2×10^{-6} m^3 s^{-1}, and cannot be measured using a rotameter, a bubble flow meter was used to measure the CO_2 flow rate. It comprises of the following:

(i)   A rubber ball having a volume of about 50 cc containing a soap solution is attached to the bottom of a calibrated glass tube

(ii) The gas inlet to this glass tube is located above the rubber ball and connected to the CO_2 cylinder through a rotameter, primarily to reduce the flow rate of CO_2 to a low value before it enters the bubble flow meter. A three-way valve is placed between the rotameter and the rubber ball in order to use its one port to vent the excess CO_2 and thereby adjust the flow rate to the bubble flow meter. The exit gas from the top of the bubble flow meter enters the gas mixer.

(iii) CO_2 flow rate from the high pressure cylinder is pre-controlled using a rotameter to less than 0.5 lpm before it enters the soap-bubble flow meter.

Compressed air metered through a calibrated rotameter, enters the gas mixer and the CO_2-air mixture then flows to the bubble column/ foam-bed reactor.

As the CO_2 gas from the cylinder passes through the graduated tube, the rubber ball is pressed to generate foam bubbles and the rise velocity with which they travel up the graduated glass tube, measured using a stop watch, gives a measure of the flow rate of CO_2.

4.1.3 Materials used: Various chemicals used as reactants, foaming agents and for the analysis of reactants and products are as follows. Sodium hydroxide (GR, MERCK Ltd. Mumbai) and Carbon-dioxide gas (Instrument Grade, Dinesh Gases Pvt. Ltd., Jaipur) were used as reactants. CTAB (GR, MERCK Ltd. Mumbai) was used as the foaming agent. Iso-amyl alcohol (GR, MERCK Ltd. Mumbai), an anti foaming agent, was used to maintain the desired foam height. Hydrochloric acid (GR, MERCK Ltd. Mumbai), oxalic acid (AR, Qualigens Pvt. Ltd., Mumbai), barium chloride (GR, MERCK Ltd. Mumbai), and phenolphthalein (AR, Loba Chemie Pvt. Ltd., Mumbai) were used for the analysis of reactants and products.

4.1.4 Experimental

(i) **Analysis of feed solution:** Na_2CO_3 present as impurity in the NaOH solution was removed by precipitating it as $BaCO_3$ through drop-wise addition of about 10 percent $BaCl_2$ solution till white precipitate continued to form and got precipitated. An aliquot of filtered NaOH solution of approximately 0.5 (N) is standardized against oxalic acid solution of known strength to get the exact normality of NaOH feed stock. An aliquot of a stock solution of HCl of approximately the same strength as that of NaOH, to be used to determine the amount of NaOH remaining unreacted in the product solution, is titrated against standard NaOH solution to find out its exact strength.

(ii) **Procedure**: NaOH solution made free from carbonate as described above was used for the preparation of feed solution. A solution of a cationic surfactant, CTAB, containing a known amount of it, was added to NaOH solution to impart foamability, mixed thoroughly and volume made up to 2.50×10^{-4} m^3 using distilled water to obtain feed solution of known strength. Exact strength of NaOH solution was calculated. An infrared (I.R.) lamp was switched on few minutes before the start of each experiment. Desired flow rate of CO_2 gas was maintained by bubble flow meter as described above. Flow rate of compressed air is adjusted using a rotameter for air. When the flow rates of CO_2 and air become steady, NaOH feed solution was poured into the reactor. A stop watch was started immediately to measure the run time. A foam-breaker sieve plate with iso-amyl alcohol applied onto it was held at the predetermined level to maintain the foam height in the column. After the experimental

run for a specified period, the flow of carbon-dioxide and air was stopped. The sieve plate was lowered down to the liquid surface of the storage section to break the foam and release the entrapped CO_2 from the foam bubbles. The column wall and the foam breaking plate was washed with distilled water. The product solution along with the wash water was collected in a stoppered volumetric flask. $BaCl_2$ solution was added drop wise to the reaction product till appearance of precipitate formation. The solution was separated from precipitate using Whatman filter paper No. 42. The resulting solution was then titrated against standard HCl solution to get the amount of unreacted NaOH. The experiment was repeated for different variables studied in this work.

Experiments in the bubble column were performed following the same procedure except that surfactant was not added to the feed solution. However, in this case maintaining a definite foam height was not required.

Details of experimental data collected, results and its discussion have been presented in chapter 5.
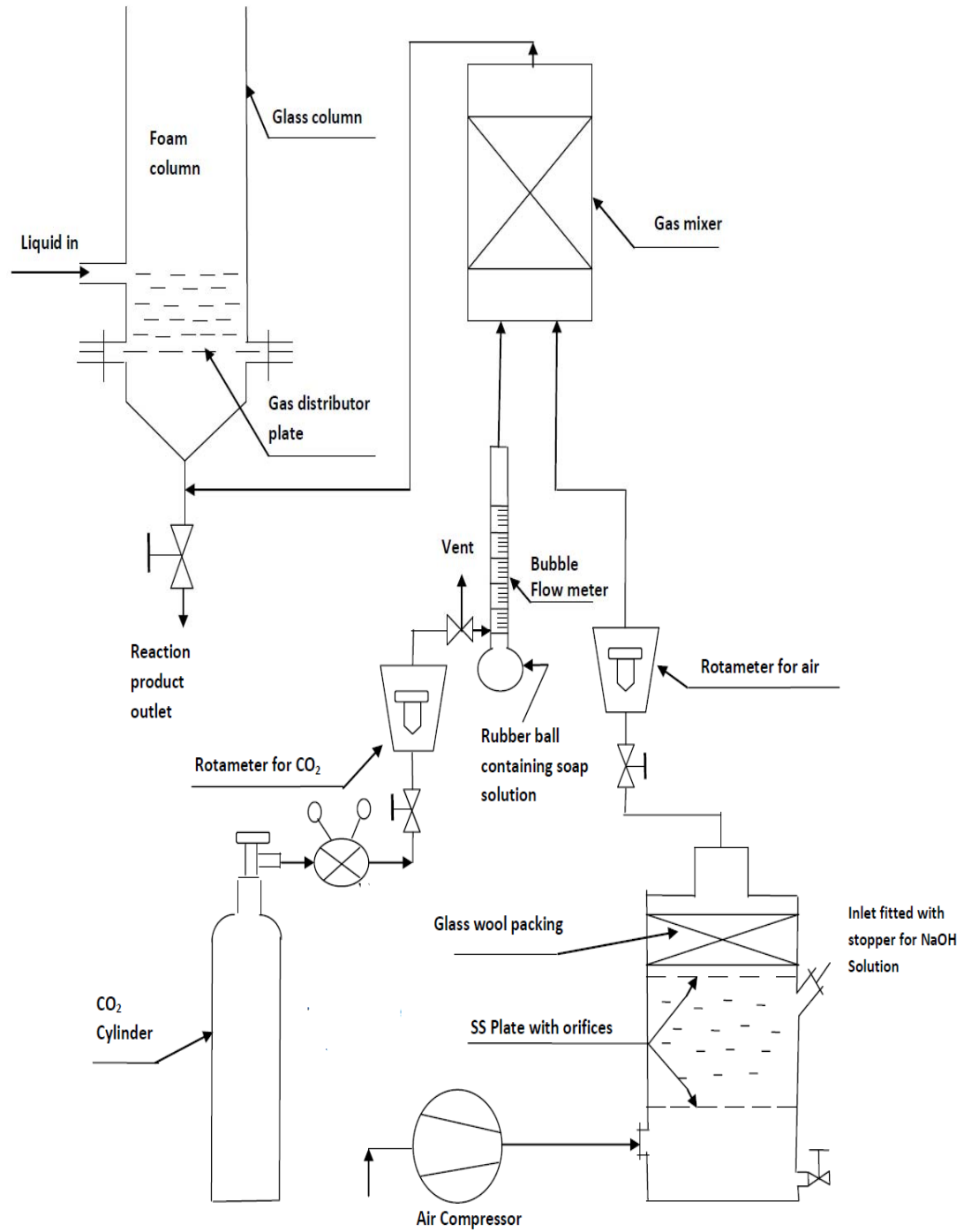
Fig 4.1: Line diagram of experimental set-up used for gas-liquid system
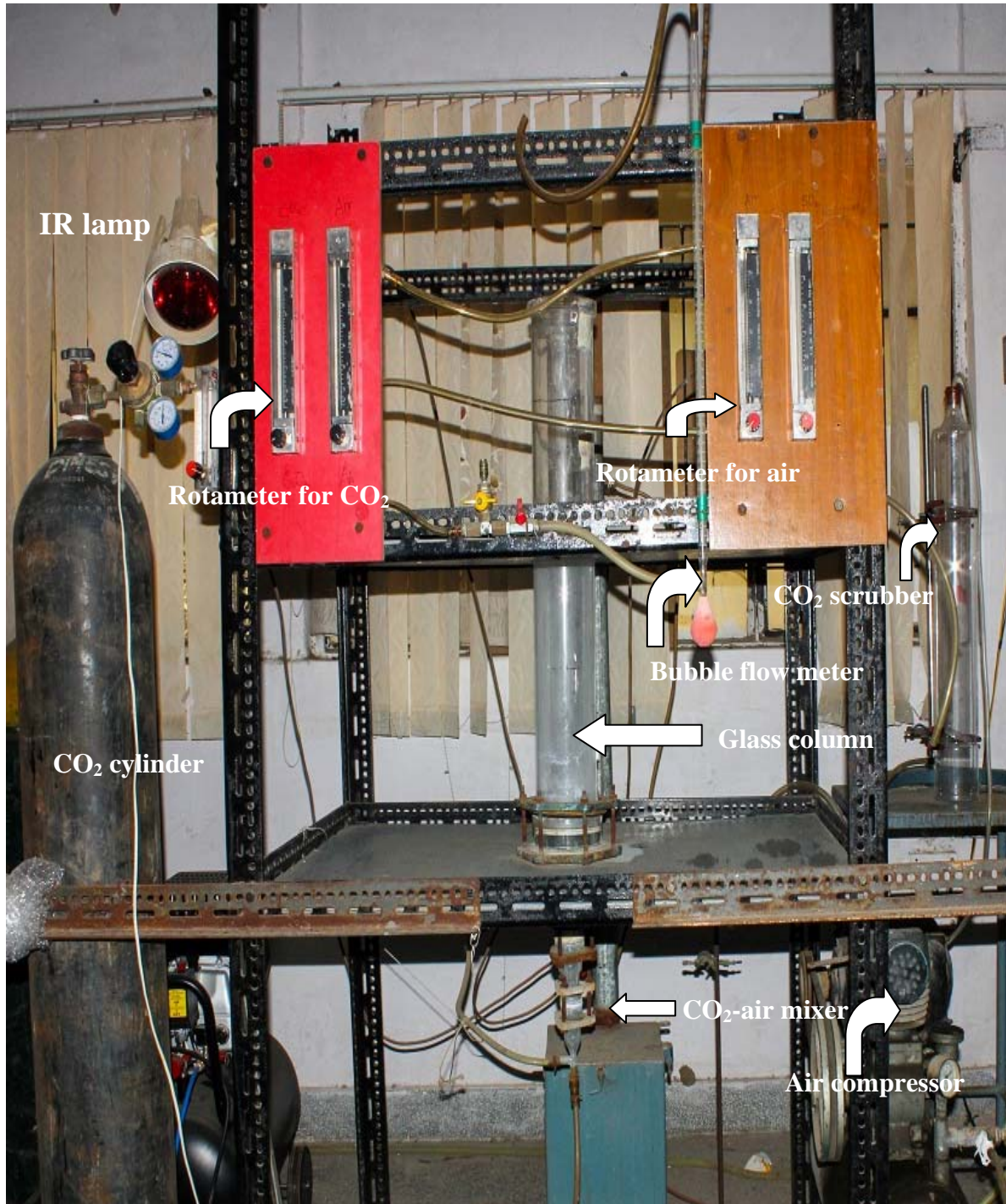
Fig 4.2 Photograph of experimental set-up used for gas-liquid system

4.2 Gas-Liquid-Solid system

4.2.1 Experiments Performed: The following experiments were performed to analyze the performance of the foam-bed reactor for carbonation of hydrated lime slurry and its comparison with that of a bubble column slurry reactor.

A. Bubble column reactor: The variables studied in this type of reactor configuration are:

(i)   Initial solids loading

(ii) Volume of slurry charged to the reactor

(iii) Superficial velocity of gas

B. Foam bed reactor: The following variables were studied for the performance analysis of a slurry-foam reactor.

(i) Initial solids loading

(ii) Volume of slurry charged to the reactor

(iii) Superficial velocity of gas

(iv) Height of foam-bed

(v) Nature of surfactant

      (a) Anionic: Sodium Dodecyl Sulfate (SDS)

      (b) Cationic: Cetyl Trimethyl Ammonium Bromide (CTAB)

      (c) Non-ionic: Octyl Phenoxy Polyethoxyethanol (Triton X-100)

(vi) Concentration of surfactant (SDS, CTAB and Triton X-100)

(vii) Concentration of CO_2 in the feed gas (10%, 25% and 50% CO_2 gas)

Other experiments performed:

      (i) Liquid hold-up measurement for each set of experiments performed

      (ii) Mass balance verification for hydrated lime

      (iii)Particle size analysis of calcium hydroxide samples and calcium carbonate products

      (iv)Effect of addition of ethylene glycol to the reaction mixture on the particle size of calcium carbonate product

      (v) Calibration of rotameters

      (vi) Surface coefficient measurement

4.2.2 Dimensions and materials of construction of foam column

Glass column

Material of construction: glass

Diameter of the column (i.d.): 10.5×10^{-2} m

Height of column: 0.74 m

Gas distributor plate

Material of construction: perspex

Thickness of plate: 2.0×10^{-3} m

Diameter of each hole: 1.0×10^{-3} m

Number of holes: 31

Orifice plate for foam breaking

Material of construction: perspex

Thickness of plate: 2.0×10^{-3} m

Diameter of each hole: 3.0×10^{-2} m

Number of holes: 57

4.2.3 Experimental set-up: The experimental set-up used for carbonation of hydrated lime slurry is shown in Figure 4.3. It is analogous to that used for the absorption of carbon-dioxide in NaOH solution described in the previous section. However, for the metering of CO_2 gas as the flow rate of gas was 10 lpm and higher pre-calibrated rotameter was used instead of bubble flow meter.

4.2.4 Materials used:

Calcium hydroxide (GR, MERCK Ltd. Mumbai) and carbon-dioxide gas (Instrument Grade, Dinesh Gases Pvt. Ltd., Jaipur) diluted with air were used as the reactants. Sodium dodecyl sulphate (AR, Qualigens Pvt. Ltd., Mumbai), CTAB (GR, MERCK Ltd. Mumbai) and Triton X-100 (SRL Chemicals Pvt. Ltd., Mumbai) were used as the foaming agents. Iso-amyl alcohol (GR, MERCK Ltd. Mumbai), an anti foaming agent was used to maintain the desired foam height. Iodine (GR, MERCK Ltd. Mumbai), potassium iodide (GR, MERCK Ltd. Mumbai), sodium thiosulphate pentahydrate (GR, MERCK Ltd. Mumbai), soluble starch (GR, MERCK Ltd. Mumbai) and potassium dichromate (GR, MERCK Ltd. Mumbai), were used in the chemical analysis of the reactants and products.

4.2.5 Experimental

(i) Slurry preparation: Calcium hydroxide being sparingly soluble in water and forms lumps when mixed with cold water, boiled distilled water was used for the preparation of slurry. A known amount of calcium hydroxide powder, 5.0×10^{-3} kg, is added to about 1.0×10^{-4} m^3 boiled distilled water taken in a 2.5×10^{-4} m^3 volumetric flask and mixed thoroughly. The slurry is shaken occasionally for about half an hour and allowed to cool. For experiments in the bubble column, volume is made up with gradual addition of distilled water and the flask was shaken simultaneously for thorough mixing.

For experiments in the foam-bed reactor, a solution of definite amount of surfactant was prepared in distilled water in a 1.0×10^{-4} m^3 beaker and added to the slurry in the volumetric flask with constant shaking before making up the volume. The slurry volume was then made up to 2.5×10^{-4} m^3 with gradual addition of distilled water and mixing the contents thoroughly.

(ii) **Procedure:** For experiments on carbonation of hydrated lime slurry, flow rate of carbon-dioxide being substantially high, a pre-calibrated rotameter was used for the metering of this gas. As with the gas-liquid system, before the start of each experiment, an I.R. lamp was switched on and carbon dioxide gas at the desired flow rate was allowed to pass through the glass column. When the flow rate became steady, 2.5×10^{-4} m^3 of hydrated lime slurry of known composition and containing a known amount of a specific surfactant was poured into the column and the reaction allowed to proceed for a pre-determined time. While for the experiments in the foam-bed reactor, the foam height was maintained using a hanging multi-orifice plate with iso-amyl alcohol applied on to its surface, for the experiments in the slurry bubble column, this was not necessary. The reaction product being slurry and results of analysis of several aliquots drawn from a product sample produced widely different results, the whole mass was analyzed iodiometrically for estimation of unreacted lime. The experiment was repeated for different times of reaction and other variables studied in this work.
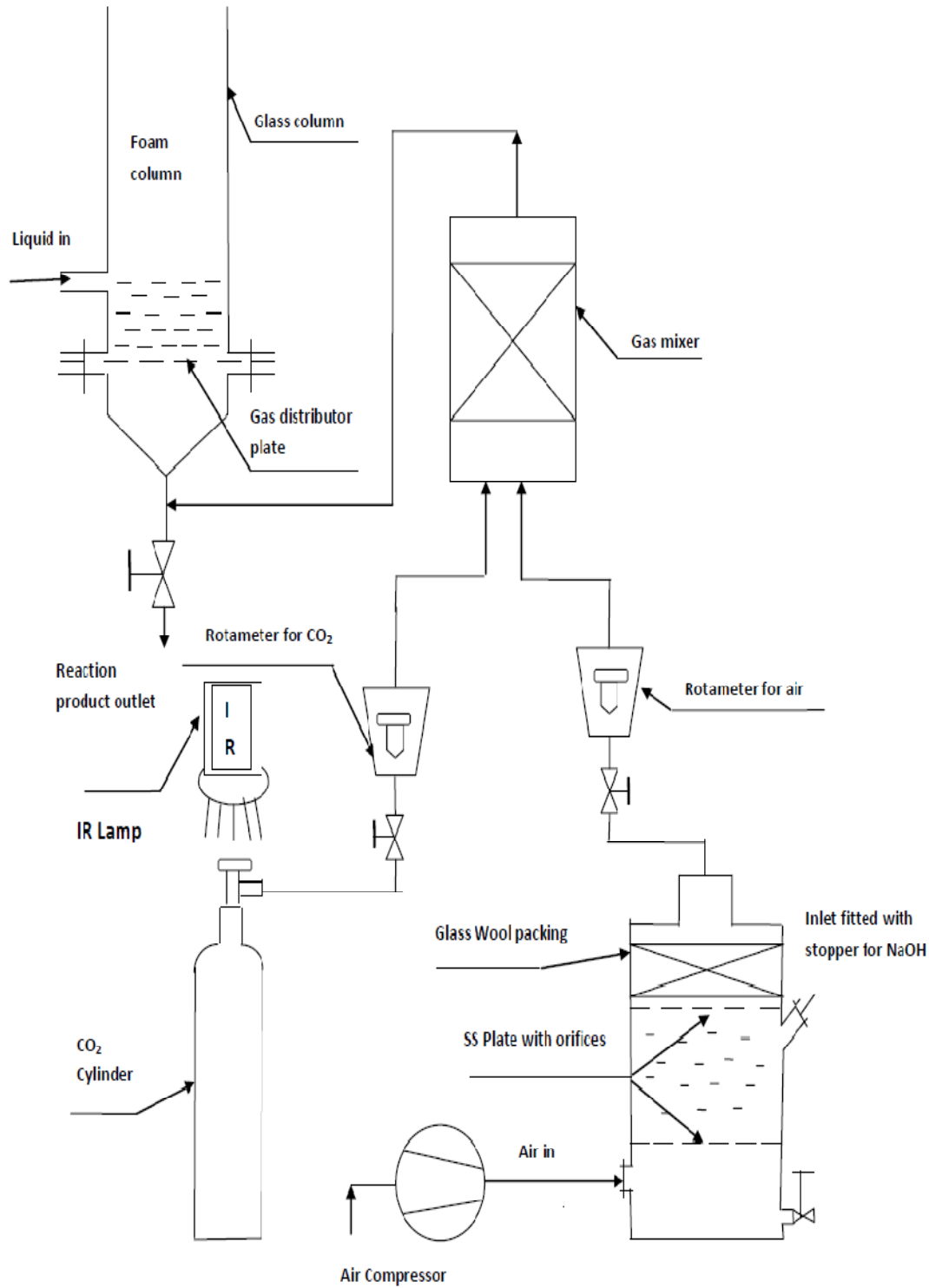
Fig 4.3 A Line diagram of experimental set-up used for gas-liquid-solid system

Figure 4.4 Experimental set-up used for gas-liquid-solid system

4.3 Measurement of parameter values

4.3.1 Liquid hold-up in foam column

Volume fraction of liquid in the gas-liquid dispersion is an important parameter governing the performance of a gas absorber or that of a gas-liquid reactor. Various methods are employed for the measurement of liquid holdup in a foam column absorber as described in chapter 2.

Measurement of liquid hold-up has been performed in the foam column using an apparatus similar to that used by Jana (2007). The apparatus used in the present work has been shown in Figure 4.5. A very similar apparatus was used earlier by Calderbank (1958) and Biswas & Kumar (1981) as well. A water-ring type vacuum pump is used for generating vacuum in a 5.0×10^{-4} m^3 capacity glass bulb. Foam is sucked into this bulb from various heights of the foam reactor and allowed to condense. Volume of condensate is measured and liquid hold-up is calculated from the knowledge of the extent of vacuum in the bulb and the volume of liquid condensed. Experiment is repeated to collect data for all the operating conditions actually used for evaluating the reactor performance.

4.3.1.1 Experimental set-up for measurement of liquid hold-up

The set-up: A schematic representation of the experimental set-up is shown in Figure 4.5. It consists of a water tank, a water pump, a rotameter for water of capacity 0 to 5 lpm, a water-ring type vacuum pump with a vacuum gauge fitted to it, a catch pot and a glass bulb connected to a liquid hold-up sampler.

(a)

(b)
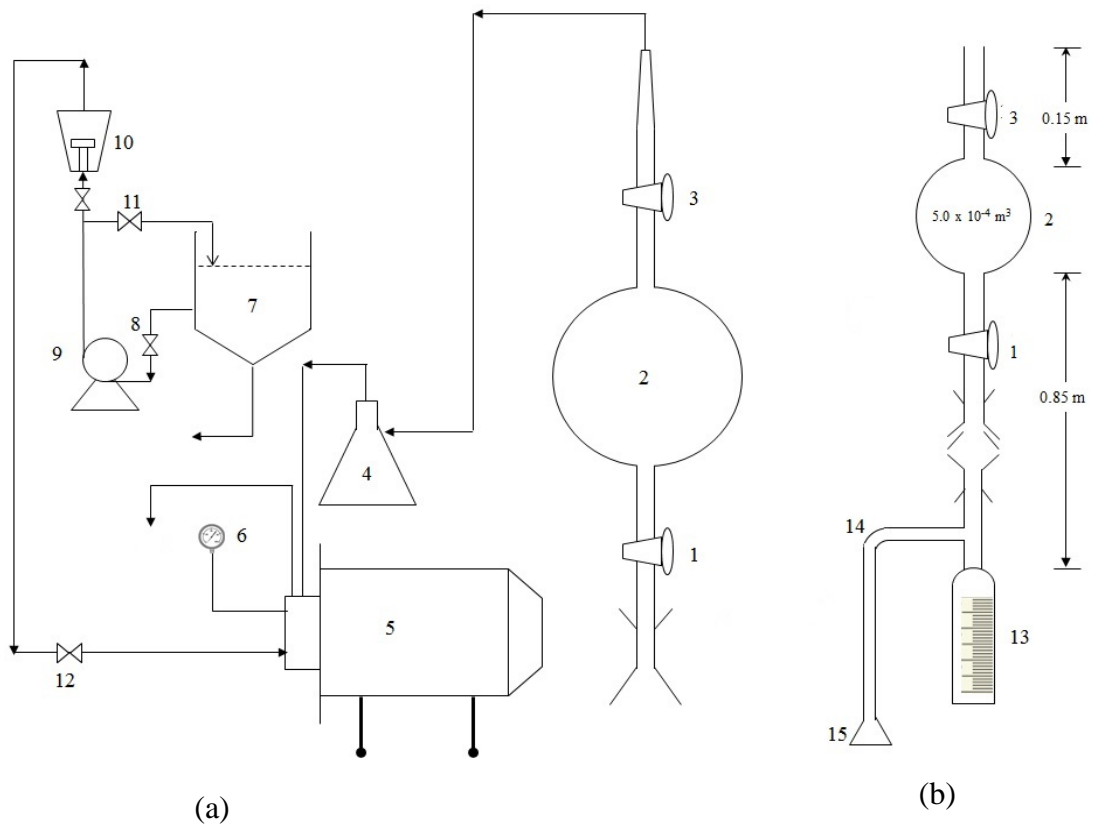
Figure 4.5: Set-up for measurement of liquid hold-up in a foam column

Legend

(a) Vaccum assembly fitted with glass bulb.

1-3. Vacuum stop cock 2. Glass bulb 4. Catch Pot 5. Water ring type vacuum pump 6. Vacuum gauge 7. Water tank   8. Tap 9. Water Pump   10. Rotameter for water 11-12. Taps

 (b) Liquid hold-up sampler with bulb

2.   Glass bulb   1-3. Vacuum stop cocks   13. Graduated tube 14. Suction tube   15.Cup
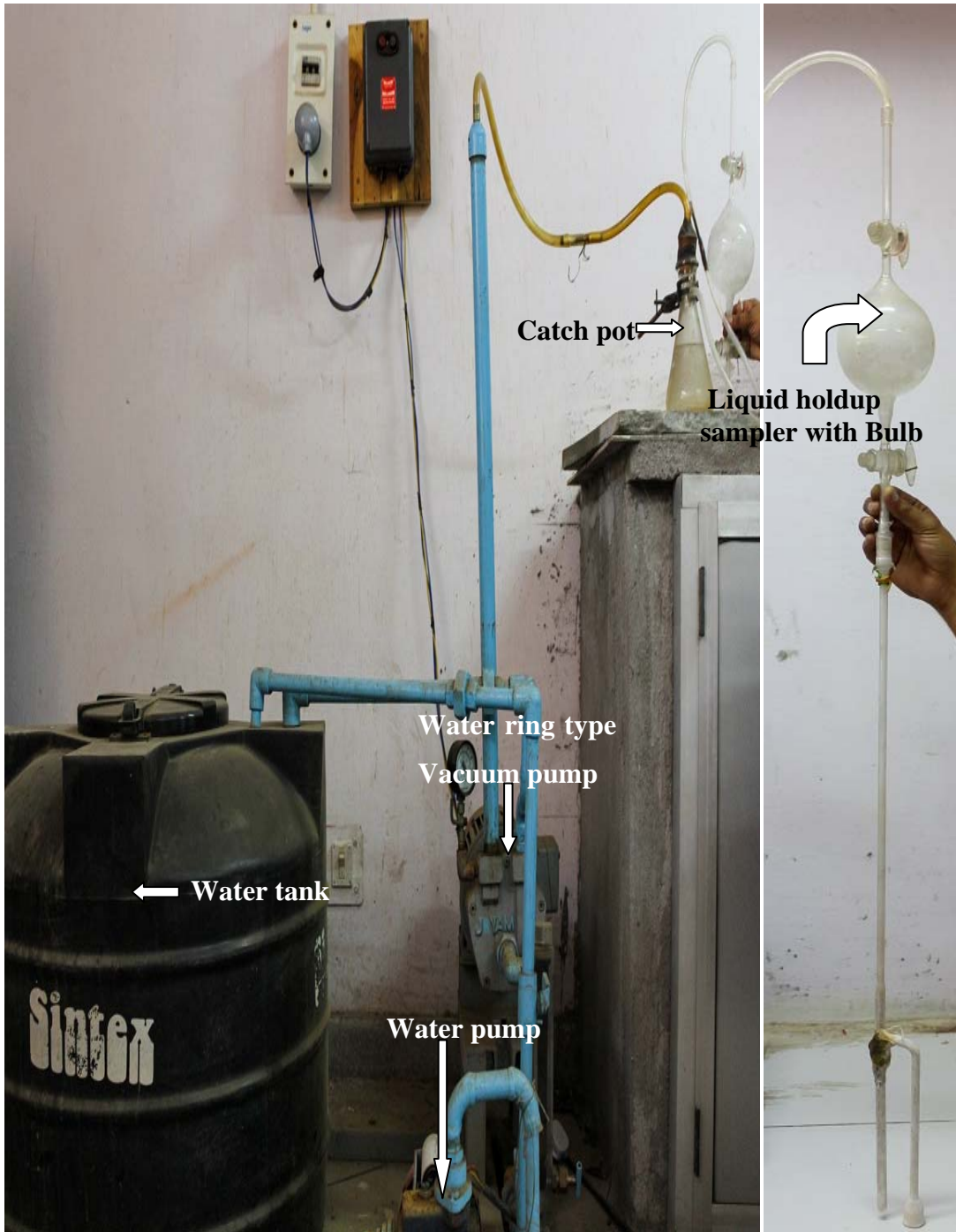
Figure 4.6 Photograph of experimental set-up for measurement of liquid hold-up in foam column

Experimental procedure:

(i)   Hydrated lime slurry containing same solids loading as those used in the experiments for performance studies of a foam bed reactor were prepared.

(ii)   Grease was applied to vacuum stop cocks (1) and (3) of the foam suction assembly. Glass bulb was then connected to the catch pot. Stop cock (1) was kept shut and stop cock (3) was opened.

(iii)   Water was filled in the water tank (7) and water pump (9) was switched on. Water-inlet valve (12) to the vacuum pump was opened. Water-flow rate was adjusted to $8.5 \times 10^{-5} \text{ m}^3 \text{ s}^{-1}$ with the help of rotameter (10) and the bypass valve (11) fully open.

(iv)   When the maximum attainable steady vacuum was attained (about 695 mm Hg), the stop cock (3) was shut. The water-inlet valve to the vacuum pump was closed. Vacuum pump and water pump were switched off.

(v)   Glass bulb (2) was then disconnected from catch pot and connected to the suction tube with the help of ground glass joint.

(vi)   Carbon dioxide-air mixture at definite flow rate (same as those used in experiments to study the performance of foam bed reactor mentioned earlier) were allowed to flow through the empty column.

(vii)   Carbonation reaction was performed in the foam reactor as described in section 4.2.5. The suction tube connected to the glass bulb is inserted into the column.

(viii)   The stop cock (1) was opened slowly to suck the foam into the glass bulb which is already under vacuum.

(ix)   Stop clock (1) was shut when the foam stopped flowing into the bulb.

(x)   Volume of condensate is measured using the tube connected to the sampler. A $2.5 \times 10^{-6} \text{ m}^3$ graduated cylinder is used for this purpose when the volume of condensate is more.

(xi)   The experiments are repeated with the other sets of experimental conditions used for collection of experimental data for carbonation of hydrated lime slurry.

(xii)   Details of liquid holdup calculations have been shown in appendix 4B.1 and experimental data in chapter 5 part II.

4.3.2 Hydrated lime content of the test sample, particle size distribution and average particle size

Percentage of hydrated lime content of the test samples have been determined using iodiometric method. These are found to be 94.76 and 95.27 percent in samples supplied by CDH and MERCK Ltd., respectively. Detailed procedure for estimation of hydrated lime content has been presented in Appendix 4A.5.

The PSDs play a significant role in governing the reactor performance and used in present work for reactor simulation. Particle-size distribution (PSDs) of reactant $Ca(OH)_2$ and product $CaCO_3$ have been measured using CILAS- 940 particle-size analyzer and Mastersizer 2000 E. The $Ca(OH)_2$ sample from two suppliers, CDH and MERCK Ltd. were used in performing the present experimental work and the particle sizes of both the samples were measured using the above particle-size analyzers. Ethyl alcohol was used as the dispersant. The particle size distribution was used for reactor simulation. The entire particle size distribution of each sample was divided in 12 volume fractions for reactor simulation. The fractions are chosen to maintain the particle size in each fraction at low value for a purpose of reactor simulation. The average particle-diameter in a given fraction is taken as the arithmetic mean of the smallest and largest diameters comprising fraction (Jana and Bhaskarwar, 2010). Details of particle size distributions of lime and percentages of hydrated lime in various test samples are reported in Chapter 5 part II.

4.3.3 Mass balance verification for hydrated lime in bubble- and foam-column reactors

<u>Bubble column</u>

Percentage of calcium hydroxide and that of impurity, primarily $CaCO_3$, in the test sample were estimated by chemical analysis followed by use of equation (4A.5). A batch of slurry of known solids loading, prepared using approximately 5.0×10^{-3} kg hydrated lime in 2.5×10^{-4} m^3 of distilled water, was made to react completely by performing experiments in a bubble column. The minimum time required for complete reaction was determined by trial experiments *in priori*. The slurry along with the liquid used for column washing was collected in a glass beaker (B$_1$) of known weight.

The top of the beaker was covered and the slurry was allowed to settle overnight. The supernatant liquid was carefully transferred by decantation to within about 1 cm from the surface of the precipitate into another beaker (B_2) of known weight. The solution kept in beaker B_2 was evaporated to dryness and the weight, negligibly small, of solid was determined.

The residual water left out in beaker B_1 was evaporated first with mild heating and constant gentle shaking, to avoid splashing of the slurry by letting off the vapor formed at the inner part of the bottom surface of the beaker, till the slurry ceased to flow. The heating was then continued by holding the beaker a few inches above the heater and with a slow rotation of it. On continued heating, cracks were found to develop at different locations of the drying solid. The rate of heating was then increased and the dried solid disintegrated into small thin platelets.

Heating, cooling and weighing of the dried solid along with the beaker were continued till constant weight was obtained.

The total mass of product $CaCO_3$ obtained from B_1 and B_2 was found to be equal to the sum of the estimated mass of $CaCO_3$ from the stoichiometry, taking into account the percentage of hydrated lime and the various impurities present in the sample as determined by its chemical analysis.

<u>Foam column</u>

CTAB was used as the surfactant for carrying out the carbonation reaction in a foam-bed reactor. The procedure adopted for bubble column for verification of mass balance was adopted for this case also. Contrary to our expectations, the product slurry could be easily evaporated to dryness and there was no difficulty in doing so, although a surfactant was present. At the temperature of experiment only about 4 x 10^6 kg of $CaCO_3$ dissolves in 2.50 x 10^{-4} m^3 of water. The mass of solid obtained by evaporation of solution in beaker B_2 was found to be approximately equal to the mass, 0.1358 x 10^{-3} kg, of CTAB used for the preparation of slurry. The mass balance was then verified as for the bubble column described above.

4.4. Effect of addition of ethylene glycol to the reaction mixture on the particle size of product CaCO₃

To estimate the change in the particle size of precipitated calcium carbonate, 2-5 ml of ethylene glycol was added to the slurry and SDS was used as the foaming agent. Particle size was found to reduce with high concentration of mono ethylene glycol (Flaten et.al. 2009). Ethylene glycol is highly viscous in nature; it increases the viscosity of media that helps in the reduction of particle size. Addition of ethylene glycol to the slurry increased the viscosity of slurry reduces the agglomeration of particles.

Chapter 5

RESULTS & DISCUSSION

PART I: GAS-LIQUID SYSTEM- Absorption of CO$_2$ in NaOH solution

New Models have been developed and presented in Chapter 3 for absorption of CO$_2$ in sodium hydroxide solution in bubble column and foam-bed reactors using lean carbon-dioxide gas. In order to validate these models, a series of experiments have been performed in semi-batch mode in these reactors. For validation of the proposed model of the bubble column reactor, the reaction was carried out without any addition of surfactant to the reactant solution, while for that of the foam-bed reactor model, a known amount of the surfactant CTAB was added to the solution prior to feeding to the foam-bed reactor for generation of experimental data in the foam-bed reactor.

The reaction between dissolved CO$_2$ and NaOH occurs in a zone close to the interface. Dissolved CO$_2$ diffusing into this reaction zone gets fully consumed by reaction with NaOH. Subsequently, more NaOH diffuse into the reaction zone from the bulk liquid and also dissolved CO$_2$ from the gas-liquid interface and the reaction continues to occur in this zone. Concentration of dissolved CO$_2$ in the bulk liquid, therefore, during the entire reaction period remains at zero level, i.e., $C_{Ab}=0$. Mass transfer with chemical reaction is thus modelled according to the theory of gas absorption in agitated liquid. However, in a foam-bed reactor while the mechanism of mass transfer with chemical reaction in the storage section is identical with that in the bubble column, in the foam section it closely resembles to absorption into quiescent liquid as the column of foam moves upwards like a rod and there being no relative movement between the gas pocket and the surrounding films into which absorption occurs.

For reactor simulation, as evident from the models, values of the various parameters, viz., $\bar{\varepsilon}_G$, k_l^0, $C_{Ai}(= C_A^*)$, D_A, k_2, a'_{bc} are needed for simulation of reactors. $\bar{\varepsilon}_G$ has been obtained using the correlation developed by Shulman and Molstad (1950), k_l^0 has been estimated using Higbi's (1935) penetration theory of mass transfer. Liquid-phase diffusion coefficient D_A has been obtained using the correlation proposed by Haq (1982) and the reaction rate constant k_2 estimated following Astarita (1967). C_{Ai} is obtained using Henry's law. In the estimation of k_2 and Henry's law coefficient, effect of ionic strength has been taken into account. All the experiments have been conducted at 30±1°C.

Partial pressure required for estimation of interfacial concentration in the liquid phase was taken as the average of those at the inlet and exit of the bubble column reactor. Further, interfacial resistance in the gas phase in the well stirred storage section is assumed negligibly small for the reason that solubility of carbon-dioxide gas in water is substantially low and liquid phase resistance is much higher compared to that in the gas phase. At the relatively high superficial velocity of gas used in the present experiments, bubbles are idealized as spherical and bubble swarm velocity is used for the estimation of gas-liquid contact time in the storage section. Mechanism of mass transfer in the storage section of the foam bed reactor is treated similar to that in the bubble column. For calculation of reaction rate in the foam section, the average partial of those at the foam section inlet, same as that at the exit from the storage, and of that at the exit of this section is used.

It was decided to study the above reaction under the conditions of pseudo-first order reaction kinetics and therefore to operate the reactor in a semi-batch mode. For maintaining the requirements of pseudo-first order reaction, the concentration of sodium hydroxide in the feed solution was kept high, 0.23 to 0.87 (N) and that of carbon-dioxide gas low, 0.22 to 0.49% by volume. In order to find out the suitable range of gas velocities to be used in the experimental studies, trial run was made with different combinations of gas velocities and concentration of CO_2 gas. In the lower range of gas velocities, foam was found to be more stable with a higher concentration of CO_2 gas. While weeping occurred when superficial gas velocity was below 2.7 x 10^{-2} m/s, recirculation of foam was observed above 10 x 10^{-2} m/s. The calculated values of the *rise-velocities* of gas bubbles in the storage section were, however, substantially higher depending on the liquid hold-up. At the low concentration of CO_2 gas used in the present experiments, foam was found to be more unstable as the gas rate was reduced at a fixed concentration of CO_2 gas. At about 0.49% CO_2 gas used in the present experiments, foam was found to be stable at and above superficial velocity of 4.4 x 10^{-2} m/s. At lower concentrations, higher gas rate was required for generation of stable foam.

Because of substantially higher gas-liquid interfacial area in a foam reactor, it was expected that conversion would be much higher than that in a bubble column reactor under otherwise identical operating conditions. For a comparison of the relative performance of the two reactors, experiments in the bubble column were performed

without any surfactant added to the reaction mixture. Similar experiments were conducted with addition of a cationic surfactant, CTAB (0.054% w/w) for the reason that substantially lower amount compared to the other type of surfactant generated stable foam under otherwise identical operating conditions. For generation of experimental reactor-performance data and validation of the bubble column and foam-bed reactor models with respect to the pertinent parameters additional series of experiments were performed, viz. effects of initial concentration of sodium hydroxide in solution and that of CO_2 in the feed gas, volume of solution charged to the reactor and the superficial velocity of gas on conversion of NaOH. Height of foam-bed was maintained at 20 cm throughout as at higher heights conversion of NaOH was found not to vary with height any more. Details of experimental data have been shown in tabular form in Appendix 5B. The figures depicting the variation of conversion of NaOH with time for different values of the variables have been shown in Figures 5.1.1 to 5.1.4. Three sets of experiments for each of the variables mentioned above have been carried out for evaluation of the performance of the two reactors.

For simulation of bubble column reactor, average of the inlet and exit partial pressures were used for estimation of the interfacial concentration of carbon-dioxide in the liquid phase. Conversion vs time data is found to be linear. From the experimental data of conversion of NaOH, moles of NaOH and that of CO_2, using the reaction stoichiometry, reacted per second was calculated. From the knowledge of volume of CO_2 entering and reacted per second and the flow rates of diluents gas, partial pressure of CO_2 in the exit gas is calculated. Average partial pressure was used for simulation of bubble column reactor as mentioned above.

For the simulation of foam-bed reactor, conversions are calculated over a small time interval separately for both the sections of the reactor. This required partial pressure of CO_2 at the exit of the storage section which is same as the inlet to the foam section for estimation of its average partial pressures in the two sections of the reactor. From the knowledge of liquid holdup in the foam sections and those of column diameter and foam height, volume of liquid in storage section is estimated. Trial value of conversion in the storage section was estimated from the conversion data obtained in a bubble column, operated under otherwise similar experimental conditions, using a linear interpolation between conversion and volume of liquid. Minor adjustment in the conversions were made by trial to fit the total conversion and thus to obtain the

final partial pressures. The average partial pressures thus obtained were used for the simulation. Concentrations of reactants in the storage section at the end of the time interval were estimated using the material balance equations and the procedure is repeated over the entire period of interest. The exit partial pressure of CO_2 was calculated using the experimental conversion data, inlet flow rates of CO_2 and air, and the reaction stoichiometry.

5.1 Effects of different variables on conversion of sodium hydroxide

5.1.1 Effect of concentration of sodium hydroxide in bubble-column and foam-bed reactors

The effect of concentration of sodium hydroxide on its conversion has been shown in Fig. 5.1.1a. Concentration of sodium hydroxide in the feed solution was varied from 9.08 (0.227 N) to 34.64 kg m^{-3} (0.866 N). CO_2 concentration at the reactor inlet and superficial velocity of gas were maintained at 3.59 x 10^{-3} mole fraction and 9.66 x 10^{-2} m/s respectively for all the experiments performed for the studies of this variable. Volume of solution charged to the reactor was 2.5 x 10^{-4} m^3. As the experiments were conducted in the bubble column, no surfactant was added to the reactant solution and there was no foam, whatsoever in the column. It is observed that after a given time of reactor operation, conversion of sodium hydroxide reduces with an increase in its concentration in the feed solution when other variables are kept unchanged. One obvious reason for this reduction is that solubility of CO_2 reduces with an increase in the concentration of NaOH in the solution. For the present case, this varies from 0.227 kg moles /m^3 to 0.866 kg moles /m^3 (0.227 x 10^{-6} g moles /cm^3 to 0.866 x 10^{-6} g moles /cm^3 corresponding to a bulk partial pressure of CO_2 equal to 0.0036 atm) as the concentration of NaOH varies from 0.22 (N) to 0.87 (N). On the contrary, the total mass of NaOH reacted in a given time of reactor operation is found to be higher for a higher initial concentration of it in the solution. For example, after 30 sec of reactor operation mass of NaOH reacted = 0.2070 x 10^{-3} kg for 0.87 (N) NaOH solution; 0.1485 x 10^{-3} kg for 0.43 (N) and 0.1089 x 10^{-3} kg for 0.23(N) of NaOH solution respectively. However, the fraction of the total initial mass of NaOH reacted during the same time interval reduced with each successive increment in concentration and caused a reduction in conversion.
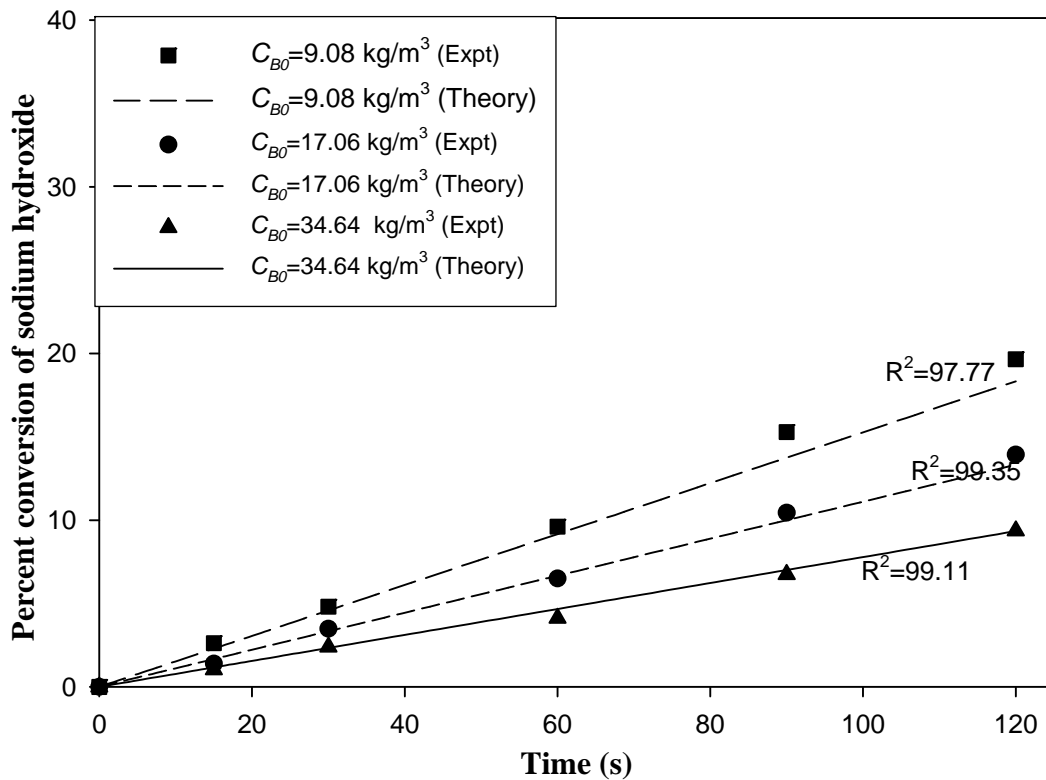
Figure 5.1.1a Effect of concentration of sodium hydroxide on conversion in bubble-column contactor

Parameters	■	●	▲
Surfactant	none	none	none
H_f (m)	0.0	0.0	0.0
V_l (m^3)$\times 10^4$	2.5	2.5	2.5
V_G (m/s)$\times 10^2$	9.66	9.66	9.66
Q_{CO_2} (m^3/s) x10^6	3.0	3.0	3.0
Q_{air} (m^3/s) x10^6	833.0	833.0	833.0

Experimental data and parameter values have been shown in Tables 5B.1.1 to 5B.1.3

It may be observed that percent conversion of sodium hydroxide varies linearly with time. This is attributed to the fact that CO_2 is the limiting component which is continuously supplied at a definite rate while high concentration of NaOH is maintained in the reaction zone by diffusion from the liquid bulk. Gas-liquid interfacial area for absorption of CO_2 in the liquid remain unchanged during the entire course of reaction. As the reaction does not occur in the bulk of the liquid, bulk

concentration of NaOH is unimportant so long as it remains high to maintain the required rate of diffusion to the reaction zone.

These experiments were also performed in a foam-bed reactor with the same values of the variables and parameters. CTAB was used as the surface active agent and a foam height of 20×10^{-2} m was maintained for all the three sets of experiments performed. Experimental results have been shown in Figure 5.1.1b. Conversions of sodium hydroxide after a definite time of reactor operation and under otherwise similar experimental conditions are found to be substantially higher in a foam-bed reactor than that in the bubble column reactor. Although total amount of liquid in the foam section is only about 14% of that charged to the reactor, average increment in conversion in the foam-bed reactor after 90 sec of reactor operation are found to be higher by about 40 percent over that in the bubble column reactor. Several fold increase in the interfacial area is considered to be the primary reason for this increase in conversion of NaOH. The model predictions are found to agree well with the experimental data.
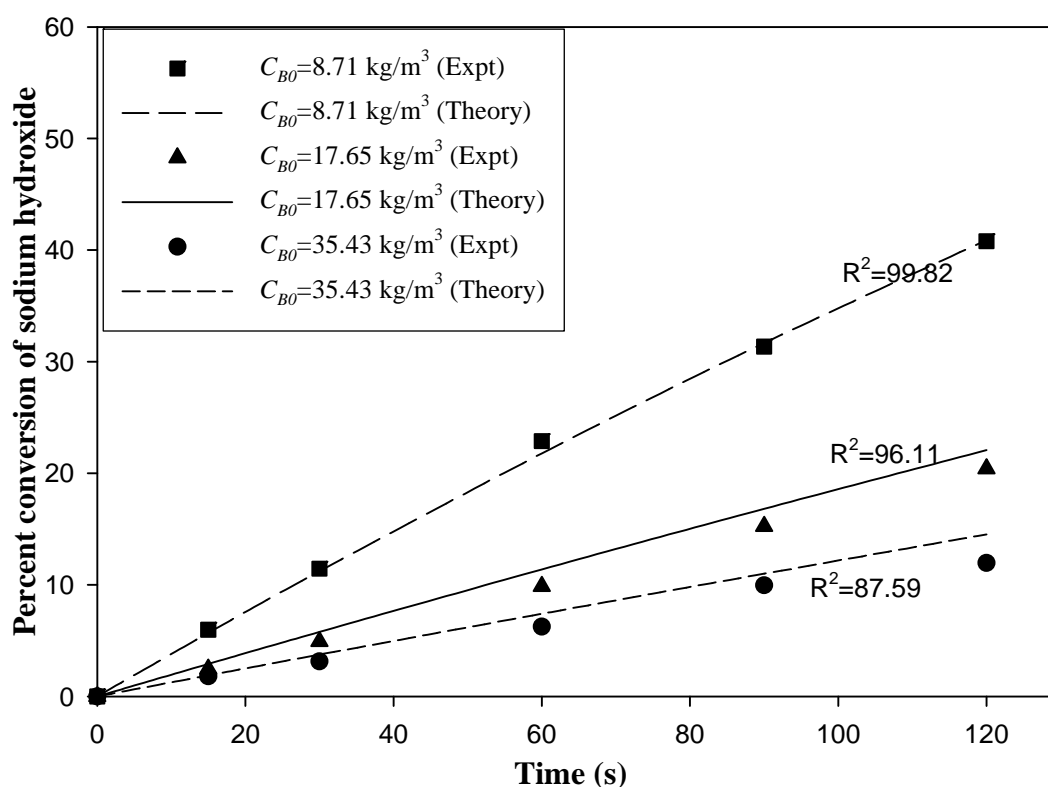
Figure 5.1.1b Effect of NaOH concentration on conversion in a foam-bed reactor

Parameters	■	▲	●	Variables	■	▲	●
Surfactant	CTAB	CTAB	CTAB				
H_f (m)	0.2	0.2	0.2	$\overline{\varepsilon_{Gs}}$	0.38	0.38	0.38
V_G (m/s)$\times 10^2$	9.66	9.66	9.66	$\overline{\varepsilon_l}$	0.013	0.036	0.039
Q_{CO_2} (m^3/s) x10^6	3.0	3.0	3.0				
Q_{air} (m^3/s) x10^6	833.0	833.0	833.0				
V_l (m^3)$\times 10^4$	2.5	2.5	2.5				

Experimental data and parameter values have been shown in Tables 5B.2.1 to 5B.2.3

5.1.2 Effect of superficial velocity of gas on conversion of sodium hydroxide in bubble-column and foam-bed reactors

Superficial velocity of gas was varied from 4.35 x 10^{-2} to 9.67 x 10^{-2} m s^{-1} to study its effect on conversion of NaOH at constant values of the other variables. Results of experiments performed in bubble column reactor have been shown in Figure 5.1.2a. Conversion of sodium hydroxide is found to increase with an increase in the superficial velocity of gas. Bubble size becomes larger with an increase in the superficial velocity of gas. This tends to reduce the specific gas-liquid interfacial area. Higher gas velocity also reduces the gas liquid contact time in the column which is partially nullified by the higher gas holdup in the bubble column and thus higher volume of gas-liquid dispersion. These effects tend to lower the rate of gas absorption. On the other hand, turbulence in the bubble column increases with an increase in the superficial velocity of gas and leads to higher values of gas-liquid mass transfer coefficient in the column. Gas holdup in the bubble column increases from 0.27 to 0.39 as the superficial velocity of gas varies from 4.35 x 10^{-2} to 9.67 x 10^{-2} m/s (Shulman and Molstad, 1950). These manifest in higher rates of gas absorption, reaction and consequently higher conversion after a given time of reactor operation.

Effect of superficial velocity of gas on conversion of NaOH in a *foam-bed reactor* has been shown in Figure 5.1.2b. 540 ppm CTAB in NaOH solution was used for the generation of a stable foam column. A comparison of the experimental data of the two figures shows that conversions obtained experimentally are substantially higher in the foam-bed reactor over that in the bubble column reactor at a given value of superficial

velocity. This is again due to the much higher rate of gas absorption resulting from the very large gas-liquid interfacial area created in the foam section. The conversions are also found to increase with an increase in the superficial velocity of gas. Concentration of surfactant being substantially small, its effect on gas absorption has been considered negligible in the development of the model. The model predictions are found to agree well with the experimental data generated in this study.
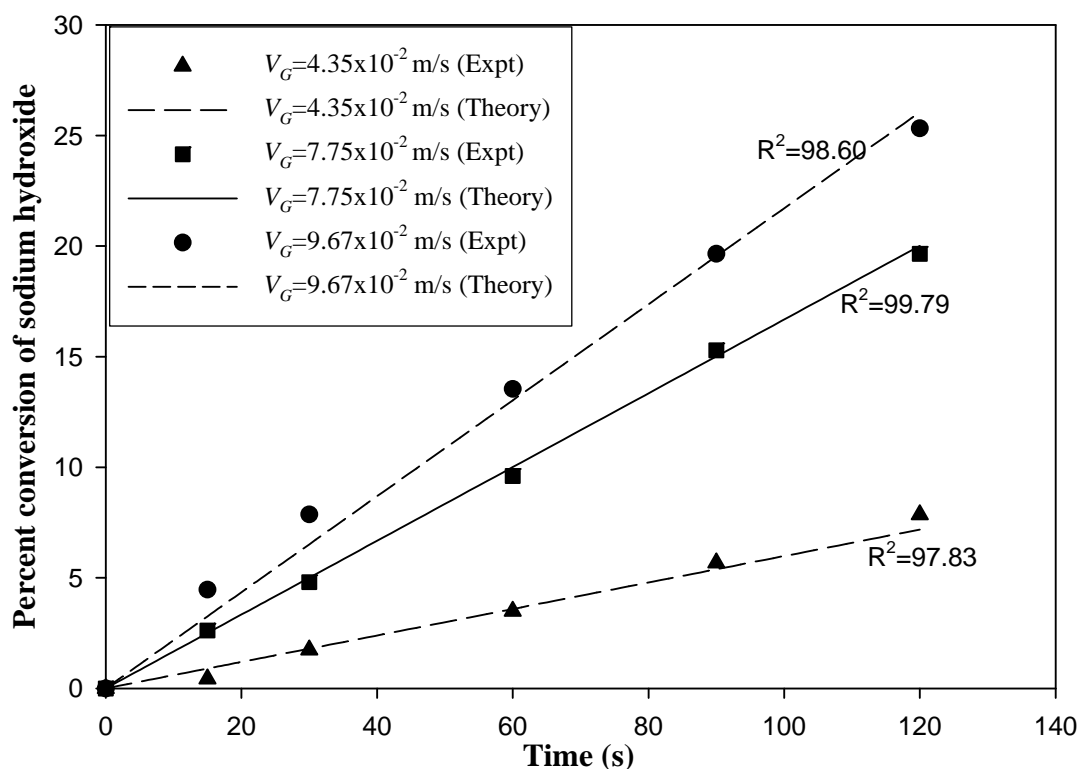
Figure 5.1.2a Effect of superficial gas velocity on conversion in a bubble-column reactor

Parameters	▲	■	●
C_{B0} (kg/m^3)	9.047	9.047	9.047
Surfactant	none	none	none
H_f (m)	0.0	0.0	0.0
Q_{CO_2} (m^3/s) x10^6	1.8	3.33	4.1
Q_{air} (m^3/s) x10^6	375.0	667.0	833.0
V_l (m^3)×10^4	2.5	2.5	2.5

Experimental data and parameter values have been shown in Tables 5B.3.1 to 5B.3.3

Figure 5.1.2b Effect of superficial gas velocity on conversion in a foam-bed reactor

Parameters	■	●	▲
C_{B0} (kg/m^3)	17.65	17.65	17.65
Surfactant	CTAB	CTAB	CTAB
H_f (m)	0.2	0.2	0.2
Q_{CO_2} (m^3/s) x10^6	1.8	3.33	4.1
Q_{air} (m^3/s) x10^6	375.0	667.0	833.0
V_l (m^3)×10^4	2.5	2.5	2.5

Variables	■	●	▲
$\overline{\varepsilon_{Gs}}$	0.29	0.34	0.39
$\overline{\varepsilon_l}$	0.01	0.034	0.038

Experimental data and parameter values have been shown in Tables 5B.4.1 to 5B.4.3

5.1.3 Effect of volume of solution charged into the reactor on conversion of sodium hydroxide in a foam-bed reactor

Volume of sodium hydroxide solution charged into the reactor was varied from 2.5 x10^{-4} to 5.0 x10^{-4} m^3. Effect of volume of solution charged into the reactor on conversion of NaOH in a foam-bed reactor has been shown in Fig. 5.1.3. It is observed that percent conversion of sodium hydroxide reduces as volume of solution fed to the reactor is increased with all other parameters and variables kept constant.

The total amount of sodium hydroxide is larger in the larger volume of solution fed to the reactor, concentration being same in all the solutions. Initial mass of sodium hydroxide taken for reactions in the three different volumes of feed solution are therefore, 4.41×10^{-3}, 6.22×10^{-3} and 8.82×10^{-3} kg. Higher gas-liquid contact time, because of the higher liquid height in the storage section for a larger volume of the liquid feed, lead to higher amount of NaOH to react over a given time of reactor operation. Besides the above factors favouring larger mass of NaOH reacted in a given time higher rate of reaction, conversion is found to reduce because of the higher total initial mass in the denominator in the definition used for conversion calculation.
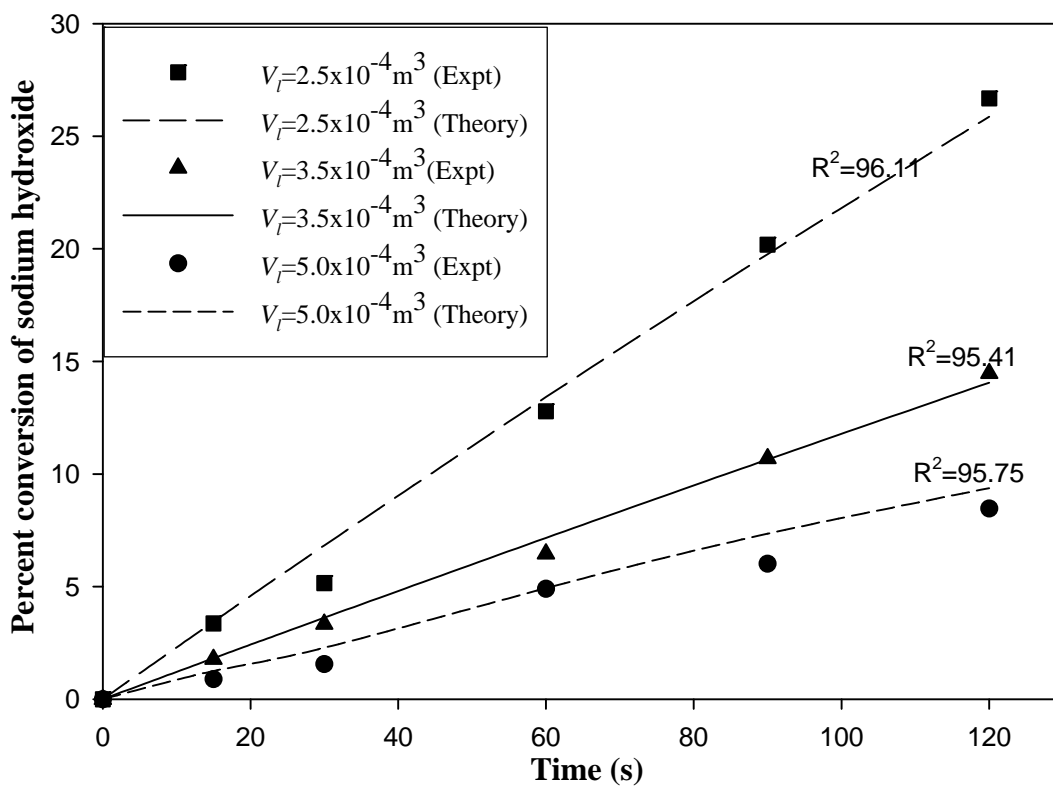
Figure 5.1. 3 Effect of solution volume charged into the reactor on conversion in a foam-bed reactor

Parameters	■	▲	●
C_{B0} (kg/m^3)	17.65	17.65	17.65
Surfactant	CTAB	CTAB	CTAB
H_f (m)	0.2	0.2	0.2
V_G (m/s)×10^4	9.66	9.66	9.66
Q_{CO2} (m^3/s) x10^6	3.0	3.0	3.0
Q_{air} (m^3/s) x10^6	833.0	833.0	833.0

Variables	■	▲	●
$\overline{\varepsilon_{Gs}}$	0.38	0.29	0.27
$\overline{\varepsilon_l}$	0.036	0.057	0.063

Experimental data and parameter values have been shown in Tables 5B.5.1 to 5B.5.3

5.1.4 Effect of concentration of carbon dioxide gas on conversion of sodium hydroxide in a foam-bed reactor

Figure 5.1.4 shows the effect of concentration of CO_2 in the feed gas on conversion of NaOH. Concentration of carbon-dioxide gas was varied from 0.22 to 0.49 percent by volume by diluting with air to study its effect on conversion of sodium hydroxide in a foam-bed reactor. 540 ppm CTAB was used as the foaming agent. It is observed from the figure that percent conversion increases with an increase in the concentration of carbon dioxide gas.

Simultaneous absorption and reaction of carbon dioxide with NaOH has been reported to be a liquid phase controlled process. Interfacial concentration of CO_2 in the liquid phase increases with an increase in its concentration in the gas phase. The increased driving force for mass transfer causes an increase in the rates of gas absorption, reaction and therefore the conversion.
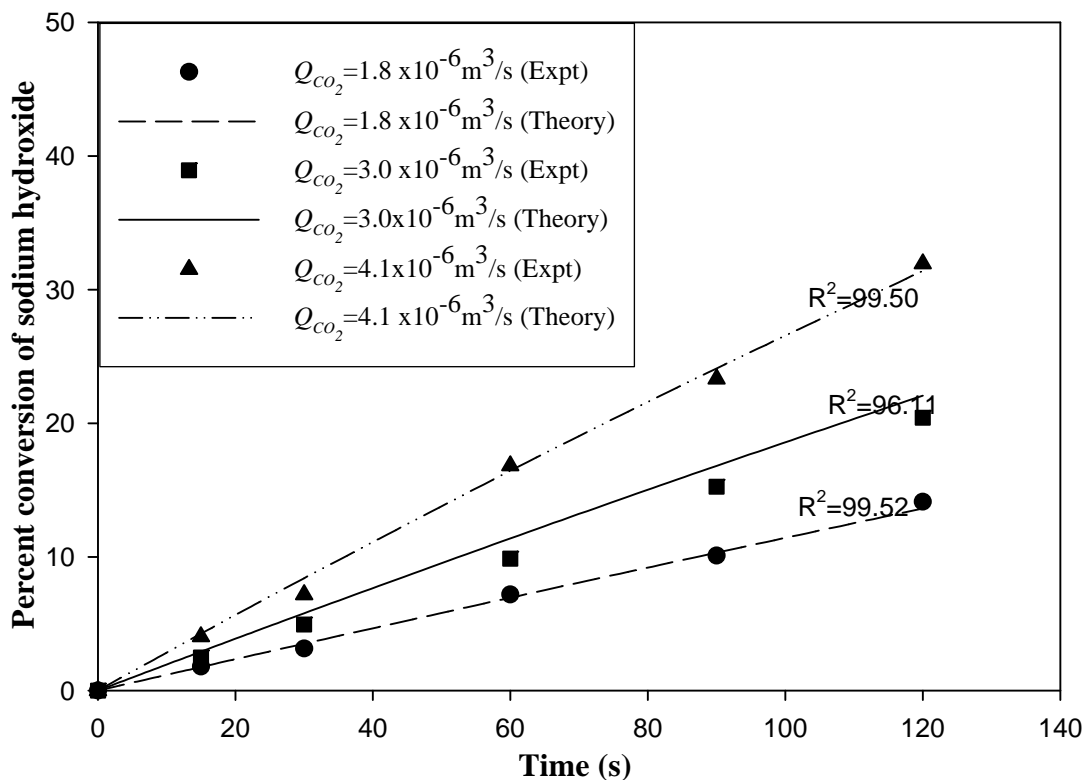
Fig 5.1.4. Effect of concentration of carbon dioxide gas on conversion of NaOH in a foam-bed reactor

Parameters	●	■	▲	Variables	●	■	▲
C_{B0} (kg/m^3)	17.65	17.65	17.65	$\overline{\varepsilon_{Gs}}$	0.37	0.38	0.39
Surfactant	CTAB	CTAB	CTAB	$\varepsilon_{,}$	0.033	0.036	0.038
H_f (m)	0.2	0.2	0.2				
V_G (m/s)$\times 10^2$	59.66	9.66	9.66				
Q_{air} (m^3/s) x10^6	833.0	833.0	833.0				
V_l (m^3)$\times 10^4$	2.5	2.5	2.5				

Experimental data and parameter values have been shown in Tables 5B.6.1 to 5B.6.3

PART II: GAS-LIQUID-SOLID SYSTEM-Absorption of CO_2 in lime slurry

Models developed for slurry and slurry-foam reactors for carbonation of hydrated lime using lean carbon di-oxide gas were presented in Chapter 3. To verify the proposed models, a series of experiments were carried out in a semi batch mode of operation in both the reactors. For a comparison of the performance of the slurry foam reactor with that of the bubble-column slurry reactor, first few experiments were carried out without addition of surfactant to the slurry. It may be observed from the models that for simulation of these reactors, values of the various parameters viz. liquid hold up in the foam column ($\overline{\varepsilon_l}$), particle size distribution ($d_{pk}'s$), solid-liquid mass-transfer coefficient (k_{sl}) and gas-liquid mass transfer coefficient ($k_l^0 a_b$) were needed. Values of d_{pk} and $\overline{\varepsilon_l}$ were measured experimentally. Solid–liquid mass transfer coefficient, k_{sl}, was obtained by fitting models to the experimental data. Trial experiments were carried out to find out the minimum superficial gas velocity required to generate stable foam column with the minimum concentration of CO_2 used in the present studies. $k_l^0 a_b$ was estimated using correlation reported in the literature for carbonation of hydrated lime slurry using lean CO_2 gas.

The subsequent series of experiments were performed with the objective of generating experimental data for comapring the performance of slurry-foam reactor with the bubble-column slurry reactor with respect to the important parameters, viz, initial loading of lime, slurry volume charged into the reactor, superficial gas velocity, foam height, nature of surfactant, concentration of surfactant, concentration of CO_2 gas and effect of addition of ethylene glycol.

For verifying the validity of the models developed, the values of k_{sl} required for fitting the model to the experimental data are compared with those reported in the literature. These values are observed to vary from 0.45 x 10^{-6} m/s to 2.0 x10^{-6} m/s for slurry reactor and from 0.65 x 10^{-6} to 0.25 x 10^{-4} m/s for the slurry foam reactor. However, Stangle and Mahalingam (1990) reported k_{sl} values to vary in the range 2 x 10^{-8} - 3 x 10^{-7} m/s and these low values were attributed to the surface coverage of lime particles by surfactant molecules as the authors used very high concentration of surfactant for generating foam. Secondly, the authors obtained k_{sl} values semi-

theoretically by fitting their model to the experimental data. They developed their model considering foam section only whereas the gas concentration and average particle size were measured upstream of the foam generation section described in this work as storage section. Neglecting the contribution of storage section towards gas absorption, solid dissolution and reaction is also considered to be an important reason for the low values of k_{sl} observed by the authors. In the present investigation, however, storage section has been observed to contribute significantly towards gas absorption and conversion and due consideration has been given for generation of foam-bed reactor model. Various investigators used different concentration of CO_2 gas for carbonation reaction and k_{sl} values are observed to increase significantly with an increase in its concentration. Superficial velocity of gas in slurry reactor and concentration of CO_2 gas in slurry-foam reactor are observed to have the most significant effect on the values of k_{sl}. A dimensionless correlation has been developed for k_{sl} in terms of different variables studied in this work.

5.2 Results of parameter estimation

5.2.1 Estimation of liquid holdup in the foam column

Liquid hold up for such reactions in which bulk concentration of reactant enhances the rate of reaction, in the foam column is an important parameter for evaluation of performance of such reactors. Liquid holdup values for carbonation of lime slurry in foam-bed reactor have been measured for all the variables studied in the present work, viz., different solid loadings, volume of slurry charged into the reactor, superficial velocity of gas, foam height, concentration of surfactants, etc. In the calculation of liquid hold-up, the volume fraction of solids in the slurry, being very small 0.9 to 1.8 percent by volume has been assumed negligible. The height-average liquid hold-up values are determined from measured liquid hold up profile. The details of experimental setup and procedure for measurement of liquid hold-up in foam column and sample calculations have been reported in chapter 4.

Experimental data and the calculated values of average liquid hold-up are shown in the following tables:

Table 5.2.1.1 Liquid hold-up in slurry-foam reactor (For the experiments-Effect of solids loading on conversion of lime)

Sample batch No. of $Ca(OH)_2$: 03097 (CDH)

CO_2 gas flow rate = 0.333 x 10^{-4} m^3/s

Air flow rate = 3.0 x 10^{-4} m^3/s

Slurry volume = 2.5 x 10^{-4} m^3

Foam height = 0.4 m

Surfactant = SDS (4000ppm)

Distance from Slurry foam interface at which suction was applied (m) × 10^2	Solids loading, kg/m^3		
	20	40	60
	Volume of liquid sucked into the sampling bulb (m^3) × 10^6		
0	55	60	45.5
3	11	11.5	10.5
5	8	8.4	7.2
10	3.1	3	2.7
20	1.8	1.7	1.4
39	1.2	1.0	0.9
Average liquid holdup	0.0106	0.0104	0.00849

Table 5.2.1.2 Liquid hold-up in slurry foam reactor (For the experiments-Effect of foam height on conversion)

Sample batch No. of $Ca(OH)_2$: 03097 (CDH)

CO_2 gas flow rate = 0.333 x 10^{-4} m^3/s

Air flow rate = 3.0 x 10^{-4} m^3/s

Solid loading= 40 kg/m^3

Slurry volume = 2.5 x 10^{-4} m^3

Surfactant = SDS (4000 ppm)

Distance from Slurry foam interface at which suction was applied (m) × 10^2	Foam height, m		
	0.2	0.4	0.6
	Volume of liquid sucked into the sampling bulb (m^3) × 10^6		

0	52	60	60.6
3	10	11.5	11.7
5	6.5	8.4	9.0
10	2.0	3.0	4.2
19	1.1	1.7	2.1
39	------	1.0	1.4
59	--------	--------	0.4
Average liquid holdup	0.0147	0.0104	0.0084

Table 5.2.1.3 Liquid hold-up in slurry foam reactor (For the experiments-Effect of slurry volume on conversion of lime)

 Sample batch No. of $Ca(OH)_2$: 03097 (CDH)

 CO_2 gas flow rate = 0.333 x 10^{-4} m^3/s

 Air flow rate = 3.0 x 10^{-4} m^3/s

 Solid loading= 40 kg/m^3

  Foam height = 0.4 m

 Surfactant = SDS (4000ppm)

Distance from Slurry foam interface at which suction was applied (m) × 10^2	Slurry volume, m^3		
	2.5 x 10^{-4}	3.5 x 10^{-4}	5.0 x 10^{-4}
	Volume of liquid sucked into the sampling bulb (m^3) × 10^6		
0	60	65	50
3	11.5	11.0	10.0
5	8.4	8.2	6.5
10	3.0	4.2	2.0
20	1.7	3.0	1.0
39	1.0	2.8	0.6
Average liquid holdup	0.0104	0.0129	0.0080

Table 5.2.1.4 Liquid hold-up in slurry-foam reactor (For the experiments-Effect of superficial velocity of gas on conversion of lime)

 Sample batch No. of $Ca(OH)_2$: 03097 (CDH)

 Solid loading = 40 kg/m^3

Slurry volume = 2.5 x 10^{-4} m^3

Foam height = 0.4 m

Surfactant = SDS (4000ppm)

Distance from Slurry foam interface at which suction was applied (m) $\times 10^2$	Superficial velocity of gas, (m/s) x 10^2		
	3.85	5.77	7.70
	Volume of liquid sucked into the sampling bulb (m^3) $\times 10^6$		
0	60	65.5	72
3	11.5	14.3	17.0
5	8.4	10.5	12.3
10	3.0	4.0	6.5
20	1.7	2.5	4.0
39	1.0	1.6	2.0
Average liquid holdup	0.0104	0.0128	0.0162

Table 5.2.1.5 Liquid hold-up in slurry-foam reactor (For the experiments-Effect of nature of surfactant on conversion)

Sample batch No. of $Ca(OH)_2$: MH0M601992 (MERCK)

CO_2 gas flow rate = 0.333 x 10^{-4} m^3/s

Air flow rate = 3.0 x 10^{-4} m^3/s

Solid loading = 40 kg/m^3

Slurry volume = 2.5 x 10^{-4} m^3

Foam Height = 0.4m

Distance from Slurry foam interface at which suction was applied (m) $\times 10^2$	Surfactant (Concentration)		
	SDS (4000 ppm)	CTAB (540 ppm)	Triton-X-100 (960 ppm)
	Volume of liquid sucked into the sampling bulb (m^3) $\times 10^6$		
0	48	73	51
3	13.0	28.0	10.5
5	8.0	8.0	8.4
10	6.2	5.8	3.1

20	4.2	3.8	1.8
39	2.0	3.0	1.0
Average liquid holdup	0.0134	0.0331	0.0099

Table 5.2.1.6 Liquid hold-up in slurry-foam reactor (For the experiments-Effect of concentration of surfactant on conversion)

Sample batch No. of $Ca(OH)_2$: MH0M601992 (MERCK)

CO_2 gas flow rate = 0.333 x 10^{-4} m^3/s

Air flow rate = 3.0 x 10^{-4} m^3/s

Solid loading = 20 kg/m^3

Slurry volume = 2.5 x 10^{-4} m^3

Surfactant = SDS

Distance from Slurry foam interface at which suction was applied (m) × 10^2	Surfactant Concentration (ppm)			
	2000	4000	8000	16000
	Volume of liquid sucked into the sampling bulb (m^3) × 10^6			
0	47	48	35	16
3	13	14	19	4.6
5	8	13	12	8.7
10	6.2	6.9	5.4	5.2
20	4.2	6.0	5.8	3.6
39	2.0	2.2	2.6	0.8
Average liquid holdup	0.0134	0.0162	0.0151	0.0085

Table 5.2.1.7 Liquid hold-up in slurry-foam reactor (For the experiments-Effect of concentration of surfactant on conversion)

Sample batch No. of $Ca(OH)_2$: MH0M601992 (MERCK)

CO_2 gas flow rate = 0.333 x 10^{-4} m^3/s

Air flow rate = 3.0 x 10^{-4} m^3/s

Solid loading = 20 kg/m^3

Slurry volume = 2.5 x 10^{-4} m^3

Surfactant: CTAB

Distance from Slurry foam interface at which suction was applied (m) $\times 10^2$	Surfactant Concentration (ppm)			
	200	540	1000	1620
	Volume of liquid sucked into the sampling bulb (m^3) $\times 10^6$			
0	73	52	80	75
3	28	25	19	15
5	8.0	13.0	5.6	5.2
10	5.8	5.8	2.8	3.2
20	3.8	4.0	3.4	3.5
39	3.0	2.8	1.4	1.8
Average liquid holdup	0.0276	0.0331	0.0140	0.0098

Table 5.2.1.8 Liquid hold-up in slurry-foam reactor (For the experiments-Effect of concentration of surfactant on conversion)

Sample batch No. of Ca(OH)$_2$: MH0M601992 (MERCK)

CO$_2$ gas flow rate = 3.33 x 10^{-5} m^3/s

Air flow rate = 3.0 x 10^{-4} m^3/s

Solid loading = 20 kg/m^3

Slurry volume = 2.5 x 10^{-4} m^3

Surfactant: Triton-X-100

Distance from Slurry foam interface at which suction was applied (m) $\times 10^2$	Surfactant Concentration (ppm)			
	320	960	2400	4800
	Volume of liquid sucked into the sampling bulb (m^3) $\times 10^6$			
0	45	51	68	61
3	10	10.5	12	11
5	8.3	8.5	8.5	7.8
10	4.8	3.2	3.2	3.4
20	2.0	1.8	2.6	1.7
39	1.0	1.0	2.0	0.9
Average liquid holdup	0.0102	0.0109	0.0126	0.0106

It is observed from Table 5.2.1.8 that on increasing surfactant concentration, the value of liquid hold-up shows an increasing trend possibly due to the increase in foam stability owing to a reduction in the film drainage rate. Liquid hold-up for ionic surfactant is found to be higher than for non-ionic surfactant under identical experimental conditions.

5.2.2 Particle size distribution and average particle size

Particle size distributions (PSDs) of reactant $Ca(OH)_2$ and product $CaCO_3$ were measured using CILAS 940 particle size analyser and MALVERN MASTERSIZER 2000E. Particle-size distributions obtained from CILAS 940 particle size analyzer for both the reactant samples have been shown in figures 5.2.2.1 and 5.2.2.2. Particle size distribution is indicative of the measure of solid-liquid interficial area in a slurry reactor and essentially need to be incorporated in the models. Two hydrated lime samples supplied by CDH Pvt. Ltd., batch No: 03097 and the other by MERCK Pvt. Ltd., batch No. MH0M601992, were used in present studies. The respective volume-average particle diameters, 8.67 μm and 6.04 μm, were measured using a CILAS 940 particle size analyzer. The entire particle size distribution was divided into 12 volume fractions and used for reactor simulation. Details of the reduced fractions are shown in tables 5.2.2.1 and 5.2.2.2.
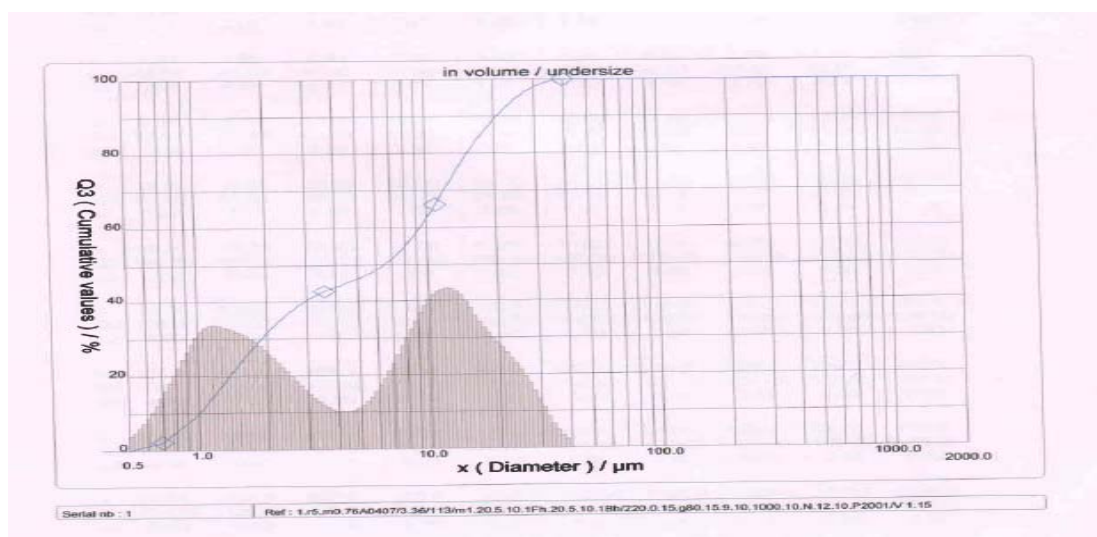
CDH, Batch no. 03097

Figure 5.2.2.1 Particle size distribution (CILAS 940 particle size analyzer)

Table 5.2.2.1 Particle size distribution of hydrated lime sample (batch no. 03097)

Average particle size= 8.67 μm

Sr. No. of fraction	Volume fraction of particles	Average particle diamter (μm)	Sr. No. of fraction	Volume fraction of particles	Average particle diameter (μm)
1	0.1185	0.9	7	0.0996	16.5
2	0.0876	1.55	8	0.0363	20.5
3	0.0988	2.2	9	0.0398	25.0
4	0.1890	4.05	10	00113	30.0
5	0.2195	8.15	11	0.0046	34.0
6	0.0932	12.5	12	0.0018	40.0
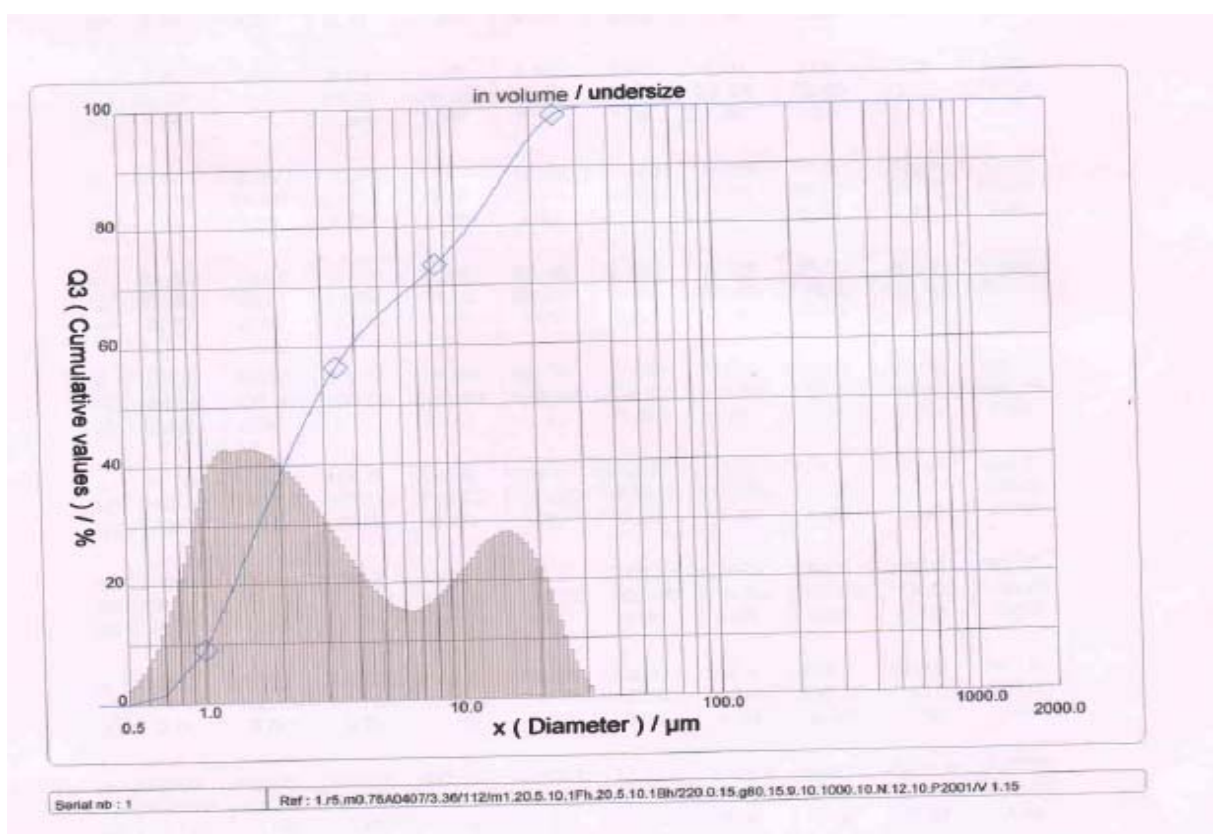
MERCK, Batch no. MH0M601992

Figure 5.2.2.2 Particle size distribution (CILAS 940 particle size analyzer)

Table 5.2.2.2   Particle size distribution of hydrated lime sample (batch no. MH0M601992)

Average particle size= 6.04 μm

Sr. No. of fraction	Volume fraction of particles	Average particle diamter (μm)	Sr. No. of fraction	Volume fraction of particles	Average particle diameter (μm)
1	0.092	0.75	7	0.0531	6.0
2	0.1662	1.25	8	0.063	8.5
3	0.1221	1.75	9	0.1022	12.5
4	0.1488	2.5	10	0.0767	17.5
5	0.0777	3.5	11	0.0536	26.25
6	0.0446	4.5	12	0.0160	33.0

The particle size distribution of reactant $Ca(OH)_2$ from B. No. MH0M601992 and obtained using MALVERN MASTERSIZER 2000E, has been shown in figure 5.2.2.3,
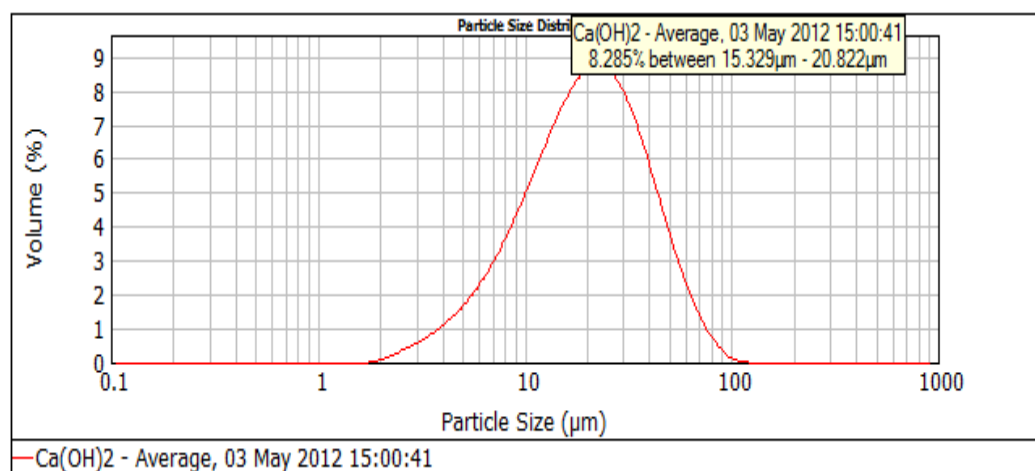
Batch no. MH0M601992

Figure 5.2.2.3 Particle size distribution (MALVERN MASTERSIZER 2000E)

While that of $CaCO_3$ obtained by complete carbonation of hydrated lime, batch no. MH0M601992, with SDS as the foaming agent in a foam-bed reactor has been shown in figure 5.2.2.4.
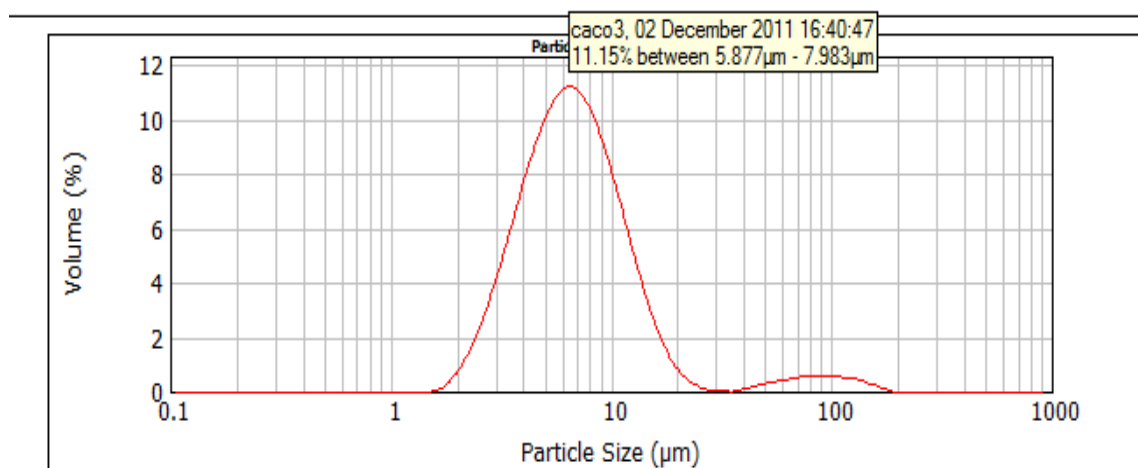
Figure 5.2.2.4 Particle size distribution of product CaCO₃ with SDS as a foaming agent (MALVERN MASTERSIZER 2000E)

It is observed that particle size of product calcium carbonate present with maximum volume percent, 11.15%, varies from 5.88 μm to 7.98 μm. The particle size distribution of product CaCO₃, obtained from carbonation of Ca(OH)₂ sample of batch no. MH0M601992, in a foam-bed reactor with CTAB as the foaming agent has been shown in figure 5.2.2.5. It is observed that particle size of product calcium carbonate present with maximum volume percent, 8.65%, varies from from 3.9 μm to 5.3 μm.

Table 5.2.2.3   Particle size distribution of CaCO₃ using SDS and CTAB as the foaming agents

S.No.	Surfactant used	% volume of particles	Particle size (μm)	Specific surface area, m²/g	Surface weighted mean diameter of particles (μm)
1.	SDS	11.15	5.8-7.9	0.424	5.777
2.	CTAB	8.65	3.9-5.3	0.413	5.928
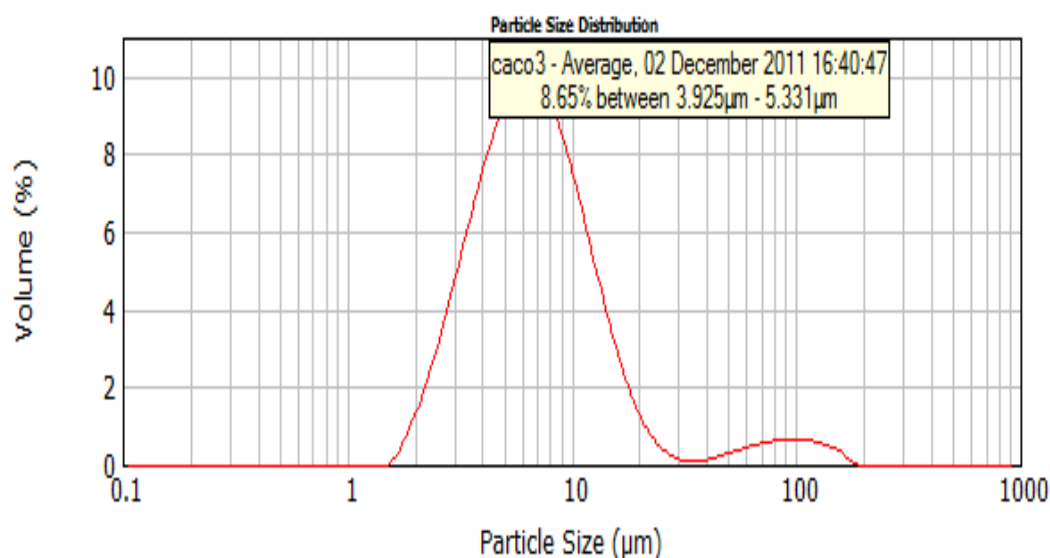
Figure 5.2.2.5 Particle size distribution of product CaCO$_3$ with CTAB as a foaming agent (MALVERN MASTERSIZER 2000E)

5.3 Effects of different variables on conversion of hydrated lime in bubble column and foam-bed slurry reactors

5.3.1 Effect of initial solids loading on conversion of lime

The effect of initial loading of calcium hydroxide on its conversion in the short bubble column reactor has been shown in Figure 5.3.1*a* and, that in the foam-bed reactor in Figure 5.3.1b. Initial loading was varied from 20 to 60 kg/m^3 with all the other variables kept unchanged for the different sets of experiments. It is observed that the conversion of lime reduces with an increase in its initial loading although the total mass of lime reacted after a given time of reactor operation increases marginally with an increase in the solids loading. Volume of solvent in the feed slurry being the same in each case, surface area of suspended particles per unit volume of slurry increases with an increase in the initial solids loading. This leads to an increase in the rate of solids dissolution and hence the rate of reaction. The observed values of the reduced conversion with increased solids loading, is therefore due to the definition used for its calculation, initial solids loading appearing in the denominator. Flow rates of CO$_2$ and air were maintained at 3.33 x 10^{-5} m^3/s and 30 x 10^{-5} m^3/s, respectively.
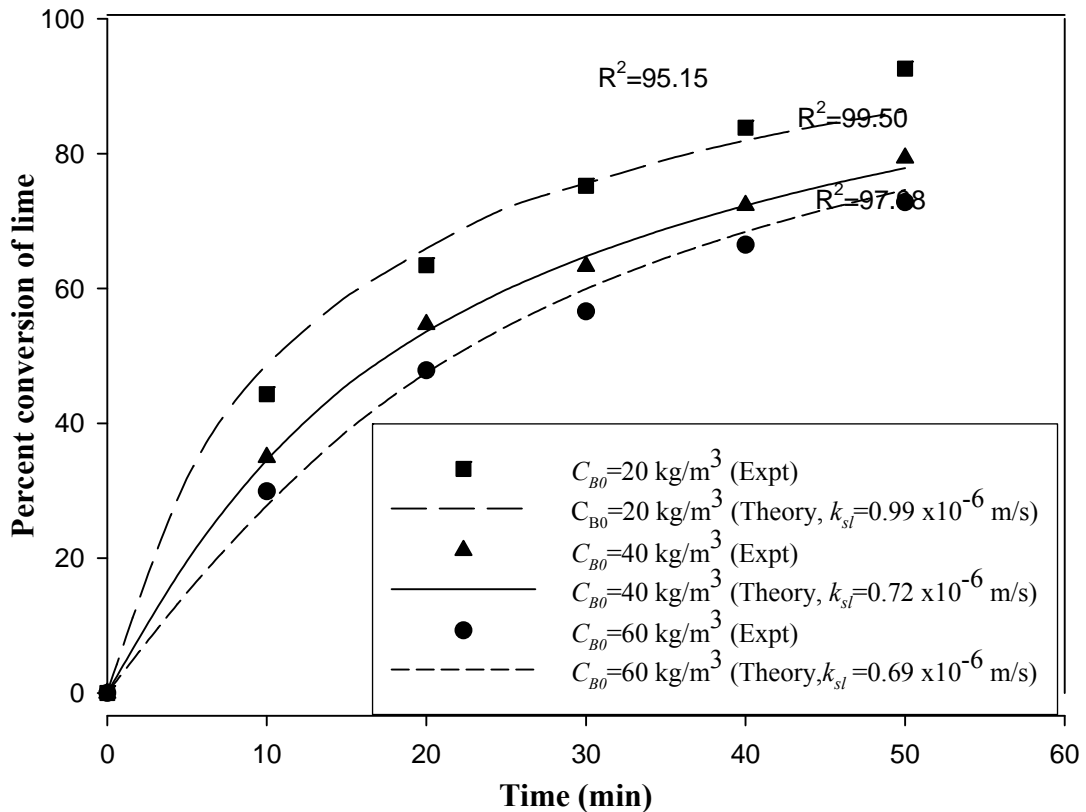
Figure 5.3.1a Effect of initial loading of lime on conversion in a bubble-column reactor (sample make &batch no.: CDH, 03097)

Experimental data and parameter values have been shown in Tables 5E.1.1 to 5E.1.3

Parameters	■	▲	●
Surfactant	none	None	none
H_f (m)	0.0	0.0	0.0
V_G (m/s)$\times 10^2$	3.85	3.85	3.85
V_l (m^3)$\times 10^4$	2.5	2.5	2.5
Q_{CO_2}(m^3/s)$\times 10^4$	0.33	0.33	0.33
Q_{air} (m^3/s)$\times 10^4$	3.0	3.0	3.0

Increased solids loading increases the viscosity of the slurry and is one of the possible reasons for the reduced value of solid-liquid mass-transfer coefficient.

Conversion of lime in the foam-bed reactor, shown in Fig. 5.3.1b, is however substantially higher than that in the bubble column reactor. This is attributed to the substantially high surface area created in the foam section with the consequent increase in the rate of absorption of carbon-dioxide gas. Presence of particles in the

region of large gas-liquid interfacial area supplying a reactant to the liquid phase is another reason for higher conversion. In the present investigation, k_{sl} is found to decrease from 0.99 x10^{-6} to 0.69 x10^{-6} m s^{-1} for bubble column- and from 0.63 x10^{-5} to 0.35 x10^{-5} m s^{-1} for foam-bed reactors as the solids loading is increased in the above range.
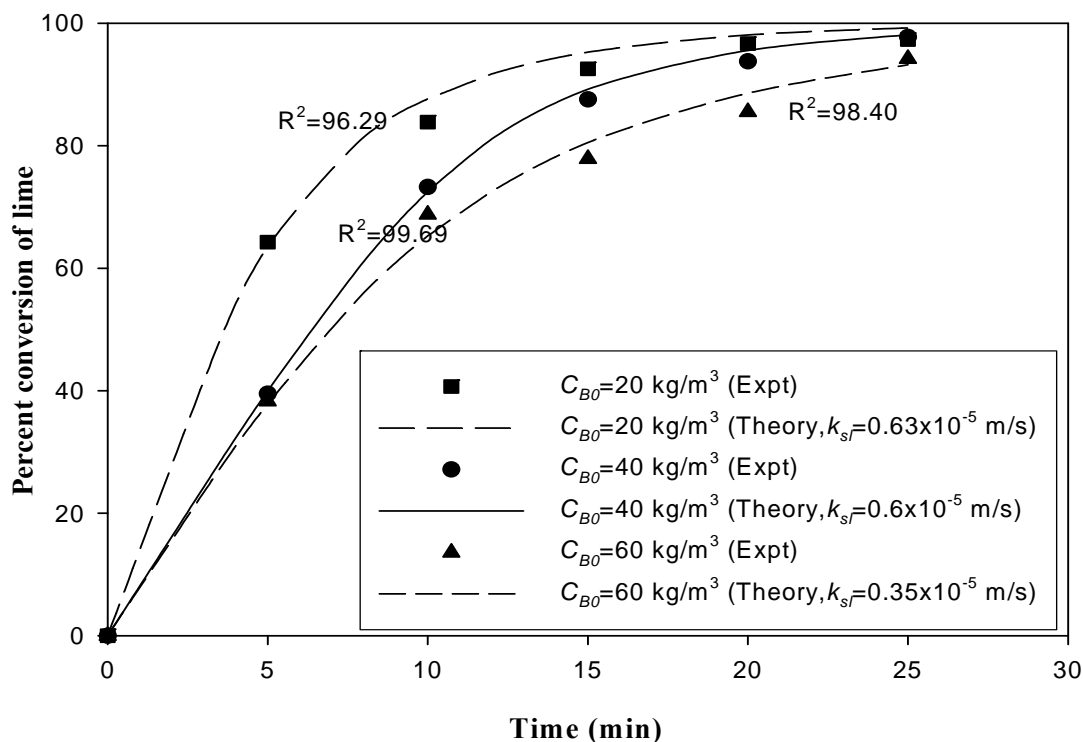
Figure 5.3.1b Effect of initial loading of lime on conversion in a foam-bed reactor (sample make &batch no. : CDH, 03097)

Experimental data and parameter values have been shown in Tables 5E.2.1 to 5E.2.3

Parameters/variables	■	●	▲
Surfactant	SDS	SDS	SDS
C_s (ppm)	4000	4000	4000
H_f (m)	0.4	0.4	0.4
V_G (m/s)$\times 10^2$	3.85	3.85	3.85
V_l (m^3)$\times 10^4$	2.5	2.5	2.5
$\overline{\varepsilon_l} \times 10^2$	1.01	1.04	0.8495

$Q_{CO_2}(m^3/s) \times 10^4$	0.33	0.33	0.33
$Q_{air} (m^3/s) \times 10^4$	3.0	3.0	3.0

5.3.2 Effect of superficial velocity of gas on conversion

Superficial velocity of gas was varied from 3.85 to 7.70 $\times 10^{-2}$ m s^{-1} to study its effect on conversion of lime in the bubble column and foam-bed reactors. In the latter, stable foam column was generated using SDS as the foaming agent.
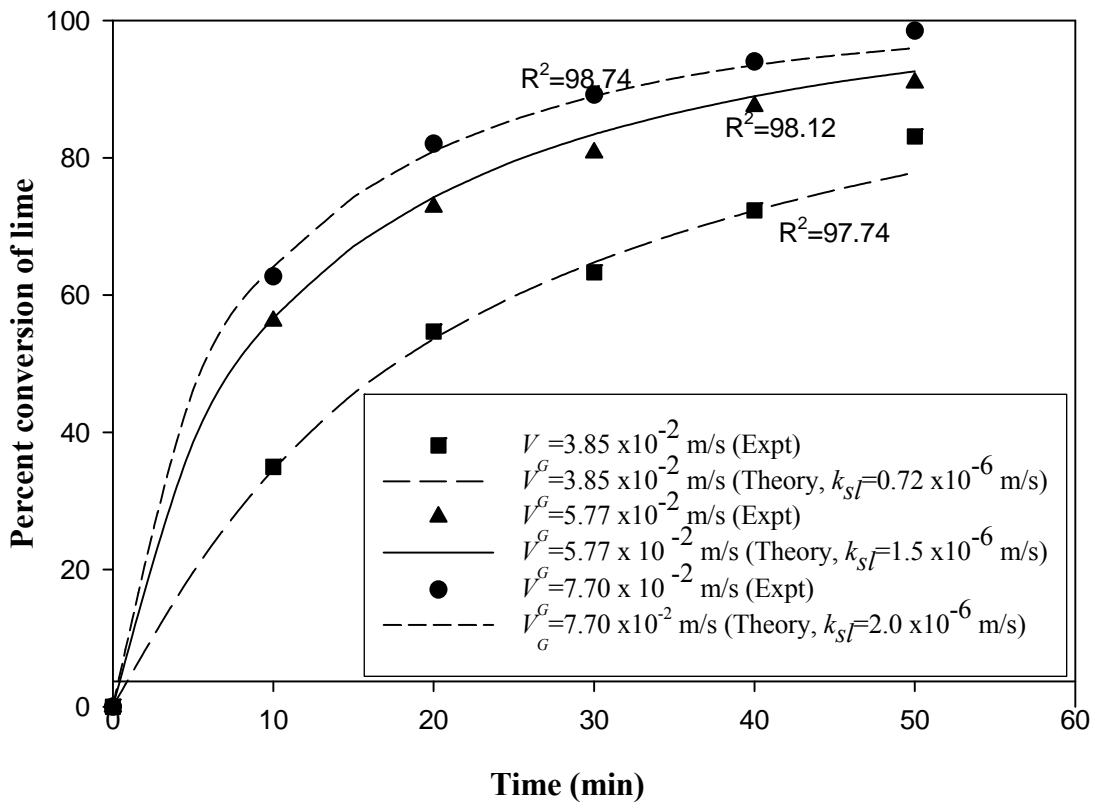
Figure 5.3.2a Effect of superficial velocity of gas on conversion of lime in a bubble-column reactor (sample batch no.: CDH, 03097)

Experimental data and parameter values have been shown in Tables 5E.3.1 to 5E.3.3

Parameters	■	▲	●
Surfactant	none	none	none
H_f (m)	0.0	0.0	0.0
C_{B0} (kg/m^3)	40	40	40
V_l (m^3) $\times 10^4$	2.5	2.5	2.5
$Q_{CO_2}(m^3/s) \times 10^4$	0.33	0.5	0.67
$Q_{air}(m^3/s) \times 10^4$	3.0	4.5	6.0

Graphical representations of the experimental data for the two cases have been shown in Figures 5.3.2a and 5.3.2b respectively. Conversion of lime increases as the superficial gas velocity is increased at constant values of the other variables including molar concentration of CO_2 in the feed gas mixture in both the reactors.
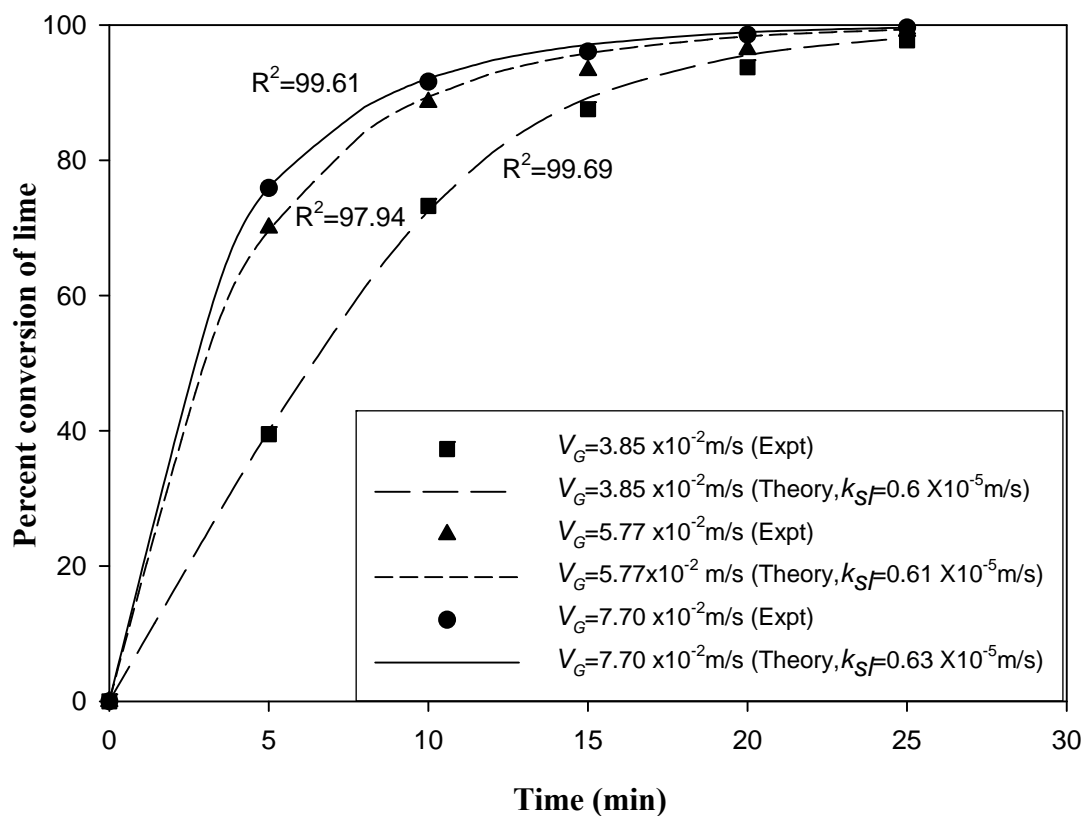
Figure 5.3.2b Effect of superficial velocity of gas on conversion of lime in a foam-bed reactor (sample batch no.: CDH, 03097)

Experimental data and parameter values have been shown in Tables 5E.4.1 to 5E.4.3

Parameters/ variables	■	▲	●
Surfactant	SDS	SDS	SDS
C_s (ppm)	4000	4000	4000
H_f (m)	0.4	0.4	0.4
C_{B0} (kg/m^3)	40	40	40
V_l (m^3)$\times 10^4$	2.5	2.5	2.5
$\overline{\varepsilon_l} \times 10^2$	1.04	1.28	1.62
Q_{CO_2}(m^3/s)$\times 10^4$	0.33	0.5	0.67
Q_{air} (m^3/s)$\times 10^4$	3.0	4.5	6.0

Increase in turbulence with higher superficial velocity of gas cause higher values of gas-liquid and gas-liquid-solid mass-transfer coefficients in a bubble column reactor. Increased rates of gas absorption and solid dissolution accompanied by chemical reaction, result in higher conversion of lime.

As with the other variables, extent of conversion after a given time of reactor operation in the foam-bed reactor is observed to be substantially higher over that in the bubble column reactor. Increase in turbulence in the storage section of a foam-bed reactor occurs by two ways. Bubble size becomes larger and the number of bubbles formed per unit time increases with an increase in the gas flow rate. Larger number of bubbles of larger size passing through the column of liquid in a given time increases turbulence in the storage section. Secondly, liquid hold-up in the foam section increases due to higher superficial velocity of gas. This causes an increase in the foam drainage rate by gravity as well. Larger quantity of suspended particles contained in the slurry therefore moves to the region of very large gas-liquid interfacial area facilitating increased rates of reaction of the absorbed gas and the dissolved solids in the foam film close to the gas-liquid interface. Gravity drainage rate from the film surfaces being directly proportional to the liquid holdup, rate of surface renewal of the foam films due to surface drainage occur at a faster rate. The resulting higher values of mass transfer coefficients in both storage and foam sections thus contribute to higher conversion of lime due to higher rates of gas absorption, solid dissolution and chemical reaction.

5.3.3 Effect of volume of slurry charged into the reactor on conversion

Figure 5.3.3a shows the effect of volume of slurry charged into the bubble column reactor on conversion of lime at constant values of the other variables. Three sets of experiments were performed by varying the volume of a batch of slurry from 2.5×10^{-4} to 5.0×10^{-4} m^3. It is observed from the figure that conversion of lime is reduced as the volume of slurry charged to the reactor is increased. Solids loading in the slurry is, however, kept constant by mixing hydrated lime proportionately to the volume of solvent used for its preparation. The surface area per unit volume of slurry, therefore, remains same in each of the feed slurry. However, total amount of solids in the slurry volume of 5.0×10^{-4} m^3 being twice than that in 2.5×10^{-4} m^3, total solid-liquid interfacial area available for solid dissolution in the former is higher by a factor of two

compared to that in the latter. Hydrated lime being sparingly soluble, amount of dissolved lime available in a larger volume of reactant slurry is proportionately larger.
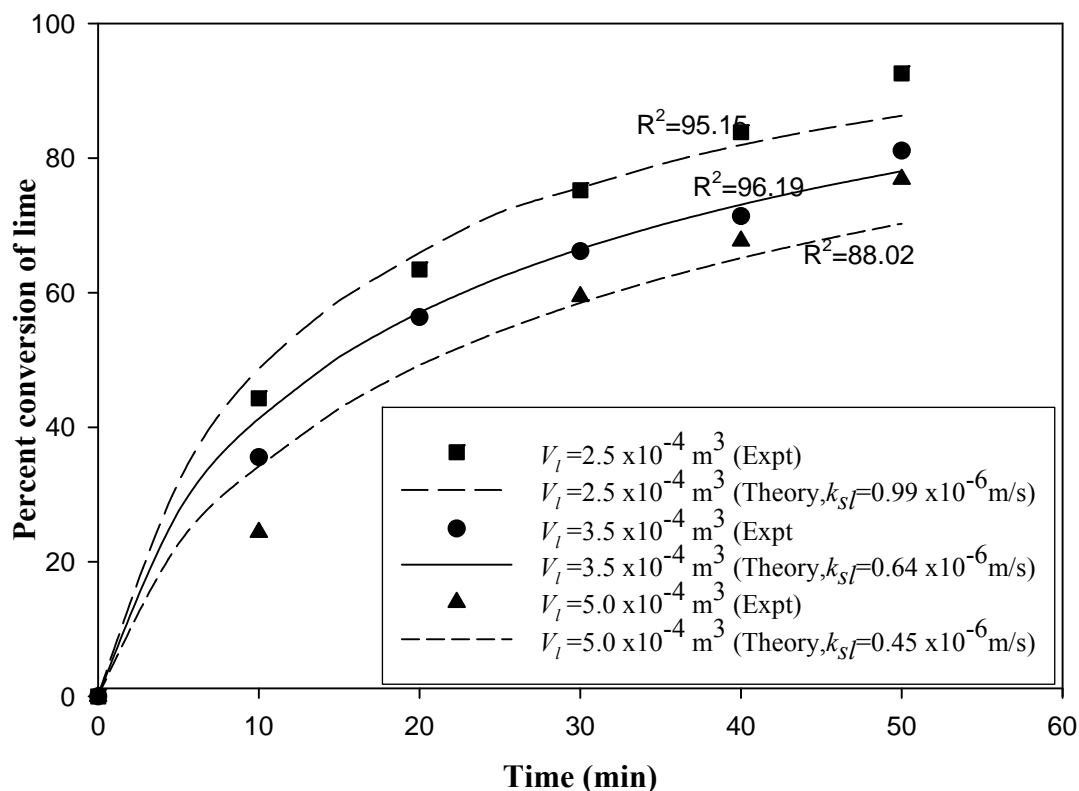
Figure 5.3.3a Effect of slurry volume charged into the reactor on conversion of lime in a bubble-column contactor (sample batch no.: CDH, 03097)

Experimental data and parameter values have been shown in Tables 5E.5.1 to 5E.5.3

Parameters	■	●	▲
C_{B0} (kg/m^3)	20	20	20
H_f (m)	0.0	0.0	0.0
V_G (m/s)$\times 10^2$	3.85	3.85	3.85
Surfactant	none	none	none
Q_{CO_2} (m^3/s)$\times 10^4$	0.33	0.33	0.33
Q_{air} (m^3/s)$\times 10^4$	3.0	3.0	3.0

Liquid height in the column being larger for a larger volume of the slurry feed, gas-liquid contact time also becomes proportionately larger. These aspects, therefore, favors larger amount of dissolved solid to undergo reaction over a given period of reactor operation. On the other hand, increased liquid height causes a lowering in each of the gas-liquid and solid-liquid mass-transfer coefficient due to reduced intensity of

agitation of the slurry, superficial velocity of gas being kept unchanged. This is likely to lower the rate of reaction per unit volume of slurry. The observed experimental data of reduced conversion therefore indicate that the effect of larger quantity of solids fed to the reactor contained in the larger slurry volume on the conversion calculation dominates over the combined effect of all the above factors. k_{sl} reduces from 0.99 x 10^{-6} to 0.45 x 10^{-6} m/s as slurry volume increases from 2.5 x 10^{-4} to 5.0 x 10^{-4} m^3.
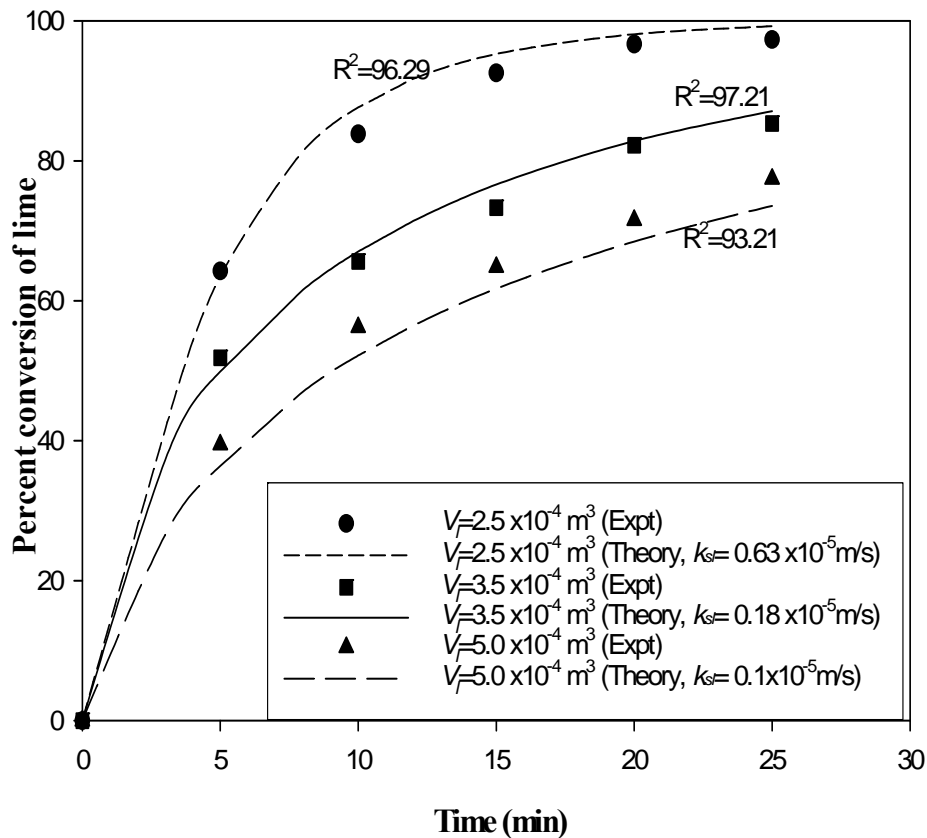
Figure 5.3.3b Effect of slurry volume charged into the reactor on conversion in a foam-bed reactor (sample batch no.: CDH, 03097)

Experimental data and parameter values have been shown in Tables 5E.6.1 to 5E.6.3

Parameters /variables	●	■	▲
Surfactant	SDS	SDS	SDS
C_s (ppm)	4000	4000	4000
H_f (m)	0.4	0.4	0.4
V_G(m/s)×10^2	3.85	3.85	3.85

C_{B0} (kg/m^3)	20	20	20
$\overline{\varepsilon_l} \times 10^2$	1.04	1.29	0.80
Q_{CO_2}(m^3/s)$\times 10^4$	0.33	0.33	0.33
Q_{air} (m^3/s)$\times 10^4$	3.0	3.0	3.0

In the foam-bed reactor, the conversion of lime is observed to be higher *for a given volume of slurry* over that in the bubble column reactor under otherwise similar experimental conditions. As observed in the cases of other variables, this is attributed mainly to the substantially higher gas-liquid interfacial area. Model is found to agree well to the experimental data for solid-liquid mass-transfer coefficient values in the range 0.1 x 10^{-5} to 0.63 x 10^{-5} m/s. These values are in close agreement with those reported by Ramachandran and Sharma (1969).

5.3.4 Effect of Foam height on conversion of hydrated lime

Effect of foam height on conversion of hydrated lime has been shown in Figure 5.3.4. Initial solids loading and concentration of carbon-dioxide gas was maintained all throughout the three sets of experiments at 40 kg m^{-3} and 10 volume percent respectively. It is observed that percent conversion of lime increases with an increase in the height of foam column. Gas remains in contact with the liquid for a longer period in a taller foam column and total gas-liquid interfacial area in a taller column is substantially higher than those in a shorter foam column. Although volume of slurry per volume of gas-liquid dispersion $\left(\overline{\varepsilon_l}\right)$ reduces marginally with an increase in the foam height, total volume of slurry in the foam column increases as the foam height is increased. Superficial velocity of gas and volume of feed-slurry being same in each set of experiments, reduced volume of slurry in the storage section associated with a taller foam column generates higher turbulence resulting in higher values of gas-liquid and solid-liquid mass-transfer coefficient.

Combined effects of all the above factors contribute to higher rates of gas absorption, reaction and conversion of lime in a taller foam column. k_{sl} values vary from 0.25 x 10^{-5} to 0.75 x 10^{-5} m/s as the foam heights vary from 0.2 to 0.6 m.
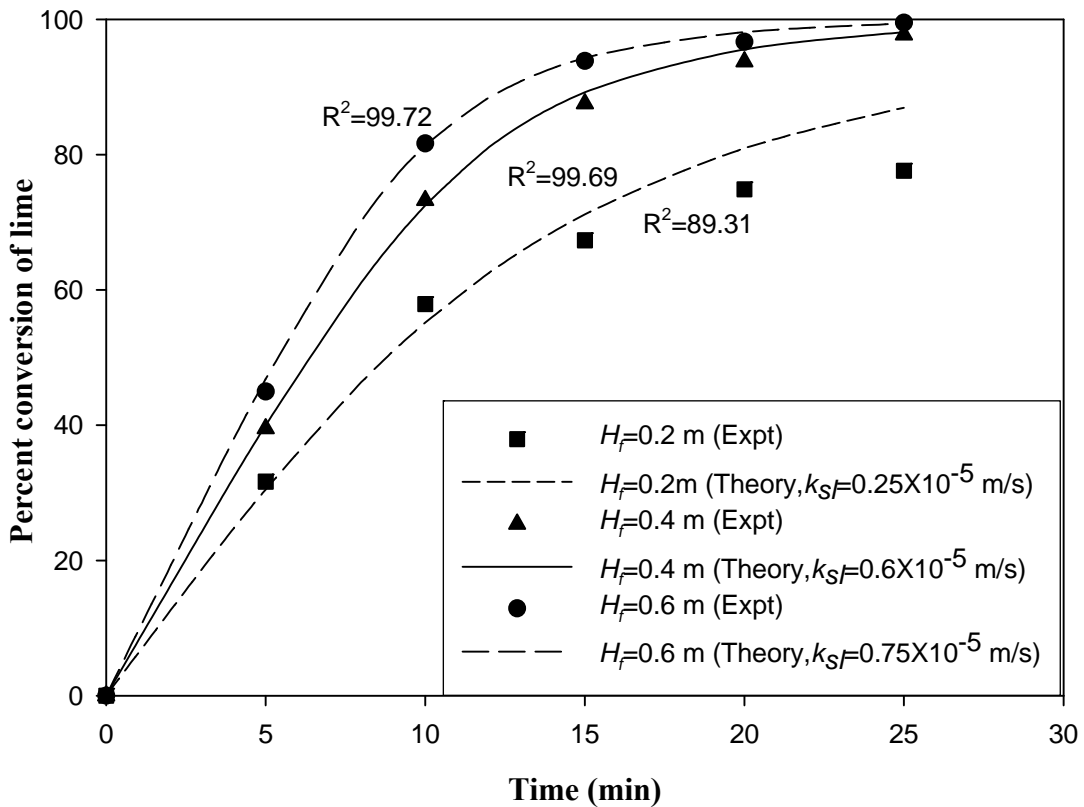
Figure 5.3.4 Effect of foam height on conversion in a foam-bed reactor (sample batch no.: CDH, 03097)

Experimental data and parameter values have been shown in Tables 5E.7.1 to 5E.7.3

Parameters/variables	■	▲	●
Surfactant	SDS	SDS	SDS
C_s (ppm)	4000	4000	4000
V_G (m/s)$\times 10^2$	3.85	3.85	3.85
C_{B0} (kg/m^3)	40	40	40
V_l (m^3)$\times 10^4$	2.5	2.5	2.5
$\overline{\varepsilon_l} \times 10^2$	1.47	1.04	0.84
Q_{CO_2}(m^3/s)$\times 10^4$	0.33	0.33	0.33
Q_{air} (m^3/s)$\times 10^4$	3.0	3.0	3.0

5.3.5 Effect of nature of surfactant

Figure 5.3.5 shows the effect of nature of surfactant on conversion of hydrated lime in a foam bed reactor.
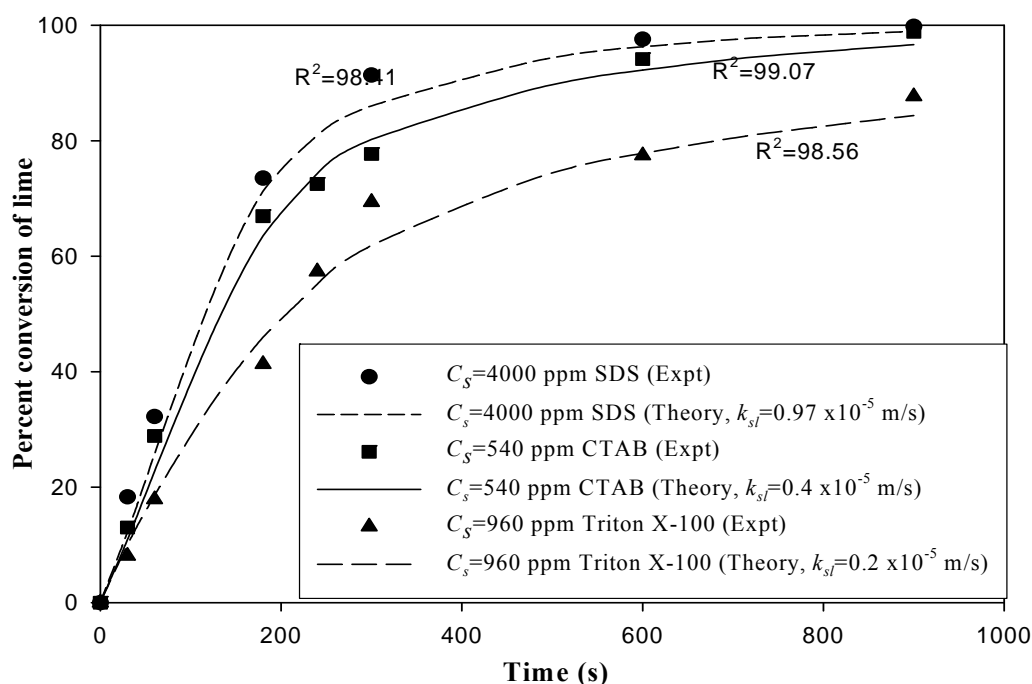
Figure 5.3.5 Effect of nature of surfactant on conversion of lime in a foam-bed reactor (sample batch no.: MERCK, MH0M601992)

Experimental data and parameter values have been shown in Tables 5E.8.1 to 5E.8.3

Parameters/variables	●	■	▲
Surfactant	SDS	CTAB	Triton X-100
C_s (ppm)	4000	540	960
H_f (m)	0.4	0.4	0.4
V_G (m/s)$\times 10^2$	3.85	3.85	3.85
C_{B0} (kg/m^3)	20	20	20
$\overline{\varepsilon_l} \times 10^2$	1.62	3.31	1.09
Q_{CO_2}(m^3/s)$\times 10^4$	0.33	0.33	0.33
Q_{air} (m^3/s)$\times 10^4$	3.0	3.0	3.0

It is observed that higher conversion is obtained with all three surfactants used i.e. sodium dodecyl sulfate (SDS), cetyl trimethyl ammonium bromide (CTAB) and octyl phenoxy polyethoxyethanol (Triton X-100) as compared to that when no surfactant is used. Conversion of lime is seen to be much higher when ionic surfactants (SDS and CTAB) are used as foaming agent compared to that when non ionic surfactant is used.

Presence of ions at the gas-liquid interface inhibits bubble coalescence and the resultant decrease in average bubble diameter also alter $k_l^{\ 0}$. In such cases, the volumetric mass-transfer coefficient, $k_l^{\ 0}a_b$ increases 2-10 times (Riet,1979). Thus the increase in conversion of calcium hydroxide in a foam bed reactor may be the result of an increase in the volumetric mass transfer coefficient. For given height of foam column, the number of bubbles are larger for ionic surfactants, resulting in higher liquid hold up and interfacial area which causes larger absorption of CO_2 gas and hence a higher conversion.

5.3.6   Effect of concentration of sodium dodecyl sulphate (SDS)

Four different concentrations of SDS: 2000, 4000, 8000 and 16000 ppm in hydrated lime slurry were used for studies of their effects on conversion of lime. The conversion, shown in figure 5.3.6, is found to increase with an increase in the surfactant concentration in the lower concentration range. Above 8000 ppm, conversion of lime is found to reduce.

Variation in the solid-liquid mass- transfer coefficient, k_{sl} is also found to follow the similar trend. It increases from 0.6 x 10^{-5} m/s to 0.99 x 10^{-5} m/s and then reduces to 0.3 x 10^{-5} m/s. A plausible explanation for such variations is that increased concentration of SDS, at its low level, increases the stability of foams resulting in an increase in the foam film thickness and thereby the slurry hold-up in the foam column. Increased turbulence due to reduced volume of slurry in the storage section and greater slurry movement in the foam section lead to higher gas-liquid and gas-liquid-solid mass transfer coefficient. Increased rates of gas absorption, solid dissolution and reaction therefore produces higher conversion of lime. At higher concentrations of SDS, surface coverage of lime particles by molecules of sodium dodecyl sulfate may be a possible reason for the reduced conversion of lime.
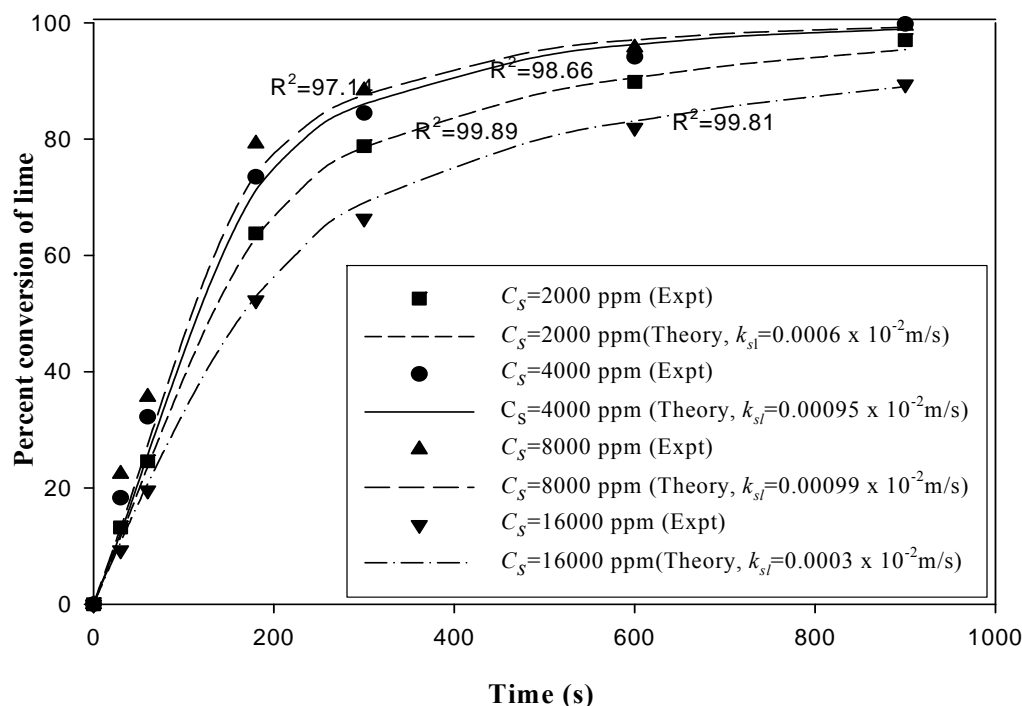
Figure 5.3.6 Effect of surfactant (SDS) concentration on conversion in a foam-bed reactor(sample batch no.: MERCK, MH0M601992)

Experimental data and parameter values have been shown in Tables 5E.9.1 to 5E.9.4

Parameters/variables	■	●	▲	▼
C_s (ppm)	2000	4000	8000	16000
H_f (m)	0.4	0.4	0.4	0.4
V_G (m/s)$\times 10^2$	3.85	3.85	3.85	3.85
C_{B0} (kg/m^3)	20	20	20	20
V_l (m^3)$\times 10^4$	2.5	2.5	2.5	2.5
$\overline{\varepsilon_l} \times 10^2$	1.34	1.62	1.51	0.85
Q_{CO_2}(m^3/s)$\times 10^4$	0.33	0.33	0.33	0.33
Q_{air} (m^3/s)$\times 10^4$	3.0	3.0	3.0	3.0

Jana and Bhaskarwar (2011) also reported reduced conversion of lime in a foam-bed reactor at such high concentrations of SDS in lime slurry. Reduction in the measured values of Zeta potential (28.1 mV) of a suspension of hydrated lime particles in distilled water in comparison to that produced (-45.8 mV) by a suspension of particles

in 8000 ppm solution of SDS, was assumed due to the accumulation of the anions of SDS at the positively charged surface of the calcium hydroxide particles in the slurry. In the present work, a similar reason is assumed for the partial surface coverage of lime particles by SDS molecules for the reduction in the rate of dissolution of calcium hydroxide particles in suspension and hence the conversion.

Stangle and Mahalingam (1990) used substantially high concentration of SDS (1.5% by weight) in their studies for carbonation of hydrated lime using 10 percent CO_2 gas in a *continuously operated foam-bed reactor*. For the low values of k_{sl} obtained, these authors also reported the possibility of partial surface coverage of lime particles by sodium dodecyl sulphate in slurry.

5.3.7 Effect of concentration of CTAB on conversion of lime

Effect of concentration of CTAB on conversion of lime in the foam-bed reactor has been shown in Figure 5.3.7. Four sets of experiments were performed with CTAB concentrations 200, 540, 1000 and 1620 ppm. The minimum concentration of CTAB required for generation of a stable foam column at 10 percent CO_2 by volume and at the minimum total gas flow rate of 3.33×10^{-4} m^3 s^{-1} (20 lpm) is 200 ppm. The maximum concentration of surfactant used here, 1620 ppm CTAB, corresponds to approximately 4.79 times its CMC.

A similar trend in the conversion of lime is observed as it is found with SDS. The conversion of lime first increases with the increase in CTAB concentration at low levels, while at higher concentrations of the cationic foaming agent, i.e.>540 ppm, the conversion of lime decreases, as was also observed for SDS.
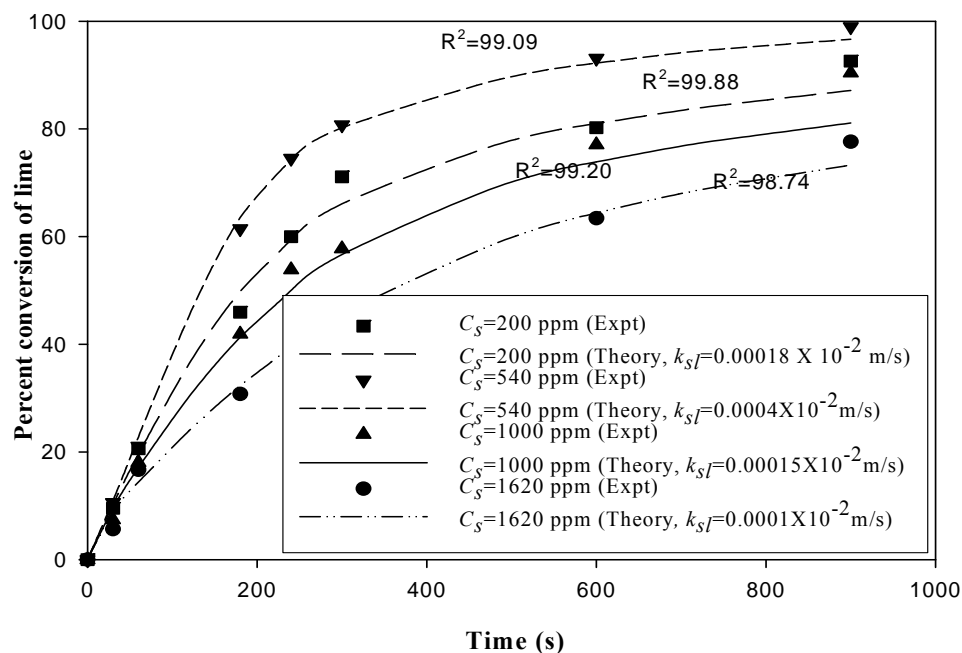
Figure 5.3.7 Effect of surfactant (CTAB) concentration on conversion in a foam-bed reactor (sample batch no.: MERCK, MH0M601992)

Experimental data and parameter values have been shown in Tables 5E.10.1 to 5E.10.4

Parameters/variables	■	▼	▲	●
H_f (m)	0.4	0.4	0.4	0.4
V_G (m/s)$\times 10^2$	3.85	3.85	3.85	3.85
C_{B0} (kg/m^3)	20	20	20	20
V_l (m^3)$\times 10^4$	2.5	2.5	2.5	2.5
$\overline{\varepsilon_l} \times 10^2$	2.76	3.31	1.40	0.98
Q_{CO_2}(m^3/s)$\times 10^4$	0.33	0.33	0.33	0.33
Q_{air} (m^3/s)$\times 10^4$	3.0	3.0	3.0	3.0

The solid-liquid mass-transfer coefficient is also found to increase from 0.18 x 10^{-5} to 0.4 x 10^{-5} m/s with an increase in CTAB concentration in the low concentration region and then decrease to 0.1 x 10^{-5} m/s at highest concentration (1620 ppm) used for experiments. This trend in the variation of k_{sl} with concentration of CTAB is found to be similar to that with SDS and in all probability for similar reasons as indicated by Jana and Bhaskarwar (2011). For their studies of carbonation of hydrated lime with

pure carbon-dioxide gas in presence of CTAB, they estimated the zeta potential of a suspension of hydrated lime particles in water and also in a suspension of particles in 1000 ppm solution of CTAB. They observed the zeta potential, 28.1 mV in 1000 ppm CTAB solution in distilled water to increase to 42.8 mv in the slurry of lime particles prepared using 1000 ppm CTAB solution. This increase in zeta potential was attributed to the accumulation of cations of CTAB on the surface of lime particles due to solid-chain interaction (Tadros, 1987) or because of bilayer adsorption of the surfactant.

5.3.8 Effect of concentration of Triton X-100 on conversion of lime

The effect of concentration of Triton X-100 on conversion of lime has been shown in Fig. 5.3.8. For studies of the effect of concentration of this non-ionic surfactant on reactor performance, four different concentrations of Triton X-100 in lime slurry, viz., 320 ppm, 960 ppm, 2400 ppm and 4800 ppm were chosen. Conversion of lime is found to increase with an increase in the surfactant concentration and decrease at its higher concentrations. Solid-liquid mass-transfer coefficient, k_{sl} is also found to increase from 0.9×10^{-6} m/s to 0.3×10^{-5} m/s with an increase in the concentration of surfactant, and then decrease to 0.65×10^{-6} m/s at the highest concentration (4800 ppm) used in the experiments, as was the case observed with cationic and anionic surfactants.
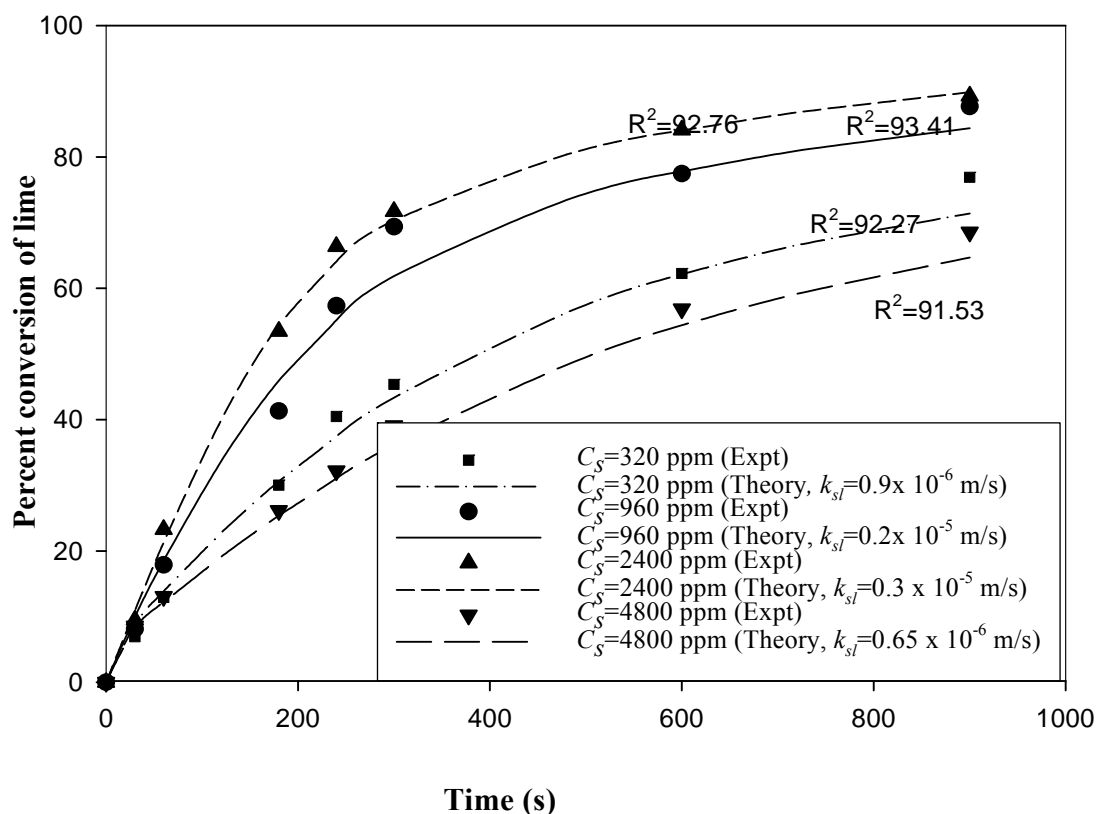
Figure 5.3.8 Effect of surfactant (Triton X-100) concentration on conversion of lime in a foam-bed reactor (sample batch no.: MERCK, MH0M601992)

Experimental data and parameter values have been shown in Tables 5E.11.1 to 5E.11.4

Parameters/variables	■	●	▲	▼
H_f (m)	0.4	0.4	0.4	0.4
V_G (m/s)$\times 10^2$	3.85	3.85	3.85	3.85
C_{B0} (kg/m^3)	20	20	20	20
V_l (m^3)$\times 10^4$	2.5	2.5	2.5	2.5
$\overline{\varepsilon_l} \times 10^2$	1.02	1.09	1.26	1.06
Q_{CO_2}(m^3/s)$\times 10^4$	0.33	0.33	0.33	0.33
Q_{air} (m^3/s)$\times 10^4$	3.0	3.0	3.0	3.0

In the lower concentration range, foam films become more stable and hence thicker with an increase in the concentration of surfactant. This prohibits the coalescence of bubbles and the enormous new surface area generated augment the dissolution of carbon-dioxide substantially. The increased consumption rate of lime from solution by

reaction with this absorbed carbon-dioxide causes dissolution of lime particles at a faster rate and therefore the solid-liquid mass transfer coefficient value is increased.

With increased concentration of Triton X-100, the bulk viscosity of slurry increases and consequently, lamellae of foam bubbles leaving the storage section become thicker. This reduces inter-bubble diffusion of gas and prevents the decrease in interfacial area caused by bubble coalescence. Thicker films also lead to larger concentration gradients of the dissolved component *A*. Drainage rate from thicker films being larger due to gravity, the rate of surface renewal is also enhanced. Also, thicker films for a given foam height in foam section imply a reduced volume of slurry in the storage section with a consequent increase in turbulence. Combined effect of all these factors possibly improves the gas-liquid and solid-liquid mass-transfer coefficients and lead to higher observed rate of reaction and conversion.

Stangle and Mahalingam (1990) compared the value of k_{sl} they obtained in the three-phase foam reactor with those obtained from a slurry bubble column reactor by Ramachandran and Sharma (1969). k_{sl} values in the foam reactor were found to be lower by several order of magnitude relative to that in a bubble column reactor. The authors (Stangle and Mahalingam, 1990) used 1% (v/v) of Triton X-100 for all the experiments they reported in their study. Their explanation of the lower value of k_{sl} due to partial surface coverage of lime particles by adsorption of surfactant molecules appears plausible.

Solid-liquid mass-transfer coefficient values obtained in the present work are about two orders of magnitude larger than that reported by Stangle and Mahalingam (1990). Concentration of CO_2 used are same, 10 percent, in both the cases. While, Stangle and Mahalingam (1990) used much higher concentration of Triton X-100 (10,000 ppm), the present work uses only 4800 ppm. Thus, surface coverage by surfactant molecules that impart resistance to dissolution of particles in the liquid phase is substantially less and lead to higher value of k_{sl}.

5.3.9 Effect of concentration of carbon-dioxide gas on conversion of lime

Concentration of carbon-dioxide gas in the feed gas mixture was varied from 10 to 50 percent by volume to study its effect on conversion of hydrated lime. Experimental data has been shown in Fig. 5.3.9. Simultaneous absorption and reaction of carbon-

dioxide gas with the dissolved lime, and, dissolution of lime being rate limiting steps (Juvekar and Sharma, 1973) in the carbonation reaction of hydrated lime slurry, higher concentration of carbon-dioxide in the feed gas is observed to increase the conversion of lime substantially. Interfacial concentration of carbon-dioxide in the liquid phase increases with an increase in its concentration in the gas phase. This increases the rate of reaction and the concentration of dissolved lime is thereby reduced at a faster rate. This phenomenon renders more lime to dissolve in the liquid to restore its solubility. Thus, an increase in the concentration of CO_2 in the gas phase leads to an increase in the rate of absorption of carbon-dioxide in the liquid, rate of dissolution of lime and that of its reaction leading to higher conversion of lime. It is observed from Figure 5.3.9 that present model fits well to the experimental data for values of k_{sl} in the range 0.9 x 10^{-5} to 0.25 x 10^{-5} m s^{-1}.
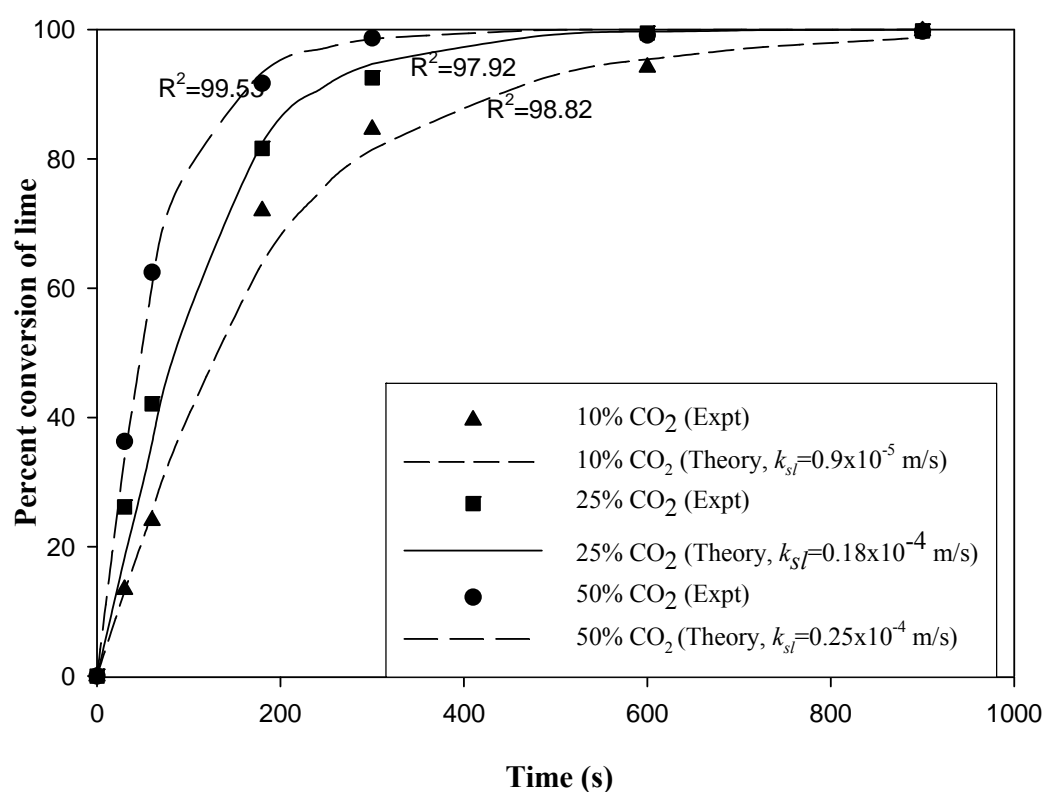
Figure 5.3.9 Effect of CO_2 concentration on conversion of lime in a foam-bed reactor (sample batch no.: MERCK, MH0M601992)

Experimental data and parameter values have been shown in Tables 5E.12.1 to 5E.12.3

Parameters/variables	●	■	▲
Surfactant	SDS	SDS	SDS
C_s (ppm)	4000	4000	4000
H_f (m)	0.4	0.4	0.4
V_G (m/s)$\times 10^2$	3.85	3.85	3.85
C_{B0} (kg/m^3)	20	20	20
$\overline{\varepsilon_l} \times 10^2$	1.62	1.62	1.62
Q_{CO_2}(m^3/s)$\times 10^4$	0.33	0.83	1.67
Q_{air} (m^3/s)$\times 10^4$	3.0	2.5	1.67

5.3.10 Effect of initial particle size on conversion of lime

Figure 5.3.10 shows the effect of initial size of hydrated lime particles on conversion in a foam bed reactor for two different Ca(OH)$_2$ samples supplied by CDH and MERCK Pvt. Ltd.
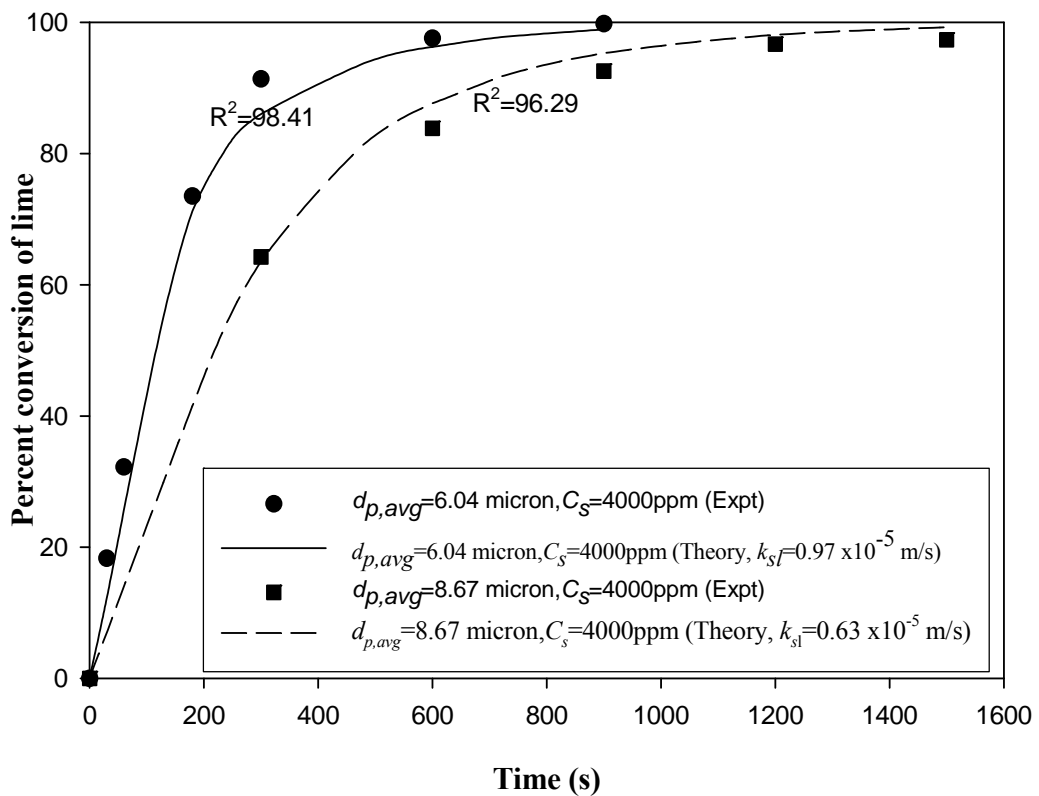
Figure 5.3.10 Effect of initial particle size on conversion of lime in a foam-bed reactor

Experimental data and parameter values have been shown in Tables 5E.13.1 to 5E.13.3.

Parameters/variables	●	■
Surfactant	SDS	SDS
C_s (ppm)	4000	4000
H_f (m)	0.4	0.4
V_G (m/s)$\times 10^2$	3.85	3.85
C_{B0} (kg/m^3)	20	20
$\overline{\varepsilon_l} \times 10^2$	1.62	1.01
Q_{CO_2} (m^3/s)$\times 10^4$	0.33	0.33
Q_{air} (m^3/s)$\times 10^4$	3.0	3.0

Carbonation of lime was performed with 4000 ppm SDS for both the samples. Two different initial particle sizes of average diameter 6.04 µm and 8.67 µm were used for experimental studies. Values of the parameters have been shown in Fig. 5.3.10. Higher conversion was observed at all times for the slurry containing smaller particles (6.04 μm) than for the slurry containing larger particles (8.67 μm). For a given solids loading, solid-liquid interfacial area per unit volume of slurry is larger for smaller particles than with larger particles. This enhances the rate of dissolution of solids and thus higher rate of reaction and conversion.

Table 5.3.1 Comparison of solid-liquid mass transfer coefficient, k_{sl} obtained in present study with other investigators

Investigators	**CO$_2$ concentration in liquid phase by volume**	**With/with out surfactant**	*Solid liquid mass transfer coefficient k_{sl} m/s*
Stangle & Mahalingam, 1990	10%	With surfactant at high concentration	2×10^{-8} -3×10^{-7}
Present Work	**10-50%**	**SDS, CTAB & Triton X-100**	$\mathbf{1\times 10^{-6}}$ **-2.5×10^{-5}**
Ramachandran & Sharma,1969	40%	Without surfactant	2×10^{-5} -8×10^{-5}
Jana,2010	100%	SDS, CTAB & Triton X-100	1×10^{-5} -8.9×10^{-5}

5.3.11 Effect of addition of ethylene glycol on particle size of product

Figure 5.3.11 shows the effect of addition of ethylene glycol on particle size of product $CaCO_3$ generated in the carbonation of lime in a slurry-foam reactor.
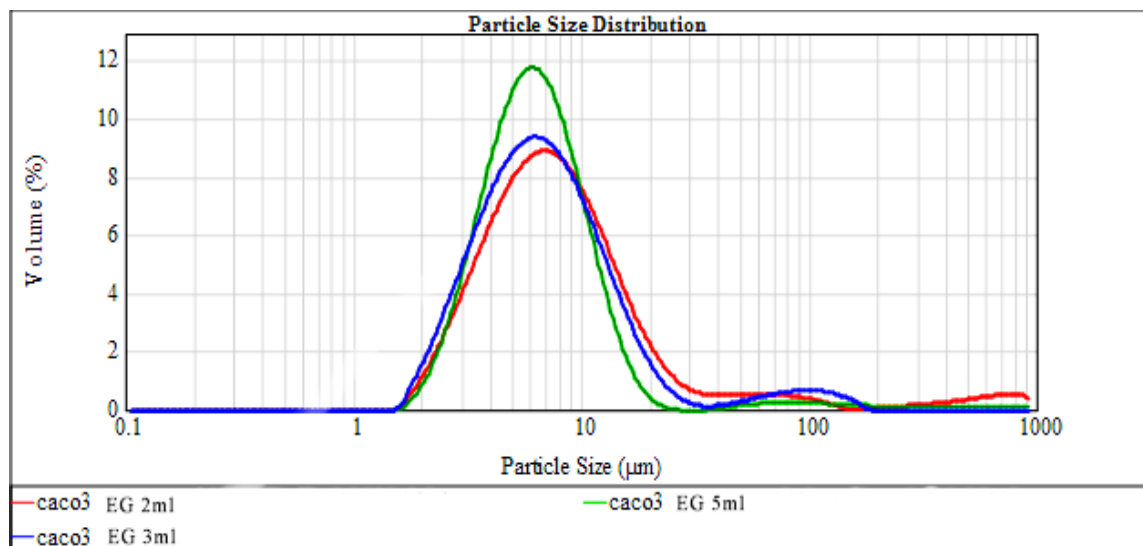
Figure 5.3.11 Comparison of particle size distribution of product $CaCO_3$ with addition of ethylene glycol (MALVERN MASTERSIZER 2000E)

2-5 ml ethylene glycol was added to the slurry and SDS was used as the foaming agent. After complete carbonation of lime particle size of product was measured using MALVERN MASTERSIZER 2000E. It is observed that the particle size reduces and specific surface area increases when ethylene glycol is added to the reactant slurry. Addition of ethylene glycol to the slurry increases its viscosity. This prohibits the agglomeration of particles but presence of ethylene glycol reduces the rate of absorption of CO_2 and thus reduces the conversion of hydrated lime. Details of the effect of addition of ethylene glycol on particle size and specific surface area of product $CaCO_3$ has been shown in Table 5.3.11.1.

Table 5.3.11.1 Comparison of particle size and specific surface area on addition of ethylene glycol to slurry-foam reactor

S.No.	Amount of ethylene glycol added, m^3 x 10^6	At volume % of particles	Particle size (μm)	Specific surface area, m^2/g	Surface weighted mean diameter of particles (μm)

1.	2	8.829	6.5-8.8	0.384	6.374
2.	3	9.313	5.8-7.8	0.429	5.702
3.	5	11.76	5.3-7.2	0.438	5.588

5.4 Thermo-gravemetric analysis (TGA), X-ray diffraction (XRD) and Field Emission Scanned Electron Microscope (FESEM) analysis of reactant and product:

While the sample received from MERCK (P) Ltd is free flowing and particles take time to settle from the slurry prepared along with surfactant, that received from CDH (P) Ltd is sticky in nature, agglomerates in slurry and settles down quickly, possibly due to some difference in composition of lime samples. TGA and XRD analysis of samples were therefore performed.

5.4.1 Thermo-gravemetric analysis (TGA)

TGA of lime samples of different batch numbers supplied by MERCK (P) Ltd and CDH (P) Ltd have been performed to evaluate their thermal decomposition characteristics. The Thermo-gravimetric analyses (TGA) of calcium hydroxide supplied by MERCK (P) Ltd, batch No. MH0M601992, has been shown in figure 5.4.1a. It is observed that as the temperature is raised from 30°C to 110°C, reduction in weight is negligibly small indicating that the sample is perfectly dry. From 110°C to 330°C, at which decomposition of $Ca(OH)_2$ starts, the reduction in weight is insignificant. With further heating, weight of sample reduces by about 24% when it attains 460°C indicating complete decomposition of $Ca(OH)_2$. On further heating weight of sample reduces further by about 3% due to decomposition of $CaCO_3$ and other impurities.

Figure 5.4.1b shows the percentage decrease in weight as the sample, supplied by CDH (P) Ltd, is heated at a rate of 10°C/min in an atmosphere of nitrogen. In the temperature range, 10°C to 110°C, about 0.5% weight reduced which in all probability is due to the removal of moisture contained in it. With the propagation of heating from 110°C to 330°C, about 1% additional reduction in weight is observed. This is attributed to some impurities, not confirmed in the present studies. As the temperature is raised further, about 23% reduction in weight is observed in the temperature range
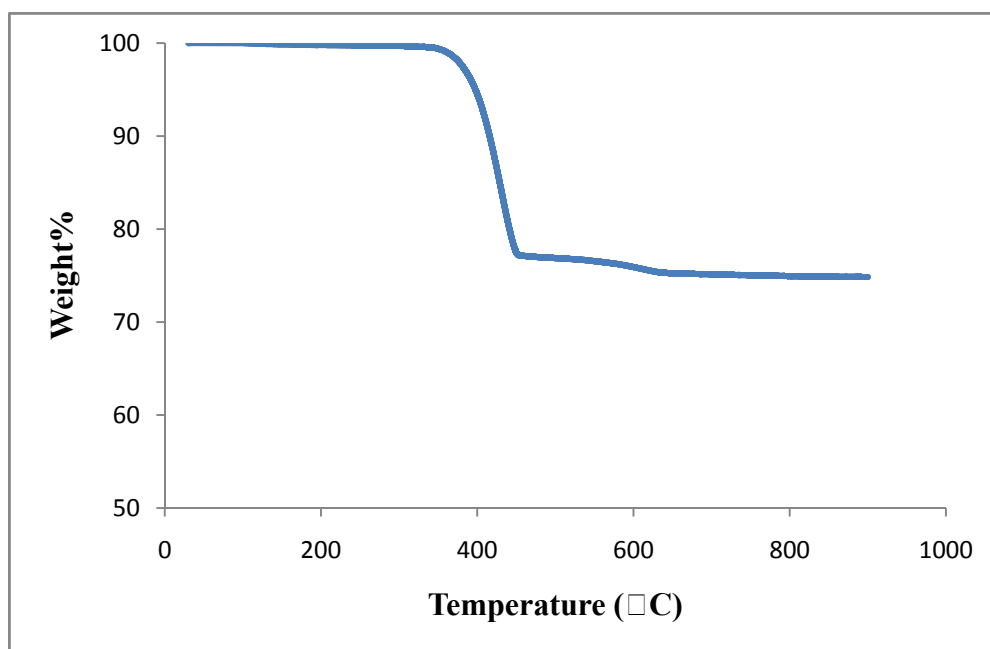
Figure 5.4.1a **Thermo-gravimetric analyses (TGA) of hydrated lime supplied by MERCK (P) Ltd. used in the experimental studies**
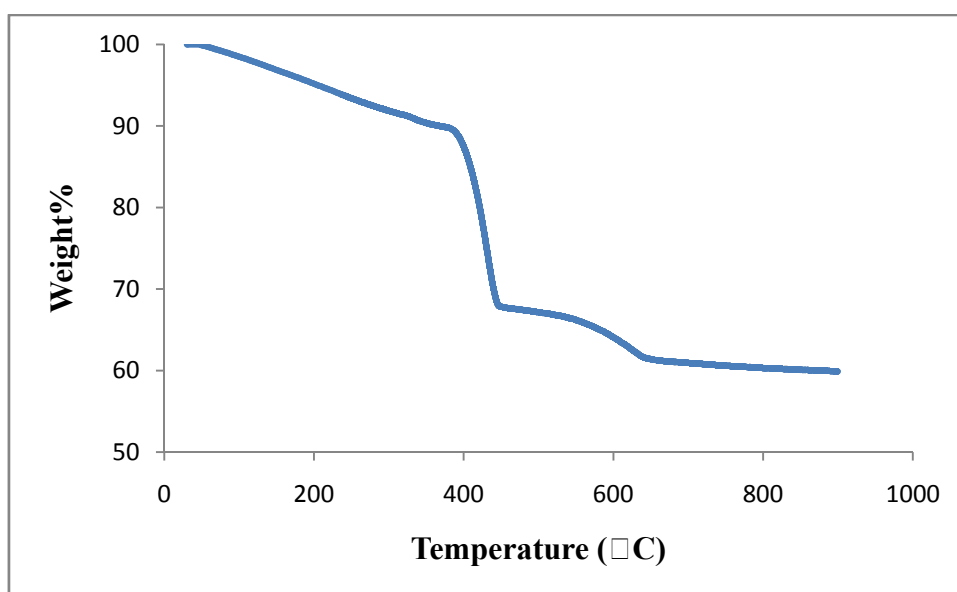
Figure 5.4.1b **Thermo-gravimetric analyses (TGA) of hydrated lime supplied by CDH (P) Ltd. used in the experimental studies**

$330^{\circ}C$ to $460^{\circ}C$ which is due to the decomposition of $Ca(OH)_2$, the latter being present only about 94%. Finally, about 3% additional decrease in weight is observed in the

temperature range 460°C to 900 C and evidently, this is due to the decomposition of $CaCO_3$.

5.4.2 X-ray diffraction (XRD)

Relative amount of different lattice forms of particles present in the samples of $Ca(OH)_2$ have been evaluated by X-ray diffraction. XRD spectra of samples of $Ca(OH)_2$, supplied by MERCK (P) Ltd and CDH (P) Ltd., have been shown in figures 5.4.2a and 5.4.2b, respectively. CuK-α has been used to characterize the samples with a 2θ range of 10°–80°. While the lime particles in the sample supplied by MERCK (P) Ltd are more crystalline, those present in the sample supplied by CDH (P) Ltd contains relatively more amorphous particles. Product PCC is found to contain all the three morphological forms: calcite, vaterite and aragonite. Figures 5.4.2c and 5.4.2d show the XRD peaks of $CaCO_3$ representing the crystalline structures present in it. Both the stable polymorphs of PCC i.e. calcite and aragonite is produced when SDS and CTAB are used as the foaming agents for carbonation of hydrated lime in a foam bed reactor. Peaks of calcite are observed more predominantly compared to aragonite when CTAB is used as a foaming agent while aragonite form is preferably produced when the foaming agent used is SDS. XRD spectra of $Ca(OH)_2$ and $CaCO_3$ are found to agree well with the JCPDS (Joint Committee on Powder Diffraction Standards).
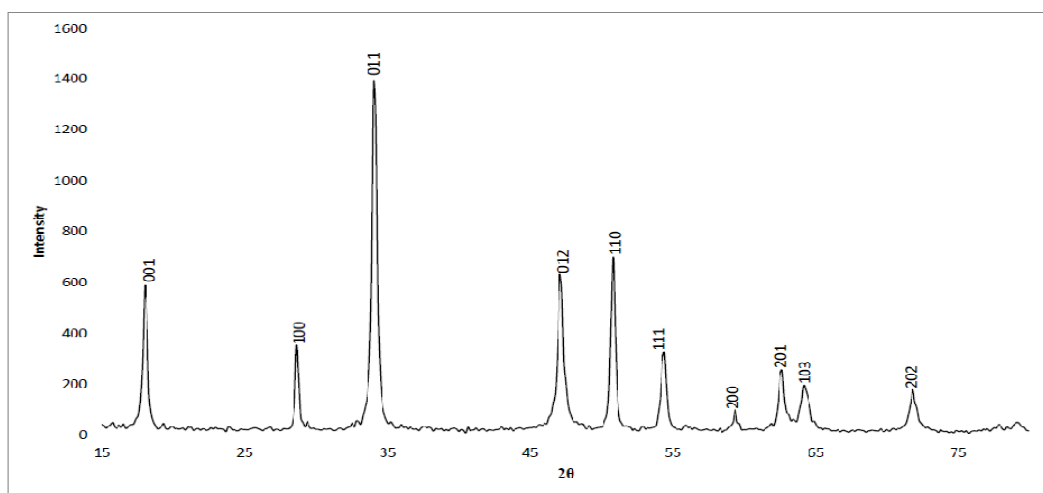
Figure 5.4.2a XRD pattern of reactant Ca(OH)$_2$ supplied by MERCK Pvt. Ltd.
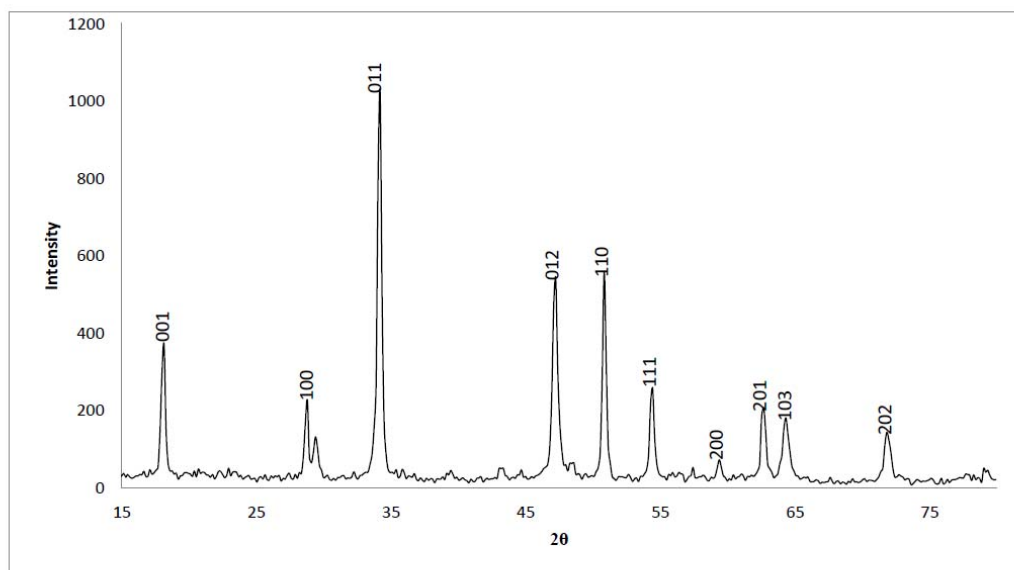
Figure 5.4.2b XRD pattern of reactant Ca(OH)₂ supplied by CDH Pvt. Ltd.
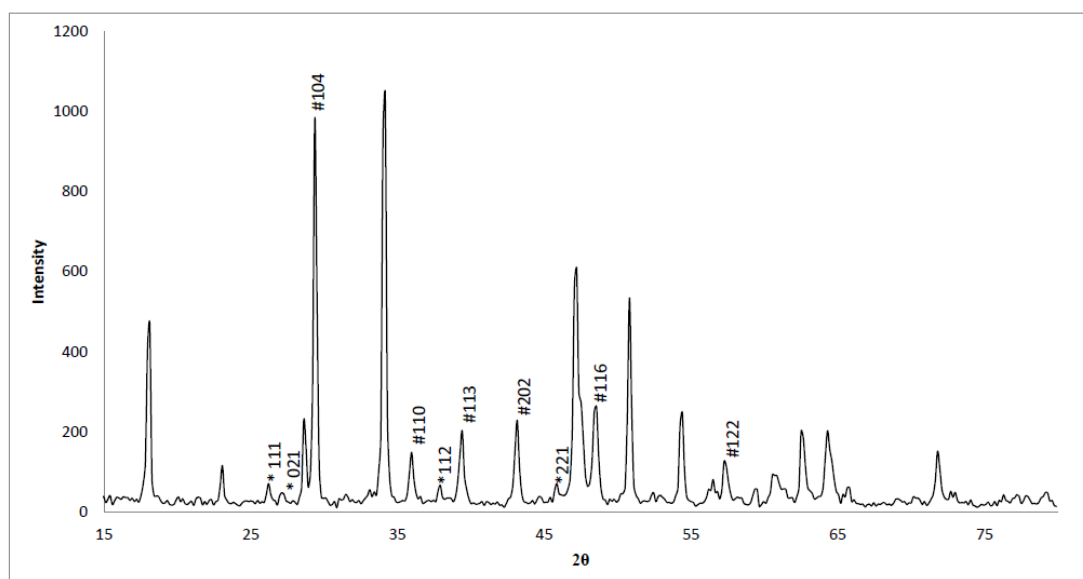
(#calcite, *aragonite)

Figure 5.4.2c XRD pattern of product CaCO₃ using SDS
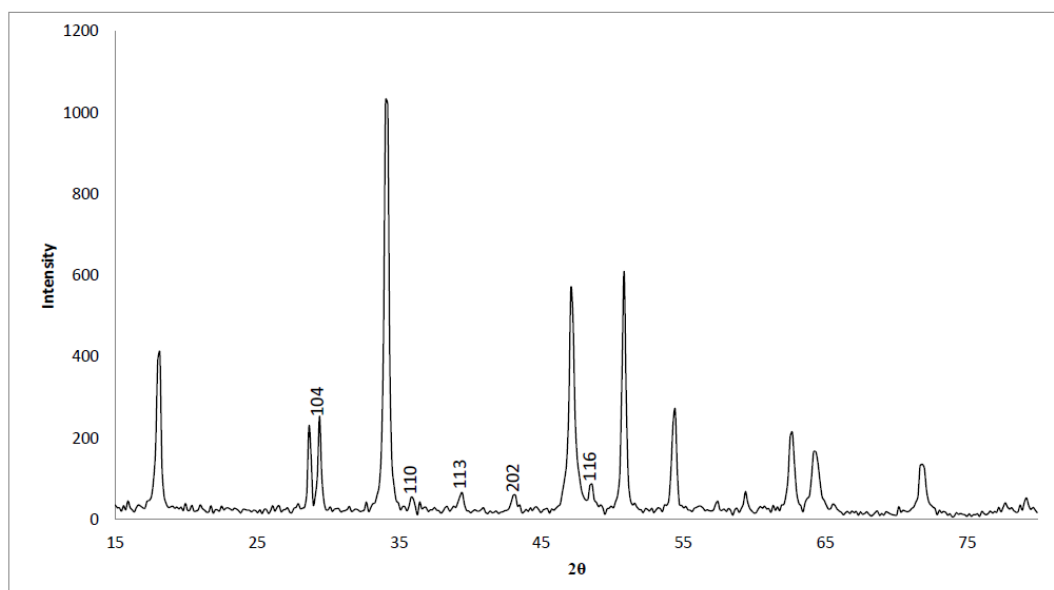
Figure 5.4.2d XRD pattern of product CaCO$_3$ using CTAB

5.4.3 Morphological analysis of products

The morphology of the product resulting from complete carbonation of hydrated lime in the presence of surfactant has been studied by *Field Emission Scanning Electron Microscope (FESEM).* The particles of CaCO$_3$ have a strong tendency to get agglomerated due to their high surface energy. Therefore it is difficult to determine the primary particle size precisely. Images of the particles are therefore obtained from SEM analysis and shown in figures 5.4.3a and 5.4.3b for products obtained with SDS and CTAB as the foaming agent. Calcite crystals display the spherical or rhombohedral structure while aragonite precipitates with needle-like agglomerates. Percentage of calcite formed is therefore substantially more as compared to aragonite form when CTAB is used as the foaming agent. FESEM results are therefore found to agree well with that obtained from XRD. It is observed from figure 5.4.3a that needle like particles are more abundant than spherical or rhombohedral. Aragonite is therefore the preferred morphological form produced in the carbonation reaction in the presence of SDS as the foaming agent. However, as seen from figure 5.4.3b spherical form of particles are much more in quantity than needle shaped particles. Therefore, calcite is the preferred morphological form of particles produced in presence of CTAB, used as the foaming agent.
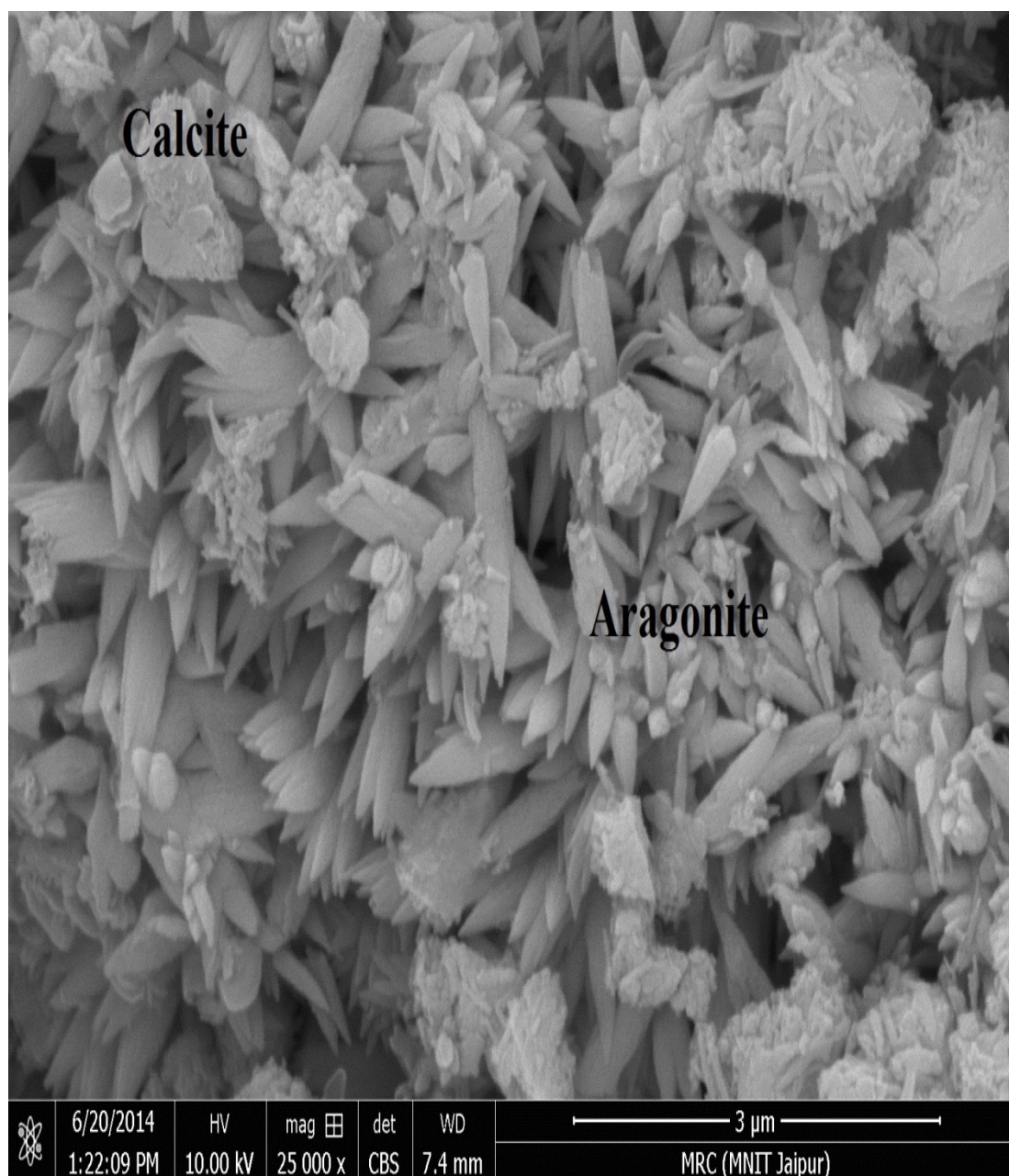
Figure 5.4.3a. FESEM image of product precipitated CaCO$_3$ resulting from complete carbonation of precipitated CaCO$_3$ sample using SDS as a foaming agent
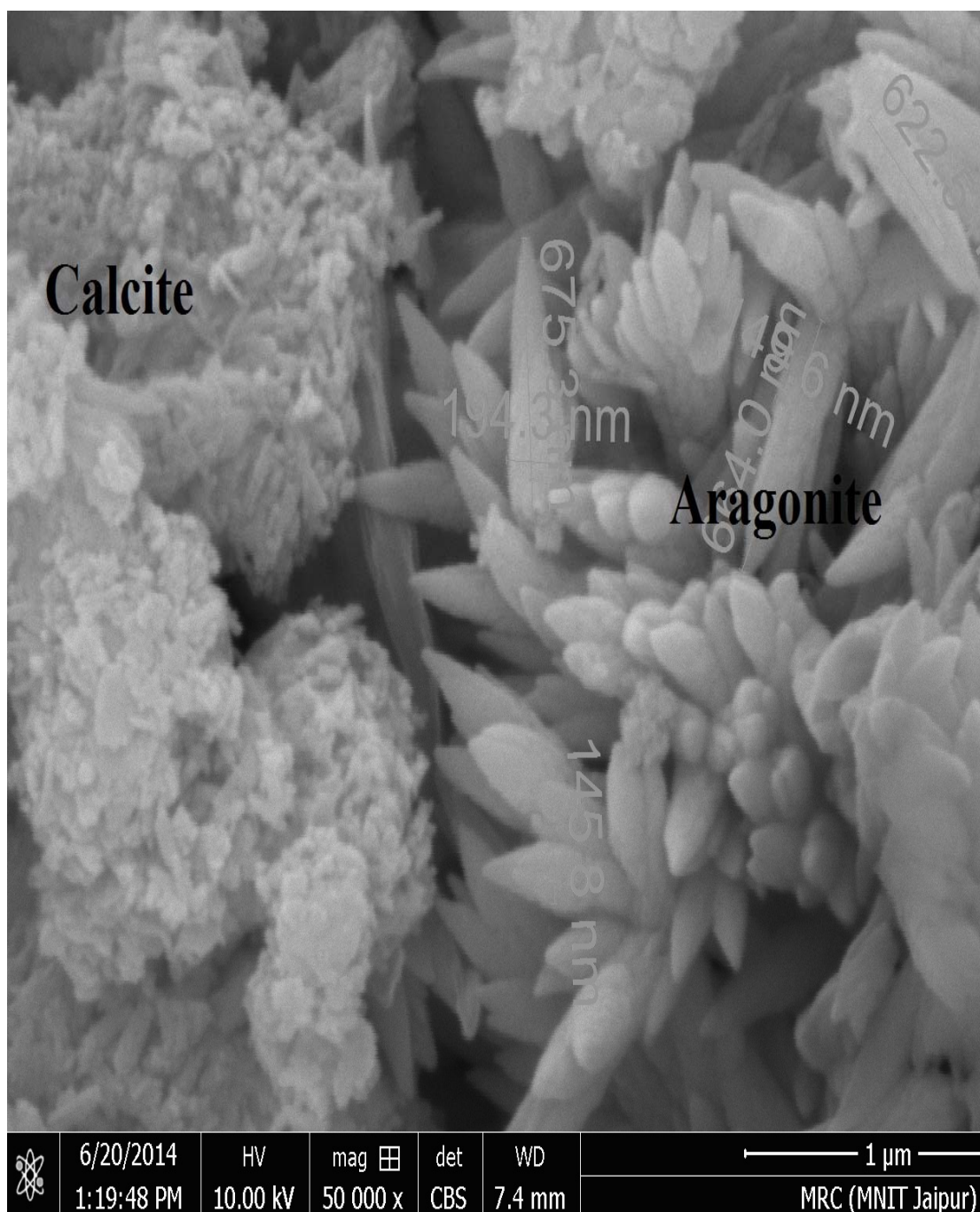
Figure 5.4.3b FESEM image of product precipitated CaCO₃ resulting from complete carbonation of precipitated CaCO₃ sample using CTAB as a foaming agent

5.5 Dimensionless correlation for k_{sl}

Solid-liquid mass transfer coefficient has been observed to increase with the increase of concentration of CO_2 gas, superficial velocity gas, foam height etc, while it reduces with initial loading of lime, volume of feed slurry. k_{sl} is also found to depend on several other operating variables, viz., C_s, $\bar{\varepsilon_l}$, d_p etc. It is therefore necessary to develop a correlation using the dimensionless variables. Both the additive and conventional power law relations were tried to find out a suitable correlation as a function of operating variables for k_{sl} estimation. These k_{sl} values estimated by the two methods were used to test the fitting of the reactor model to the experimental data. New k_{sl} values from the additive correlation, when used for reactor simulation, better agreement of the model to the experimental data were obtained. Hence, the additive correlation was accepted for estimation of k_{sl} for the present system. The following dimensionless correlation has been developed using experimental data collected with the above variables.

In order to develop the dimensionless correlation, the following variables have been used: k_{sl}, D_B, d_p, g_c, $m_B^T(0)/V_l$, h, H_f, V_G, C_G, C_s, μ_{eff}, $\bar{\varepsilon_l}$ and ρ_l

Number of variables: 13

Number of dimensions needed to describe the above variables: 4; these are F, M, L and θ.

Number of dimensionless groups that can be formed using above variables =13-4=9

The variables chosen for core groups are: D_B d_p g_c and μ_{eff}

The nine dimensionless groups to be formed, denoted by π_i (i=1,2,3,......,9),

can be written as:

$$\pi_1 = \left(D_B^p.d_p^q.g_c^r.\mu_{eff}^s\right)(k_{sl})^1$$

$$\pi_2 = \left(D_B^p.d_p^q.g_c^r.\mu_{eff}^s\right)(H_f)^1$$

$$\pi_3 = \left(D_B^p . d_p^q . g_c^r . \mu_{eff}^s\right)(h)^1$$

$$\pi_4 = \left(D_B^p . d_p^q . g_c^r . \mu_{eff}^s\right)(C_s)^1$$

$$\pi_5 = \left(D_B^p . d_p^q . g_c^r . \mu_{eff}^s\right)(V_g)^1$$

$$\pi_6 = \left(D_B^p . d_p^q . g_c^r . \mu_{eff}^s\right)(C_G)^1$$

$$\pi_7 = \left(D_B^p . d_p^q . g_c^r . \mu_{eff}^s\right)(\rho_l)^1$$

$$\pi_8 = \left(D_B^p . d_p^q . g_c^r . \mu_{eff}^s\right)(\overline{\varepsilon_l})^1$$

$$\pi_9 = \left(D_B^p . d_p^q . g_c^r . \mu_{eff}^s\right)(m_B^T(0)/V_l)^1$$

The dimensionless groups obtained are as follows:

$$\pi_1 = \frac{k_{sl} . d_p}{D_B} \qquad \pi_2 = \frac{m_B^T(0) . D_B}{\mu_{eff} . V_l} \qquad \pi_3 = \frac{V_G . d_p}{D_B}$$

$$\pi_4 = \frac{H_f}{d_p} \qquad \pi_5 = \frac{h}{d_p} \qquad \pi_6 = \frac{C_s . D_B}{\mu_{eff}}$$

$$\pi_7 = \frac{\rho_l . D_B}{\mu_{eff}} \qquad \pi_8 = \frac{1 - \overline{\varepsilon_l}}{\overline{\varepsilon_l}} \qquad \pi_9 = \frac{C_G . D_B}{\mu_{eff}}$$

In the correlations described below

$$Y = \pi_1 \qquad x_1 = \pi_2 \qquad x_2 = \pi_3 \qquad x_3 = \pi_4 \qquad x_4 = \pi_5 \qquad x_5 = \pi_6 \qquad x_6 = \pi_7$$

$$x_7 = \pi_8 \qquad x_8 = \pi_9$$

x_1 to x_9 and Y are calculated for each set of experimental data using variables and parameters actually used in the experiments. Using 'data fit', a curve-fitting software the following correlations were developed.

$R^2 = 0.974996151$

$$Y = ax_1 + bx_2 + cx_3 + dx_4 + ex_5 + fx_6 + gx_7 + hx_8 + i$$

$$\frac{k_{sl}.d_p}{D_B} = \left(-1.1357006 \times 10^{-6}\right)\left(\frac{m_B^T(0).D_B}{\mu_{eff}.V_l}\right) + \left(1.842149 \times 10^{-4}\right)\left(\frac{V_G.d_p}{D_B}\right) + \left(31998.5312\right)\left(\frac{H_f}{d_p}\right) +$$

$$\left(-1.024186 \times 10^{-8}\right)\left(\frac{h}{d_p}\right) + \left(-5.6862 \times 10^{-5}\right)\left(\frac{C_s.D_B}{\mu_{eff}}\right) + \left(2.23274 \times 10^{-7}\right)\left(\frac{\rho_l.D_B}{\mu_{eff}}\right) + \left(1.7856 \times 10^{-7}\right)$$

$$\left(\frac{1-\overline{\varepsilon_l}}{\overline{\varepsilon_l}}\right) + \left(6.40399 \times 10^{-5}\right)\left(\frac{C_G.D_B}{\mu_{eff}}\right) + \left(-1475132290.16719\right)$$

Chapter 6

CONCLUSION

&

RECOMMENDATION FOR FUTURE WORK

Conclusions

New mathematical models have been developed for absorption of lean CO_2 gas in NaOH solution under condition of fast pseudo-first order reaction kinetics in short bubble column- and foam-bed reactors operated in semi-batch mode. Models have also been developed for absorption of 10 to 50 percent CO_2 gas from its mixture with air in bubble column- and foam-bed *slurry reactors*. For the fast gas-liquid reaction, liquid holdup does not play a role while for the moderately fast slurry reaction; liquid holdup is important and has been incorporated in the model. The data published in the literature on foam-bed reactors and the models have been reanalyzed. Experiments have been performed in the above reactors for the systems chosen to verify if the contribution of the storage section towards gas absorption and reaction is negligible, as it has been claimed in the published literature, compared to that in the foam section although the storage constitutes 65 to 85 percent of the total liquid charged to the reactor. Storage have been observed to be the main section governing the performance of the foam reactor and in the present work, the foam reactor models have been developed taking into consideration the contributions of both the sections. When there is no foam, the foam reactor models reduce to those of the bubble column reactors.

The models developed have been validated through generation of experimental data. The variables investigated are : effects of initial concentration of NaOH, superficial velocity of gas, volume of solution charged into the reactor and concentration of CO_2 gas on conversion of NaOH for the gas-liquid system and, initial loading of hydrated lime in slurry, superficial velocity of gas, height of foam column, volume of slurry charged into the reactor, initial size distribution of lime particles (samples received from different manufacturers), concentration of CTAB, SDS and triton X-100 used as foaming agents, and, concentration of CO_2 in the feed gas for the slurry reaction. The model predictions for a foam-bed reactor are found to agree well to the experimental data and the reduced model also successfully explained the experimental data obtained on a short slurry-bubble column reactor. These new performance data are the first of their kind reported in the literature on foam-bed reactors.

Increase in the conversion of lime or NaOH with an increase in the superficial velocity of gas is attributed to the higher gas-liquid and solid-liquid mass-transfer coefficients, and to the higher liquid hold-up in the foam column. Increased concentration of CO_2 in the feed gas results in an increase in its rates of absorption, reaction and conversion

of lime/ NaOH. The increase in conversion in the foam reactors over the conventional bubble column reactors, and with the increase in foam height is credited to the increase in the gas-liquid interfacial area, higher liquid hold-up and larger gas-liquid contact times.

The decrease in the conversions of lime and that of NaOH with the increase in solids loading/ concentration of NaOH and with the increase in volume of slurry/ solution charged into the reactor is primarily due to the definition used for its calculation, and partly due to the decrease in the mass-transfer coefficients under less turbulent conditions in the storage section. Concentration of dissolved lime in solution slowly decreases due to reaction even as more of lime comes into solution by dissolution of particles. This decrease in the concentration of lime has been taken into account by assuming second-order reaction kinetics in the model equations for storage section of the slurry-foam reactor.

Liquid hold-up, an important variable for the slurry-foam reactor, has been measured at different heights of the foam column, for all the experimental conditions used and its average value over the foam column-height has been estimated. Material balance of the reactants and products for the slurry reaction has been verified through experiments.

SEM and XRD analyses of PCC products obtained by complete carbonation of hydrated lime indicate that while calcite is the predominant morphological form obtained with CTAB as the foaming agent, aragonite is formed in appreciable quantity with SDS. XRD analyses indicate presence of $CaCO_3$ impurities and percent, respectively, in samples received from CDH and MECRK Ltd.

Solid-liquid mass- transfer coefficient values are found to vary more significantly with the superficial velocity of gas and with the concentrations of CO_2 gas. Its variation with the solids loading, volume of feed slurry, concentration of surfactants and with foam height is rather low. A dimensionless correlation has been developed for solid-liquid mass transfer coefficient using the experimental data collected for carbonation of hydrated lime slurry as functions of concentration of carbon-dioxide gas, superficial

velocity of gas, etc and other variables/parameters studied for collection of experimental data.

Recommendations for future work

1. Ionic and non-ionic surfactants mixed in various proportions may be used as the foaming agent and its effect on conversion of hydrated lime / NaOH may be studied.

2. The effects of the following variables/parameters on conversion of lime in a foam-bed reactor have not been studied in the present work. It is recommended here that the effects of these variables may be studied in a future work.

   (i) The effect of temperature of slurry, reactant gas and that of NaOH feed solution on their conversion.

   (ii) Effect of concentrations, between 50 and 100 volume percent, of CO_2 gas on conversion of hydrated lime.

   (iii) The effect of diameter of the foam column on conversion of reactants.

   (iv) The effect of diameter of orifices of the gas-distributor plate (variation of gas-bubble size).

3. Performances of the gas-liquid/ gas-liquid-solid bubble column and foam-bed reactors have been studied for semi-batch mode of operation. Future work may aim at studying the performances of these reactors for continuous flow.

4. A foam-bed reactor being advantageous for treatment of large quantity of gas using a small amount of liquid, it can be usefully employed for pollution abatement problems, especially for removal of dusts and harmful components from exhaust gases. It may be studied as a slurry reactor for desulfurization of exhaust gas using lime/ limestone, carbon-dioxide removal from exhaust gases emanating from furnaces, thermal power plants, etc.

5. While aragonite has been observed to be the major crystalline form obtained as product when SDS is used as the foaming agent but it is calcite when CTAB is used for this purpose. Aragonite being a highly desired morphological form for medical purposes, detailed studies of the above aspects are required to maximize the production of aragonite and elimination of surfactants as impurities from the

products. Products from slurry-foam reactors may be stored over long period for studies on growth rates, shape of crystals of PCC produced using different surfactants as foaming agents, etc.

6. Other ionic and non-ionic surfactants may be used to study the performances of the systems employed in the present work and to find out the best surfactant to obtain the desired morphology of the PCC crystals.

7. Performance of the gas-liquid foam-bed reactor has been studied using only CTAB as the foaming agent. Anionic and non-ionic surfactants and different concentrations of these may be used to study the effect of these variables.

8. Possible synthesis of nano particles of $CaCO_3$ in foam-bed reactors by carbonation of soluble calcium salts and containing suitable foaming agents may be investigated.

APPENDICES

APPENDIX 2A

2A. 1 Bubble formation at orifice: Bubble diameter and terminal rise velocity of bubbles

2A.1.1 Bubble diameter

The size of gas bubbles depends on the rate of gas flow through the orifices, the orifice diameter, the fluid properties and the extent of turbulence in the liquid. For horizontally placed orifice plates, turbulence in the liquid solely due to rising bubbles and orifices separated by at least $3d_{b0}$ apart, the following correlations have been proposed by various investigators for air-water system.

Very low gas rates

For liquids having viscosities similar to that of water, diameter can be computed by equating the bouyant force on the bubble which tends to lift the bubble away from the orifice to surface tension which tends to retain it at the surface. Thus at the time of detachment of the bubble, the two forces being equal, one can write

$$\left(\frac{\pi}{6}\right)d_{b0}^3 \Delta\rho g / g_c = \pi d_0 \sigma \tag{2A.1}$$

This simplifies to,

$$d_{b0} = \left(\frac{6d_0\sigma\ g_c}{g\ \Delta\rho}\right)^{\frac{1}{3}} \tag{2A.2}$$

This has been shown to be true for orifice diameters up to 10×10^{-6} m.

For large liquid viscosities, up to 1000 cp, the following correlation has been proposed (Davidson and Schuler, 1960) to be applicable,

$$d_{b0} = 2.312\left(\frac{\mu_l Q_{G0}}{\rho_L g}\right)^{\frac{1}{4}} \tag{2A.3}$$

Intermediate flow rates, $Q_{G0} > [20\ (d_o\sigma g_c)^5/(\ g\Delta\rho)^2\ \rho_L^3]^{1/6}$ but $Re_o<2100$ (Leibson et al., 1956)

$$d_b = 0.0287 d_0^{1/2} R_{eG0}^{1/3} \qquad\qquad (2A.4)$$

where, d_b and d_o are in metres and $R_{eG,o} = d_o V_o \rho_G / \mu_G$

Large gas rates (Leibson et al., 1956)

$$d_{b0} = 0.0071 R_{eG}^{0.05} \qquad\qquad (2A.5)$$

Correlations for specific interfacial area, gas holdup and additional correlations for bubble diameter in conventional reactors are listed in Table 2.3.
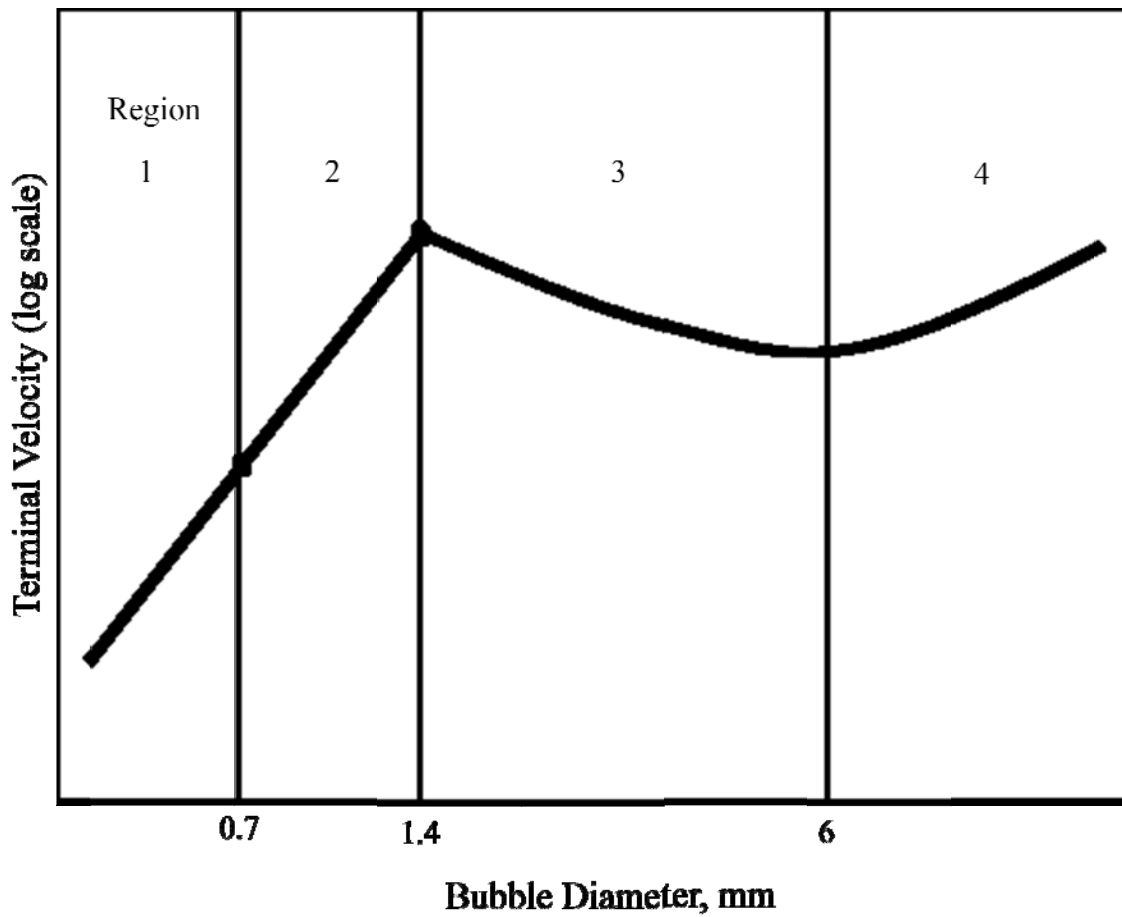
Figure 2A.1 Terminal Velocity of Single gas bubbles

2A.1.2 Terminal rise velocity of single and swarms of bubbles

Rise velocity of single bubble

The following correlations have been proposed (Mendelson, 1967) for estimation of steady state rise velocity of single bubbles:

(i) $d_{b0} < 0.7 \, x10^{-6} \, m$

The bubbles are spherical and the terminal velocity is given by Stoke's Law:

$$V_t = \frac{g d_{b0}^2 \Delta \rho}{18 \mu_L}$$

(2A.6)

(ii) $0.7 \, mm < d_p < 1.4 \, mm$

The gas within the bubbles circulates and it rises at a faster rate. Specific correlations are not available.

(iii) $1.4 \, mm < d_p < 6 \, mm$:

The bubbles are not spherical and follow a zigzag path.

$d_p > 6$ mm: The bubbles have a spherically shaped cap. For low viscosity liquids,

$$V_t = \sqrt{\frac{2 \sigma g_c}{d_{b0} \rho_L} + \frac{g d_{b0}}{2}}$$

(2A.7)

Bubble swarm velocity: Velocity of swarms of bubbles rising through a column of liquid has been given by Marrucci (1965). Details have been presented in chapter 3.

2A. 2 Carbon dioxide: The greenhouse gas - *An overview*

2A.2.1 Production and consumption

It appears imperative to become familiarize with the specific and important aspects of raw material being used in this study.

Carbon dioxide has limited solubility in water, reversibly getting converted to H_2CO_3. The hydration equilibrium constant of carbonic acid is

$$K_h = \frac{[H_2CO_3]}{[CO_2(aq)]} = 1.70x10^{-3} (at \; 25°C)$$

(2A.8)

Only a small fraction of the carbon dioxide is converted to carbonic acid but remains as CO_2 and not affecting the pH of the solution.

Production: For almost all practical purposes, CO_2 is obtained as a byproduct from numerous process operations and used as raw material in large tonnages in industries for the manufacture of chemicals, fertilizers etc. after necessary purification.

(i) Hydrogen manufacture by steam reforming of petroleum products (ii) NH_3 synthesis (iii) Fermentation (iv) Quicklime manufacture (v) Pig iron in blast furnace (vi) Cement industries (vii) Petroleum refinery (viii) Natural gas processing plants (ix) Power plants (coal/ natural gas)

2A.2.2 Purification of CO_2 from its mixture with other gases present as impurities

The most widely used industrial process for the removal of CO_2 from gas mixtures employ one of a variety of alkaline solutions. Both physical and chemical absorption processes have been employed for the purpose. There are two important solvents used extensively for this purpose, viz., an aqueous solution of mono-ethanol amine and the other being hot potassium carbonate.

Aqueous solution of mono-ethanol amine under pressure reacts with CO_2 at room temperature. The MEA solution is then stripped with steam at 90–120°C at near atmospheric pressure in a reactivation column to dissociate the MEA.CO_2 complex. This process has the disadvantage of severe corrosion at elevated temperature especially at that part of the tower where CO_2 concentration in solution is high. Stainless steel or a corrosion inhibitor is used to mitigate this problem.

The other solvent extensively used is aqueous solution of sodium or potassium carbonate. CO_2 produced by water gas reaction or steam reforming of naphtha is separated from H_2 preferably with aqueous solution of K_2CO_3/ $KHCO_3$ rather than Na_2CO_3/ $NaHCO_3$ solution. This is attributed to the fact that larger amount of CO_2 is dissolved in the former than that in the latter before the solution becomes saturated and needs regeneration. Secondly, the ionic strength effect on the rate and equilibrium constants is more favorable with the K_2CO_3 solution.

Although it is possible to remove CO_2 to a value as low as 0.1% by volume using K_2CO_3 solution, it has been observed economical to operate the tower for purity levels of 1% and greater. CO_2 is absorbed under pressure in hot K_2CO_3 solution at temperatures close to its boiling point and regenerate it at the same temperature but at a pressure close to atmosphere. This reduces steam consumption and eliminates heat exchangers.

Specific catalysts and promoters are added to the solution for process improvements.

In alkaline solution, the following reactions are known to occur.

$$CO_2 + H_2O \leftrightarrow H_2CO_3 \rightarrow HCO_3^- \ H^+ \qquad \text{(2A.9 i)}$$

$$CO_2 + OH^- \rightarrow HCO_3^- \qquad \text{(2A.9 ii)}$$

Reaction (ii) is known to be faster than (i). As the reaction involves ion, the rate constant k_{OH}^- is affected by the ionic strength of the solution. In reality, the reactive alkaline solution is buffered by the presence of several anions, as when carbonate-bicarbonate buffered solutions of sodium or potassium are used.

Concentration of hydroxyl ions are obtained from the two rapid reactions:

$$HCO_3^- \leftrightarrow H^+ + CO_3^{2-} \qquad \text{(2A.9 iii)}$$

$$H_2O \leftrightarrow H^+ + OH^- \qquad \text{(2A.9 iv)}$$

Eliminating the concentration of H^+ ions one obtains,

$$[OH^-] = \frac{Kw[CO_3^{2-}]}{[K_2][HCO_3^-]} \qquad \text{(2A.10)}$$

k_2 is the second ionization constant for carbonic acid and K_w is the ion product for water.

Rate of gas absorption depends on its solubility which in turn is affected by the concentration of ions in solution at the interface. The Henry's law coefficient for the solution is related to its value in pure water by the empirical equation:

$$\log \frac{H}{H_o} = -hI \qquad \text{(2A.11)}$$

Where, I is the ionic strength calculated as,

$$I = \frac{1}{2} \sum z_i^2 C_i \qquad (2A.12)$$

And $h = h_+ + h_- + h_G$ $\qquad (2A.13)$

Physical solvent Processes

There are several such processes:

(i) Rectisol process: The solvent used is methanol at -60° C.

(ii) Fluor solvent process: Propylene carbonate, a non-aqueous solvent is used for absorption of CO_2 gas.

(iii) Sulfinol process: Tetrahydrothiophene dioxide, an organic solvent is used for the absorption of CO_2 gas.

(iv) Selexol process: Dimethyl ether of polyethylene glycol is used for the absorption of SO_2 gas.

(v) Purisol process: N-methyl-2-pyrrolidone

(vi) Ammonia process: Aqueous ammonia solution is used as solvent.

(vii) Water at high pressure: solubility of water being poor at low pressure, absorption operation is performed at high pressure.

2A.2.3 Consumption of CO_2: (a) In the manufacture of (i) Urea (ii) Methanol (iii) Metal carbonates and bicarbonate (iv) Sodium salicylate (v) Wine making (vi) Carbonated soft drink (vii) Pulp and paper manufacturing, (b) Production aid or as solvent (i) Supercritical extraction (ii) Enhanced oil recovery: CO_2 dislodges oil trapped in the pores of underground rock. Friction is reduced in presence of CO_2 and flow of oil through the rock to the well is enhanced (iii) Manufacture of dry ice.

2A.2.4 Danger associated with the release of CO_2 into atmosphere: Among the fossil fuels, coal accounts for the maximum quantity of CO_2 generated per unit of energy produced.

CO$_2$ emission and the Global warming effect

Carbon dioxide among the other green house gases, methane, nitrous oxide, ozone and water vapor is known to be the major concern on global warming. Increase in the average temperature of the air and sea water is universally known as *Global Warming*. Since 1750, the year of Industrial Revolution, Industrial Growth and burning of Fossil Fuels CO$_2$ concentration in the atmosphere has increased from 280 to 392 ppm.

Visible light enters through the glass into a green house and is converted to infrared (heat) radiation. However, the glass being opaque to infrared, it cannot go out and the greenhouse remains warm. Water vapor and CO$_2$ in the atmosphere absorb the outgoing heat radiation and send it back to Earth.

Preventive measures:

CCS (carbon capture and sequestration)

After capture from large stationary sources, CO$_2$ is compressed, transported by pipe line, train/truck/ship etc) to site and injected underground (depleted oil and gas fields, deep coal seams and saline formations; geologic storage includes porous rock which must prevent upward migration of CO$_2$.

CCS is a three-step process*:*

(i) Capture of CO$_2$ from process or power plants using an MEA absorption tower in place of the conventional stack, desorption of CO$_2$ gas and recycling the regenerated solvent to the absorber.

(ii) Transport of the captured and compressed CO$_2$ usually by pipe lines to the storage site

(iii) Underground injection of the CO$_2$, a mile or more beneath the surface, into rock formations.

*Limitations***:**

- Energy penalty (10 to 40 percent of the energy produced by a power plant).
- May lead to doubling of coal plant costs

2A.2.5 Kyoto Protocol

An international treaty that sets binding obligations on industrialized countries to reduce emissions of green house gases.

APPENDIX 3A

3A.1 Verification for pseudo-first order condition

<u>**Physico-chemical data**</u>

D_A = 2.2595 x 10^{-5} cm^2/s at 30°C

k_2 = 1.3981x10^7 cm^3/g mole. s

C_{B0} = 0.44136 x 10^{-3} g moles/ cm^3

D_B =1.7979 x 10^{-5} cm^2/s

z=2.0

$C_A{}^*$ = 0.6914 x 10^{-7} g moles cm^{-3}

<u>**Conditions for pseudo-first order reaction :**</u>

$$Ha = \frac{\sqrt{k_2 C_{OH^-} D_{AB}}}{k_l}$$

$$\frac{\sqrt{(1.398x10^7 cm^3 / gmol.s)(0.44136x10^{-3} gmol / cm^3)(2.2595x10^{-5} cm^2 / s)}}{0.0261(cm/s)}$$

=14.30

$$E_a/Ha = (1 + \frac{D_B C_{B0}}{z D_A C_A{}^*} / \frac{\sqrt{k_2 C_{OH^-} D_{AB}}}{k_l})$$

$$= [1 + \frac{(1.7979 \times 10^{-5})(0.44136 \times 10^{-3})}{(2)(2.2595 \times 10^{-5})(0.6914 \times 10^{-7})}]/14.30$$

$$= [1+(0.2539x10^4)]/ 14.30$$

$$= 2540/ 14.30$$

$$= 177.6$$

$$\frac{k_l a}{k_2 C_{B0}}$$

$$= \frac{(0.0261)(0.9699)}{(1.398x10^7)(0.44136x10^{-3})}$$

$$= 4.103x10^{-6}$$

Ha being much larger than 2 and E_a/Ha much larger than 5, the reaction is pseudo-first order.

APPENDIX 4A

4A.1 Preparation and standardization of solutions for absorption of CO_2 gas in NaOH solution

Preparation of 0.1 N sodium hydroxide solution

8.4×10^{-3} kg of sodium hydroxide pellets were weighed on a watch glass and dissolved in approximately 2.0×10^{-4} m^3 of boiled-out distilled water and mixed thoroughly. When the pellets dissolved 2×10^{-3} m^3 of volumetric flask make up with distilled water.

Preparation of 0.1 N solution of hydrochloric acid

Approximately 18×10^{-6} m^3 of pure concentrated hydrochloric acid was pipette-out and poured into the 2×10^{-3} m^3 of volumetric flask having 5×10^{-4} m^3 of distilled water. The resultant solution was make up to liter mark with distilled water and mix thoroughly.

Preparation 0.1 N solution of oxalic acid (primary standard)

6.45×10^{-3} kg oxalic acid weighed and dissolved in 25×10^{-6} m^3 distilled water and mixed thoroughly. The solution was make up to 1×10^{-3} m^3 mark.

Standardization of 0.1 N sodium hydroxide solution

Sodium hydroxide solution reacts with atmospheric CO_2 and contamination of sodium carbonate was formed that affect the strength of the base solution. Barium chloride solution was added into the sodium hydroxide solution to precipitate CO_3^{--}. The barium carbonate was precipitated and the solution was filtered using whattman filter paper. Then the solution was titrated against 0.1 N oxalic acid solution in the presence of phenolphthalein as a indicator. The end point was reached when pale pink colour persists for 30 sec. The reaction is given below:

$$2\,NaOH\ (aq) + H_2C_2O_4 .2H_2O(s) \rightarrow Na_2C_2O_4(aq) + 4H_2O \qquad (4A.1)$$
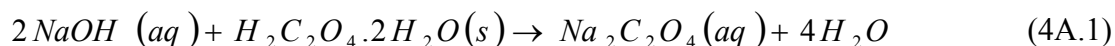
Standardization of hydrochloric acid

5×10^{-5} m^3 sodium hydroxide solution (carbonate free) was taken in the conical flask and 2-3 drops of phenolphthalein was added into it. This solution was titrated against hydrochloric acid solution to know the exact normality. The pale pink colour shows the end point of the titration.

4A.2 Determination of unreacted NaOH concentration in the product solution

Barium chloride solution was added into the product solution to precipitate CO_3^{--}. The barium carbonate was precipitated and the solution was filtered using whattman filter paper. Then the solution was titrated against HCl in the presence of phenolphathalein as an indicator. The titration gives the volume required to neutralize the NaOH present in the solution.

4A.3 Sample calculation for conversion of sodium hydroxide

Initial NaOH in $5 \times 10^{-5} m^3$

$$N_1 V_{1(NaOH)} = N_2 V_{2(HCl)}$$

$$Normality \ of \ NaOH = \frac{N_2 \times V_2}{V_1} N$$

$$Amount \ of \ NaOH \ in \ 250 \ ml \ solution = \frac{Eq. \ wt. \ of \ NaOH \times 250 \times N_1}{1000}$$

$$= X \ g$$

Unreacted NaOH in 15s *in* 50 *ml* =

$$\frac{Normality \ of \ HCl \times volume \ of \ HCl \ required \ to \ neutralized \ NaOH}{50}$$

$$= Z \ N$$

Amount of unreated NaOH in 250 *ml after* 15s *of reaction time*

$$= \frac{Eq.wt.of \ NaOH \times 250 \times Z}{1000}$$

$$= Y \ g$$

$$\% \ conversion = \frac{X - Y}{X} \times 100$$

4A.4   Preparation and standardization of solutions for carbonation of hydrated lime slurry

Preparation of 0.2 N iodine solution

About 80 x 10^{-3} kg of potassium iodide was dissolved in 30 x10^{-6} m^3 of distilled water in a 2.0 x 10^{-3} m^3 volumetric flask and shaken thoroughly till complete dissolution. About 50.8 x10^{-3} kg of iodine was then added to the flask. The contents were shaken

well till iodine dissolved completely. Distilled water was then added to make the solution volume up to the mark.

Preparation of sodium-thiosulfate Solution

Approximately 0.1 N sodium thiosulfate solution was prepared by dissolving 25.0 x 10^{-3} kg of A. R. grade crystallized sodium thiosulfate pentahydrate ($Na_2S_2O_3.5H_2O$) in about 500 x 10^{-6} m^3 freshly prepared distilled water in a 2.0 x 10^{-3} m^3 volumetric flask. After complete dissolution of the particles, volume of the solution was made up to the mark using distilled water. About 10 mg of Hg(II) iodide was added to the solution for its stabilization for storage for a few days.

Preparation of 0.1N potassium dichromate solution (Primary standard)

Approximately 4.903 x10^{-3} kg of potassium dichromate (AR grade) was weighed and dissolved in about 250.0 x 10^{-6} m^3 freshly boiled distilled water in a 1.0 x 10^{-3} m^3 volumetric flask. Volume of the solution was then made upto the mark using distilled water. The normality of the solution was estimated as the ratio of actual weight of potassium dichromate taken for preparation of the solution to its equivalent weight.

Preparation of starch solution

About 2.0 g of soluble starch was taken and a paste was made with little amount of freshly boiled distilled water. This was poured into 200.0 x 10^{-6} m^3 of boiling water in a beaker. The solution was boiled for one minute with constant stirring using a glass rod. It was allowed to cool and 2 to 3 g of KI was added into it for preserving it for several days.

Standardization of thiosulphate solution

About 100.0 x 10^{-6} m^3 of freshly boiled distilled water was taken in a 500.0 x 10^{-6} m^3 conical flask. Approximately 3.0 x10^{-3} kg of KI and 2.0 x 10^{-3} kg of sodium hydrogen carbonate were added and dissolved thoroughly. About 6.0 x 10^{-6} m^3 of HCl was added to this solution. 25.0 x10^{-6} m^3 of potassium dichromate solution of known normality was added and the resultant solution was placed in dark for 5 minutes to complete the reaction:

$$Cr_2O_7^{2-} + 6I^- + 14 H^+ \longrightarrow 2 Cr^{3+} + 3 I_2 + 7 H_2O \qquad (4A.2)$$
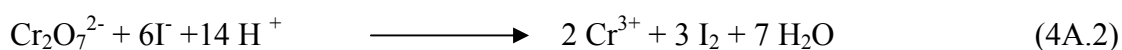
After about 5 min, the stopper and the side wall of the flask were washed with distilled water. The solution was diluted to about 300.0×10^{-6} with distilled water and titrated with sodium thiosulphate solution till the solution attains yellowish-green color. Thiosulphate reacts rapidly and stoichiometrically with the iodine liberated by the above reaction under usual experimental condition (pH <5)

$$2 \, S_2O_3^{2-} + I_3^- \longrightarrow 3I^- + S_4O_6^{2-} \tag{4A.3}$$
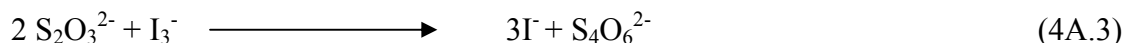
About 3.0×10^{-6} to 5.0×10^{-6} m^3 of starch solution was at this instant when the colour of the solution changed to dark blue. Thereafter, thiosulphate solution was added drop wise till the color changed from blue to light green which indicated the end of the titration.

Standardization of 0.2 N iodine solution:

The iodine solution is standardized with sodium thiosulfate solution of known normality. 25.0×10^{-6} m^3 of iodine solution was taken in a 500.0×10^{-6} m^{-3} conical flask. About 100.0×10^{-6} m^{-3} of distilled water was added it. The diluted iodine solution was titrated using standard sodium thiosulphate solution until its deep violet color turns into pale yellow. About 2.0×10^{-6} m^3 of starch solution was added when the color of the solution turns into deep blue. Drop wise addition of thiosulphate solution was continued toll the contents become colorless indicating the end point of titration.

4A.5 Chemical analysis of hydrated lime reactant sample and product slurry for estimation of percentage of hydrated lime content

4A.5.1 Analysis of hydrated lime reactant sample

Materials used

Standard solutions of sodium thiosulfate, 0.1N; iodine solution (0.2 N) and starch indicator solution.

Procedure

Hydrated lime sample was accurately weighed close to a value of 1.0×10^{-3} kg in a glass-stoppered 2.50×10^{-4} m^3 conical flask and about 3.0×10^{-5} m^3 of boiling water is added to it. The contents are shaken for about 15 minutes and cooled. Standard solution of iodine added to it with constant shaking of the flask. Deep violet color of

iodine is seen disappear. Addition of iodine and shaking of the flask is continued till violet color of iodine is observed to persist. Presence of excess iodine indicated that lime has exhausted by reaction. The solution is transferred quantitatively to a 5.0×10^{-4} m^3 volumetric flask and the solution volume is made up to the mark by diluting with distilled water.

Excess iodine present in the solution is determined by pipetting out 2.5×10^{-5} m^3 of the solution titrating it with a standard sodium-thiosulphate solution. Starch indicator was used to determine the end point of titration. A blank determination is also carried out using the same amount of iodine solution as with the sample.

Working equation for estimation of hydrated lime content in the sample

The following equation for estimation of hydrated lime content in a test sample has been taken from Jana (2007).

$$\text{Percentage of hydrated lime by mass} = 74.1 \times \frac{\left(V_{th,b} - V_{th,s}\right)\left(N\right)}{M} \tag{4A.5}$$

Where, $V_{th,b}$ = Volume of thiosulphate solution required for blank titration

$V_{th,s}$ = Volume of thiosulphate solution required to titrate the excess iodine present

4A.5.2 Estimation of unreacted lime in the product slurry

Materials used

Standard solutions of sodium thiosulfate, 0.1N; iodine solution (0.2 N) and starch indicator solution.

Procedure

An aliquot of 50.0×10^{-6} m^3 from the product slurry (20.0×10^{-6} m^3) was titrated with thiosulfate solution to determine the excess iodine present in the slurry and thus calculate the amount of unreacted lime in the whole mixture. By doing this, consumption of thiosulfate solution could be reduced. However, several aliquots from product slurry generated widely different titer values when titrated against a standard thiosulphate solution. It therefore indicates that suspended particles of unreacted lime present in different aliquots were different. Hence, the entire volume of product slurry, 20.0×10^{-4} m^3, was titrated against thiosulphate solution for each experiment.

Working equation for estimation of unreacted lime content in the product slurry

The following analysis has been taken from Jana (2007).

The total volume of product slurry including the column wash water and the iodine solution, known amount, added to it to consume the unreacted lime is made up to 2000 ml (V_{final}) adding excess distilled water, if required. To reduce the volume of iodine solution required to be added, its normality was kept at a relatively high value, approximately 0.2 (N). It appears convenient to write the working equation in terms of consumption of iodine.

Volume of iodine solution added per 25 ml of slurry = $\dfrac{(V_{I_2,add})(25)}{2000}$ ml, if the total

volume of iodine solution added to the slurry is $V_{I_2,add}$.

Again, if for standardization of 25 ml of iodine solution, volume of thiosulphate solution needed is V_{th} ml,

Volume of thiosulfate solution equivalent to the iodine **added** per 25 ml of slurry

$$= \frac{V_{th}}{25}[\frac{V_{I_2,add} \text{ x } 25}{2000}] \text{ ml} \tag{4A.6}$$

Also, if the total volume of thiosulphate solution required for titration be $V_{th,tot}$, for the estimation of excess iodine present in 2000 ml of slurry, then

Volume of thio required for **back** titration of 25 ml of slurry = $\dfrac{(V_{th,tot})(25)}{2000}$ ml

Therefore, following equation (4A.6) one obtains,

The mass of unreacted lime present in 500 ml of slurry

$$= (0.741)[\frac{V_{th}}{25}(\frac{V_{I_2,add} \text{ x } 25}{2000}) - \frac{(V_{th,tot})(25)}{2000}](N) \tag{4A.7}$$

Mass of unreacted lime present in 2000 ml slurry =

$$(4)(0.741)[\frac{V_{th}}{25}(\frac{V_{I_2,add} \text{ x } 25}{2000}) - \frac{(V_{th,tot})(25)}{2000}](N) \tag{4A.8}$$

APPENDIX 4B

4B.1 Estimation of liquid holdup from experimental data

The following data for the estimation of liquid hold-up have been collected for the experimental conditions described in chapter 5 part II.

Volume of suction bulb = 550 x 10^{-6} m^3

From the vacuum gauge, maximum vacuum generated = 690 mm Hg (approximately, as seen from the vibrating needle).

After application of maximum vacuum, water was sucked into the bulb several times. Volume of water sucked into the bulb varied from 490x10^{-6} m^3 to 500x10^{-6} m^3. Thus, the average value of vacuum generated in the bulb is (495x10^{-6} m^3/550x10^{-6} m^3) x 760 mm Hg= 684 mm Hg.

Volume of liquid collected in the bulb after complete collapse of foam sucked from the gas liquid interface is 39.0 x10^{-6} m^3.

The liquid hold-up values at the slurry-foam interface is thus: 39.0 x10^{-6} m^3 /495x10^{-6} m^3= 0.079

Liquid hold-up values estimated from the foam sucked from different heights of the foam column are shown in the following table:

Table 4B.1.1 Local liquid hold-up value in a slurry foam column

Distance from Slurry foam interface at which suction was applied (m) × 10^2	Volume of liquid sucked into the sampling bulb (m^3) × 10^6	Liquid hold-up ε_l Dimensionless
0.0	60.0	0.121212
3.0	11.5	0.023232
5.0	8.4	0.01697
10.0	3.0	0.006061
20.0	1.7	0.003434
39.0	1.0	0.00202

The above liquid hold-up values are plotted against height of foam and the height-average liquid hold-up is obtained as 0.0103668.

APPENDIX 4C

Measurement of surface coefficient

An apparatus similar to that used by Jana (2007) was used for experimental determination of surface coefficient of saturated lime solution containing different concentrations of various surfactants (cationic, anionic and nonionic) used for carbonation of hydrated lime slurry in the foam bed reactor. Volume of CO_2 gas absorbed from the lean gaseous mixture is estimated using the manometer reading and the correlation proposed by Jana and Bhaskarwar (2011). The surface coefficient is then calculated following Blank and Roughton (1960)

4C.1 Experimental setup for measurement of surface coefficient:

The experimental set-up for measurement of surface coefficient is shown In Figure 4C.1. It consists of a water ring type vacuum pump, pump tank, ballast vessel, vacuum stop cocks, a carbon dioxide gas cylinder, catch pot, mercury manometer, water manometer, valves and gas absorption cells.

4C.2 Procedure for measurement of surface coefficient:

(i) **Preparation of surfactant solution**: Saturated solution of calcium hydroxide was prepared by mixing about 5.0 x10^{-3} kg of it in 2.0 x10^{-4} m^3 of hot distilled water in 2.0 x10^{-3} m^3 volumetric flask. The mixture was shaken thoroughly for about one hour and allowed to cool. With gradual addition of cold distilled water, the mixture is shaken intermittently and the volume made up to 2.0 x10^{-3} m^3. The solution of hydrated lime containing suspended particles is shaken occasionally for several hours and allowed to settle overnight. Clear saturated solution of lime is separated by decantation. Known amount of surfactant was added to this saturated solution of lime to prepare different concentration of surfactant solutions in saturated lime solution for carrying out experiments.

Figure 4C.1 Experimental set-up for measurement of surface coefficient
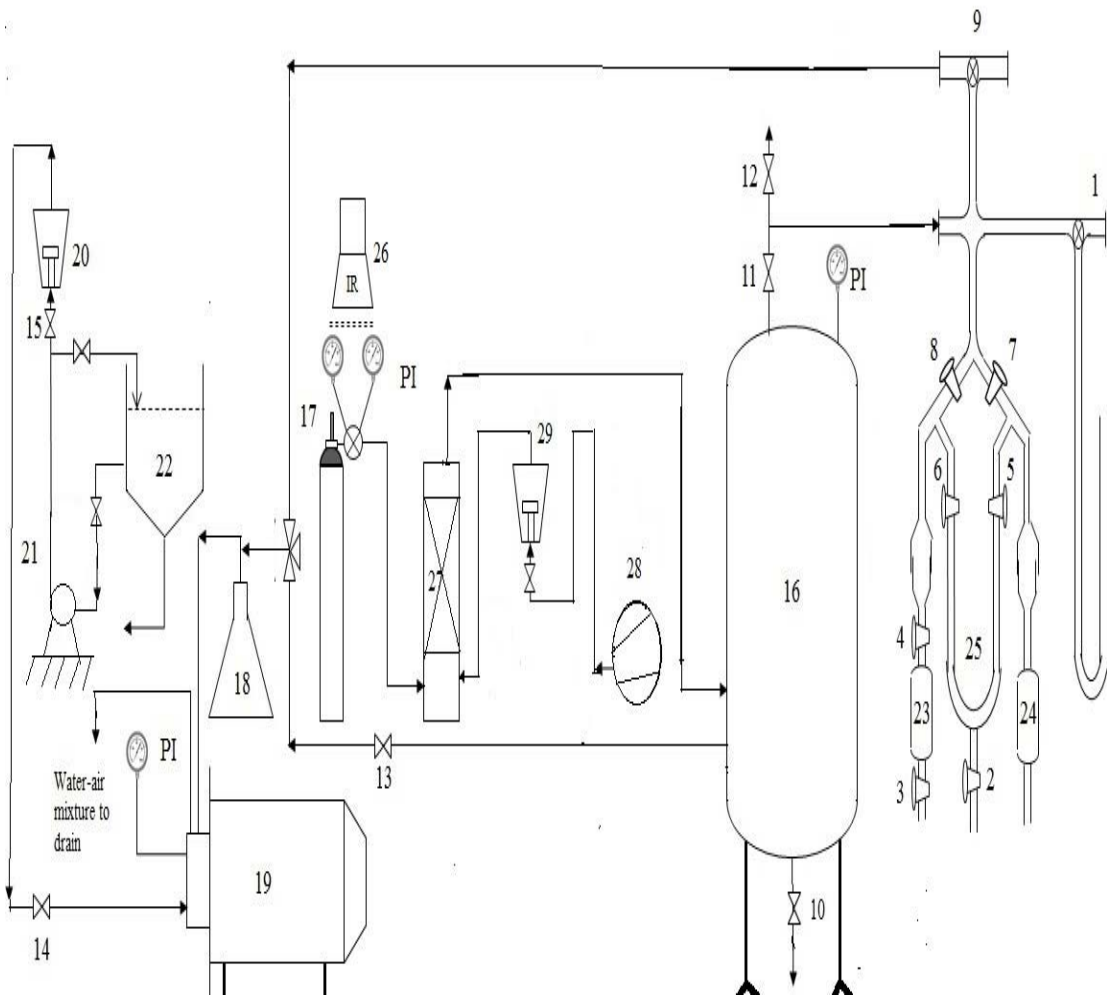
Figure 4C.2 Line diagram of experimental set-up used for measurement of Surface transfer coefficient

Legend

1-9. Vacuum stop cocks 10-15. Valves 16. Ballast vessel 17. CO_2 cylinder 18. Catch pot 19. Water-ring type vacuum pump 20. Rotameter for water   21. Water pump 22.water tank 23. Gas-absorption cell 24.Dummy cell   25. Differential water manometer 26. Infrared lamp 27. Mixing zone 28. Air compressor 29. Rotameter for air

(ii) **Technique**: Water is filled in the water tank and the vacuum pump is switched on. Gas absorption data in the manometric apparatus is collected for estimation of surface coefficient by following the below mentioned steps:

(a)   Valves (11)-(13) and vacuum stop cocks (1)-(3) closed, vacuum stop cock (9) opened, the entire system is evacuated. Vacuum stop cock (2) is opened and water is sucked into the differential manometer (25) to the desired level. Vacuum stop cock (2) is then closed.

(b) Vacuum stop cocks (3), (4) and (8) were opened, and, (5) and (6) were shut. Test solution was sucked into the gas-absorption cell upto the desired level. Vacuum stop cock (3) was then shut and the system was evacuated for degassing the solution.

(c) All the vacuum stop cocks were shut, and the system was left undisturbed for few minutes so that the foam bubbles formed on the surface of solution get collapsed.

(d) Vacuum stop cock (9) and valve (11) were then shut and valve (13) was opened to evacuate the low pressure gas storage vessel (16). Valves (11) and (13) were shut and the ballast vessel (16) was filled with lean carbon dioxide gas having the same composition as those used in the experiments. Gas filling and evacuation was repeated twice to avoid the dilution of the gas mixture with the residual impurity present in the vessel when its filling was started.

(e) Valve (11) and vacuum stop cock (1) were opened, valve (10) and vacuum stop cocks (7-9) shut, the gas pressure in vessel (16) was adjusted to one atmosphere by bleeding the excess gas through valve (12) by monitoring the vessel pressure with the help of mercury manometer (26).

(f)   Vacuum stop cock (5-8) were opened and the system was allowed to come to equilibrium. Change in gas pressure in vessel (7) is found to be negligibly small.

(g) Vacuum stop cock (4) is opened and a stop watch started to mark the beginning of an experiment. Vacuum stop cocks (7) and (8) are closed, and, (5) and (6) opened. Differential heights of the water column, caused by the absorption of CO_2 in the absorption cell and the resultant decrease in pressure in the left arm of the manometer (25), are recorded as functions of time.

(h) Valve (12) closed and vacuum broken by opening the inlet valve to catch pot. Vacuum stop cocks (7) and (8) opened, and, (5) and (6) closed. Then stop cocks (3) and (4) are opened to drain the solution from the absorption cell.

(i) For collection of more experimental data, the absorption cell is removed and rinsed with fresh test solution. The cell is placed back in position and steps (b) to (i) are repeated for each set of data.

4C.3 Sample calculation for surface mass transfer coefficient from experimental data

Cross sectional area of absorption cell, $A_b = 1.66 \times 10^{-3}$ m^2

Cross sectional area of manometer tube, $A_t = 3.125 \times 10^{-5}$ m^2

Total initial volume of gas in reference cell, $V_{r0} = 2.2803 \times 10^{-4}$ m^3

Total initial volume of gas in absorption cell, $V_{a0} = 6.0375 \times 10^{-5}$ m^3

$R = 8.314 \times 10^3$ (kg. m^2)/s^2.kmol. ^{0}K

$P_s = 1.03125 \times 10^5$ N/m^2

$V_{ms} = 22.414 \times 10^{-3}$ m^3/kmol

$T_s = 273$ ^{0}K

$P_{a0} = 1.03125 \times 10^5$ N/m^2

$P_{r0} = 1.03125 \times 10^5$ N/m^2

$\rho_m = 1000$ kg / m^3

For absorption of gas in saturated lime solution containing 2000 ppm SDS, the manometer reading Δh_m at 15 sec is 9×10^{-3} m.

Volume of gas in reference cell, $V_r = V_{r0} + (h_m/2) A_t$

$V_r = 2.2803 \times 10^{-4} + (9 \times 10^{-3}/2)(3.125 \times 10^{-5}) = 2.28171 \times 10^{-4}$ m^3.

Pressure of gas in reference cell, $P_r = \dfrac{P_{r0} V_{r0}}{V_r}$

$$= (1.03125 \times 10^5)(2.2803 \times 10^{-4})/ (2.28171 \times 10^{-4})$$

$$= 101262.28 \text{ N/m}^2$$

Pressure of gas in the absorption cell, $P_a = P_r - h_m \rho_m g$

$$= 101262.28 - (0.009)(1000)(9.81)$$

$$= 101173.98 \text{ N/m}^2$$

Molar volume of gas in absorption cell, $V_m = \dfrac{P_s V_{ms}}{T_s} \dfrac{T}{P_a}$

$V_m = (1.03125 \times 10^5)(22.414)(303)/(273)(101173.98)$

$\quad = 24.89 \text{ m}^3/ \text{ k mol}$

Volume of gas in absorption cell after time t_a, $V_a = V_{a0} - (h_m/2)(A_t)$

$V_a = 6.0375 \times 10^{-5} - (0.009/2)\,(3.125 \times 10^{-5}) = 6.0234 \times 10^{-5}\,\text{m}^3$

Volume of gas absorbed during 15 sec, $V_{ab} = (n_0 - n_{ta})\, V_{MG}$

$V_{ab} = \dfrac{1}{RT}\left(P_{a0}V_{a0} - P_a V_a\right)V_{MG}$

$\quad = 2.3043 \times 10^{-7}\,\text{m}^3$

Similarly calculate the volume absorbed for different manometer readings at different time. And plot the graph, time vs volume of gas absorbed for with and without surfactant. From trend- line equation, the volume of gas absorbed in the two cases is obtained.

Time (s)	Volume of gas absorbed (m³) × 10⁶ (without any surfactant)	Volume of gas absorbed (m³)× 10⁶(with SDS 2000 ppm)
0	0	0
15	0.5877	0.2304
30	1.2482	0.89304
45	1.8545	1.37481
60	2.1564	1.57705
75	2.4074	1.77892
90	2.5327	1.93008
105	2.6828	1.98042
120	2.8827	2.08104
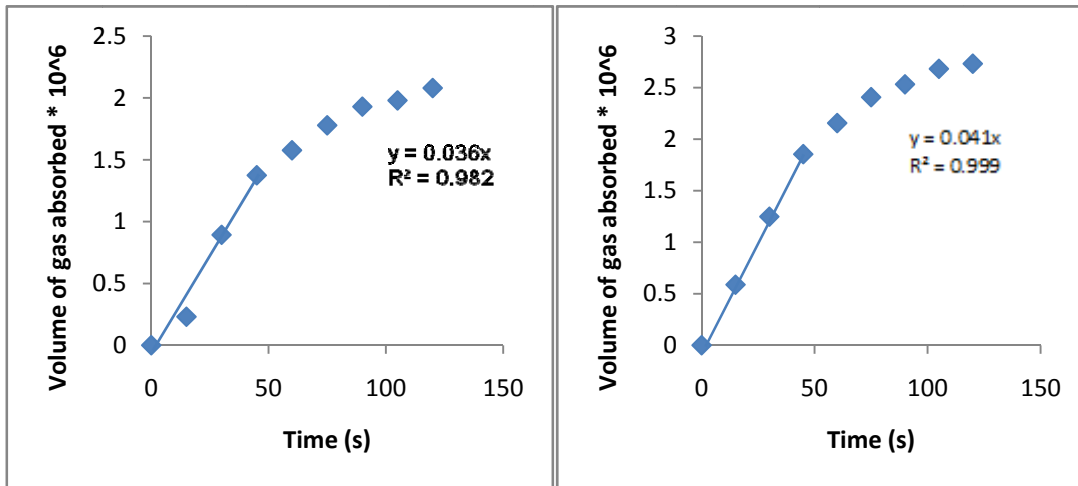
Fig. 4C.3 Volume of gas absorbed with time in saturated lime solution containing 2000 ppm SDS

a) With SDS 2000 ppm   b)   Without surfactant

$U_0 = (0.041 \times 60) \times 10^{-6} = 2.46 \times 10^{-6} \, m^3/min$ (Without surfactant)
$U_f = (0.036 \times 60) \times 10^{-6} = 2.16 \times 10^{-6} \, m^3/min$ (With surfactant)

The fraction reduction in uptake rate, $r = 1 - \dfrac{2.16 \times 10^{-6}}{2.46 \times 10^{-6}} = 0.122$

So $k_s = \dfrac{U_f}{A_b P_a r} \dfrac{1}{60\alpha} = 2.927 \times 10^{-4} \, m/s$

Similar calculations have been done for other sets of experimental data.

APPENDIX 5A

SAMPLE CALCULATIONS

5A.1 Sample calculation for NaOH-CO$_2$ system

CO$_2$ of fixed concentration is supplied continuously to the reactor while the concentration of NaOH in the batch of liquid phase reactant fed to the reactor get reduced with time although the concentration of NaOH is maintained substantially high during the entire period of reaction. Calculation is performed for a very small time interval over which NaOH concentration is assumed to remain constant. The new concentration at the end of time interval becomes initial concentration for the next time interval. Time-conversion data is found to follow approximately the trend of a straight line.

For running the simulation, a value of the saturation solubility of CO$_2$ is required. Since, solubility of CO$_2$ varies with the ionic strength of NaOH solution, the batch of NaOH fed to the reactor will have a particular solubility value for CO$_2$ at the start and a different value at the end of reactor operation when the NaOH concentration is reduced.

Using the experimental time-conversion data and material balance over a small time interval, average (of that inlet to and exit from the reactor) partial pressure of CO$_2$ both at the start of experiment as well as at the end of reactor operation are estimated. Solubility of CO$_2$ at these partial pressure values is used as the starting trial value for reactor simulation. There is no fitting parameter in the model.

5A.1.1 For bubble column

a) Temperature: 30 °C
b) Initial mass of NaOH in solution = 4.2652 g (Ref. Fig. 5a.1.1a)
c) Concentration of NaOH solution = 0.426 N
d) P_{Ab} at reactor inlet: 3.588 x 10^{-3} atm (Q_{CO_2}: 3 cm^3 s^{-1} Q_{air}: 833 cm^3 s^{-1})

 (Gas phase resistance has been neglected and $P_{Ab} = P_{Ai}$)

 Experimental conversion-time data are found to be linear.

B. *Solubility of CO_2* in the reaction mass in the bubble column *at the time of start of the batch reactor operation* (Ref. fig. 5.1.1a)

1. Experimental conversion -time data is found to be closely linear.

   Mass of NaOH reacted (during the first 15 s period of experimental run) = 0.00396 g s^{-1}

   Moles NaOH reacted $= 9.9 \times 10^{-5} gmol\ s^{-1}$

   Moles of CO_2 reacted $= 4.95 \times 10^{-5} gmol\ s^{-1}$

   Volume of CO_2 reacted

   $$= 4.95 \times 10^{-5} \times 22400 = 1.1088\ cm^3 s^{-1} at\ 0°C\ and\ 1\ atm\ pressure$$

   $$= \frac{(1.1088 \times 303)}{273} = 1.2307 cm^3 at\ 30°C\ and\ 1\ atm\ pressure$$

   Partial pressure of CO_2 at reactor exit $= \dfrac{(3 - 1.2307)}{833 + 1.7693} = 0.00212\ atm$

   Avg. partial pressure of CO_2 in the column, $P_{Ai,avg} = \dfrac{(0.003589 + 0.00212)}{2}$

   $$= 0.002854\ atm$$

   Average C_{Ai} in the column *at the start of experiment*, $C_{Ai} = H.P_{Ai,ang}$

   $$= (2.6089 \times 10^{-5})(0.002854) = 0.745 \times 10^{-7}\ gmol\ cm^{-3}$$

   Details of calculation of H is shown below:

   Ionic Effect on solubility:

   $$\log_{10}\left(\frac{H}{H_w}\right) = -hI \qquad \text{(Eqn. 3.19)}$$

   $$h = h_+ + h_- + h_w = 0.091 + 0.066 - 0.02133 = 0.1357 \quad \text{(Eqn.3.25)}$$

   $$I = \frac{1}{2}\sum z_i^2 C_i = \frac{1}{2}\left[(0.5)(1)^2 + (0.5)(1)^2\right] = 0.5 \qquad (i = 1\ for\ Na^+\ and\ i = 2\ for\ OH^-)$$

   $$\text{(Eqn. 3.20)}$$

   $$\log H_w = 4.117 - 0.059T + 7.885 \times 10^{-5} T^2 \qquad \text{(Eqn. 3.22)}$$

   $$= 3.014\ x\ 10^{-7}\ kmol\ m^{-3}\ Pa^{-1} = 3.05\ x\ 10^{-5}\ g\ mol\ cm^{-3}\ atm^{-1}\ (for\ T = 303\ °K)$$

$$\log_{10}\left(\frac{H}{H_w}\right) = -0.06785$$

$$H = \left(3.05 \times 10^{-5}\right)\left(0.85536\right) = 2.6089 \times 10^{-5} \, g \, mol \, cm^3 atm^{-1}\left(at \, the \, start \, of \, \text{exp}t\right)$$

C. ***Solubility of CO_2*** in the reaction mass in the bubble column ***at the end of batch reactor operation***

Conversion after 120 sec = 17.86%

Mass of NaOH remaining unreacted in the product solution = 4.265-0.7617 = 3.5033 g

Normality of NaOH in the product solution= 0.35 (N)

h= 0.1357 I=0.35 (calculations performed as in 'B' above)

$$\log_{10}\left(\frac{H}{H_w}\right) = -0.0475$$

$$\left(\frac{H}{H_w}\right) = 0.8964$$

$$H = H_w\left(0.8964\right) = \left(3.05 \times 10^{-5}\right)\left(0.8964\right) = 2.734 \times 10^{-5} \, g \, mol \, cm^{-3} atm^{-1}$$
$$\left(at \, the \, end \, of \, \text{exp}t\right)$$

Solubility of CO_2 at the end of batch reactor operation (when normality of NaOH in solution is 0.35 N) at 30℃ is obtained following the above (as in **'B'**) procedure. Average partial pressure required for this is calculated from the **molar rate of reaction** *at the end of batch reactor operation* which in turn is obtained from the experimental data in a similar way as shown in **'B'** above.

D.   Reactor Simulation

Experimental conditions

Normality of NaOH feed solution: 0.426 (N)

Volume of feed solution: 250 cm^3

Mass of NaOH in feed solution = 4.2652 g,

Q_{CO_2}= 0.192 lpm,

Q_{air} = 50 lpm

Physico-chemical data

Cross-sectional area of column = 86.54 cm^2

No of holes on the distributor plate = 31

Superficial velocity of gas = 9.66 cm s^{-1}

Gas holdup = 0.29   (Shulman and Molstad,1950)

Diffusion coefficient of carbon-dioxide in liquid phase = 2.2595 x 10^{-5} cm^2/s

Partial pressure of component *A* at reactor inlet: 0.0038 atm.

Reaction rate constant at 30 C, k_2 = 1.398 x 10^7 cm^{3}g mol^{-1} atm^{-1} (Eqn. 3.23)

$R_{BA} = 2$

$u_{single} = 23.41 \; cm$ (Eqn. 3.30)

$u_{swarm} = 13.52 \; cm$ (Eqn. 3.29)

d_{b0} = 0.573 cm

$t_c = \dfrac{d_{b0}}{u_{swarm}} = 0.042 \; s$

Residence time of bubble in column = $\dfrac{h_d}{u_{swarm}} = 0.3 \; s$

Height of dispersion, h_d = 4.07 cm

$k_l^0{}_{avg} = 0.026 \; cm \; s^{-1}$

 Density of feed solution = 1.02 x 10^{-3} g cm^{-3}

Viscosity of liquid, $\mu_l = 0.01 g \; cm^{-1}s^{-1}$

Surface tension of liquid, 72 dyne cm^{-1}

In the present work, the theoretical predictions of conversion-time data have been assumed to follow a linear trend. A value of C_{Ai} in the bubble column is required for the reactor simulation. The average value of C_{Ai} at the start of experiment, found to be 0.745 x 10^{-7} gmol cm^{-3} as shown in part '*B*' above, was used as the initial guess. Model was found to agree well to the experimental data for a value of C_{Ai} = 0.7694 x 10^{-7} gmol cm^{-3}.

APPENDIX 5B

5B Experimental data for carbonation of sodium hydroxide in Bubble Column Reactor and Foam Bed Reactor (Gas-liquid system)

5B.1 Bubble-column reactor data

Table 5B.1.1 Effect of concentration of sodium hydroxide (0.87N) on conversion (figure 5.1.1a)

Gas flow rate:

CO_2 flow rate: 3.0×10^{-6} m^3/s
Air flow rate: 833×10^{-6} m^3/s

Normality of NaOH solution= 0.87 (N)

Normality of HCl solution= 0.49 (N)

Volume of NaOH solution= 2.5×10^{-4} m^3

Foam height: none

Surfactant: none

Time of reaction (s)	HCl consumed, (m^3)$\times 10^6$	Unreacted NaOH (kg) $\times 10^3$	Percent Conversion	
			Experimental	Theoretical
0	87.5	8.6590	0.00	0.00
15	86.6	8.5699	1.04	1.02
30	85.4	8.4512	2.40	2.04
60	83.9	8.3027	4.11	4.07
90	82.6	8.1741	5.60	6.02
120	80.8	7.9960	7.65	8.14

Table 5B.1.2 Effect of concentration of sodium hydroxide (0.43N) on conversion (figure 5.1.1a)

Gas flow rate:

CO_2 flow rate: 3.0×10^{-6} m^3/s
Air flow rate: 833×10^{-6} m^3/s

Normality of NaOH solution= 0.43 (N)

Normality of HCl solution= 0.49 (N)

Volume of NaOH solution = 2.5×10^{-4} m^3

Foam height: none

Surfactant: none

Time of reaction (s)	HCl consumed (m^3)$\times 10^6$	Unreacted NaOH (kg) x 10^3	Percent Conversion	
			Experimental	Theoretical
0	43.1	4.2652	0.00	0.00
15	42.5	4.2058	1.39	2.10
30	41.6	4.1167	3.48	4.20
60	39.4	3.8990	8.58	8.40
90	37.8	3.7407	12.29	12.60
120	35.4	3.5032	17.86	16.80

Table 5B.1.3 Effect of concentration of sodium hydroxide (0.23 N) on conversion (figure 5.1.1a)

Gas flow rate:

CO_2 flow rate: 3.0×10^{-6} m^3/s
Air flow rate: 833×10^{-6} m^3/s

Normality of NaOH solution= 0.23 (N)

Normality of HCl solution= 0.50 (N)

Volume of NaOH solution = 2.5×10^{-4} m^3

Foam height: none

Surfactant: none

Time of reaction (s)	HCl consumed (m^3)$\times 10^6$	Unreacted NaOH (kg x 10^3)	Percent Conversion	
			Experimental	Theoretical
0	22.9	2.2662	0.00	0.00
15	22.3	2.2068	2.62	2.50
30	21.8	2.1573	4.81	5.00

60	20.7	2.0485	9.61	10.01
90	19.4	1.9198	15.28	15.01
120	18.4	1.8209	19.65	20.01

5B.2 Foam-Bed Reactor data

Table 5B.2.1 Effect of concentration of sodium hydroxide (0.87 N) on conversion (figure 5.1.1b)

Gas flow rate:

CO_2 flow rate: 3.0 x10^{-6} m^3/s
Air flow rate: 833 x10^{-6} m^3/s

Normality of NaOH solution= 0.22 (N)

Normality of HCl solution= 0.49 (N)

Volume of NaOH solution = 2.5X10^{-4} m^3

Foam height: 0.2 m

Surfactant: C-TAB

Time of reaction (s)	HCl consumed (m^3)$\times 10^6$	Unreacted NaOH (kg) x 10^3	Percent Conversion	
			Experimental	Theoretical
0	89.5	8.8569	0.00	0.00
15	87.9	8.6986	1.79	1.88
30	86.7	8.5798	3.13	3.74
60	83.9	8.3027	6.26	7.40
90	80.6	7.9762	9.94	10.99
120	78.8	7.7980	11.96	14.52

Table 5B.2.2 Effect of concentration of sodium hydroxide (0.44 N) on conversion (figure 5.1.1b)

Gas flow rate:

CO_2 flow rate: 3.0 x10^{-6} m^3/s

Air flow rate: 833 x10^{-6} m^3/s

Normality of NaOH Solution= 0.44 (N)

Normality of HCl solution= 0.50 (N)

Volume of NaOH solution = 250 x10^{-6} m^3

Foam height: 0.2 m

Surfactant: C-TAB

Time of reaction (s)	HCl consumed (m^3)× 10^6	Unreacted NaOH (kg) x 10^3	Percent Conversion	
			Experimental	Theoretical
0	44.6	4.4136	0.00	0.00
15	43.5	4.3048	2.47	2.91
30	42.4	4.1959	4.93	5.78
60	40.2	3.9782	9.87	11.38
90	37.8	3.7407	15.25	16.81
120	35.5	3.5131	20.40	22.07

Table 5B.2.3 Effect of concentration of sodium hydroxide (0.22 N) on conversion (figure 5.1.1b)

Gas flow rate:

CO$_2$ flow rate: 3.0 x10^{-6} m^3/s
Air flow rate: 833 x10^{-6} m^3/s

Normality of NaOH solution=0.89 (N)

Normality of HCl= 0.49 (N)

Volume of NaOH solution = 2.5 x10^{-4} m^3

 Foam height: 0.2 m

Surfactant: C-TAB

Time of reaction (s)	HCl consumed (m^3)× 10^6	Unreacted NaOH (kg) x 10^3	Percent Conversion	
			Experimental	Theoretical
0	20.1	2.1768	0	0

15	18.9	2.0468	5.97	5.69
30	17.8	1.9277	11.44	11.22
60	15.5	1.6786	22.89	21.78
90	13.8	1.4945	31.34	31.67
120	11.9	1.2887	40.80	40.89

Table 5B.3 Bubble-column reactor

Table 5B.3.1 Effect of superficial velocity of gas (4.35×10^{-2} m/s) on conversion (figure 5.1.2a)

Gas flow rate:

CO_2 flow rate: 1.8×10^{-6} m^3/s
Air flow rate: 375×10^{-6} m^3/s

Normality of NaOH solution= 0.23 (N)

Normality of HCl solution = 0.49 (N)

Volume of NaOH solution = 250×10^{-6} m^3

Foam height: none

Surfactant: none

Time of reaction (s)	HCl consumed (m^3)$\times 10^6$	Unreacted NaOH (kg) x 10^3	Percent Conversion	
			Experimental	Theoretical
0	44.6	4.4136	0.00	0.00
15	44.2	4.3740	0.90	0.89
30	43.9	4.3443	1.57	1.79
60	43	4.2553	3.59	3.59
90	42.1	4.1662	5.61	5.38
120	41.2	4.0772	7.62	7.18

Table 5B.3.2 Effect of superficial velocity of gas (7.75x10^{-2} m/s) on conversion (figure 5.1.2a)

Gas flow rate:

CO_2 flow rate: 3.33 x10^{-6} m^3/s
Air flow rate: 666.67 x10^{-6} m^3/s

Normality of NaOH solution= 0.23 (N)

Normality of HCl = 0.49 (N)

Volume of NaOH solution = 250 X10^{-6} m^3

Foam height: none

Surfactant: none

Time of reaction (s)	HCl consumed (m^3)× 10^6	Unreacted NaOH (kg) x 10^3	Percent Conversion	
			Experimental	Theoretical
0	43.1	4.2652	0.00	0.00
15	42.5	4.2058	2.62	2.50
30	41.6	4.1167	4.80	5.00
60	39.4	3.8990	9.61	10.00
90	37.8	3.7407	15.28	15.01
120	35.4	3.5032	19.65	20.01

Table 5B.3.3 Effect of superficial velocity of gas (9.67x10^{-2} m/s) on conversion (figure 5.1.2a)

Gas flow rate:

CO_2 flow rate: 4.34 x10^{-6} m^3/s
Air flow rate: 833.0 x10^{-6} m^3/s

Normality of NaOH solution=0.23 (N)

Normality of HCl = 0.49 (N)

Volume of NaOH solution = 250 x 10^{-6} m^3

Foam height: none

Surfactant: none

Time of reaction (s)	HCl consumed $(m^3) \times 10^6$	Unreacted NaOH (kg) x 10^3	Percent Conversion	
			Experimental	Theoretical
0	44.6	4.4136	0	0.00
15	42.6	4.2157	4.48	3.26
30	41.4	4.0969	7.17	6.51
60	38.6	3.8199	13.45	13.03
90	36.7	3.6318	17.71	19.54
120	33.5	3.3152	24.89	26.05

Table 5B.4 Foam-bed reactor

Table 5B.4.1 Effect of superficial velocity of gas on conversion of sodium hydroxide (NaOH= 0.44 N) (figure 5.1.2b)

Gas flow rate:

CO_2 flow rate: 1.8 x10^{-6} m^3/s
Air flow rate: 375 x10^{-6} m^3/s
Superficial velocity of gas: 4.35x10^{-2} m/s

Normality of NaOH solution = 0.44 (N)

Normality of HCl =0.49 (N)

Volume of NaOH solution = 2.5 x10^{-4} m^3

Foam height: 0.2 m

Surfactant: C-TAB

Time of reaction (s)	HCl consumed $(m^3) \times 10^6$	Unreacted NaOH (kg) x 10^3	Percent Conversion	
			Experimental	Theoretical
0	44.6	4.4136	0.00	0.0000
15	44.2	4.3740	0.90	1.72
30	43.4	4.2949	2.69	3.44
60	42.1	4.1662	5.60	6.87
90	40.1	3.9683	10.09	10.31

| 120 | 38.7 | 3.8298 | 13.23 | 13.76 |

Table 5B.4.2 Effect of superficial velocity of gas on conversion of sodium hydroxide (NaOH= 0.44 N) (figure 5.1.2b)

Gas flow rate:

CO_2 flow rate: 3.33 x10^{-6} m^3/s
Air flow rate: 667 x10^{-6} m^3/s
Superficial velocity of gas: 7.75 x10^{-2} m/s

Normality of NaOH solution = 0.44 (N)

Normality of HCl = 0.49 (N)

Volume of NaOH solution = 2.5 x10^{-4} m^3

Foam height: 0.2 m

Surfactant: C-TAB

Time of reaction (s)	HCl consumed (m^3)$\times 10^6$	Unreacted NaOH (kg) $\times 10^3$	Percent Conversion	
			Experimental	Theoretical
0	44.6	4.4136	0.00	0.00
15	43.1	4.2652	3.36	4.22
30	41.4	4.0969	7.17	8.34
60	37.4	3.7011	16.14	16.32
90	35.1	3.4735	21.30	23.94
120	31.1	3.0777	30.27	31.19

Table 5B.4.3 Effect of superficial velocity of gas on conversion of sodium hydroxide (NaOH= 0.44 N) (figure 5.1.2b)

Gas flow rate:

CO_2 flow rate: 4.1 x10^{-6} m^3/s
Air flow rate: 833 x10^{-6} m^3/s
Superficial velocity of gas: 9.66x10^{-2} m/s

Normality of NaOH solution =0.44 (N)

Normality of HCl = 0.49 (N)

Volume of NaOH solution = 2.5×10^{-4} m^3

Foam height: 0.2 m

Surfactant: C-TAB

Time of reaction (s)	HCl consumed (m^3)$\times 10^6$	Unreacted NaOH (kg) x 10^3	Percent Conversion	
			Experimental	Theoretical
0	44.6	4.4136	0.00	0.00
15	42.8	4.2355	4.04	4.80
30	40.4	3.9980	9.42	9.49
60	35.9	3.5527	19.51	18.50
90	32.8	3.2459	26.46	27.05
120	29.1	2.8797	34.75	35.12

Table 5B.5 Foam Bed Reactor

Table 5B.5.1 Effect of volume of sodium hydroxide solution charged into the reactor on conversion (figure 5B.1.3)

Gas flow rate:

> CO$_2$ flow rate: 3.0×10^{-6} m^3/s
> Air flow rate: 833×10^{-6} m^3/s

Normality of NaOH solution = 0.44 (N)

Normality of HCl = 0.49 (N)

Volume of NaOH solution = 2.5×10^{-4} m^3

Foam height: 0.2 m

Surfactant: C-TAB

Time of reaction (s)	HCl consumed (m^3)$\times 10^6$	Unreacted NaOH (kg) $\times 10^3$	Percent Conversion	
			Experimental	Theoretical
0	44.6	4.4136	0.00	0.00
15	43.5	4.3048	2.47	2.91

30	42.4	4.1959	4.93	5.78
60	40.2	3.9782	9.87	11.38
90	37.8	3.7407	15.25	16.81
120	35.5	3.5131	20.40	22.07

Table 5B.5.2 Effect of volume of sodium hydroxide solution charged into the reactor on conversion (figure 5B.1.3)

Gas flow rate:

CO_2 flow rate: 3.0 x10^{-6} m^3/s
Air flow rate: 833 x10^{-6} m^3/s

Normality of NaOH solution = 0.44 (N)

Normality of HCl = 0.49 (N)

Volume of NaOH solution = 3.5 x10^{-4} m^3

Foam height: 0.2 m

Surfactant: C-TAB

Time of reaction (s)	HCl consumed (m^3)$\times 10^6$	Unreacted NaOH (kg) $\times 10^3$	Percent Conversion	
			Experimental	Theoretical
0	44.8	6.2068	0	0
15	44.1	6.1098	1.56	2.04
30	43.3	5.9990	3.35	4.05
60	41.6	5.7634	7.14	8.03
90	40.0	5.5418	10.71	11.91
120	38.4	5.3201	14.29	15.72

Table 5B.5.3 Effect of volume of sodium hydroxide solution charged into the reactor on conversion (figure 5B.1.3)

Gas flow rate:

CO_2 flow rate: 3.0 x10^{-6} m^3/s

Air flow rate: 833 x10^{-6} m^3/s

Normality of NaOH solution = 0.44 (N)

Normality of HCl = 0.49 (N)

Volume of NaOH solution = 5.0 x10^{-4} m^3

Foam height: 0.2 m

Surfactant: C-TAB

Time of reaction (s)	HCl consumed (m^3)$\times 10^6$	Unreacted NaOH (kg) x 10^3	Percent Conversion	
			Theoretical	Experimental
0	44.9	8.8866	0	0
15	44.3	8.7679	1.34	1.68
30	43.7	8.6491	2.67	3.21
60	42.5	8.4116	5.35	6.23
90	41.3	8.1741	8.02	9.21
120	39.7	7.8574	11.58	12.13

Table 5B.6 Foam Bed Reactor

Table 5B.6.1 Effect of concentration of Carbon-dioxide gas on conversion of sodium hydroxide (figure 5B.1.4)

Partial pressure of CO$_2$ solution: 2.16x10^{-3}atm

Gas flow rate:

CO$_2$ flow rate: 1.8 x10^{-6} m^3/s
Air flow rate: 833 x10^{-6} m^3/s

Normality of NaOH solution= 0.44 (N)

Normality of HCl = 0.49 (N)

Volume of NaOH solution = 2.5 x10^{-4} m^3

Foam height: 0.2 m

Surfactant: C-TAB

Time of	HCl consumed	Unreacted NaOH	Percent Conversion

reaction (s)	(ml)	(kg) x 10^3	Experimental	Theoretical
0	44.6	4.413616	0.00	0.00
15	43.8	4.334448	1.79	1.98
30	43.2	4.275072	3.14	3.94
60	41.4	4.096944	7.17	7.80
90	40.1	3.968296	10.09	11.59
120	38.3	3.790168	14.12	15.29

Table 5B.4.2 Effect of concentration of Carbon-dioxide gas on conversion of sodium hydroxide (figure 5B.1.4)

Partial pressure of CO_2 gas: 3.59 x10^{-3} atm

Gas flow rate:

CO_2 flow rate: 3.0 x10^{-6} m^3/s
Air flow rate: 833 x10^{-6} m^3/s

Normality of NaOH solution= 0.44 (N)

Normality of HCl = 0.49 (N)

Volume of NaOH solution = 2.5 x10^{-4} m^3

Foam height: 0.2 m

Surfactant: C-TAB

Time of reaction (s)	HCl consumed (m^3) x10^6	Unreacted NaOH (kg) x 10^3	Percent Conversion	
			Experimental	Theoretical
0	44.6	4.4136	0	0
15	43.5	4.3048	2.47	2.91
30	42.4	4.1959	4.93	5.78
60	40.2	3.9782	9.87	11.38
90	37.8	3.7407	15.25	16.81
120	35.5	3.5131	20.40	22.07

Table 5B.6.3 Effect of concentration of Carbon-dioxide gas on conversion of sodium hydroxide (figure 5B.1.4)

Partial pressure of CO_2 : 4.90 x10^{-3} atm

Gas flow rate:

CO_2 flow rate: 4.1 x10^{-6} m^3/s
Air flow rate: 833 x10^{-6} m^3/s

Normality of NaOH solution= 0.44 (N)

Normality of HCl = 0.49 (N)

Volume of NaOH solution = 2.5 x10^{-4} m^3

Foam height: 0.2 m

Surfactant: C-TAB

Time of reaction (s)	HCl consumed (ml)	Unreacted NaOH (kg) x 10^3	Percent Conversion	
			Experimental	Theoretical
0	44.6	4.4136	0	0
15	42.8	4.2355	4.04	4.25
30	40.4	3.9980	7.17	8.40
60	35.9	3.5527	16.81	16.44
90	32.8	3.2459	23.32	24.10
120	30.8	3.0480	31.94	31.40

APPENDIX 5C

5C.1 Calibration of rota-meters

The rotameter is an instrument used for measurement of flow rate of gas. The calibration of rotameters has been done by volume displacement method. A tank of 300 l capacity was filled upto 2/3 of its capacity. An inverted glass bottle with markings on its wall and completely filled with water was immersed into the water tank in the inverted position. Carbon dioxide gas was allowed to flow through the rotameter and when the flowrate reached a steady value, the tube connected to the exit of the rotameter was slowly inserted into the glass bottle. A stopwatch was immediately started to measure the time of flow. After the desired time, the tube was removed from the bottle. The volume of water displaced was noted from the attached scale on the outside wall of glass bottle (Table 5C.1.1).

Table 5C.1.1 Calibration of CO_2 rotameter by volume-displacement method

Rotameter reading, lpm (m^3/s)	Measured (by displacement of water) gas flow rates, lpm (m^3/s)
2.0 (3.33 x 10^{-4})	2.15 (3.58 x 10^{-4})
3.0 (5.0 x 10^{-4})	3.25 (5.41 x 10^{-4})
4.0 (6.66 x 10^{-4})	4.3 (7.16 x 10^{-4})
5.0 (8.33 x 10^{-4})	5.4 (9.02 x 10^{-4})
8.0 (13.33 x 10^{-4})	8.6 (14.33 x 10^{-4})
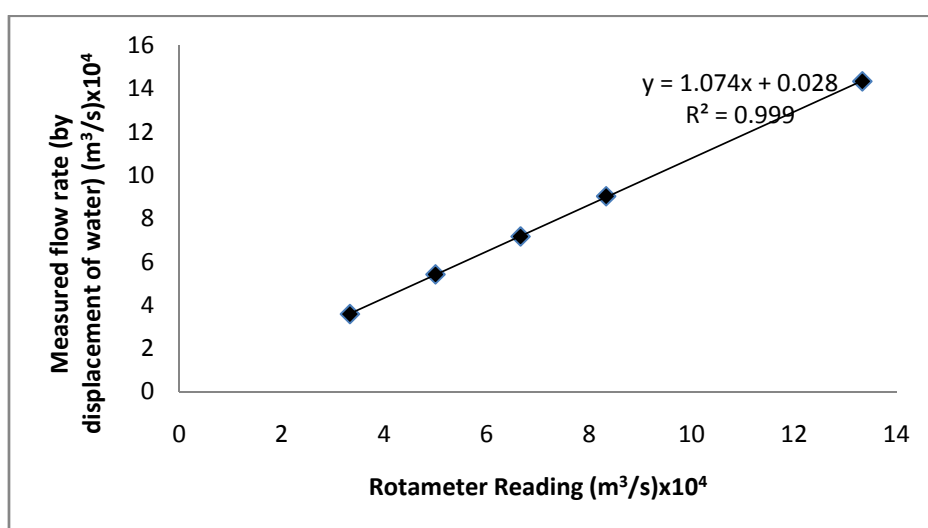
Figure 5C.1.1 Calibration of rotameter for CO_2 by volume-displacement method

Table 5C.1.2 Calibration of air rotameter by volume-displacement method

Rotameter reading, lpm (m^3/s)	Measured (by displacement of water) air flow rates, lpm (m^3/s)
5.0 (8.33 x 10^{-4})	5.3 (8.33 x 10^{-4})
8.0 (13.33 x 10^{-4})	8.4 (14.0 x 10^{-4})
10.0 (16.66 x 10^{-4})	10.7 (17.83 x 10^{-4})
18.0 (30.0 x 10^{-4})	18.9 (31.5x 10^{-4})
27.0 (45.0 x 10^{-4})	29.0 (48.33 x 10^{-4})

Figure 5C.1.2 Calibration of rotameter for air by volume-displacement method

The same experiment was repeated for different flow rates of air. The measured flow rate was plotted against rotameter reading (Figure 5C.1.2).

5C.2 Coefficient of Determination, R^2

The R^2 i.e. coefficient of determination is the best suitable method for finding out the goodness of fit between experimental and simulated results. The value of R^2 can determine by the following relation:

$$R^2 = 100 \left[1 - \frac{\sum \left(y_{i.\exp t} - y_{i,pred} \right)^2}{\sum \left(y_{i,\exp t} - y_{i,\exp t,avg} \right)^2} \right]$$

APPENDIX 5D

SAMPLE CALCULATIONS

5D.1 Sample calculation for verification of gas-liquid-solid Ca(OH)$_2$-CO$_2$ system reactor model for its finding out its agreement with the experimental data

A. Experimental conditions

i. Temperature= 30°C

ii. Total Initial loading of hydrated lime, $m_B^T(0)$ = 5.0 x 10^{-3},10 x 10^{-3} & 15 x 10^{-3}, kg

iii. Bulk pressure *of* carbon di-oxide at reactor inlet, P_{Ab} : 0.25, 0.5 & 0.1 atm

iv. Superficial velocity of gas, V_G = 3.847 x10^{-2} , 5.77 x10^{-2} & 7.70 x10^{-2} m/s

v. Flow rate of CO$_2$, Q_{CO_2} =0.33 x 10^{-4}, 0.5 x 10^{-4} & 0.67 x 10^{-4} m^3/s

vi. Flow rate of air, Q_{air} = 3.0 x 10^{-4}, 4.5 x 10^{-4} & 6.0 x 10^{-4} m^3/s

vii. Volume of slurry charged initially into the reactor, V_{sl} = 2.5 x10^{-4}, 3.5 x 10^{-4} & 5.0 x10^{-4} m^3

viii. Foam height, H_f = 0.2, 0.4 & 0.6 m

ix. Radius of the reactor column, r_C =5.25 x10^{-2} m

x. Number of holes in the distributor plate, H_N =31

xi. Average liquid holdup in the foam section,$\overline{\varepsilon_l}$ = 1.06 x10^{-2} m (ref. table 5.2.1.5)

   (Detail data presented in table 5.2.1.1 to 5.2.1.8)

xii. Surfactant SDS= 2000, 4000, 8000 & 16000 ppm

B. Physico-chemical parameters

i. Diffusion Coefficient for *A* in liquid at 30° C, D_A = 2.2024 x 10^{-9} m^2/s

ii. Diffusion Coefficient for *B* in liquid at 30° C, D_B = 1.7979 x 10^{-9} m^2/s

iii. Acceleration due to gravity, g = 9.81 m s^{-2}

iv. Solubility of hydrated lime in water at 30°c, C_B^* = 2.0664 x10^{-2} k mol/m^3

v. Second order rate constant for the system, k_2 = 1.24 x10^4 m^3/ (kmol .s)

vi. Henry's constant for gas absorption in aqueous solution at 30℃, $H = 2.6089 \times 10^{-5}$ gmol/(cm^3 atm)

Estimation of bubble radius, r_{b0} :

The volume of bubbles formed in a foam bed reactor is calculated using expression given by Kumar and Kuloor, 1970:

$$V_{b0} = (0.976) \left(\frac{Q_G}{H_N} \right)^{1.2} \bigg/ g^{0.6}$$

$$= (0.976) \left(\frac{376.8 \times 10^{-6}}{31} \right)^{1.2} \bigg/ (9.81)^{0.6}$$

$$= 3.1343 \times 10^{-7} \, m^3$$

The average radius of bubbles is obtained as:

$$r_{b0} = \left(\frac{3V_{b0}}{4\pi} \right)^{0.3333}$$

$$= 4.2169 \times 10^{-3} \, m$$

Estimation of the value of Q_f, V_{fl}, t_c^*, a and V

Solubility of carbon dioxide gas in water at 30°c, C_A^*

$$C_A^* = H \times p_{Ai}$$

Gas phase resistance has been assumed to be negligible.

$$p_{Ai} = \frac{\left(p_{Ai,inlet} + p_{Ai,exit} \right)}{2}$$

$$C_A^* = \left(2.6089 \times 10^{-5} \right) \times (0.0026)$$
$$= 6.942 \times 10^{-5} \, k \, mol / m^3$$

Drainage rate, $Q_f = \dfrac{Q_G . \overline{\varepsilon_l}}{\left(1 - \overline{\varepsilon_l} \right)}$

$$= \frac{(376.8 \times 10^{-6})(0.01)}{(1 - 0.01)}$$

$$= 3.81 \times 10^{-6} \, m^3 / s$$

Time of contact of gas with the liquid films in the foam bed, t_c^* :

$$t_c^* = \frac{H_f \pi r_c^2 \left(1 - \overline{\varepsilon_l}\right)}{Q_G}$$

$$= \frac{0.2 \times 3.14 \times \left(5.25 \times 10^{-2}\right)^2 \times \left(1 - 0.01\right)}{\left(376.8 \times 10^{-6}\right)}$$

$$= 4.55 \, s$$

5D.1.1 Sample calculation for conversion of Ca(OH)$_2$ in foam-bed reactor from experimental data

Sample calculation for conversion of hydrated lime using experimental data for 20 kg/m^3 initial loading of hydrated lime in a 0.4 m foam column for 300s using SDS as the foaming agent (ref: table 5E.2.1) are given below:

Initial weight of hydrated lime in 2.5 x 10^{-4} m^3 of water = 5.0052x 10^{-3} kg

Purity of Calcium Hydroxide in sample = 94.76%

Normality of Thiosulphate solution =0.098 N $\approx$ 0.1 N

Volume of thiosulphate required to neutralize 25 x 10^{-6} m^3 of iodine solution = 58.9 x 10^{-6} m^3

Reaction time = 300 s

Volume of iodine added to the product slurry = 230 x 10^{-6} m^3

Total volume of thiosulphate solution required for neutralization of the excess iodine present in 2.0 x 10^{-3} m^3 of slurry= 78.9 x 10^{-6} m^3

Mass of unreacted calcium hydroxide present in 500 ml slurry =

$$(0.741)\left[\frac{V_{th}}{25}\left(\frac{V_{I_2add}}{2000}\times 25\right)-\left(\frac{V_{th,tot}\times 25}{2000}\right)\right](N)$$

Mass of unreacted calcium hydroxide present in 2.0×10^{-3} m^3 slurry =

$$(4)(0.741)\left[\frac{V_{th}}{25}\left(\frac{V_{I_2add}}{2000}\times 25\right)-\left(\frac{V_{th,tot}\times 25}{2000}\right)\right](N)$$

$$=(4)(0.741)\left[\frac{58.9}{25}\left\{\frac{230}{2000}\times 25\right\}-\left\{\frac{78.9\times 25}{2000}\right\}\right](0.09842)$$

$$=1.68823\times 10^{-3}\text{ kg}$$

Mass of Ca(OH)$_2$ retained in the beaker (not transferred, N.T.)=

$$(0.741)\left[\frac{V_{th}}{25}\left(\frac{V_{I_2add}}{2000}\times 25\right)-\left(\frac{V_{th,tot}\times 25}{2000}\right)\right](N)$$

$$=(0.741)\left[\frac{58.9}{25}\left\{\frac{20}{2000}\times 25\right\}-\left\{\frac{21.5\times 25}{2000}\right\}\right](0.1)$$

$$=0.0234\text{ g}$$

$$Conversion=\frac{Mass\ of\ \text{lim}e\ reacted}{Mass\ of\ \text{lim}e\ ch\arg ed\ into\ the\ reactor}\times 100$$

$$=\frac{(M)(\%purity)-Mass\ of\ Ca(OH)_2\ unreacted-N.T.}{(M)(\%purity)-N.T.}\times 100$$

$$=\frac{5.0052\times 0.9476-1.68823-0.023355}{5.0052\times 0.9476-0.023355}\times 100$$

$$=64.23\%$$

5D.1.2 Sample calculation for conversion of Ca(OH)$_2$ in foam-bed reactor after 300 s of reactor operation using the model developed in the present work

The reactor simulation with the values of parameters/ variables mentioned above yield the following values after 300 s of reactor operation (ref. table 5E.2.1).

$$C_B^T(0) = \frac{(mass\ of\ sample\ taken)(percentage\ of\ calcium\ hydroxide\ in\ sample)}{(M_B)(Volume\ of\ solvent)}$$

$$C_B^T(0) = \frac{(5.0052 \times 10^{-3})(0.9476)}{(74.1)(250.0 \times 10^{-6})}$$

$$= 0.25602\ k\ mol/m^3$$

$$C_B^T(0) = C_B(t) + \sum_i \left(n_{pi} \frac{\pi d_{pi}^3}{6} \right) \frac{\rho_B}{M_B} \frac{V_{sl}}{V_l}$$

$$= (0.16249) + (0.00849)\frac{(2.2 \times 10^3)(253.4 \times 10^{-6})}{(74.1)(250.0 \times 10^{-6})}$$

$$= 0.09347\ k\ mol/m^3$$

$$Conversion = \frac{C_B^T(0) - C_B^T(t)}{C_B^T(0)} \times 100 = \frac{0.25602 - 0.09347}{0.25602} \times 100 = 63.49\%$$

Conversion obtained experimentally = 64.23%

APPENDIX 5E

5E. Experimental data for carbonation of hydrated lime in bubble-column and slurry-foam reactor

5E.1 Bubble-column reactor

Table 5E.1.1 Effect of initial loading (20 kg/m^3) on conversion of hydrated lime (Figure 5.3.1a)

Sample Batch No.: 03097 (Make: CDH)

Gas flow rate:

CO_2 gas flow rate: 0.333 x 10^{-4} m^3 /s
Air flow rate: 3.0 x 10^{-4} m^3 /s
Volume of solvent in slurry = 2.5 x 10^{-4} m^3

Volume of thio solution required for titration against 25 ml I_2 solution = 54.9 x 10^{-6} m^3

Surfactant: none   Normality of thiosulfate solution = 0.98N

Foam height: none

Time (s)	Initial mass of sample in feed slurry (kg)x10^3	Vol of I_2 solution added to prod slurry (v_{I_2}) (m^3)x10^6	Vol of Thio sol^n req for excess I_2 in prod slurry $(V_{th,tot})$ (m^3) x10^6	Mass of $Ca(OH)_2$ retained in the beaker (kg)x10^3	Mass of unreacted $Ca(OH)_2$ in prod slurry (W_B) (kg) x10^3	Percent conversion	
						Expt	Theory
600	5.0061	370	90.6	0.0179	2.6324	44.29	48.67
1200	5.0016	260	98.3	0.0259	1.7235	63.43	65.93
1800	5.0087	200	117.8	0.0189	1.1719	75.21	75.59
2400	5.0089	150	120.2	0.0267	0.7628	83.84	81.94
3000	5.0081	100	123.5	0.0266	0.0301	92.57	86.29

Table 5E.1.2 Effect of initial loading (40 kg/m^3) on conversion of hydrated lime (Figure 5.3.1a)

Sample Batch No.: 03097 (Make: CDH)

Gas flow rate:

CO_2 gas flow rate: 0.333 x 10^{-4} m^3 /s
Air flow rate: 3.0 x 10^{-4} m^3 /s
Volume of solvent in slurry = 2.5 x 10^{-4} m^3

Volume of thio solution required for titration against 25 ml I_2 solution=54.9 x 10^{-6}m^3

Surfactant: none   Normality of thiosulphate solution =0.98N

Foam height: none

Time (s)	Initial mass of sample in feed slurry (kg)x10^3	Vol of I_2 solution added to prod slurry (v_{I_2}) (m^3)x10^6	Vol of Thio sol^n req for excess I_2 in prod slurry $\left(V_{th,tot} \right)$ (m^3) x10^6	Mass of Ca(OH)$_2$ retained in the beaker (kg)x10^3	Mass of unreacted Ca(OH)$_2$ in prod slurry (W_B) (kg) x10^3	Percent conversion	
						Expt	Theory
600	10.0548	760	85.6	0.0214	6.1838	34.95	34.54
1200	10.0054	540	90.3	0.0231	4.2863	54.68	53.61
1800	10.0610	450	98.7	0.0336	3.4864	63.30	64.75
2400	10.0347	350	100.5	0.0194	2.6251	72.34	72.29
3000	10.0240	250	50.4	0.0341	1.9530	79.36	77.85

Table 5E.1.3 Effect of initial loading (60 kg/m^3) on conversion of hydrated lime (figure 5.3.1a)

Sample Batch No: 03097 (Make: CDH)

Gas flow rate:

CO_2 gas flow rate: 0.333 x 10^{-4} m^3 /s
Air flow rate: 3.0 x 10^{-4} m^3 /s
Volume of solvent in slurry = 2.5 x 10^{-4} m^3

Volume of thio solution required for titration against 25 ml I_2 solution=54.9 x 10^{-6} m^3

Surfactant: none   Normality of thiosulfate solution =0.98N

Foam height: none

Time (s)	Initial mass of sample in feed slurry (kg)x10^3	Vol of I_2 solution added to prod slurry (v_{I_2}) (m^3)x10^6	Vol of Thio sol^n req for excess I_2 in prod slurry $(V_{th,tot})$ (m^3) x10^6	Mass of $Ca(OH)_2$ retained in the beaker (kg)x10^3	Mass of unreacted $Ca(OH)_2$ in prod slurry (W_B) (kg) x10^3	Percent conversion	
						Expt	Theory
600	15.0431	1200	76.5	0.0186	9.9778	29.91	27.79
1200	15.0054	900	80.8	0.0321	7.3979	47.85	47.48
1800	15.0061	760	90.7	0.0196	6.1652	56.58	59.92
2400	15.0304	600	100.2	0.0340	4.7630	66.48	68.39
3000	15.0241	500	110.6	0.0193	3.8704	72.78	74.61

5E.2 Foam-bed reactor

Table 5E.2.1 Effect of initial loading (20 kg/m^3) on conversion of hydrated lime (figure 5.3.1b)

Sample batch no.: 03097 (Make: CDH)

Gas flow rate:

CO_2 gas flow rate: 0.333 x 10^{-4} m^3 /s
Air flow rate: 3.0 x 10^{-4} m^3 /s
Volume of solvent in slurry = 2.5 x 10^{-4} m^3

Volume of thio solution required for titration against 25 ml I_2 solution=58.9 x 10^{-6} m^3

Surfactant: SDS (4000 ppm)   Normality of thiosulfate solution =0.09842N

Foam height: 0.4 m

Time (s)	Initial mass of sample in feed slurry (kg)x10^3	Vol of I$_2$ solution added to prod slurry (v_{I_2}) (m^3)x10^6	Vol of Thio sol^n req for excess I$_2$ in prod slurry $(V_{th,tot})$ (m^3) x10^6	Mass of Ca(OH)$_2$ retained in the beaker (kg)x10^3	Mass of unreacted Ca(OH)$_2$ in prod slurry (W_B) (kg) x10^3	Percent conversion	
						Expt	Theory
180	5.0046*	--------	--------	--------	--------	-------	41.46
300	5.0052	230	78.9	0.0234	1.6882	64.23	63.49
480	5.0046*	--------	--------	--------	--------	-------	81.42
600	5.0092	160	167.8	0.0279	0.7627	83.84	87.65
720	5.0046*	--------	--------	--------	--------	-------	91.73
900	5.0054	120	186.4	0.0259	0.8922	92.55	95.28
1200	5.0029	80	145.3	0.0196	0.3999	96.66	98.08
1500	5.0004	70	130.3	0.0195	0.3207	97.32	99.24

*Average weight of calcium hydroxide

Table 5E.2.2 Effect of initial loading (40 kg/m^3) on conversion of hydrated lime (figure 5.3.1b)

Sample batch no.: 03097 (Make: CDH)

Gas flow rate:

CO$_2$ gas flow rate: 0.333 x 10^{-4} m^3 /s
Air flow rate: 3.0 x 10^{-4} m^3 /s
Volume of solvent in slurry = 2.5 x 10^{-4} m^3

Volume of thio solution required for titration against 25 ml I$_2$ solution=58.9 x 10^{-6} m^3

Surfactant: SDS (4000 ppm)   Normality of thiosulfate solution =0.098N

Foam height: 0.4 m

Time (s)	Initial mass of sample in feed slurry (kg)x10^3	Vol of I$_2$ solution added to prod slurry (v_{I_2}) (m^3)x10^6	Vol of Thio sol^n req for excess I$_2$ in prod slurry $(V_{th,tot})$ (m^3) x10^6	Mass of Ca(OH)$_2$ retained in the beaker (kg)x10^3	Mass of unreacted Ca(OH)$_2$ in prod slurry (W_B) (kg) x10^3	Percent conversion	
						Expt	Theory
180	10.0444*	--------	--------	--------	--------	-------	24.25
300	10.0491	800	310.3	0.0315	5.7413		39.97

						39.51	
480	10.0444[*]	--------	--------	--------	--------	-------	61.11
600	10.0514	400	245.6	0.0304	2.5409	73.24	72.5
720	10.0444[*]	--------	--------	--------	--------	-------	81.12
900	10.0185	250	265.8	0.0253	1.1785	87.55	89.21
1200	10.0961	160	213.6	0.0196	0.5957	93.76	95.56
1500	10.0069	100	176.4	0.0195	0.2159	97.72	98.11

*Average weight of calcium hydroxide

Table 5E.2.3 Effect of initial loading (60 kg/m^3) on conversion of hydrated lime (figure 5.3.1b)

Sample batch no.: 03097 (Make: CDH)

Gas flow rate:

CO$_2$ gas flow rate: 0.333 x 10^{-4} m^3 /s
Air flow rate: 3.0 x 10^{-4} m^3 /s
Volume of solvent in slurry = 2.5 x 10^{-4} m^3

Volume of thio solution required for titration against 25 ml I$_2$ solution=58.9 x 10^{-6} m^3

Surfactant: SDS (4000 ppm)   Normality of thiosulfate solution = 0.098N

Foam height: 0.4 m

Time (s)	Initial mass of sample in feed slurry (kg)x10^3	Vol of I$_2$ solution added to prod slurry (v_{I_2}) (m^3)x10^6	Vol of Thio sol^n req for excess I$_2$ in prod slurry ($V_{th,tot}$) (m^3) x10^6	Mass of Ca(OH)$_2$ retained in the beaker (kg)x10^3	Mass of unreacted Ca(OH)$_2$ in prod slurry (W_B) (kg) x10^3	Percent conversion	
						Expt	Theory
180	15.0196[*]	--------	--------	--------	--------	-------	23.34
300	15.0092	1100	70.2	0.0208	9.1942	35.26	37.81
480	15.0196[*]	--------	--------	--------	--------	-------	55.96
600	15.0659	550	75.5	0.0304	4.4498	68.76	65.26
720	15.0196[*]	--------	--------	--------	--------	-------	72.54
900	15.0091	400	80.0	0.0145	3.1447	77.87	80.52
1200	15.0046	290	120.5	0.0303	2.0520	85.54	88.58
1500	15.0094	110	32.8	0.0302	0.8254	94.18	93.21

*Average weight of calcium hydroxide

5E.3 Bubble-column reactor

Table 5E.3.1 Effect of superficial gas velocity (3.85×10^{-2} m/s) on conversion of hydrated lime (figure 5.3.2a)

Sample Batch No: 03097 (Make: CDH)

Gas flow rate:

CO_2 gas flow rate: 0.333×10^{-4} m^3 /s
Air flow rate: 3.0×10^{-4} m^3 /s

Initial solids loading = 40 kg/ m^3

Volume of solvent in slurry = 2.5×10^{-4} m^3

Volume of thio solution required for titration against 25 ml I_2 solution = 54.9×10^{-6} m^3

Surfactant: none   Normality of thiosulfate solution =0.1N

Foam height: none

Time (s)	Initial mass of sample in feed slurry (kg)x10^3	Vol of I_2 solution added to prod slurry (v_{I_2}) (m^3)x10^6	Vol of Thio sol^n req for excess I_2 in prod slurry ($V_{th,tot}$) (m^3) x10^6	Mass of Ca(OH)$_2$ retained in the beaker (kg)x10^3	Mass of unreacted Ca(OH)$_2$ in prod slurry (W_B) (kg) x10^3	Percent conversion	
						Expt	Theory
300	10.0359	--------	--------	--------	--------	-------	19.57
600	10.0548	760	85.6	0.0214	6.1838	34.95	34.54
900	10.0359*	--------	--------	--------		-------	45.62
1200	10.0054	540	90.3	0.0231	4.2863	54.68	53.61
1500	10.0359*	--------	--------	--------		-------	59.81
1800	10.0610	450	98.7	0.0336	3.4864	63.30	64.75
2100	10.0359*	--------	--------	--------	--------	-------	68.84
2400	10.0347	350	100.5	0.01939	2.6251	72.34	72.288
2700	10.0359*	--------	--------	--------	--------	-------	75.26
3000	10.0240	200	30.5	0.0341	1.9530	83.11	77.85

*Average weight of calcium hydroxide

Table 5E.3.2 Effect of superficial gas velocity (5.77 x 10^{-2} m/s) on conversion of hydrated lime (Figure 5.3.2a)

Sample Batch No: 03097 (Make: CDH)

Gas flow rate:

CO_2 gas flow rate: 0.5 x 10^{-4} m^3 /s
Air flow rate: 4.5 x 10^{-4} m^3 /s

Initial solids loading = 40 kg/ m^3

Volume of solvent in slurry = 2.5 x 10^{-4} m^3

Volume of thio solution required for titration against 25 ml I_2 solution=54.6 x 10^{-6} m^3

Surfactant: none   Normality of thiosulfate solution =0.1N

Foam height: none

Time (s)	Initial mass of sample in feed slurry (kg)x10^3	Vol of I_2 solution added to prod slurry (v_{I_2}) (m^3)x10^6	Vol of Thio sol^n req for excess I_2 in prod slurry $(V_{th,tot})$ (m^3) x10^6	Mass of $Ca(OH)_2$ retained in the beaker (kg)x10^3	Mass of unreacted $Ca(OH)_2$ in prod slurry (W_B) (kg) x10^3	Percent conversion	
						Expt	Theory
300	10.0145[*]	--------	--------	--------	--------	-------	38.51
600	10.0098	540	60.7	0.0189	4.1446	56.22	56.60
900	10.0145[*]	--------	--------	--------	--------	-------	67.08
1200	10.0231	350	70.5	0.0279	2.5709	72.85	74.24
1500	10.0145[*]	--------	--------	--------	--------	-------	79.50
1800	10.0076	260	75.4	0.0205	1.8245	80.72	83.42
2100	10.0145[*]	--------	--------	--------	--------	-------	86.47
2400	10.0053	190	95.7	0.0271	1.1829	87.49	88.96
2700	10.0145[*]	--------	--------	--------	--------	-------	90.98
3000	10.0269	150	95.3	0.0188	0.8607	90.92	92.59

*Average weight of calcium hydroxide

Table 5E.3.3 Effect of superficial gas velocity (7.78 x 10^{-2} m/s) on conversion of hydrated lime (Figure 5.3.2a)

Sample Batch No: 03097 (Make: CDH)

Gas flow rate:

CO_2 gas flow rate: 0.666×10^{-4} m^3/s

Air flow rate: 6.0×10^{-4} m^3/s

Initial loading = 40 kg/m^3

Volume of solvent in slurry = 2.5×10^{-4} m^3

Volume of thio solution required for titration against 25 ml I_2 solution=54.6×10^{-6} m^3

Surfactant: none   Normality of thiosulfate solution =0.1N

Foam height: none

Time (s)	Initial mass of sample in feed slurry (kg)x10^3	Vol of I_2 solution added to prod slurry (v_{I_2}) (m^3)x10^6	Vol of Thio sol^n req for excess I_2 in prod slurry ($V_{th,tot}$) (m^3) x10^6	Mass of $Ca(OH)_2$ retained in the beaker (kg)x10^3	Mass of unreacted $Ca(OH)_2$ in prod slurry (W_B) (kg) x10^3	Percent conversion	
						Expt	Theory
300	10.0145*	--------	--------	--------	--------	-------	46.06
600	10.0087	450	30.8	0.0289	3.5272	62.70	64.12
900	10.0145*	--------	--------	--------	--------	-------	74.27
1200	10.0256	230	43.5	0.0279	1.6999	82.05	80.95
1500	10.0145*	--------	--------	--------	--------	-------	85.54
1800	10.0276	150	51.2	0.0306	1.0241	89.19	88.97
2100	10.0145*	--------	--------	--------	--------	-------	91.57
2400	10.0074	100	65.4	0.0271	0.5667	94.00	93.48
2700	10.0145*	--------	--------	--------	--------	-------	94.90
3000	10.0031	50	70.8	0.0289	0.1423	98.49	95.97

*Average weight of calcium hydroxide

5E.4 Foam-bed reactor

Table 5E.4.1 Effect of superficial gas velocity (3.85×10^{-2} m/s) on conversion of hydrated lime (Figure 5.3.2a)

Sample Batch No.: 03097 (Make: CDH)

Gas flow rate:

CO_2 gas flow rate: 3.33×10^{-5} m^3/s

Air flow rate: 3.0×10^{-4} m^3/s

Initial loading = 40 kg/m^3

Volume of solvent in slurry = 2.5×10^{-4} m^3

Volume of thio solution required for titration against 25 ml I_2 solution=58.9 x $10^{-6} m^3$

Surfactant: SDS (4000 ppm)   Normality of thiosulfate solution =0.98N

Foam height: 0.4 m

Time (s)	Initial mass of sample in feed slurry (kg)x10^3	Vol of I_2 solution added to prod slurry (v_{I_2}) (m^3)x10^6	Vol of Thio sol^n req for excess I_2 in prod slurry $\left(V_{th,tot}\right)$ (m^3) x10^6	Mass of $Ca(OH)_2$ retained in the beaker (kg)x10^3	Mass of unreacted $Ca(OH)_2$ in prod slurry (W_B) (kg) x10^3	Percent conversion	
						Expt	Theory
180	10.0444*	--------	--------	--------	--------	-------	24.25
300	10.0491	800	310.3	0.0315	5.7413	39.51	39.97
480	10.0444*	--------	--------	--------	--------	-------	61.11
600	10.0514	400	245.6	0.0304	2.5409	73.24	72.5
720	10.0444*	--------	--------	--------	--------	-------	81.12
900	10.0185	250	265.8	0.0253	1.1785	87.55	89.21
1200	10.0961	160	213.6	0.0196	0.5957	93.76	95.56
1500	10.0069	100	176.4	0.0195	0.2159	97.72	98.11

*Average weight of calcium hydroxide

Table 5E.4.2 Effect of superficial gas velocity (5.77 x 10^{-2} m/s) on conversion of hydrated lime (Figure 5.3.2b)

Sample batch no.: 03097 (Make: CDH)

Gas flow rate:

CO$_2$ gas flow rate: 0.5 x 10^{-4} m^3 /s

Air flow rate: 4.5 x 10^{-4} m^3 /s

Initial loading = 40 kg/m^3

Volume of solvent in slurry = 2.5 x $10^{-4} m^3$

Volume of thio solution required for titration against 25 ml I_2 solution=58.9 x 10^{-6} m^3

Surfactant: SDS (4000 ppm)   Normality of thiosulfate solution =0.098N

Foam height: 0.4 m

Time (s)	Initial mass of sample in feed slurry (kg)x10³	Vol of I₂ solution added to prod slurry (v_{I_2}) (m³)x10⁶	Vol of Thio solⁿ req for excess I₂ in prod slurry $\left(V_{th,tot}\right)$ (m³) x10⁶	Mass of Ca(OH)₂ retained in the beaker (kg)x10³	Mass of unreacted Ca(OH)₂ in prod slurry (W_B) (kg) x10³	Percent conversion Expt	Percent conversion Theory
180	10.0444*	--------	--------	----------	--------	-------	50.18
300	10.0491	380	80.2	0.0197	2.8502	70.01	69.59
480	10.0444*	--------	--------	----------	--------	-------	84.17
600	10.0514	180	110.8	0.0190	1.0846	88.59	89.40
720	10.0444*	--------	--------	----------	--------	-------	92.84
900	10.0185	130	120.8	0.0223	0.6346	93.30	95.83
1200	10.0961	100	132.4	0.0180	0.34442	96.39	98.32
1500	10.0069	70	135.3	0.0179	0.0855	99.10	99.33

*Average weight of calcium hydroxide

Table 5E.4.3 Effect of superficial gas velocity (7.7 x 10^{-2} m/s) on conversion of hydrated lime (Figure 5.3.2b)

Sample batch no.: 03097 (Make: CDH)

Gas flow rate:

CO_2 gas flow rate: 0.666 x 10^{-4} m³ /s

Air flow rate: 6.0 x 10^{-4} m³ /s

Initial loading = 40 kg/ m³

Volume of solvent in slurry = 2.5 x 10^{-4} m³

Volume of thio solution required for titration against 25 ml I₂ solution=56.7 x 10^{-6} m³

Surfactant: SDS (4000 ppm)   Normality of thiosulfate solution =0.98N

Foam height: 0.4 m

Time (s)	Initial mass of sample in feed slurry (kg)x10³	Vol of I₂ solution added to prod slurry (v_{I_2}) (m³)x10⁶	Vol of Thio solⁿ req for excess I₂ in prod slurry $\left(V_{th,tot}\right)$ (m³) x10⁶	Mass of Ca(OH)₂ retained in the beaker (kg)x10³	Mass of unreacted Ca(OH)₂ in prod slurry (W_B) (kg) x10³	Percent conversion Expt	Percent conversion Theory

Time (s)	Initial mass	Vol of I_2	Vol of Thio	Mass of Ca(OH)$_2$ retained	Mass of unreacted Ca(OH)$_2$	Percent conversion	
						Expt	Theory
180	10.0322*	--------	--------	-	--------	-------	59.19
300	10.0039	320	100.8	0.0197	2.2789	75.91	76.01
480	10.0322*	--------	--------	----------	--------	-------	87.88
600	10.0961	150	120.9	0.0190	0.7997	91.62	92.16
720	10.0322*	-------------	--------	----------	--------	-------	94.78
900	10.0331	100	124.6	0.0223	0.3727	96.07	97.09
1200	10.0272	70	120.9	0.01801	0.1381	98.54	98.93
1500	10.0009	40	80.6	0.0179	0.0369	99.61	99.61

*Average weight of calcium hydroxide

5E.5 Bubble-column reactor

Table 5E.5.1 Effect of slurry volume (2.5×10^{-4} m^3) on conversion of hydrated lime (Figure 5.3.3a)

Sample Batch No: 03097 (Make: CDH)

Gas flow rate:

CO_2 gas flow rate: 0.333×10^{-4} m^3 /s
Air flow rate: 3.0×10^{-4} m^3 /s

Initial loading = 20 kg/ m^3

Volume of thio solution required for titration against 25 ml I_2 solution = 54.9×10^{-6} m^3.

Surfactant: none   Normality of thiosulfate solution = 0.1N

Foam height: none

Time (s)	Initial mass of sample in feed slurry (kg)x10^3	Vol of I_2 solution added to prod slurry (v_{I_2}) (m^3)x10^6	Vol of Thio sol^n req for excess I_2 in prod slurry ($V_{th,tot}$) (m^3) x10^6	Mass of Ca(OH)$_2$ retained in the beaker (kg)x10^3	Mass of unreacted Ca(OH)$_2$ in prod slurry (W_B) (kg) x10^3	Percent conversion	
						Expt	Theory
180	5.0046*	--------	--------	--------	--------	-------	41.46
300	5.0052	230	78.9	0.0234	1.6882	64.23	63.49
480	5.0046*	--------	--------	--------	--------	-------	81.42
600	5.0092	160	167.8	0.0279	0.7627	83.84	87.65
720	5.0046*	--------	--------	--------	--------	-------	91.73
900	5.0054	120	186.4	0.0259	0.8922	92.55	95.28
1200	5.0029	80	145.3	0.0196	0.3999	96.66	98.08
1500	5.0004	70	130.3	0.0195	0.3207	97.32	99.24

*Average weight of calcium hydroxide

Table 5E.5.2 Effect of slurry volume (3.5×10^{-4} m^3) on conversion of hydrated lime (figure 5.3.3a)

Sample Batch No: 03097 (Make: CDH)

Gas flow rate:

CO_2 gas flow rate: 0.333×10^{-4} m^3 /s
Air flow rate: 3.0×10^{-4} m^3 /s

Initial loading = 28 kg/ m^3

Volume of thio solution required for titration against 25 ml I_2 solution=58.6×10^{-6} m^3.

Surfactant: none   Normality of thiosulfate solution =0.1N

Foam height: none

Time (s)	Initial mass of sample in feed slurry (kg)x10^3	Vol of I_2 solution added to prod slurry (v_{I_2}) (m^3)x10^6	Vol of Thio sol^n req for excess I_2 in prod slurry $\left(V_{th,tot}\right)$ (m^3) x10^6	Mass of $Ca(OH)_2$ retained in the beaker (kg)x10^3	Mass of unreacted $Ca(OH)_2$ in prod slurry (W_B) (kg) x10^3	Percent conversion	
						Expt	Theory
300	7.0287*	-------	-------	--------	-------	-------	27.47
600	7.0234	530	70.9	0.0292	4.2715	35.53	41.28
900	7.0287*	-------	-------	-------	-------	-------	50.44
1200	7.0086	370	76.4	0.0339	2.8839	56.35	57.06
1500	7.0287*	-------	-------		-------	-------	62.28
1800	7.0964	300	82.1	0.0302	2.2648	66.17	66.49
2100	7.0287*	-------	-------	--------	-------	-------	70.04
2400	7.0053	260	90.7	0.0340	1.8916	71.36	73.08
2700	7.0287*	-------	-------	--------	-------	-------	75.73
3000	7.0097	190	102.5	0.0299	1.2502	81.09	78.05

*Average weight of calcium hydroxide

Table 5E.5.3 Effect of slurry volume (5×10^{-4} m^3) on conversion of hydrated lime (figure 5.3.3a)

Sample Batch No: 03097 (Make: CDH)

Gas flow rate:

CO_2 gas flow rate: 0.333×10^{-4} m^3 /s

Air flow rate: 3.0 x 10^{-4} m^3 /s

Initial loading = 40 kg/ m^3

Volume of thio solution required for titration against 25 ml I$_2$ solution=58.6 x 10^{-6} m^3.

Surfactant: none   Normality of thiosulfate solution =0.1N

Foam height: none

Time (s)	Initial mass of sample in feed slurry (kg)x10^3	Vol of I$_2$ solution added to prod slurry (v_{I_2}) (m^3)x10^6	Vol of Thio sol^n req for excess I$_2$ in prod slurry ($V_{th,tot}$) (m^3) x10^6	Mass of Ca(OH)$_2$ retained in the beaker (kg)x10^3	Mass of unreacted Ca(OH)$_2$ in prod slurry (W_B) (kg) x10^3	Percent conversion	
						Expt	Theory
300	10.0353*	-------	-------	--------	-------	-------	22.63
600	10.0099	850	30.6	0.023593	7.1536	24.39	34.17
900	10.0353*	-------	-------	-------	-------	-------	42.78
1200	10.0436	670	35.2	0.021405	5.5983	41.04	49.21
1500	10.0353*	-------	-------	-------	-------	-------	54.26
1800	10.0618	470	43.6	0.020584	3.8582	59.45	58.48
2100	10.0353*	-------	-------	-------	-------	-------	62.06
2400	10.0352	380	50.5	0.023319	3.0638	67.70	65.13
2700	10.0353*	-------	-------	--------	-------	-------	67.84
3000	10.0261	280	55.3	0.019308	2.1916	76.89	70.25

*Average weight of calcium hydroxide

5E.6 Foam-bed reactor

Table 5E.6.1 Effect of slurry volume (2.5 x 10^{-4}m^3) on conversion of hydrated lime (figure 5.3.3b)

Sample batch no.: 03097 (Make: CDH)

Gas flow rate:

CO$_2$ gas flow rate: 0.333 x 10^{-4} m^3 /s
Air flow rate: 3.0 x 10^{-4} m^3 /s

Initial loading = 20 kg/ m^3

Volume of thio solution required for titration against 25 ml I$_2$ solution=58.9 x 10^{-6} m^3

Surfactant: SDS (4000 ppm)   Normality of thiosulfate solution =0.98N

Foam height: 0.4 m

Time (s)	Initial mass of sample in feed slurry (kg)x10³	Vol of I₂ solution added to prod slurry (v_{I_2}) (m³)x10⁶	Vol of Thio solⁿ req for excess I₂ in prod slurry ($V_{th,tot}$) (m³) x10⁶	Mass of Ca(OH)₂ retained in the beaker (kg)x10³	Mass of unreacted Ca(OH)₂ in prod slurry (W_B) (kg) x10³	Percent conversion	
						Expt	Theory
180	5.0046*	--------	--------	--------	--------	-------	41.46
300	5.0052	200	78.9	0.0233	1.4305	69.67	63.49
480	5.0046*	--------	--------	--------	--------	-------	81.42
600	5.0092	160	167.8	0.0279	0.7627	83.84	87.65
720	5.0046*	--------	--------	--------	--------	----------	91.73
900	5.0054	130	186.4	0.0259	0.4371	90.73	95.28
1200	5.0029	100	145.3	0.0196	0.3293	93.03	98.08
1500	5.0004	80	167.8	0.0195	0.0754	98.40	99.24

*Average weight of calcium hydroxide

Table 5E.6.2 Effect of slurry volume ($3.5 \times 10^{-4} m^3$) on conversion of hydrated lime (Figure 5.3.3b)

Sample Batch No.: 03097 (Make: CDH)

Gas flow rate:

CO_2 gas flow rate: $0.333 \times 10^{-4} m^3$ /s

Air flow rate: $3.0 \times 10^{-4} m^3$ /s

Initial loading = 28 kg/ m^3

Volume of thio solution required for titration against 25 ml I_2 solution=$58.9 \times 10^{-6} m^3$

Surfactant: SDS (4000 ppm)   Normality of thiosulfate solution =0.1004N

Foam height: 0.4 m

Time (s)	Initial mass of sample	Vol of I₂ solution added to	Vol of Thio solⁿ req for	Mass of Ca(OH)₂ retained	Mass of unreacted Ca(OH)₂	Percent conversion	

	in feed slurry (kg)x10^3	prod slurry (v_{I_2}) (m^3)x10^6	excess I_2 in prod slurry ($V_{th,tot}$) (m^3) x10^6	in the beaker (kg)x10^3	in prod slurry (W_B) (kg) x10^3	Expt	Theory
180	7.0328*	--------	--------	--------	--------	-------	37.20
300	7.0089	400	70.2	0.0208	3.1804	51.96	49.88
480	7.0328*	--------	--------	--------	--------	-------	61.59
600	7.1207	300	73.4	0.0197	2.3097	65.67	67.04
720	7.0328*	--------	--------	--------	--------	-------	71.41
900	7.0045	240	80.3	0.0145	1.7690	73.29	76.62
1200	7.0264	170	80.9	0.0196	1.1655	82.44	82.84
1500	7.0034	150	90.7	0.0195	0.9579	85.52	87.10

*Average weight of calcium hydroxide

Table 5E.6.3 Effect of slurry volume (5.0 x 10^{-4}m^3) on conversion of hydrated lime (figure 5.3.3b)

Sample Batch No.: 03097 (Make: CDH)

Gas flow rate:

CO_2 gas flow rate: 0.333 x 10^{-4} m^3 /s

Air flow rate: 3.0 x 10^{-4} m^3 /s

Initial loading = 40 kg/ m^3

Volume of thio solution required for titration against 25 ml I_2 solution=58.9 x 10^{-6} m^3

Surfactant: SDS (4000 ppm)   Normality of thiosulfate solution =0.1004N

Foam height: 0.4 m

Time (s)	Initial mass of sample in feed slurry (kg)x10^3	Vol of I_2 solution added to prod slurry (v_{I_2}) (m^3)x10^6	Vol of Thio sol^n req for excess I_2 in prod slurry ($V_{th,tot}$) (m^3) x10^6	Mass of Ca(OH)_2 retained in the beaker (kg)x10^3	Mass of unreacted Ca(OH)_2 in prod slurry (W_B) (kg) x10^3	Percent conversion	
						Expt	Theory
180	10.0064*	--------	--------	--------	--------	-------	26.48
300	10.0011	700	80.7	0.0315	5.7195	39.45	36.38
480	10.0064*	--------	--------	--------	--------	-------	47.03
600	10.0042	520	90.8	0.0304	4.1363	56.23	52.18
720	10.0064*	--------	--------	--------	--------	-------	56.45

900	10.0120	430	100.3	0.0253	3.3284	64.82	61.73
1200	10.0063	360	110.5	0.0304	2.6898	71.54	68.45
1500	10.0083	300	120.9	0.0303	2.1365	77.40	73.57

*Average weight of calcium hydroxide

5E.7 Foam-bed reactor

Table 5E.7.1 Effect of foam height (0.2 m) on conversion of hydrated lime (figure 5.3.4)

Sample batch no.: 03097 (Make: CDH)

Gas flow rate:

CO_2 gas flow rate: 3.33×10^{-5} m^3 /s

Air flow rate: 3.0×10^{-4} m^3 /s

Initial loading = 40 kg/ m^3

Volume of solvent in slurry = 2.5×10^{-4} m^3

Volume of thio solution required for titration against 25 ml I_2 solution = 58.6×10^{-6} m^3

Surfactant: SDS (4000 ppm)   Normality of thiosulfate solution = 0.1004N

Time (s)	Initial mass of sample in feed slurry (kg)x10^3	Vol of I_2 solution added to prod slurry (v_{I_2}) (m^3)x10^6	Vol of Thio sol^n req for excess I_2 in prod slurry ($V_{th,tot}$) (m^3) x10^6	Mass of $Ca(OH)_2$ retained in the beaker (kg)x10^3	Mass of unreacted $Ca(OH)_2$ in prod slurry (W_B) (kg) x10^3	Percent conversion	
						Expt	Theory
180	10.0231*	--------	--------	------- -	--------	-------	18.66
300	10.0423	780	50.6	0.0317	6.4824	31.65	30.45
480	10.0231*	--------	--------	----------	--------	-------	46.35
600	10.0089	500	80.6	0.0294	3.9797	57.91	55.16
720	10.0231*	--------	--------	----------	--------	-------	62.53
900	10.0123	400	90.5	0.0295	3.0889	67.34	71.16
1200	10.0231	320	97.8	0.0301	2.3785	74.88	80.92
1500	10.0287	290	98.3	0.0299	2.1203	77.62	86.94

*Average weight of calcium hydroxide

Table 5E.7.2 Effect of foam height (0.4 m) on conversion of hydrated lime (figure 5.3.4)

Sample batch no: 03097 (Make: CDH)

Gas flow rate:

CO$_2$ flow rate: 0.333 x 10^{-4} m^3 /s

Air flow rate: 3.0 x 10^{-4} m^3 /s

Initial loading = 40 kg/ m^3

Volume of solvent in slurry = 2.5 x 10^{-4} m^3

Volume of thio solution required for titration against 25 ml I$_2$ solution=58.9 x 10^{-6} m^3

Surfactant: SDS (4000 ppm)   Normality of thiosulfate solution =0.1004N

Time (s)	Initial mass of sample in feed slurry (kg)x10^3	Vol of I$_2$ solution added to prod slurry (v_{I_2}) (m^3)x10^6	Vol of Thio sol^n req for excess I$_2$ in prod slurry $\left(V_{th,tot} \right)$ (m^3) x10^6	Mass of Ca(OH)$_2$ retained in the beaker (kg)x10^3	Mass of unreacted Ca(OH)$_2$ in prod slurry (W_B) (kg) x10^3	Percent conversion	
						Expt	Theory
180	10.0444*	--------	--------	--------	--------	-------	24.25
300	10.0491	800	310.3	0.0315	5.7413	39.51	39.97
480	10.0444*	--------	--------	--------	--------	-------	61.11
600	10.0514	400	245.6	0.0304	2.5409	73.24	72.5
720	10.0444*	--------	--------	--------	--------	-------	81.12
900	10.0185	250	265.8	0.0253	1.1785	87.55	89.21
1200	10.0961	160	213.6	0.0196	0.5957	93.76	95.56
1500	10.0069	100	176.4	0.0195	0.2159	97.72	98.11

*Average weight of calcium hydroxide

Table 5E.7.3 Effect of foam height (0.6 m) on conversion of hydrated lime (figure 5.3.4)

Sample batch no.: 03097 (Make: CDH)

Gas flow rate:

CO$_2$ gas flow rate: 0.333 x 10^{-4} m^3 /s

Air flow rate: 3.0 x 10^{-4} m^3 /s

Initial loading: 40 kg/ m^3

Volume of solvent in slurry: 2.5 x 10^{-4} m^3

Volume of thio solution required for titration against 25 ml I$_2$ solution=58.9 x 10^{-6} m^3

Surfactant: SDS (4000 ppm)   Normality of thiosulfate solution =0.1004N

Time (s)	Initial mass of sample in feed slurry (kg)x10^3	Vol of I$_2$ solution added to prod slurry (v_{I_2}) (m^3)x10^6	Vol of Thio sol^n req for excess I$_2$ in prod slurry ($V_{th,tot}$) (m^3) x10^6	Mass of Ca(OH)$_2$ retained in the beaker (kg)x10^3	Mass of unreacted Ca(OH)$_2$ in prod slurry (W_B) (kg) x10^3	Percent conversion	
						Expt	Theory
180	10.0359*	--------	--------	------- -	--------	-------	28.51
300	10.0548	650	90.3	0.0317	5.2265	44.96	46.78
480	10.0359*	--------	--------	----------	--------	-------	70.18
600	10.0054	250	110.4	0.0294	1.7343	81.65	81.36
720	10.0359*	--------	--------	----------	--------	-------	88.46
900	10.0610	120	120.7	0.0295	0.5855	93.84	94.31
1200	10.0347	90	124.3	0.0301	0.3160	96.67	98.11
1500	10.0240	60	128.0	0.0299	0.0461	99.51	99.39

*Average weight of calcium hydroxide

5E.8 Foam-bed reactor

Table 5E.8.1 Effect of nature of surfactant (SDS) on conversion of hydrated lime (figure 5.3.5)

Sample batch no.: MH0M601992 (Make: MERCK)

Gas flow rate:

CO_2 gas flow rate: 0.333 x 10^{-4} m^3 /s

Air flow rate: 3.0 x 10^{-4} m^3 /s

Initial loading: 20 kg/ m^3

Volume of solvent in slurry: 2.5 x 10^{-4} m^3

Volume of thio solution required for titration against 25 ml I$_2$ solution=54.6 x 10^{-6} m^3

Surfactant concentration: 4000 ppm   Normality of thiosulfate solution =0.1004N

Foam height: 0.4 m

Time (s)	Initial mass of sample in feed slurry (kg)x10^3	Vol of I$_2$ solution added to prod slurry (v_{I_2}) (m^3)x10^6	Vol of Thio sol^n req for excess I$_2$ in prod slurry ($V_{th,tot}$) (m^3) x10^6	Mass of Ca(OH)$_2$ retained in the beaker (kg)x10^3	Mass of unreacted Ca(OH)$_2$ in prod slurry (W_B) (kg) x10^3	Percent conversion	
						Expt	Theory
30	5.0120	500	50.3	0.0199	3.8749	18.07	12.20
60	5.0082	430	78.2	0.0207	3.2025	32.26	25.65
120	5.0114*	--------	--------	----------	--------	-------	51.49

180	5.0102	200	100.3	0.0222	1.2517	73.51	71.20
240	5.0114*	--------	--------	---------	--------	-------	80.93
300	5.0138	110	130.4	0.0232	0.4086	91.36	86.02
480	5.0114*	--------	--------	---------	--------	-------	93.75
600	5.0123	80	143.8	0.0209	0.1150	97.57	96.26
720	5.0114*	--------	--------	---------	--------	-------	97.75
900	5.0121	70	150.2	0.0217	0.0099	99.79	98.92

*Average weight of calcium hydroxide

Table 5E.8.2 Effect of nature of surfactant (CTAB) on conversion of hydrated lime (figure 5.3.5)

Sample batch no.: MH0M601992 (Make: MERCK)

Gas flow rate:

CO_2 gas flow rate: 0.333×10^{-4} m^3 /s

Air flow rate: 3.0×10^{-4} m^3 /s

Initial loading = 20 kg/ m^3

Volume of solvent in slurry = 2.5×10^{-4} m^3

Volume of thio solution required for titration against 25 ml I_2 solution=54.6×10^{-6} m^3

Surfactant concentration: 540 ppm   Normality of thiosulfate solution =0.106N

Foam height = 0.4 m

Time (s)	Initial mass of sample in feed slurry (kg)x10^3	Vol of I_2 solution added to prod slurry (v_{I_2}) (m^3)x10^6	Vol of Thio sol^n req for excess I_2 in prod slurry ($V_{th,tot}$) (m^3) x10^6	Mass of $Ca(OH)_2$ retained in the beaker (kg)x10^3	Mass of unreacted $Ca(OH)_2$ in prod slurry (W_B) (kg) x10^3	Percent conversion	
						Expt	Theory
30	5.0098	560	40.9	0.0173	4.1148	13.01	10.89
60	5.0273	490	54.3	0.0195	3.4351	27.89	22.75
120	5.0165*	--------	--------	---------	--------	-------	45.30
180	5.0023	240	69.1	0.0196	1.5609	66.93	63.50
240	5.0415	210	75.3	0.0202	1.3076	72.51	74.29
300	5.0217	190	100.4	0.0193	1.0563	77.71	80.20
480	5.0165*	--------	--------	---------	--------	-------	88.97
600	5.0076	100	123.8	0.01814	0.2773	94.13	92.21
720	5.0165*	--------	--------	---------	--------	-------	94.45
900	5.0054	70	122	0.0184	0.0553	98.83	96.63

*Average weight of calcium hydroxide

Table 5E.8.3 Effect of nature of surfactant (Triton X 100) on conversion of hydrated lime (Figure 5.3.5)

Sample batch no.: MH0M601992 (Make: MERCK)

Gas flow rate:

CO_2 gas flow rate: 0.333 x 10^{-4} m^3 /s

Air flow rate: 3.0 x 10^{-4} m^3 /s

Initial loading = 20 kg/ m^3

Volume of solvent in slurry = 2.5 x 10^{-4} m^3

Volume of thio solution required for titration against 25 ml I_2 solution = 48.6 x 10^{-6} m^3

Surfactant concentration: 960 ppm   Normality of thiosulfate solution = 0.1004N

Foam height = 0.4 m

Time (s)	Initial mass of sample in feed slurry (kg)x10^3	Vol of I_2 solution added to prod slurry (v_{I_2}) (m^3)x10^6	Vol of Thio sol^n req for excess I_2 in prod slurry ($V_{th,tot}$) (m^3) x10^6	Mass of $Ca(OH)_2$ retained in the beaker (kg)x10^3	Mass of unreacted $Ca(OH)_2$ in prod slurry (W_B) (kg) x10^3	Percent conversion	
						Expt	Theory
30	5.0077	600	60.5	0.0247	4.3432	8.10	9.94
60	5.0254	550	76.9	0.0277	3.8971	17.88	18.52
120	5.0278*	--------	--------	---------	--------	-------	33.66
180	5.0343	400	67.3	0.0183	2.7896	41.32	45.93
240	5.0832	320	100.8	0.0246	2.0472	57.34	55.13
300	5.0128	260	136.4	0.0286	1.4493	69.37	61.83
480	5.0278*	--------	--------	---------	--------	-------	73.44
600	5.0124	170	58.6	0.0284	1.0678	77.43	77.80
720	5.0278*	--------	--------	---------	--------	-------	80.93
900	5.0186	140	123.4	0.0264	0.5842	87.67	84.37

*Average weight of calcium hydroxide

5E.9 Foam-bed reactor

Table 5E.9.1 Effect of concentration of surfactant (SDS) on conversion of hydrated lime (figure 5.3.6)

Sample batch no.: MH0M601992 (Make: MERCK)

Gas flow rate:

CO_2 gas flow rate: 3.33 x 10^{-5} m^3 /s

Air flow rate: 3.0×10^{-4} m^3/s

Initial loading = 20 kg/m^3

Volume of solvent in slurry = 2.5×10^{-4} m^3

Volume of thio solution required for titration against 25 ml I$_2$ solution=54.6×10^{-6} m^3

Concentration of surfactant: 2000 ppm

Normality of thiosulfate solution:0.1004N

Foam height = 0.4 m

Time (s)	Initial mass of sample in feed slurry (kg)x10^3	Vol of I$_2$ solution added to prod slurry (v_{I_2}) (m^3)x10^6	Vol of Thio sol^n req for excess I$_2$ in prod slurry $\left(V_{th,tot}\right)$ (m^3) x10^6	Mass of Ca(OH)$_2$ retained in the beaker (kg)x10^3	Mass of unreacted Ca(OH)$_2$ in prod slurry (W_B) (kg) x10^3	Percent conversion	
						Expt	Theory
30	5.0079	520	30.8	0.0228	4.1099	13.10	11.47
60	5.0031	450	25.1	0.0318	3.5625	24.57	23.56
120	5.0299*	--------	--------	---------	--------	-------	45.97
180	5.0213	230	40.9	0.0218	1.7164	63.77	63.013
240	5.0299*	--------	--------	---------	--------	-------	72.90
300	5.0107	150	58.3	0.0289	1.0017	78.77	78.58
480	5.0299*	--------	--------	---------	--------	-------	87.25
600	5.0841	90	65.4	0.0225	0.4879	89.83	90.55
720	5.0299*	--------	--------	---------	--------	-------	92.92
900	5.0520	50	70.8	0.0223	0.1428	97.00	95.37

*Average weight of calcium hydroxide

Table 5E.9.2 Effect of concentration of surfactant (SDS) on conversion of hydrated lime (figure 5.3.6)

Sample batch no.: MH0M601992 (Make: MERCK)

Gas flow rate:

CO$_2$ gas flow rate: 0.333×10^{-4} m^3/s
Air flow rate: 3.0×10^{-4} m^3/s

Initial loading = 20 kg/m^3

Volume of solvent in slurry = 2.5×10^{-4} m^3

Volume of thio solution required for titration against 25 ml I$_2$ solution=54.6×10^{-6} m^3

Concentration of surfactant: 4000 ppm

Normality of thiosulfate solution:0.1004N

Foam height = 0.4 m

Time (s)	Initial mass of sample in feed slurry (kg)x10³	Vol of I₂ solution added to prod slurry (v_{I_2}) (m³)x10⁶	Vol of Thio solⁿ req for excess I₂ in prod slurry ($V_{th,tot}$) (m³) x10⁶	Mass of Ca(OH)₂ retained in the beaker (kg)x10³	Mass of unreacted Ca(OH)₂ in prod slurry (W_B) (kg) x10³	Percent conversion	
						Expt	Theory
30	5.0120	500	50.3	0.0199	3.8749	18.07	12.20
60	5.0082	430	78.2	0.0207	3.2025	32.26	25.65
120	5.0114*	--------	--------	---------	--------	-------	51.49
180	5.0102	200	100.3	0.0222	1.2517	73.51	71.20
240	5.0114*	--------	--------	---------	--------	-------	80.93
300	5.0138	110	130.4	0.0232	0.4086	91.36	86.02
480	5.0114*	--------	--------	---------	--------	-------	93.75
600	5.0123	80	143.8	0.0209	0.1150	97.57	96.26
720	5.0114*	--------	--------	---------	--------	-------	97.75
900	5.0121	70	150.2	0.0217	0.0099	99.79	98.92

*Average weight of calcium hydroxide

Table 5E.9.3 Effect of concentration of surfactant (SDS) on conversion of hydrated lime (Figure 5.3.6)

Sample batch no.: MH0M601992 (Make: MERCK)

Gas flow rate:

CO_2 gas flow rate: 0.333 x 10⁻⁴ m³ /s

Air flow rate: 3.0 x 10⁻⁴ m³ /s

Initial loading = 20 kg/ m³

Volume of solvent in slurry = 2.5 x 10⁻⁴ m³

Volume of thio solution required for titration against 25 ml I₂ solution=54.6 x 10⁻⁶ m³

Concentration of surfactant: 8000 ppm   Normality of thiosulfate solution:0.1004N

Foam height = 0.4 m

Time (s)	Initial mass of sample in feed slurry (kg)x10³	Vol of I₂ solution added to prod slurry (v_{I_2}) (m³)x10⁶	Vol of Thio solⁿ req for excess I₂ in prod slurry ($V_{th,tot}$) (m³) x10⁶	Mass of Ca(OH)₂ retained in the beaker x10⁻³ (kg)	Mass of unreacted Ca(OH)₂ in prod slurry (W_B) (kg) x10³	Percent conversion	
						Expt	Theory
30	5.0187	470	40.8	0.0309	3.6665	22.43	13.01

60	5.0153	400	56.3	0.0279	3.0402	35.65	27.30
120	5.0174*	--------	--------	---------	--------	-------	54.53
180	5.0176	150	63.7	0.0302	0.9817	79.22	73.99
240	5.0174*	--------	--------	---------	--------	-------	82.81
300	5.0184	100	70.4	0.0189	0.5505	88.35	87.59
480	5.0174*	--------	--------	---------	--------	-------	94.82
600	5.0164	60	76.8	0.0291	0.2018	95.73	97.05
720	5.0174*	--------	--------	---------	--------	-------	98.30
900	5.0181	40	80.6	0.0290	0.0251	99.47	99.25

*Average weight of calcium hydroxide

Table 5E.9.4 Effect of concentration of surfactant (SDS) on conversion of hydrated lime (Figure 5.3.6)

Sample batch no.: MH0M601992 (Make: MERCK)

Gas flow rate:

CO_2 gas flow rate: 0.333×10^{-4} m^3 /s

Air flow rate: 3.0×10^{-4} m^3 /s

Initial loading = 20 kg/m^3

Volume of solvent in slurry = 2.5×10^{-4} m^3

Volume of thio solution required for titration against 25 ml I_2 solution = 54.6×10^{-6} m^3

Concentration of surfactant: 16000 ppm   Normality of thiosulfate solution: 0.1004N

Foam height = 0.4 m

Time (s)	Initial mass of sample in feed slurry (kg)x10^3	Vol of I$_2$ solution added to prod slurry (v_{I_2}) (m^3)x10^6	Vol of Thio sol^n req for excess I$_2$ in prod slurry ($V_{th,tot}$) (m^3) x10^6	Mass of Ca(OH)$_2$ retained in the beaker (kg) x10^3	Mass of unreacted Ca(OH)$_2$ in prod slurry (W_B) (kg) x10^3	Percent conversion	
						Expt	Theory
30	5.0079	550	50.2	0.0228	4.2815	9.27	10.56
60	5.0031	480	30.4	0.0318	3.7865	19.59	20.65
120	5.0298*	--------	--------	---------	--------	-------	38.74
180	5.0753	300	40.9	0.0218	2.2851	52.27	52.90
240	5.0298*	--------	--------	---------	--------	-------	62.61
300	5.0135	230	74.8	0.0289	1.5903	66.32	69.04
480	5.0298*	--------	--------	---------	--------	-------	79.33
600	5.0114	150	98.5	0.0225	0.8522	81.97	83.10
720	5.0298*	--------	--------	---------	--------	-------	85.90
900	5.0678	90	60.4	0.0223	0.5065	89.40	89.03

*Average weight of calcium hydroxide

5E.10 Foam-bed reactor

Table 5E.10.1 Effect of concentration of surfactant (CTAB) on conversion of hydrated lime   (Figure 5.3.7)

Sample batch no.: MH0M601992 (Make: MERCK)

Gas flow rate:

CO$_2$ gas flow rate: 0.333 x 10^{-4} m^3 /s

Air flow rate: 3.0 x 10^{-4} m^3 /s

Initial loading = 20 kg/ m^3

Volume of solvent in slurry = 2.5 x 10^{-4} m^3

Volume of thio solution required for titration against 25 ml I$_2$ solution=54.6 x 10^{-6} m^3

Concentration of surfactant: 200 ppm   Normality of thiosulfate solution:0.106N

Foam height = 0.4 m

Time (s)	Initial mass of sample in feed slurry (kg)x10^3	Vol of I$_2$ solution added to prod slurry (v_{I_2}) (m^3)x10^6	Vol of Thio sol^n req for excess I$_2$ in prod slurry $(V_{th,tot})$ (m^3) x10^6	Mass of Ca(OH)$_2$ retained in the beaker (kg) x10^3	Mass of unreacted Ca(OH)$_2$ in prod slurry (W_B) (kg) x10^3	Percent conversion	
						Expt	Theory
30	5.0465	600	70.4	0.0247	4.3043	9.52	10.17
60	5.0003	530	77.9	0.0277	3.7404	20.60	19.58
120	5.0384*	--------	--------	---------	--------	-------	36.38
180	5.0643	390	100.2	0.0183	2.5840	45.95	49.81
240	5.0326	290	80.4	0.0246	1.8983	59.99	59.40
300	5.0306	230	98.5	0.0286	1.3691	71.11	66.07
480	5.0384*	--------	--------	---------	--------	-------	76.95
600	5.0316	180	111.3	0.0284	0.9371	80.23	80.97
720	5.0384*	--------	--------	---------	--------	-------	83.88
900	5.0631	110	123.6	0.0264	0.3544	92.58	87.14

*Average weight of calcium hydroxide

Table 5E.10.2 Effect of concentration of surfactant (CTAB) on conversion of hydrated lime (Figure 5.3.7)

Sample batch no.: MH0M601992 (MERCK)

Gas flow rate:

CO$_2$ gas flow rate: 0.333 x 10^{-4} m^3 /s

Air flow rate: 3.0 x 10^{-4} m^3 /s

Initial loading = 20 kg/ m^3

Volume of solvent in slurry = 2.5 x 10^{-4} m^3

Volume of thio solution required for titration against 25 ml I_2 solution=54.6 x 10^{-6} m^3

Concentration of surfactant: 540 ppm   Normality of thiosulfate solution:0.106N

Foam height = 0.4 m

Time (s)	Initial mass of sample in feed slurry (kg)x10^3	Vol of I_2 solution added to prod slurry (v_{I_2}) (m^3)x10^6	Vol of Thio sol^n req for excess I_2 in prod slurry ($V_{th,tot}$) (m^3) x10^6	Mass of $Ca(OH)_2$ retained in the beaker (kg) x10^3	Mass of unreacted $Ca(OH)_2$ in prod slurry (W_B) (kg) x10^3	Percent conversion	
						Expt	Theory
30	5.0098	560	40.9	0.01726	4.1148	13.01	10.89
60	5.0273	490	54.3	0.0195	3.4351	27.89	22.75
120	5.0165*	--------	--------	---------	--------	-------	45.31
180	5.0023	240	69.1	0.0196	1.5609	66.93	63.50
240	5.0415	210	75.3	0.0202	1.3076	72.51	74.30
300	5.0217	190	100.4	0.0193	1.0563	77.71	80.21
480	5.0165*	--------	--------	---------	--------	-------	88.98
600	5.0076	100	123.8	0.01814	0.2773	94.13	92.22
720	5.0165*	--------	--------	---------	--------	-------	94.45
900	5.0054	70	122	0.0184	0.0553	98.83	96.63

*Average weight of calcium hydroxide

Table 5E.10.3 Effect of concentration of surfactant (CTAB) on conversion of hydrated lime (Figure 5.3.7)

Sample batch no.: MH0M601992 (MERCK)

Gas flow rate:

CO_2 gas flow rate: 0.333 x 10^{-4} m^3 /s

Air flow rate: 3.0 x 10^{-4} m^3 /s

Initial loading = 20 kg/ m^3

Volume of solvent in slurry = 2.5 x 10^{-4} m^3

Volume of thio solution required for titration against 25 ml I_2 solution=48.6 x 10^{-6} m^3

Concentration of surfactant: 1000 ppm   Normality of thiosulfate solution:0.106N

Foam height = 0.4 m

Time (s)	Initial mass of sample	Vol of I_2 solution added to	Vol of Thio sol^n req for	Mass of $Ca(OH)_2$ retained	Mass of unreacted $Ca(OH)_2$	Percent conversion

	in feed slurry (kg)$\times 10^3$	prod slurry (v_{I_2}) (m^3)$\times 10^6$	excess I_2 in prod slurry $\left(V_{th,tot}\right)$ (m^3) $\times 10^6$	in the beaker (kg) $\times 10^3$	in prod slurry (W_B) (kg) $\times 10^3$	Expt	Theory
30	5.0098	550	50.2	0.0198	4.3775	7.40	9.54
60	5.0285	550	78.6	0.0182	3.8904	18.04	17.10
120	5.0198*	--------	--------	---------	--------	-------	30.32
180	5.0024	420	118.1	0.0189	2.7427	41.91	41.31
240	5.0005	320	67.4	0.0187	2.1784	53.85	50.01
300	5.0296	280	74.8	0.0191	2.2851	57.72	56.67
480	5.0198*	--------	--------	---------	--------	-------	69.07
600	5.0027	190	93.4	0.0180	1.0838	77.05	73.86
720	5.0198*	--------	--------	---------	--------	-------	77.33
900	5.0654	110	97.0	0.0175	0.4589	90.41	81.09

*Average weight of calcium hydroxide

Table 5E.10.4 Effect of concentration of surfactant (CTAB) on conversion of hydrated lime (Figure 5.3.7)

Sample batch no.: MH0M601992 (MERCK)

Gas flow rate:

CO_2 gas flow rate: 0.333 x 10^{-4} m^3 /s

Air flow rate: 3.0 x 10^{-4} m^3 /s

Initial loading = 20 kg/ m^3

Volume of solvent in slurry = 2.5 x 10^{-4} m^3

Volume of thio solution required for titration against 25 ml I_2 solution = 48.6 x 10^{-6} m^3

Concentration of surfactant: 1620 ppm   Normality of thiosulfate solution: 0.106N

Foam height = 0.4 m

Time (s)	Initial mass of sample in feed slurry (kg)$\times 10^3$	Vol of I_2 solution added to prod slurry (v_{I_2}) (m^3)$\times 10^6$	Vol of Thio sol^n req for excess I_2 in prod slurry $\left(V_{th,tot}\right)$ (m^3) $\times 10^6$	Mass of $Ca(OH)_2$ retained in the beaker (kg) $\times 10^3$	Mass of unreacted $Ca(OH)_2$ in prod slurry (W_B) (kg) $\times 10^3$	Percent conversion	
						Expt	Theory
30	5.0062	610	50.4	0.0247	4.4592	5.66	8.84
60	5.0128	550	65.0	0.0277	3.9438	16.66	14.38
120	5.0095*	--------	--------	---------	--------	-------	23.96
180	5.0325	470	76.4	0.0183	3.2883	30.76	32.33
240	5.0083	430	87.9	0.0246	2.9377	37.86	39.53

300	5.0027	400	90.5	0.0286	2.6984	42.87	45.63
480	5.0095*	--------	--------	---------	--------	-------	58.64
600	5.0015	290	93.4	0.0284	1.7279	63.39	64.38
720	5.0095*	--------	--------	---------	--------	-------	68.62
900	5.0024	190	100.2	0.0264	1.0571	77.61	73.27

*Average weight of calcium hydroxide

5E.11 Foam-bed reactor

Table 5E.11.1 Effect of concentration of surfactant (Triton-X 100) on conversion of hydrated lime (figure 5.3.8)

Sample batch no.: MH0M601992 (MERCK)

Gas flow rate:

CO_2 gas flow rate: 0.333×10^{-4} m^3 /s

Air flow rate: 3.0×10^{-4} m^3 /s

Initial loading = 20 kg/ m^3

Volume of solvent in slurry = 2.5×10^{-4} m^3

Volume of thio solution required for titration against 25 ml I_2 solution=48.6×10^{-6} m^3

Concentration of surfactant: 320 ppm   Normality of thiosulfate solution:0.106N

Foam height = 0.4 m

Time (s)	Initial mass of sample in feed slurry (kg)x10^3	Vol of I_2 solution added to prod slurry (v_{I_2}) (m^3)x10^6	Vol of Thio sol^n req for excess I_2 in prod slurry ($V_{th,tot}$) (m^3) x10^6	Mass of $Ca(OH)_2$ retained in the beaker (kg) x10^3	Mass of unreacted $Ca(OH)_2$ in prod slurry (W_B) (kg) x10^3	Percent conversion	
						Expt	Theory
30	5.0087	610	65.4	0.0187	4.4003	6.92	8.69
60	5.0205	590	96.3	0.0188	4.1263	12.92	13.84
120	5.015*	--------	--------	---------	--------	-------	22.74
180	5.0253	480	87.9	0.0190	3.3194	30.01	30.59
240	5.0012	430	120.5	0.0187	2.8097	40.48	37.43
300	5.0143	400	119.0	0.0189	2.5865	45.35	43.32
480	5.015*	--------	--------	---------	--------	-------	56.27
600	5.0178	290	108.5	0.0192	1.7879	62.25	62.11
720	5.015*	--------	--------	---------	--------	-------	66.55
900	5.0172	190	90.6	0.0169	1.0948	76.89	71.39

*Average weight of calcium hydroxide

Table 5E.11.2 Effect of concentration of surfactant (Triton X 100) on conversion of hydrated lime (figure 5.3.8)

Sample batch no.: MH0M601992 (MERCK)

Gas flow rate:

CO$_2$ gas flow rate: 0.333 x 10^{-4} m^3 /s

Air flow rate: 3.0 x 10^{-4} m^3 /s

Initial loading = 20 kg/ m^3

Volume of solvent in slurry = 2.5 x 10^{-4} m^3

Volume of thio solution required for titration against 25 ml I$_2$ solution=48.6 x 10^{-6} m^3

Concentration of surfactant: 960 ppm   Normality of thiosulfate solution:0.1004N

Foam height = 0.4 m

Time (s)	Initial mass of sample in feed slurry (kg)x10^3	Vol of I$_2$ solution added to prod slurry (v_{I_2}) (m^3)x10^6	Vol of Thio sol^n req for excess I$_2$ in prod slurry $\left(V_{th,tot}\right)$ (m^3) x10^6	Mass of Ca(OH)$_2$ retained in the beaker (kg) x10^3	Mass of unreacted Ca(OH)$_2$ in prod slurry (W_B) (kg) x10^3	Percent conversion	
						Expt	Theory
30	5.0077	600	60.5	0.0247	4.3432	8.10	9.94
60	5.0254	550	76.9	0.0277	3.8971	17.88	18.52
120	5.0278*	--------	--------	---------	--------	-------	33.66
180	5.0343	400	67.3	0.0183	2.7896	41.31	45.93
240	5.0832	320	100.8	0.0246	2.0472	57.34	55.13
300	5.0128	260	136.4	0.0286	1.4493	69.37	61.83
480	5.0278*	--------	--------	---------	--------	-------	73.44
600	5.0124	170	58.6	0.0284	1.0678	77.44	77.80
720	5.0278*	--------	--------	---------	--------	-------	80.93
900	5.0186	140	123.4	0.0264	0.5842	87.67	84.37

*Average weight of calcium hydroxide

Table 5E.11.3 Effect of concentration of surfactant (Triton X 100) on conversion of hydrated lime (figure 5.3.8)

Sample batch no.: MH0M601992 (MERCK)

Gas flow rate:

CO$_2$ gas flow rate: 0.333 x 10^{-4} m^3 /s

Air flow rate: 3.0 x 10^{-4} m^3 /s

Initial loading = 20 kg/ m^3

Volume of solvent in slurry = 2.5 x 10^{-4} m^3

Volume of thio solution required for titration against 25 ml I_2 solution=48.6 x 10^{-6} m^3

Concentration of surfactant: 2400 ppm Normality of thiosulfate solution: 0.1004N

Foam height = 0.4 m

Time (s)	Initial mass of sample in feed slurry (kg)x10^3	Vol of I_2 solution added to prod slurry (v_{I_2}) (m^3)x10^6	Vol of Thio sol^n req for excess I_2 in prod slurry ($V_{th,tot}$) (m^3) x10^6	Mass of $Ca(OH)_2$ retained in the beaker (kg) x10^3	Mass of unreacted $Ca(OH)_2$ in prod slurry (W_B) (kg) x10^3	Percent conversion	
						Expt	Theory
30	5.0135	550	50.2	0.0198	4.2815	9.47	9.54
60	5.0174	460	30.4	0.0182	3.6240	23.26	17.10
120	5.0138*	--------	--------	---------	---------	---------	30.32
180	5.0197	290	40.9	0.0189	2.2038	53.45	41.31
240	5.0192	230	74.8	0.0187	1.5903	66.36	50.01
300	5.0168	210	98.5	0.0191	1.3397	71.69	56.67
480	5.0138*	--------	--------	---------	---------	---------	69.07
600	5.0071	120	60.4	0.0180	0.7502	84.11	73.86
720	5.0138*	---------	---------	---------	---------	---------	77.33
900	5.0029	90	60.4	0.0175	0.5065	89.26	81.09

*Average weight of calcium hydroxide

Table 5E.11.4 Effect of concentration of surfactant (Triton-X 100) on conversion of hydrated lime (figure 5.3.8)

Sample batch no.: MH0M601992 (MERCK)

Gas flow rate:

CO_2 gas flow rate: 0.333 x 10^{-4} m^3 /s

Air flow rate: 3.0 x 10^{-4} m^3 /s

Initial loading = 20 kg/ m^3

Volume of solvent in slurry = 2.5 x 10^{-4} m^3

Volume of thio solution required for titration against 25 ml I_2 solution=48.6 x 10^{-6} m^3

Concentration of surfactant: 4800 ppm

Normality of thiosulfate solution: 0.1004N

Foam height = 0.4 m

Time (s)	Initial mass of sample	Vol of I_2 solution added to	Vol of Thio sol^n req for	Mass of $Ca(OH)_2$ retained	Mass of unreacted $Ca(OH)_2$	Percent conversion	

	in feed slurry (kg)$\times 10^3$	prod slurry (v_{I_2}) (m^3)$\times 10^6$	excess I$_2$ in prod slurry ($V_{th,tot}$) (m^3) $\times 10^6$	in the beaker (kg) $\times 10^3$	in prod slurry (W_B) (kg) $\times 10^3$	Expt	Theory
30	5.0563	560	50.2	0.0174	4.3628	8.5390	8.19
60	5.0236	520	30.4	0.0177	4.1114	13.0508	12.20
120	5.0372*	----------	----------	----------	----------	26.1288	19.10
180	5.0283	450	40.9	0.0178	3.5037	32.1918	25.36
240	5.0342	430	74.8	0.0181	3.2151	39.0402	31.03
300	5.0150	400	98.5	0.0192	2.8832	56.8356	36.12
480	5.0372*	----------	----------	----------	----------	68.5179	48.33
600	5.0356	280	60.4	0.0189	2.0501	8.5390	54.35
720	5.0372*	--------	--------	----------	----------	13.0508	59.13
900	5.0675	210	54.2	0.0176	1.5044	26.1288	64.68

*Average weight of calcium hydroxide

5E.12 Foam-bed reactor

Table 5E.12.1 Effect of concentration of CO$_2$ gas (10%) on conversion of hydrated lime (figure 5.3.9)

Sample batch no.: MH0M601992 (MERCK)

Gas flow rate:

CO$_2$ gas flow rate: 0.333×10^{-4} m^3/s

Air flow rate: 3.0×10^{-4} m^3/s

Initial loading = 20 kg/ m^3

Volume of solvent in slurry = 2.5×10^{-4} m^3

Volume of thio solution required for titration against 25 ml I$_2$ solution=54.6×10^{-6} m^3

Concentration of surfactant: SDS (4000 ppm)

Normality of thiosulfate solution: 0.1004N

Foam height = 0.4 m

Time (s)	Initial mass of sample in feed slurry (kg)$\times 10^3$	Vol of I$_2$ solution added to prod slurry (v_{I_2}) (m^3)$\times 10^6$	Vol of Thio sol^n req for excess I$_2$ in prod slurry ($V_{th,tot}$) (m^3) $\times 10^6$	Mass of Ca(OH)$_2$ retained in the beaker (kg) $\times 10^3$	Mass of unreacted Ca(OH)$_2$ in prod slurry (W_B) (kg) $\times 10^3$	Percent conversion	
						Expt	Theory
30	5.0120	530	50.3	0.0199	4.1187	13.34	12.99
60	5.0082	480	78.2	0.0207	3.6087	24.03	25.314
90	5.0114*	--------	--------	--------	--------	-------	37.017

180	5.0102	210	100.3	0.0222	1.3330	71.94	63.83
240	5.0114[*]	--------	--------	--------	--------	-------	74.40
300	5.0138	150	130.4	0.0232	0.7335	84.57	81.40
480	5.0114[*]	--------	--------	--------	--------	-------	92.16
600	5.0123	100	143.8	0.0209	0.2775	94.16	95.38
720	5.0114[*]	--------	--------	--------	--------	-------	97.22
900	5.0121	70	150.2	0.0217	0.0099	99.79	98.73

*Average weight of calcium hydroxide

Table 5E.12.2 Effect of concentration of CO_2 gas (25%) on conversion of hydrated lime (Figure 5.3.9)

Sample batch no.:

Gas flow rate:

CO$_2$ gas flow rate: 0.833×10^{-4} m^3 /s

Air flow rate: 2.5×10^{-4} m^3 /s

Initial loading = 20 kg/ m^3

Volume of solvent in slurry = 2.5×10^{-4} m^3

Volume of thio solution required for titration against 25 ml I$_2$ solution = 48.9×10^{-6} m^3

Concentration of surfactant: SDS (4000 ppm)

Normality of thiosulfate solution: 0.1004N

Foam height = 0.4 m

Time (s)	Initial mass of sample in feed slurry (kg)x10^3	Vol of I$_2$ solution added to prod slurry (v_{I_2}) (m^3)x10^6	Vol of Thio sol^n req for excess I$_2$ in prod slurry ($V_{th,tot}$) (m^3) x10^6	Mass of Ca(OH)$_2$ retained in the beaker (kg) x10^3	Mass of unreacted Ca(OH)$_2$ in prod slurry (W_B) (kg) x10^3	Percent conversion	
						Expt	Theory
30	5.0074	500	34.6	0.0174	3.5093	26.17	18.30
60	5.0136	400	43.2	0.0265	2.7497	42.11	36.04
90	5.0115[*]	--------	--------	----------	--------	-------	52.25
180	5.0253	150	57.7	0.0176	0.8768	81.62	82.45
240	5.0115[*]	--------	--------	----------	--------	-------	90.48
300	5.0134	90	80.6	0.0247	0.3550	92.53	94.66
480	5.0115[*]	--------	--------	----------	--------	-------	98.97
600	5.0014	60	110.4	0.0182	0.0259	99.45	99.66
720	5.0115[*]	--------	--------	----------	--------	-------	99.90
900	5.0078	45	85.3	0.0274	0.0101	99.79	99.99

*Average weight of calcium hydroxide

Table 5E.12.3 Effect of concentration of CO_2 gas (50%) on conversion of hydrated lime (Figure 5.3.9)

Sample batch no.:

Gas flow rate:

CO_2 gas flow rate: 1.6667×10^{-4} m^3 /s

Air flow rate: 1.6667×10^{-4} m^3 /s

Initial loading = 20 kg/ m^3

Volume of solvent in slurry = 2.5×10^{-4} m^3

Volume of thio solution required for titration against 25 ml I_2 solution=54.6×10^{-6} m^3

Normality of thiosulfate solution: 0.1004N

Concentration of surfactant: SDS (4000 ppm)

Foam height = 0.4 m

Time (s)	Initial mass of sample in feed slurry (kg)x10^3	Vol of I_2 solution added to prod slurry (v_{I_2}) (m^3)x10^6	Vol of Thio sol^n req for excess I_2 in prod slurry $(V_{th,tot})$ (m^3) x10^6	Mass of $Ca(OH)_2$ retained in the beaker (kg) x10^3	Mass of unreacted $Ca(OH)_2$ in prod slurry (W_B) (kg) x10^3	Percent conversion	
						Expt	Theory
30	5.0179	400	58.4	0.0213	3.0324	36.28	33.54
60	5.0131	250	65.8	0.0216	1.7863	62.43	60.19
90	5.0129 *	--------	--------	-----------	--------	-------	75.96
180	5.0053	90	90.4	0.0218	0.3949	91.68	93.35
240	5.0129 *	--------	--------	-----------	--------	-------	96.87
300	5.0134	40	70.5	0.0188	0.0627	98.68	98.55
480	5.0129 *	--------	--------	-----------	--------	-------	99.87
600	5.0104	35	65.2	0.0225	0.0418	99.12	99.98
720	5.0129 *	--------	--------	-----------	--------	-------	99.99
900	5.0178	30	62.1	0.0223	0.0127	99.73	100

*Average weight of calcium hydroxide

Notation

A	Substance A, present in gas phase as well as dissolved in liquid
2a	Thickness of a liquid-foam, m
$a_1, a_2, ..., a_m$	Thickness of half-film in subsections 1,2,3,.., and m respectively, m
a_C	Cross section area of column, m^2
a_s	The interfacial area per unit volume of gas-liquid dispersion, $m^2\ m^{-3}$
a_b	Interfacial Area per bubble, $m^2\ m^{-3}$
a_p	Surface area of particles, $m^2\ m^{-3}$
a_t	Area of all the bubbles in dispersion, m^2
a_{bc}^t	Total interfacial area in the column, m^2
$a_{storagre}^t$	Total interfacial area in the storage section, m^2
A_t	Cross sectional area of the glass tube of the water manometer in the manometric apparatus, m^2
B	Substance B, present in solution/slurry as dissolved as well as dissolving particles
B_1	Constant, defined in equation (2.26)
C_{Ab}	Bulk concentration of A, $k\ mol\ m^{-3}$
C_A	Concentration of dissolved A in the liquid at any time t, $kmol\ m^{-3}$
C_{A0}	Initial concentration of reactant A dissolved in liquid in the (feed), kg m^{-3}, $k\ mol\ m^{-3}$
C_A'	Concentration of reactant A in the foam film at position x and any contact time t_c
C_{AS}	Concentration of dissolved A in the storage section at any time t, $k\ mol\ m^{-3}$
C_{Ad}	Concentration of reactant A in the drainage stream from foam to storage section, $k\ mol\ m^{-3}$
$C_A^* = C_{Ai}$	Interfacial concentration of A in the liquid phase, $k\ mol\ m^{-3}$
C_{Ad}	Concentration of dissolved A in the drainage stream from foam to storage section, $k\ mol\ m^{-3}$

C_B	Concentration of B in the liquid film (for NaOH + lean CO_2 gas system), $kmol\ m^{-3}$
$\overline{C_A}$	Average concentration of component A, $k\ mol\ m^{-3}$
C_B	Initial concentration of reactant B in liquid phase, $k\ mol\ m^{-3}$
C_{Bb}	Bulk concentration of B, $k\ mol\ m^{-3}$
C_{Bi}	Concentration of B at the solid-liquid interface in the liquid phase, $k\ mol\ m^{-3}$
C_{Bm}	Mean concentration of NaOH, $k\ mol\ m^{-3}$
C_{Bs}	Concentration of component B in the storage section, $k\ mol\ m^{-3}$
C_B^*	Solubility of component B in water, $k\ mol\ m^{-3}$
C_{B0}	Initial concentration of reactant B dissolved in liquid in the (feed), $kg\ m^{-3}$, $k\ mol\ m^{-3}$
C_{Bd}, C_{Bf}	Concentration of reactant B in the drainage stream at any time t for gas-liquid/gas-liquid-solid system, $k\ mol\ m^{-3}$
$C_{B(t)}, C_B^T(t)$	Total (dissolved in liquid as well as undissolved particles) loading of B per unit volume of solvent at any time t, $k\ mol\ m^{-3}$
$C_{B(0)}, C_B^T(0)$	Initial total loading of B per unit volume of solvent, $k\ mol\ m^{-3}$
C_s	Concentration of surfactant, ppm
D	Diameter, m
D_A	Diffusivity of species A in liquid phase, $m^2\ s^{-1}$
D_B	Diffusivity of species B in liquid phase, $m^2\ s^{-1}$
D_G	Diffusivity of gas, $m^2\ s^{-1}$
d_{b0}	Average diameter of initial spherical bubble, m
d_c	Diameter of foam column, m
d_0	Diameter of holes on the gas distributor plate, m
d_p	Average diameter of the particle in slurry, m
d_{pk}	Instantaneous value of particle diameter in the kth size fraction in slurry, m
d_{pk0}	Initial diameter of particles in the kth size fraction in slurry, m

d_s	Sauter mean bubble diameter at a given height in the foam section, m
E	Foam-expansion ratio, dimensionless
E_i	Instantaneous value of enhancement factor for gas absorption with chemical reaction, dimensionless
E_a	Average value of enhancement factor for gas absorption with chemical reaction, dimensionless
E_{cs}	Excess concentration at the surface, $k\ mol\ m^{-3}$
f	Friction factor for foam flow through a pipe, dimensionless
g	Acceleration due to gravity, $m\ s^{-2}$
H	Henry's law solubility coefficient for solution containing ions,
H_a	Hatta number
h	Height of liquid in the storage section, m
H_f	Height of foam, m
H_W	Henry's law solubility coefficient for water containing ions,
h_0	Initial height of liquid in the storage section, m
h_d	Height of dispersion, m
h_m	Differential height in manometer, m
H_T	Depth from top of foam, m
H_N	Number of holes in distributor plate, dimensionless
h	Sum of positive , negative and gas species ions
I	Ionic strength
K	a constant defined in equation (2.3)
k_c	Gas phase mass transfer coefficient, $m\ s^{-1}$
K_l	Overall liquid phase mass transfer coefficient, $m\ s^{-1}$
k_2	Second order reaction rate constant, $m^3\ kmol^{-1}s^{-1}$
$k_l a$, k_l	Liquid phase mass transfer coefficient, $m\ s^{-1}$
k_l^0	Physical liquid phase mass transfer coefficient, $m\ s^{-1}$
k_G	Gas phase mass transfer coefficient, $k\ mol\ m^{-2}.\ Pa.\ S$
k_{lr}	Gas liquid mass transfer coefficient with chemical reaction, $m\ s^{-1}$

k_s	Gas liquid mass transfer coefficient in presence of surface resistance and chemical reaction, $m\ s^{-1}$
k_{sl}	Solid- liquid mass transfer coefficient, $m\ s^{-1}$
M_B	Molecular weight of component B, $kg\ (kg\ mol)^{-1}$
$m_B^T(0)'$	Initial total loading of unreacted B per unit volume of solvent, $kg\ m^3$
$m_B^T(t)$	Total loading of unreacted B at any time t, $kg\ m^3$
N	Normality of standard solution
N_A	Molar flux of component A absorbed per unit gas-liquid interfacial area per unit time, $kmol\ m^{-2}\ s^{-1}$
$\overline{N_A}$	Average molar flux of component A absorbed per unit gas-liquid interfacial area per unit time, $kmol\ m^{-2}\ s^{-1}$
n_{bc}	Number of bubbles in the dispersion at any time in bubble column
$n_{A,abs}$	Moles of A absorbed per unit time
$n_{B,abs}$	Moles of B absorbed per unit time
n_{pk}	Number of particles in the kth size fraction per unit volume of slurry, m^3
P_{Ab}	Bulk pressure of component A, atm
P_{Ai}	Partial pressure of component A, atm
$P_{Ai,inlet}$	Partial pressure of component A inlet, atm
$P_{Ai,exit}$	Partial pressure of component A exit, atm
P_r	Pressure of carbon dioxide gas in the reference cell at any time t_a, $N\ m^{-2}$
P_{r0}	Initial pressure of carbon dioxide gas in the reference cell, $N\ m^{-2}$
P_s	Pressure of gas at NTP, $N\ m^{-2}$
Δp	pressure drop, $N\ m^{-2}$
Δp_1	Pressure drop due to the dry plate, $N\ m^{-2}\ per\ plate$
Δp_2	Pressure drop due to foam, $N\ m^{-2}\ per\ plate$
Q_d	Total flow rate of draining liquid from foam into storage section, $m^3\ s^-$
$Q_G,\ Q_{Go}$	Flow rate of gas into the storage section, $m^3\ s^{-1}$

r	Fractional reduction in the uptake rate produced by the surfactant film in the absorption cell, dimensionless
R_{BA}	The stoichiometric factor for overall reaction
r_{b0}	Average radius of bubble, m
r_c	Radius of foam column, m
R	Gas constant, $(kg \cdot m^2) (s^2 \cdot k\, mol \cdot K)^{-1}$
R_{eo}	Reynolds number, dimensionless
s	The fractional rate of surface renewal
Sc	Schmidt number, dimensionless
Sh	Sherwood number, dimensionless
θ	Time, s^{-1}
t	Time of operation of the foam-bed contactor, s
t_a	Time of gas absorption in the absorption cell, s
t_{bc}, t_c	Gas-liquid contact time in foam section, s
t_c^*	Contact time, s
t_{cs}	Gas-liquid contact time in storage section, s
t_d	Time of foam drainage, s
T	Temperature at which experiments were conducted, K
T_s	Temperature of gas at NTP, K
U_f	Uptake rate of gas in liquid in the absorption cell in presence of surface film at the gas pressure P_a, $m^3\ s^{-1}$
U_0	Uptake rate of gas in liquid in the absorption cell without any surface film at the gas pressure P_a, $m^3\ s^{-1}$
u	Uptake rate of gas in absorption cell in time 't_a' seconds, m^3
u_f	Linear velocity of foam , $m\, s^{-1}$
u_o	gas velocity through orifices, $m\, s^{-1}$
$u_{\sin gle}$	Rise velocity of single gas bubbles in the storage section, $m\ s^{-1}$
u_{swarm}	Rise velocity of swarm of gas bubbles in the storage section, $m\ s^{-1}$
V	Volume of slurry/liquid in storage section, m^3

V_a	Volume of gas in the absorption cell at any time t_a, m^3
V_{a0}	Initial volume of gas in the absorption cell, m^3
V_{ab}	Volume of gas absorbed in the absorption cell in time t_a, m^3
V_{b0}	Volume of single bubble, m^3
V_d	Volume of the liquid drained from static foam in time t_c^*, m^3
V_l	Total volume of solvent in solution/slurry, m^3
V_g	Total volume of gas in the dispersion, m^3
V_G	Superficial velocity of gas, $m\,s^{-1}$
V_{foam}^l	Volume of slurry in the foam section, m^3
V_{fo}	Initial total volume of liquid contained in foam, m^3
V_{MG}	Molar volume of gas at temperature and pressure of experiment, $m^3\,(k\;mol)^{-1}$
V_{ms}	Molar volume of gas at NTP, $m^3(k\;mol)^{-1}$
V_{pk}	Volume of a particle in the kth size fraction at any time 't' in the storage section, m^3
V_{pkd}	Volume of a particle in the kth size fraction at any time 't' in the drainage stream from foam section, m^3
V_r	Volume of gas in the reference cell at any time t_a, m^3
V_{r0}	Initial volume of gas in the reference cell, m^3
V_{sl}	Volume of slurry charged into the bubble column or foam bed reactor, m^3
$V_{l,store}$	Volume of liquid in the storage section, m^3
V_t	Terminal velocity of a single bubble, $m\,s^{-1}$
V_{th}	Volume of thiosulphate solution needed for standardization of 2.5×10^{-5} m^3 iodine solution, m^3
$V_{th,b}$	Volume of thiosulphate required to neutralize iodine solution having a volume equal to that added per 2.5×10^{-5} m^3 solution of lime sample, m^3

$V_{th,s}$	Volume of thiosulphate solution required to neutralize excess iodine present in 2.0×10^{-5} m^3 solution of lime, m^3
$V_{th,tot}$	Total volume of thiosulphate solution required for titration of 2.0×10^{-3} m^3 of product slurry, m^3
V_{thio}	Volume of thiosulphate solution, m^3
$\left(W_B\right)_{storage,\Delta t}$	Rate of consumption of B, total moles of B reacted over contact time, Δt
w	Mass of hydrated lime present per unit volume of slurry, kg
X	Percentage conversion of NaOH/Ca(OH)$_2$, dimensionless

Greek letters

$\overline{\varepsilon_G}$	Average gas holdup
ε_g	Gas holdup
$\overline{\varepsilon_l}, \varepsilon_l$	Liquid hold up
α	Solubility coefficient of carbon dioxide gas in water, m^2/N
δ	Film thickness, m
σ_l	Surface tension, $N\,m^{-1}$
λ	Pseudo-first order kinetic rate constant for the reaction, s^{-1}
ρ_B	Density of component B, $kg\,m^{-3}$
ρ_f	Density of foam, $kg\,m^{-3}$
ρ_G	Density of gas, $kg\,m^{-3}$
ρ_l	Density of liquid, $kg\,m^{-3}$
ρ_0	Density of pure solvent, $kg\,m^{-3}$
ρ_m	Density of manometer liquid, $kg\,m^{-3}$
ρ_s	Density of calcium carbonate, $kg\,m^{-3}$
ρ_{sl}	Density of slurry, $kg\,m^{-3}$
μ_{eff}	Effective viscosity, $kg\,m^{-1}s^{-1}$

μ_g viscosity of gas, *kg m⁻¹s⁻¹*

μ_l viscosity of liquid, *kg m⁻¹s⁻¹*

θ Time of exposure of liquid elements on the surface of a bubble for

absorption, s

REFERENCES

1. Akita, K. and Yoshida, F. (1973). Gas holdup and volumetric mass transfer coefficient in bubble columns. Effects of liquid properties. *Industrial and Engineering Chemistry Process Design and Development*, **12**(1), 76-80.

2. Akita, K. and Yoshida, F. (1974). Bubble size, interfacial area, and liquid-phase mass transfer coefficient in bubble columns. *Industrial and Engineering Chemistry Process Design and Development*, **13**(1), 84-91.

3. Ambulgekar, P. V., Dedhia, A. C. and Pandit A. B. (2004). Liquid drainage in static foam: Analogy with liquid drainage through packed bed. *Indian Journal of Chemical Technology*, **11**, 392-400.

4. Astarita, G. *Mass transfer with chemical reaction*. Elesevier, 1967.

5. Asolekar, S. R., Deshpande, P. K. and Kumar, R. (1988). A model for a foam-bed slurry reactor. *AIChE journal*, **34**(1), 150-154.

6. Bandyopadhyay, A. and Biswas, M. N. (2011). Determination of interfacial area in a tapered bubble column. Journal of Chemical Technology and Biotechnology, 86(9), 1211-1225.

7. Barigou, M. and Davidson, J.F. (1996). Pressure drop and liquid entrainment in a foam flowing in a vertical pipe. *Proceedings of the 2nd European Conference for Young Researchers in Chemical Engineering Leeds, U.K.*, April 2-3, 952-954.

8. Bhaskarwar, A. and Kumar, R. (1984). Oxidation of sodium sulphide in a foam bed contactor. *Chemical Engineering Science*, **39**(9), 1393-1399.

9. Bhaskarwar, A. N. and Kumar, R. (1986). Oxidation of sodium sulphide in the presence of fine activated carbon particles in a foam bed contactor. *Chemical Engineering Science*, **41**(2), 399-404.

10. Bhaskarwar, A. N. and Kumar, R. (1995). Gas-phase controlled mass transfer in a foam-bed reactor. *Chemical Engineering Communications*, **131**(1), 115-124.

11. Bhaskarwar, A. N. (1987). Analysis of gas absorption accompanied by a zero-order chemical reaction in a liquid-foam film surrounded by limited gas pockets. *Journal of Chemical Technology and Biotechnology*, **37**(3), 183-187.

12. Bhaskarwar, A. N., Desai, D. and Kumar, R. (1990). General model of a foam bed reactor. *Chemical Engineering Science*, **45**(5), 1151-1159.

13. Bhaskarwar, A. N., Kumar, R. and Gandhi, K. S. (1987). Mass transfer accompanied by a chemical reaction in an emulsion foam bed reactor. *AIChE Journal*, **33**(2), 331-335

14. Bhattacharjee, S., Kumar, R. and Gandhi, K. S. (1997). Prediction of separation factor in foam separation of proteins. *Chemical Engineering Science*, **52**(24), 4625-4636.

15. Bhattacharjee, S., Kumar, R. and Gandhi, K. S. (2001). Modeling of protein mixture separation in a batch foam column. *Chemical Engineering Science*, **56**(19), 5499-5510.

16. Bikerman, J. J. (1956). Drainage of liquid from surfaces of different rugosities. *Journal of Colloid Science*, **11**(4), 299-307.

17. Biswas, J. and Kumar, R. (1981). Mass transfer with chemical reaction in a foam bed contactor. *Chemical Engineering Science*, **36**(9), 1547-1556.

18. Biswas, J., Asolekar, S. R. and Kumar, R. (1987). Effect of surface resistance arising due to surfactant on gas absorption accompanied by a chemical reaction in a foam-bed-reactor. *The Canadian Journal of Chemical Engineering*, **65**(3), 462-469.

19. Blank, M. and Roughton, F. J. W. (1960). The permeability of monolayer to carbon dioxide. *Transactions of the Faraday Society*, **56**, 1832-1841.

20. Bogatykh, S. A. (1964). Absorption of water vapor from gases in the cyclone-foam apparatus. *Khimicheskoe Mashinostroenie, 2, 17-21.*

21. Brady, A. P. and Ross, S. (1944). The Measurement of Foam Stability. *Journal of the American Chemical Society*, **66**(8), 1348-1356.

22. Calderbank, P. H. and Rennie, J. (1962). The physical properties in foams and froths formed on sieve plates. *Transactions of the Institute of Chemical Engineering*, **40**, 3-12.

23. Calderbank, P. H. (1958). Physical rate processes in industrial fermentation. Part I: The interfacial area in gas-liquid contacting with mechanical agitation. *Transactions of the Institute of Chemical Engineering*, **36**, 443-463.

24. Calvert, J. R. (1990). Pressure drop for foam flow through pipes. *International Journal of Heat and Fluid Flow*, **11**(3), 236-241.

25. Capuder, E. and Koloini, T. (1984). Gas hold-up and interfacial area in aerated suspensions of small particles. *Chemical Engineering Research and Design*, **62**, 255-60.

26.   Caskey, J. A. and Barlage Jr, W. B. (1972). A study of the effects of soluble surfactants on gas absorption using liquid laminar jets. *Journal of Colloid and Interface Science*, **41**(1), 52-62**.**

27.   Chen, G. X., Cai, T. J., Chuang, K. T. and Afacan, A. (2007). Foaming effect on random packing performance. *Chemical Engineering Research and Design*. **85**(2), 278-282.

28.   Chen, J. F., Wang, Y. H., Guo, F., Wang, X. M. and Zheng, C. (2000). Synthesis of nanoparticles with novel technology: high-gravity reactive precipitation. *Industrial and Engineering Chemistry Research*, **39**(4), 948-954.

29.   Clift, R., Grace, J. R. and Weber, M. E. *Bubble Drops and Particles,* Academic Press, New York, p171, 236, 1978.

30.   Cullen, E. J. and Davidson, J. F. (1956). The effect of surface active agents on the rate of absorption of carbon dioxide by water. *Chemical Engineering Science*, **6**(2), 49-56.

31.   Dankwerts, P. V. *Gas-liquid reactions*. McGraw-Hill, New York, 1970.

32.   Danckwerts and Sharma M. M. (1966). The Absorption of Carbon Dioxide into Solutions of Alkalis and Amines: (with Some Notes on Hydrogen Sulphide and Carbonyl Sulphide). *Institution of Chemical Engineers*, CE244-CE280.

33.   Danckwerts, P. V., Kennedy, A. M.and Roberts, D. (1963). Kinetics of CO 2 absorption in alkaline solutions—II: Absorption in a packed column and tests of surface-renewal models. *Chemical Engineering Science*, *18***(2),** 63-72.

34.   Davidson, J. F. and Schuler, B. G. (1960).*Trans. Inst. Chem. Eng. Lond.,* **38**,144. (cited in Treybal, R.E.)

35.   Desai, D. and Kumar, R. (1985). Some experimental observations on recirculating semi-batch foam columns. *Chemical Engineering Science*, **40**(7), 1305-1308.

36.   Desai, D. and Kumar, R. (1983). Liquid holdup in semi-batch cellular foams. *Chemical Engineering Science*, **38**(9), 1525-1534.

37.   Deshpande, N. S., Dinkar, M. and Joshi, J. B. (1995). Disengagement of the gas phase in bubble columns. *Int. J. Multiphase Flow*, **21**, 1191-1201.

38.   Deshpande, N. S. and Barigou, M. (2000). The flow of gas–liquid foams in vertical pipes. *Chemical Engineering Science*, **55**(19), 4297-4309.

39. Emmert, R. E. and Pigford, R. L. (1954). Interfacial resistance-a study of gas absorption in falling liquid films. *Chemical Engineering Progress*, **50**(2), 87-93.

40. Flaten, M. E., Seiersten, M. and Andreassen, J. (2009). Polymorphism and morphology of calcium carbonate precipitated in mixed solvents of ethylene glycol and water, *Journal of Crystal Growth,* **311**, 3533-3538.

41. Gaikwad, A. A. and Bhaskarwar, A. N. (2007). Absorption of pure carbon-dioxide gas in a foam-bed reactor. *Proceedings of European Congress of Chemical Engineering, Copenhagen,* 16-20.

42. Gaikwad, A. A., Challapalli, N. and Bhaskarwar, A. N. (2010). Carbonation of barium sulfide in a foam-bed reactor. *Chemical Engineering Communications*, **197**(6), 804-829.

43. Galkina, V. P. and Gertsen, P. P. (1969). Absorption of hydrogen fluoride in a froth absorber. *Nauchnye Trudy-Permskii Politekhnicheskii Instituta,* **52**, 119-124. From: Ref. Zh., Khim. 1970, Abstr. No. 11645.

44. Gestrich, W. and Krauss, W. (1976). Specific interfacial area in bubble layers. *International Chemical Engineering*, **16**(1), 10-18.

45. Goodridge, F. and Bricknell, D. J. (1962). Interfacial resistance in the carbon dioxide-water system. *Transactions of the Institute of Chemical Engineering*, **40**, 54-60.

46. Gourich, B., Christophe, V., Essadki, A. H., Allam, F., Soulami, M. B. and Ziyad, M. (2006). Identification of flow regimes and transition points in a bubble column through analysis of differential pressure signal- Influence of the coalescence behaviour of the liquid phase. *Chemical Engineering and processing*, **45**, 214-223

47. Grishina, N. P., Mutriskov, A. Ya. And Maminov, O.V. (1971). Effect of surfactants on the degree of foaming. *Trudy Kazanskogo Khimiko-Teckhnologicheskogo Instituta*, **44**, 19-22.

48. Hartland, S. and Barber, A. D. (1974). A Model for Cellular Foam, *Transactions of the Institute of Chemical Engineering.* **52**, 43-52.

49. Haas, P. A. and Johnson, H. F. (1967). A model and experimental results for drainage of solution between foam bubbles. *Industrial and Engineering Chemistry Fundamentals*, **6**(2), 225-233.

50. Haq, M. A. (1982). Fluid-dynamics on sieve trays. *Hydrocarbon Processing*, **61**(4), 165-168.

51. Helsby, F. W. and Birt, D. C. P. (1955). Foam as a medium for gas absorption. *Journal of Applied Chemistry*, **5**(7), 347-352.

52. Heller, J. P. and Kuntamukkula, (1987). Critical review of the Foam rheology literature, *Ind. Eng. Chem. Res.,* **26**, 318-325.

53. Heuss, J. M., King, C. J. and Wilke, C. R. (1965). Gas-liquid mass transfer in cocurrent froth flow. *AIChE Journal*, **11**(5), 866-873.

54. Higbie, R. (1935). The rate of absorption of a pure gas into a still liquid during short periods of exposure. *Transactions AIChE.* **31**(2), 365-389.

55. Hoffer, M. S. and Rubin, E. (1969). Flow regimes of stable foams. *Industrial and Engineering Chemistry Fundamentals*, **8**(3), 483-490.

56. Houghton, G., McLean, A. M. and Ritchie, P. D. (1957). Mechanism of formation of gas bubble-beds. *Chemical Engineering Science*, **7**(1), 40-50.

57. Jackson, J. (1963). Gas cleaning by the foam method. *British Chemical Engineering*, **8**(5), 319-321.

58. Jacobi, W. M., Woodcock, K. E. and Grove, C. S. (1956). Theoretical investigation of foam drainage. *Industrial and Engineering Chemistry*, **48**(11), 2046-2051.

59. Jana, S. K. and Bhaskarwar, A. N. (2012). Measurement of surface-transfer coefficient values for CO2 absorption in lime solutions in presence of surfactants. *The Canadian Journal of Chemical Engineering*, **90**(1), 196-204.

60. Jana, S. K. and Bhaskarwar, A. N. (2010). Modeling gas absorption accompanied by chemical reaction in bubble column and foam-bed slurry reactors. *Chemical Engineering Science*, **65**(11), 3649-3659.

61. Jana, S. K. and Bhaskarwar, A. N. (2011). Gas absorption accompanied by chemical reaction in a system of three-phase slurry-foam reactors in series. *Chemical Engineering Research and Design*, **89**(6), 793-810.

62. Jana, S.K. (2007). Studies on a slurry foam reactor for carbonation of hydrated-lime slurry using pure carbon-dioxide gas. *Ph.D. thesis, IIT Delhi*.

63. Jones, A. G., Hostomsky, J. and Zhou, L. (1992). On the effect of liquid mixing rate on primary crystal size during the gas-liquid precipitation of calcium carbonate. *Chemical Engineering Science*, **47**(13), 3817-3824.

64. Juvekar, V. A. and Sharma, M. M. (1973). Absorption of CO_2 in a suspension of lime. *Chemical Engineering Science*, **28**(3), 825-837.

65. Kaldor, T. G. and Phillips, C. R. (1976). Aerosol scrubbing by foam. *Industrial & Engineering Chemistry Process Design and Development*, **15**(1), 199-206.

66. Kantarci, N., Borak, F., and Ulgen, K. O. (2005). Bubble column reactors. *Process Biochemistry*, **40**(**7**), 2263-2283.

67. Kawecki, W., Reith, T., Van Heuven, J. W. and Beek, W. J., 1967, Bubble size distribution in the impeller region of a stirred vessel. *Chemical Engineering Science,* **22**, 1519-1523.

68. Kojima, H., Hakuta, M., Kudoh, K., Ichinoseki, T. and Midorikawa, H. (1989). Chemical absorption into slurry in gas-sparged stirred vessel under continuous operation. *Journal of Chemical Engineering of Japan*, **22**(6), 621-627.

69. Kotaki, Y. and Tsuge, H. (1990). Reactive crystallization of calcium carbonate by gas-liquid and liquid-liquid reactions. *The Canadian Journal of Chemical Engineering*, **68**(3), 435-442**.**

70. Kister, H. Z. (2003). What caused tower malfunctions in the last 50 years?.*Chemical Engineering Research and Design*, **81**(**1**)**,** 5-26.

71. Kruglyakov, P. M. and Taube, P. R. (1965). *Zhurnal Fizicheskoi Khimii,* **38**, p. 1514. From Ref. Bikerman (1973), p. 164.

72. Kumar, A., Degaleesan, T. E., Laddha, G. S. and Hoelscher, H. E. (1976). Bubble swarm characteristics in bubble columns. *The Canadian Journal of Chemical Engineering*, **54**(6), 503-508.

73. Kumar, R. and Kuloor, N. R. *Advances in Chemical Engineering,* Vol. 8, p. 286. *Academic Press, New York*, 1970.

74. Kucka, L., Kenig, E. Y. and Gorak, A. (2002). Kinetics of the Gas-liquid reaction between carbon dioxide and hydroxide ions, *Ind. Eng. Chem. Res.,* **41(24),** 5952-5957.

75. Lee, D. J., Luo, X. and Fan, L. S. (1999). Gas disengagement technique in a slurry bubble column operated in the coalesced bubble regime. *Chemical Engineering Science*, **54**(13), 2227-2236.

76. Leibson, I., Holcomb, E. G., Cacoso, A. G. and Jacmic, J. J. (1956). Rate of flow and mechanics of bubble formation from single submerged orifices. *AIChE Journal*, **2**(3), 300-306.

77.   Lemoine, R., Behkish, A., Sehabiague, L., Heintz, Y. J., Oukaci, R., and Morsi, B. I. (2008). An algorithm for predicting the hydrodynamic and mass transfer parameters in bubble column and slurry bubble column reactors. *Fuel processing technology*, **89(4),** 322-343.

78.   Leonard, R. A. and Lemlich, R. (1965). A study of interstitial liquid flow in foam. Part I. Theoretical model and application to foam fractionation. *AIChE Journal*, **11**(1), 18-25.

79.   Lipping, D., Prokop, A. and Tanner, R. D. (2003). Variation of bubble size distribution in a protein foam fractionation column measured using a capillary probe with photoelectric sensors. *Journal of Colloid and Interface Science*, **259**(1), 180-185.

80.   Llorens, J., Mans, C. and Costa, J. (1988). Discrimination of the effects of surfactants in gas absorption. *Chemical Engineering Science*, **43**(3), 443-450.

81.   Luchinsky, G.P. (1939). New method for absorption of aerosols and gases by liquids. *Zh. Fiz. Khim.* **13**, 302.

82.   Maminov, O. V. and Usmanova, S. I. (1968). Absorption of carbon dioxide by monoethanolamine solutions in a foam apparatus. *Trudy Kazanskogo Khimikotekhnologicheskogo Instituta.* **37**, 291-297.

83.   Maminov, O. V. and Mutriskov, A. (1969). Mass transfer for behavior in foam layers. Institute of Chemical Engineers, **9**, 642.

84.   Manvelyan, M. G., Tarat, E. Ya. and Safaryan, M. A. (1967a). Carbonation of sodium metasilicate solutions in a froth apparatus [sieve-tray column]. I. Hydrodynamics conditions of similarity in a parallel- flow apparatus. *Armyanskii Khimicheskii Zhurnal,* **20**(5), 382-390.

85.   Manvelyan, M. G., Tarat, E. Ya. and Safaryan, M. A. (1967b). Carbonation of sodium metasilicate solutions in a froth apparatus [sieve-tray column]. II. Main indicators of hydrodynamics conditions and factors affecting froth formation. *Armyanskii Khimicheskii Zhurnal,* **20**(5), 390-400.

86.   Maruscak, A., Baker, C. G. J. and Bergougnou, M. A. (1971). Calcium carbonate precipitation in a continuous stirred tank reactor. *The Canadian Journal of Chemical Engineering*, **49**(6), 819-824.

87.   Marrucci, G. (1965). Rising velocity of swarm of spherical bubbles. *Industrial and Engineering Chemistry Fundamentals*, **4**(2), 224-225.

88. Mashelkar, R. A. (1970). Bubble columns. *British Chemical Engineering*, **15**(10), 1297-1297.

89. Mena, P. C., Ruzicka, M.C., Rocha, F. A., Teixeira, J. A. and Drahos, J. (2005). Effect of solids on homogeneous-heterogeneous flow regime transition in bubble columns. *Chemical Engineering Science*, **60**, 6013-6026.

90. Meikap, B. C., Kundu, G., & Biswas, M. N. (2002). Modeling of a novel multi-stage bubble column scrubber for flue gas desulfurization. *Chemical Engineering Journal*, **86(3),** 331-342

91. Mendelson, H. D. (1967). The prediction of bubble terminal velocities from wave theory. *AIChE Journal*, **13**(2), 250-253.

92. Mersmann, A. (1962). Pressure drop and foam height of aerated liquid layers on sieve trays. *VDI Forschungsheft*, **491**, 1-44.

93. Metzner, A. B. and Brown, L. F. (1956). Mass transfer in foams. *Industrial and Engineering Chemistry*, **48**(11), 2040-2045.

94. Miles, G. D., Shedlovsky, L. and Ross, J. (1945). Foam drainage. *The Journal of Physical Chemistry*, **49**(2), 93-107.

95. Morris, R. M. and Woodburn, E. T. (1967). S. A. Chemical process. Cp.98 (cited in Juvekar and Sharma, 1973).

96. Mutriskov, A. Ya., Maminov, O. V. and Ismagilov, K. G. (1964). Effect of temperature on absorption with chemical reaction under foaming conditions. *Trudy Kazanskogo Khimiko-Teckhnologicheskogo Instituta,* **32**, 152-156. From Ref. Zh., Khim. 1965, Abstr. No. 11119.

97. Mutriskov, A. Ya. and Maminov, O. V. (1975). Mass transfer during chemical reaction in a froth bed. *Mashiny I Apparaty Khim Tekhologiya,* **3**, 3-5.

98. Nakazato, T., Liu, Y., Sato, K. and Kato, K. (2002). Semi-dry process for production of very fine calcium carbonate powder by a powder-particle spouted bed. *Journal of Chemical Engineering of Japan*, **35**(5), 409-414.

99. Nishioka, G. and Ross, S. (1981). A new method and apparatus for measuring foam stability. *Journal of colloid and Interface Science*. **81(1)**, 1-7.

100. Onda, K., Sada, E. and Hiroshi, T. (1969). Interfacial areas and liquid side mass-transfer coefficients in foam columns, *Kagaku Kogaku,* **33**(5), 448-453.

101. Perrin, S., Chaudourne, S., Jallut, C. and Lieto, J. (2002). Transient state techniques for mass transfer characterization of a gas-liquid packed column. *Chemical Engineering Science*, **57**(16), 3335-3345.

102. Perry, R.H. and Green, D. *Perry's Chemical Engineers Handbook*, 6th Edn. McGraw-Hill, 1987.

103. Plevan, R. E. and Quinn, J. A. (1966). The effect of monomolecular films on the rate of gas absorption into a quiescent liquid. *AIChE Journal*, **12**(5), 894-902.

104. Plateau, J. (1873). Statique expérimentale et théorique des liquides soumis aux seules forces moléculaires (Vol. 2). Gauthier-Villars**.**

105. Ponter, A. B., Trauffler, P. and Vijayan, S. (1976). Effect of surfactant addition upon packed distillation column performance. *Industrial and Engineering Chemistry Process Design and Development*, **15**(1), 196-199.

106. Pozin, M. E., Tarat, E. Ya. And Morariu, I. (1964). Rate of absorption of carbon dioxide by monoethanoalamine foam solutions. *Khimiya I Khimicheskaya Tekhnologiya*, **7**(2), 240-245.

107. Pradhan, S. M., Sarma, Ram, Sita, D. S. H. and Khilar, K. C. (1990). Stability of aqueous foams with polymer additives. *Journal of colloid and Interface Science*.**139**, 519-526.

108. Ramachandran, P. A. and Sharma, M. M. (1969). Absorption with fast reaction in a slurry containing sparingly soluble fine particles. *Chemical Engineering Science*, **24**(11), 1681-1686.

109. Reddy, M. M. and Nancollas, G. H. (1971). Mass transfer with chemical reaction in a froth bed reactor. *Chemical Engineering Communications*, **178**(1), 103-127.

110. Reddy, S. Y. C. and Bhaskarwar, A. N. (2000).The crystallization of calcium carbonate: I. Isotope exchange and kinetics. *J. Colloid Interface Sci.***36**, 166-172.

111. Rennie, J. and Evans, F. (1962). The Formation of Froths and Foams above Sieve Plates, *British Chemical Engineering,* **7**(7), 498-502.

112. Riet, K. V. (1979). Review of measuring methods and results in non viscous gas-liquid mass transfer in stirred vessels. *Industrial and Engineering Chemistry Process Design and Development*, **18**(3), 357-364.

113. Robinson, C. W. and Wilke, C. R. (1974). Simultaneous measurement of interfacial area and mass transfer coefficients for well-mixed gas dispersion in aqueous electrolyte solutions. *AIChE Journal*, **20**(2), 285-294.

114. Rodionov, A.I., Kashnikov, A.M., Radikovskii, V.M. and Mendeleev, D.I. (1966). Determination of the phase contact [Interfacial] area and the coefficient of heat and mass transfer on sieve plates. *Telpo-I Massoperenos.* **4**, 28-37.

115. Rosen, M. J. *Surfactants and interfacial phenomena*, John Wiley and Sons, 1978.

116. Rubin, E., La Mantia, C. R., & Gaden Jr, E. L. (1967). Properties of dynamic foam columns. *Chemical Engineering Science*, **22**(8), 1117-1125.

117. Rukhadze, V. V., Gaprindashvili, V. N., Pulariani, Yu. I. and Tskalobadze, L. A. (1990). Optimization of the process of $BaCO_3$ precipitation from barium sulphide by carbon dioxide. *Soobshcheniya Akademii Nauk Gruzinskoi SSR.* **138**(2), 337-340.

118. Sada, E., Kumazawa, H. and Butt, M. A. (1977). Gas absorption with catalytic reaction. *Chemical Engineering Science*, **32**(8), 970-972.

119. Sada, E., Kumazawa, H. and Butt, M. A. (1977). Simultaneous absorption with reaction in a slurry containing fine particles. *Chemical Engineering Science*, **32**(12), 1499-1503.

120. Sada, E., Kumazawa, H. and Lee, C. H. (1984). Chemical absorption into concentrated slurry: absorptions of carbon dioxide and sulfur dioxide into aqueous concentrated slurries of calcium hydroxide. *Chemical Engineering Science*, **39**(1), 117-120.

121. Sada, E., Kumazawa, H. and Butt, M. A. (1977). Single gas absorption with reaction in a slurry containing fine particles. *Chemical Engineering Science*, **32**(10), 1165-1170.

122. Sada, E., Kumazawa, H., Lee, C. and Fujiwara, N. (1985). Gas-liquid mass transfer characteristics in a bubble column with suspended sparingly soluble fine particles. *Industrial and Engineering Chemistry Process Design and Development*, **24**(2), 255-261.

123. Sarma, Ram, Sita, D. S. H., Pandit, J. and Khilar, K.C. (1987). Enhancement of stability of aqueous foams by addition of water-soluble polymers-

measurements and analysis. *Journal of colloid and Interface Science*, **124**, 339-348.

124.   Sathe, M., Joshi, J., & Evans, G. (2013). Characterization of turbulence in rectangular bubble column. *Chemical Engineering Science*, ***100*,** 52-68.

125.   Sawyer, W. M. and F. M. Fowkes. (1958). Interaction of anionic detergents and certain polar aliphatic compounds in foams and micelles. *The Journal of Physical Chemistry,* **62**(2), 159-166.

126.   Shabel'nikov, A., P. and Mukhlenov, I., P. (1963). Studies of the absorption of moderately soluble gases under conditions of foam formation, *Khimiya I Khimicheskaya Tekhnologiya.* **6**(6), 982-990.

127.   Shah, P. S. and Mahalingam, R. (1984). Mass transfer with chemical reaction in liquid foam reactors. *AIChE journal*, **30**(6), 924-934.

128.   Sharma, D. S. H. S. R., Pandit, J. and Khilar, K. C. (1988). Enhancement of stability of aqueous foams by addition of water-soluble polymers-measurements and analysis. *Journal of Colloid and Interface Science*, **124**(1), 339-348.

129.   Sharma, M. M. and Danckwerts, P. V. (1970). Chemical methods of measuring interfacial area and mass-transfer coefficient in two-fluid systems. *British Chemical Engineering,* **15**(4), 522-528.

130.   Sharma, R K., Gaikwad, A. and Bhaskarwar, A. N. (2005). Gas absorption with chemical reaction and desorption in a foam-bed reactor. *Chemical Engineering Communications*, **192**(5), 597-619.

131.   Sharma, M. M. and Gupta, R. K. (1967). Mass-transfer characteristics of plateau columns without down comer. *Trans. Instn. Chem. Engrs.* **45(1),** T169-T175.

132.   Sherwood, T. K., Pigford, R. L. and Wilke, C. R. *Mass Transfer*, Mc-Grawhill, Kogakusha. p. 365, (Table 8.4), 1975.

133.   Shih, F. S. and Lemlich, R. (1971). Continuous foam drainage and overflow. *Industrial & Engineering Chemistry Fundamentals*, **10**(2), 254-259.

134.   Shih, S. M., Ho, C. U. S., Song, Y. S. and Lin, J. P. (1999). Kinetics of the reaction of $Ca(OH)_2$ with CO_2 at low temperature. *Industrial and Engineering Chemistry Research*, **38**(4), 1316-1322.

135. Shimizu, K., Takada, S., Minekawa, K. and Kawase, Y. (2000). Phenomenological model for bubble column reactors: prediction of gas hold-ups and volumetric mass transfer coefficients. *Chemical Engineering Journal*, **78**(1), 21-28.

136. Shulman, H. L. and Molstad, M. C. (1950). Gas-bubble columns for gas-liquid contacting. *Industrial and Engineering Chemistry*, **42**(6), 1058-1070.

137. Sherwood, T. K., Pigford, R. L. and Wilke, C. R. *Mass transfer*. McGraw-Hill, p. 365, (Table 8.4), 1975.

138. Suresh, A. K. NPTEL lecture notes. IIT Bombay.

139. Sree, R. P. (1993). Mass Transfer Accompanied by a Chemical Reaction in a Micro emulsion Foam-bed Reactor. Recent Trends in Biotechnology. *Proceedings of the Ninth National Convention of Chemical Engineering and International Symposium.* Importance of Biotechnology in Coming Decades. P 211-217.

140. Stangle, G. C. and Mahalingam, R. (1989). Mass transfer with chemical reaction during gas bubble formation in foam column reactors. *Chemical Engineering Science*, **44**(3), 507-514.

141. Stangle, G. C. and Mahalingam, R. (1990). Mass transfer with chemical reaction in a three hyphen; phase foam-slurry reactor. *AIChE journal*, **36**(1), 117-125.

142. Steiner, L., Hunkeler, R. and Hartland, S. (1977). Behavior of dynamic cellular foams. *Transactions of the Institute of Chemical Engineering*, **55**, 153-163.

143. Subramanyam, R., Katyal, P. and Bhaskarwar, A. N. (1999). Design of a foam-bed reactor system. **136**(1-2), 23-30.

144. Tadaki, T. and Maeda, S. (1964). Absorption of carbon dioxide by milk of lime in a wetted wall column. *Kagaka Kogaka*, **2**, 85.

145. Tadros, Th. F. *Solid/liquid dispersions*, p. 119. Academic Press, 1987.

146. Ternovskaya, A. N. and Belopolskii, A. P., 1950, *Zhurnal Fizicheskoi Khimii,* 24, p. 43 (cited in Cullen and Davidson 1956).

147. Thomas, P. D., Darton, R. C. and Whalley, P. B. (1995). Liquid foam structure analysis by visible light tomography. *The Chemical Engineering Journal and the Biochemical Engineering Journal*, **56**(3), 187-192.

148. Thondavadi, N. N. and Lemlich, R. (1985). Flow properties of foam with and without solid particles. *Industrial and Engineering Chemistry Process Design and Development*, **24**(3), 748-753.

149. Treybal, E. R. *Mass Transfer Operations*, Third edition, McGraw–Hill, Singapore, 1981.

150. Tsuge, H., Kotaki, Y. and Hibino, S. (1987). Reactive Crystallization of Calcium Carbonate by Liquid-liquid Reaction. *Journal of Chemical Engineering of Japan.* **20**(4), 374-379.

151. Uchida, S., Koide, K. and Shindo, M. (1975). Gas Absorption with Fast Reaction into a Slurry Containing by Liquid-liquid Reaction. *Journal of Chemical Engineering of Japan.* **20**(4), 374-379.

152. Valentine, F. H. H. *Absorption in gas-liquid dispersions: some aspects of bubble technology*. Spon, 1967.

153. Varshney, A., Agrawal, P. and Bhaskarwar, A. N. (2003). Gas absorption with zero-order chemical reaction in a foam-bed reactor. *Chemical Engineering Science*, **58**(15), 3413-3424.

154. Vogel, A. I., *Vogel's Text Book of Quantitative Chemical Analysis* (Revised by: Jeffery, G. H., Bassett, J., Mendham, J. and Denney, R. C.). 5th Edn. p.384. ELBS, London, 1989.

155. Wachi, S. and Jones, A. G. (1991). Mass transfer with chemical reaction and precipitation. *Chemical Engineering Science*, **46**(4), 1027-1033.

156. Weber, H. C. and Nilsson, K. T. (1926). The Absorption of Gases in Milk of Lime1: Part I. *Industrial and Engineering Chemistry*, **18**(10), 1070-1075.

157. Wei, S. H., Mahuli, S. K., Agnihotri, R. and Fan, L. S. (1997). High surface area calcium carbonate: pore structural properties and sulfation characteristics. *Industrial and Engineering Chemistry Research*, **36**(6), 2141-2148

158. Weissman, E. Y. and Calvert, S. (1965). Mass transfer in horizontally moving stable aqueous foams. *AIChE Journal*, **11**(2), 356-363.

159. Westerterp, K. R., Van Dierendonck, L. L. and De Kraa, J. A. (1963). Interfacial areas in agitated gas-liquid contactors. *Chemical Engineering Science*, **18**(3), 157-176.

160. Xie, W., Neethling, S. J. and Cilliers, J. J. (2004). A novel approach for estimating the average bubble size for foams flowing in vertical columns. *Chemical Engineering Science*, **59**(1), 81-86.

161. Zurakowski, S. and Glaser, R. (1965). Construction parameters of foam columns for gas drying. *Przemysl Chemiczny.* **44**(9), 510-513.

BIO-DATA

Name	:	**ISHA ARYA**
Father's Name	:	Mr. Mohan Lal Arya
Mother's Name	:	Mrs. Usha Arya
Date of Birth	:	21/02/1985
Marital Status	:	Married
Husband's Name	:	Dr. Yogesh Kumar (MBBS, MD)
Educational Qualification	:	M. Tech., Chemical Engineering, (2008), *MNIT, Jaipur*
		B.E., Biotechnology Engineering, (2006), *University of Rajasthan, Jaipur*
Job Experience	:	Visiting Professor at *J.K. Laxmipat University, Jaipur*
Scientific Memberships	:	**02** (Life associate member - International Association of Engineers
		Life associate member- Indian Institute of Chemical Engineers)
Publications	:	International Journal (01)
		International conference (02)
		National Journal (01)
		National conference (04)

Awards and Recognition:

- UGC award under the scheme of Post Graduate Scholarship for professional courses, 5000/- p.m. Scholarship for M. Tech.
- Selected for Rajiv Gandhi research fellowship 2011-2012.
- Active participation in organizing a Workshop on *Process modifications for green technology and energy integration -2012,* at MNIT –JAIPUR
- Active participation in organizing a short term course on *Recent Advances in Pollution Prevention Technologies in Process Industries-2012,* at MNIT - JAIPUR